University of Strathclyde,

Strathclyde Institute of Pharmacy and Biomedical Sciences

SAKATA Lab.

Investigating Age-Related Changes in Auditory Cortex Activity

Sarah Fouda

Supervised by Dr Shuzo Sakata

A thesis submitted in partial fulfilment of the requirements for the degree of Doctor of Philosophy

14 July 2023

Declaration

This thesis is the result of the author's original research. It has been composed by the author and has not been previously submitted for examination which has led to the award of a degree. The copyright of this thesis belongs to the author under the terms of the United Kingdom Copyright Acts as qualified by University of Strathclyde Regulation 3.50. Due acknowledgement must always be made of the use of any material contained in, or derived from, this thesis.

Signed:

Fouda Sarah

Date: 14 July 2023

Acknowledgements

I would like to express my deepest gratitude to all those who have supported and contributed to the completion of this thesis. Their guidance, encouragement, and assistance have been invaluable throughout this journey.

First and foremost, I am thankful to my supervisor, Shuzo SAKATA, for his guidance, expertise, and unwavering support. His insightful feedback, constructive criticism, and dedication to my research have played a crucial role in shaping this thesis. I would like to emphasize particularly his patience and professionalism, which I am sure will greatly influence my future career. I would like to thank the examiners and the jury for taking the time to read and provide feedback on my thesis. I am grateful to the Shuzo Sakata Lab members for their assistance, discussion, scientific sharing, and feedback on my work, as the optogenetic Lab members. I would like to particularly thank Mirna Mirkel for always being the camaraderie that I needed through this process. I would also like to mention Daniel Lyngholm as his involvement was crucial in collecting the necessary data and ensuring the validity of my findings. Thank you to Nicole Byron and Jacques Ferreira for their support, camaraderie, and feedback on my work. I would like to acknowledge the staff and resources provided by SIBPS, who facilitated my thesis management.

I am indebted to my family for their unconditional love, unwavering support, and constant belief in my abilities. Their encouragement, understanding, and sacrifices have been the pillars of my academic journey. I would like to express my heartfelt gratitude to my mom, Farida Fouda, for her unconditional support through all the phases of these three years and to my dad, Refaat Fouda, for his unwavering faith in me. I would like to thank my sisters, Princessa and Hagar Fouda, who are my anchors and my best friends. Thank you to my lovely friends, Rofayda, Maryam, Ines, team S, with who I can be myself and have fun...

I would like to express my sincere gratitude to the examiners of my thesis for their valuable time and commitment in reviewing my work.

To the esteemed readers and examiners of this thesis, thank you for your time, I sincerely hope that the findings and insights presented herein will captivate your interest and contribute to the advancement of knowledge in our shared field of study.

Thank you all.

Fouda Sarah

"Indeed, with the hardship, there is ease"

Abstract

Presbycusis is an age-related hearing loss affecting a significant portion of the ageing population over 65 years old, leading to auditory difficulties and resulting in a decrease in autonomy. Many efforts are being made in the characterization of new therapies, notably employing cochlear implants. This disease affects the peripheral level of the auditory nervous system. However, little is known about how the auditory cortex adapts to this degeneration over time of hearing. The auditory cortex plays a critical role in auditory perception and is susceptible to age-related changes that may contribute to the development and progression of presbycusis. This thesis aims to investigate the effects of aging on the AC computation and its responses to auditory peripheral loss, providing insights into the mechanisms underlying auditory processing and the impact of presbycusis on central auditory function.

We investigated neuronal activity in C57BL/6 mice background ("C57"), known as a model of early age-related hearing loss, due to a genetic deficit at the cochlear level, with the F1 hybrid of C57BL/6 and CBA/Ca backgrounds ("Hybrid mice") that does not exhibit such important hearing loss. We analysed the electrophysiological auditory cortex activity to describe the neural computation along ageing and across cell-types during spontaneous and sound stimuli.

Our findings revealed distinct activity patterns in the auditory cortex of Hybrid and C57 mice. From a young age, differences were observed in both spontaneous firing and evoked-response activity, indicating that the reception of sound shapes the functionality of the auditory cortex. Interestingly, these changes were more pronounced in inhibitory cell, suggesting their role in auditory reception and processing and highlighting the impact of presbycusis on these cell types. Furthermore, the relationship between spontaneous and evoked-response activity differed between the two strains, with implications for information processing in the auditory cortex. In addition to the electrophysiological parameters, we investigated the pupil dynamics as a measure of brain state during auditory processing. The analysis of pupil responses provided insights into the modulation of brain states and their influence on auditory perception and processing.

Contents

Contents

Contents

List of Figures

List of Figures

List of Tables

Nomenclature

$5HT3aR$ Ionotropic serotonin receptor neurons

$A1$ primary auditory cortex

ABR Auditory brainstem responses

AC Auditory cortex

AP Action potential

BS Broad-spiking cells

$C57$ C57BL/6 mice background

CE Contrast Entropy

CV Coefficient of variation of the interspike interval

dB Decibel

DCN Dorsal nuclei

EEG Electroencephalograpy

$EPSP$ Excitatory postsynaptic potential

FR Firing rate

FSU Fast-spiking units

$Hybrid$ F1 hybrid of C57BL/6 and CBA/Ca mice background

IC Inferior colliculi

IHC Inner cells

$IPSP$ Inhibitory postsynaptic potential

LFP Local field potential

MGB Medial geniculate body of the thalamus

MI Mutual information per seconds

MIs Mutual information per spikes

NR Non-responding cells

Nomenclature

NS Narrow-spiking cells

OHC Outer cells

PC Pyramidal cells

PSD Power spectrum density

$PSTH$ Peri-stimulus-time histogram

PV Calcium-binding protein parvalbumin neurons

R Responding cells

RSU Regular-spiking units

SOC Superior olivary complex

SOM Neuropeptide somatostatin neurons

$STRF$ Spectro-temporal receptive field

$T2P$ Trough to peak

VCN Ventral nuclei

Introduction

Throughout our lives, hearing undergoes significant changes and can be greatly affected by ageing (Jayakody et al. 2018). The auditory system holds a vital role in comprehending and reacting to our surroundings daily. With the global population ageing, age-related alterations are emerging as a prominent socio-economic concern that requires attention. Apart from the decline in the range of audible frequencies (Gates & Mills 2005), age-related hearing loss has a profound impact on individuals' lives and may even coexist with various neurodegenerative disorders (Lin et al. 2011, Peelle et al. 2011, Jayakody et al. 2018, Livingston et al. 2017), or mental health conditions (Lee et al. 2012, Jayakody et al. 2018, Wong et al. 2014).

Although age-related hearing loss is commonly described as a peripheral auditory impairment (Jayakody et al. 2018), few studies have explored the effects of this loss on auditory cortex activity (Fuksa et al. 2022, Gates & Mills 2005). Considering the broad capacity of the auditory cortex to adapt and its plasticity properties (Fetoni et al. 2015, Rauschecker 1999), we wanted to investigate how hearing loss shapes the activity in the auditory cortex and how it affects its capabilities (Kotak et al. 2005, Xue et al. 2023, Bishop et al. 2022). Furthermore, with the emergence of potential cortical probe therapies (Musk 2019, Beauchamp et al. 2020), we aimed to describe how auditory cortex neurons are activated during age-related hearing loss.

More specifically, our inquiries revolved around two main questions: How does the auditory cortex adjust to peripheral impairment? And how does the auditory cortex change with ageing? To address these inquiries, we conducted observations on age-related auditory cortical activity using two mouse models. The first model, the C57BL/6J mice strain, "C57", has early age-related hearing loss resulting from a gene mutation that disrupts the functioning of ear hair cell (Ohlemiller 2004). The second model, an F1 hybrid of C57BL/6 and CBA/Ca backgrounds, the "Hybrid mice", for whom the hearing deficit of C57 mice was restored, represents age-related hearing loss unrelated to peripheral pathological conditions (Frisina et al. 2011, Lyngholm & Sakata 2019, Bowen et al. 2020), where the overall ageing process affects hearing abilities.

In our study, we used electrophysiological data from silicon probes, which allowed us to monitor neural activity from a large number of cell. We followed cell activity during silence, described as 'spontaneous activity,' hypothesizing that this measurement represents the functional activity and integrity of the auditory cortex. Spontaneous neural activity is often viewed as neural noise that imposes limitations on sensory performance. However, an alternative hypothesis suggests that spontaneous firing carries information, and the distinction between these two hypotheses becomes apparent when considering its effects on the stimuli reception (Harris & Thiele 2011, Meyer-Baese et al. 2022, Eggermont 2015). Secondly, we investigated how the cell were active during the presentation of natural sounds to observe how age affects evokes-response of complex sounds and how they were differently encoded between the C57 and Hybrid mice. Finally, we compared spontaneous and evoked response activities to explore how the responsiveness to sound is affected by spontaneous activity due to peripheral impairment.

Existing evidence suggests that brain states have a significant impact on the auditory response to sound

(Matthew et al. 2015, Harris & Thiele 2011). Consequently, an aspect addressed in this thesis is understanding how the activity of the auditory cortex is influenced by levels of arousal. Therefore, the final section of our thesis is dedicated to exploring a methodology for representing brain states using pupil diameter as a measure of brain states and how it correlates with the auditory cortex activity.

This introductory chapter will begin with a description of the auditory pathway, detailing the complex process of sound encoding from the ear to the cortex. Subsequently, our focus will shift toward understanding the auditory cortex, including an analysis of its structure and functional aspects. We will then explore the effects of ageing on the auditory cortex focusing on the presbycusis. We will then, explore the brain states topic, and their link to auditory cortex functionality. Finally, we will review the principles of neuronal electrophysiology, providing a deeper understanding of the underlying mechanisms. current hypotheses regarding cortical neuronal networks, as well as the various measurements and metrics used to study them.

1.1 The auditory system

Sound is a propagating disturbance of air molecules that can be described as a wave (Figure 1.1. A). When a xylophone bar is struck, it induces an oscillatory movement of the surrounding air molecules, causing them to alternate between rarefaction (low pressure) and compression (high pressure). A sound wave is characterised by its frequency, which represents the number of rarefaction/compression cycles occurring over time, and its amplitude, which indicates the intensity of each air movement. As the frequency increases, the pitch of the sound rises. The auditory spectrum varies among species, ranging from 20 Hz to 20 kHz for humans and from 2 kHz to 100 kHz for mice (Ekdale 2016). The amplitude of a sound determines the magnitude of air deformation, which is measured using decibel levels (dB SPL) (Bizley 2017). Natural sounds consist of a combination of multiple frequencies and harmonics. Hearing is a complex phenomenon that involves various components, including sound localisation, onset/offset, decay (the rate at which the volume decreases after the initial peak), transitions between sounds (FM sweeps), discrimination from background noise, and speech (Bizley 2017, Gage & Baars 2018, Kopp-Scheinpflug et al. 2018). These features surround us at every moment, from infancy to old age.

1.1.1 The auditory pathway

1.1.1.1 The peripheral auditory system

The reception and transmission of air oscillations in the auditory system involve a remarkable sequence of events. It begins with sound waves in the environment, which enter the ear canal and cause the tympanic membrane (eardrum) to vibrate in response. This vibrations are then transmitted across the three tiny bones of the middle ear, known as the ossicles (malleus, incus, and stapes). The final bone in this chain, the stapes, interfaces with the oval window, a membrane that separates the middle ear from the fluid-filled cochlea in the inner ear. The movement of the stapes against the oval window creates fluid waves within the cochlear duct, which houses the sensory organ for hearing, the organ of Corti. As the fluid waves propagate through the cochlea, they cause the displacement of specialized hair cell within the organ of Corti. This hair cell movement leads to the generation of electrical signals, ultimately transmitting auditory information to the brain for processing and perception of sound (Pickles

2015) (Figure 1.1. BDE). The cochlea, situated in the inner ear, is the primary component of signal transduction from physical vibration to electrical signals that can be processed by the brain (Brownell 1982). It is a 2.5-shell structure filled with different liquids at varying concentrations. It comprises three fluid-filled chambers, which are separated by membranes. The scala media, positioned between the other two chambers (Figure 1.1. C), is a complex structure delimited by the Reissner and Basilar membranes (Figure 1.1. D). The basilar membrane runs along the length of the cochlea and supports the Organ of Corti, which houses the sensory cell known as hair cell (Figure 1.1. CF). The Organ of Corti extends along the entire length of the basilar membrane and contains the hair cell and stereocilia, where signal transduction occurs (Bahmer & Gupta 2018). The oscillations induced on the basilar membrane cause the Organ of Corti to move up and down, coming into contact with the tectorial membrane, which stretches the hair cell membrane and opens its channels. Due to the differences in ionic composition between cochlear liquids, the flow of ions depolarises the cell, transducing mechanical information into an electrical signal (Figure 1.1. C-F) (Casale et al. 2018). Hair cell are divided into two subgroups depending on their position on the Organ of Corti: inner hair cell (IHC), which carry the majority of auditory information and have synaptic contacts with approximately 20 auditory nerve cell, and outer hair cell (OHC), which, in contrast, have only one neuronal contact and play a role in amplifying the oscillation of the cochlear region responding to a particular frequency (Hudspeth 2013).

The stapes bone strikes the cochlear windows, a membrane-covered opening that separates the middle ear from the inner ear, thereby amplifying sound vibrations. The pressure exerted on the liquid transmits the sound wave along the basilar membrane. This membrane exhibits a gradient of rigidity from the point of articulation with the stapes (the base) to the apex (the extremity of the spiral). Consequently, the force required to bend the membrane is not uniform along the cochlea (Figure 1.1. F). High frequencies are encoded at the apex, while low frequencies are encoded at the base. This spatial organization of frequency coding is referred to as the tonotopic map. This organization is maintained throughout the auditory pathway (AP) until reaching the auditory cortex (AC) (Rhode et al. 2010). The neurons that innervate the IHCs are bipolar, their cell bodies are located in the spiral ganglion, and their processes extend into the cochlear nuclei. The auditory pathway involves the transmission of signals through various stations, from the cochlear nucleus, superior olivary, lateral lemniscus, inferior colliculus, and medial geniculate nucleus to the auditory cortex (Figure 1.2. A) (Bahmer & Gupta 2018). Each of these nuclei plays a crucial role in transmitting auditory signals to the auditory cortex.

In mice, the cochlear nuclei are vital structures located within the medulla, a part of the brainstem (Figure 1.2. A). These nuclei receive input from the auditory nerves, which carry auditory information from the cochlea. The fibres of the cochlear nerves bifurcate, with one branch connecting to the ventral cochlear nuclei (VCN) and the other to the dorsal cochlear nuclei (DCN). The neurons within these nuclei exhibit a tonotopic organization, where fibres originating from the apex of the cochlea (representing low frequencies) are located on the nuclei borders, while those from the base (representing high frequencies) penetrate deeper into the nuclei (Figure 1.2. C). This tonotopic arrangement allows for the preservation of the frequency-to-location mapping observed in the cochlea, forming bands of neurons with an isofrequency laminae structure (Haines & Mihailoff 2017).

The VCN are associated with inhibiting partially the contralateral pathway (Ingham et al. 2006, Oertel et al.

2011), enabling the selectivity of sound localization. This mechanism helps in distinguishing sounds coming from different directions. Apart from their role in auditory processing, the cochlear nuclei also contribute to the protection of the middle ear against acoustic over-stimulation through the contraction of the middle ear muscles (Oliver et al. 2003, Paul et al. 2019).
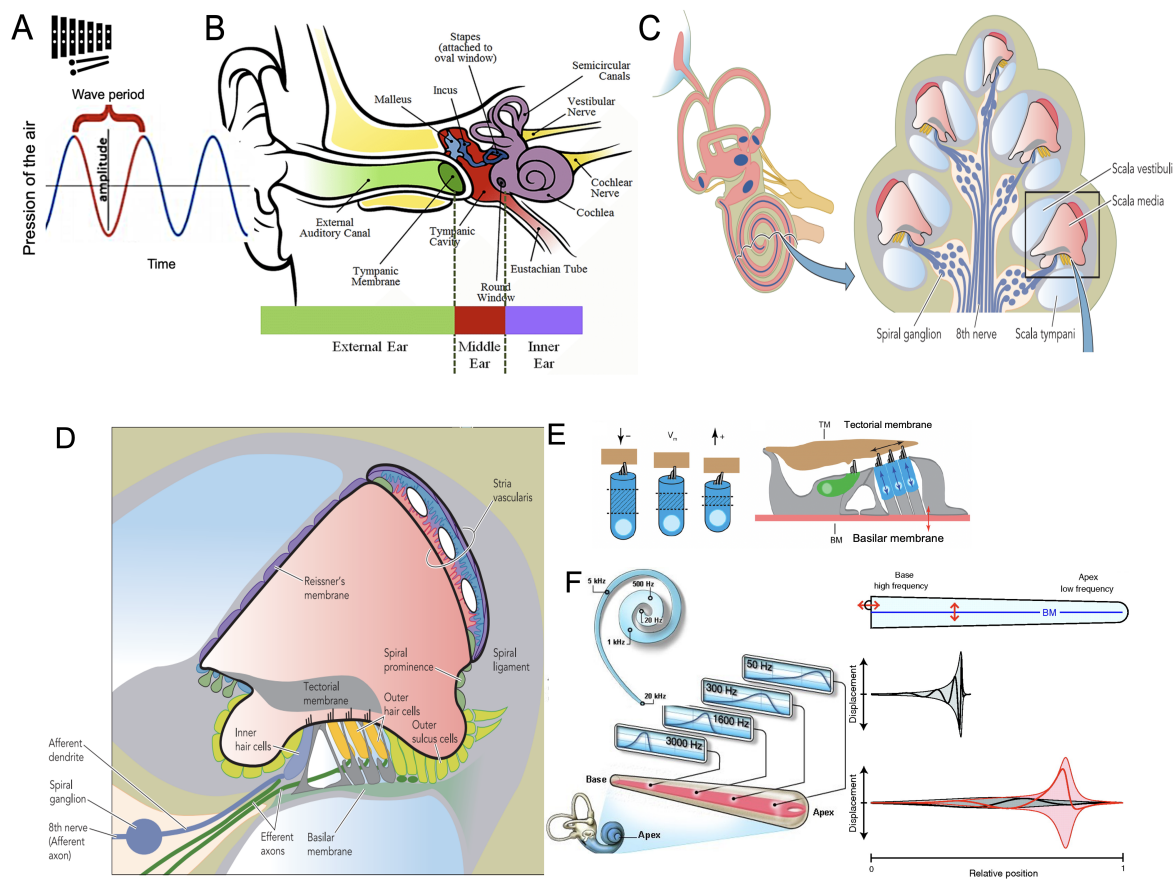
Figure 1.1: *The transduction of the auditory signal.*
(A) Schema of an auditory sound wave. (B) Representation of the ear compartments. Sounds enters the external ear and vibrates the tympanic membrane, the vibration will be amplified via the three bones of the middle ear into the cochlea. *Adapted from (Graven & Browne 2008) and (Zdebik et al. 2009).* (C) Schema of the cochlea organisation (D) Representation of the various cochlear components involved in the auditory signal transduction. (E) Schematic of the mechanical opening of channels in the hair cell. The movement of the basilar membrane induces the hit of the hair cell on the tectorial membrane, allowing for the necessary ion flux required for the polarisation of the cell and electrical transduction. (F) Representation of the tonotopic map and basilar membrane (BM) distortion along the cochlea. The rigidity of the basilar membrane increases along the cochlea causing a harder distortion at the apex *Adapted from (Peng & Ricci 2011) and (Reichenbach & Hudspeth 2010).*

1.1.1.2 The superior olivary complex

The superior olivary complex (SOC) is located in the brainstem, specifically in the pontine region. It plays a role in auditory processing and sound localization (Grothe & Park 2000). Comprising a group of nuclei, the superior olivary complex receives auditory information from both ears and integrates it to determine the direction and distance of sound sources. Through a process called binaural processing, it compares the differences in sound timing and intensity between the ears to create a three-dimensional representation of sound in space (Siveke et al. 2012). This information is then relayed to higher brain centres responsible for sound perception and interpretation. The superior olivary complex is a remarkable example of the brain's intricate mechanisms for processing auditory stimuli and enabling us to navigate our acoustic environment (Lopez-Poveda 2018, Haines & Mihailoff 2017).

Moreover, the SOC is described as the initial crucial step in the auditory analysis. Its functions include inducing auditory reflexes, alertness, and integration of auditory and visual cues (Haines & Mihailoff 2017). It has various feedback connections within itself and descending fibres to regulate peripheral processing and inputs (Grothe & Park 2000). Through a lateral efferent system, it projects to the inner hair cell, releasing dopamine to protect them from excitotoxicity. It also projects to the outer hair cell via the medial efferent system, although the exact role of this connection is unknown, it is believed to be related to the contractile state (electromotility) of the OHC (He 1997).

1.1.1.3 The inferior colliculus

The inferior colliculi are prominent structures located in the midbrain. They serve as important relay centres for auditory information, receiving inputs from the lower auditory nuclei, including the superior olivary complex and the cochlear nuclei (Paul et al. 2019); (Lee et al. 2015). The inferior colliculi play a crucial role in processing sound localisation, intensity, and frequency. They integrate and analyse the incoming auditory signals, contributing to the formation of auditory spatial maps and sound perception (Gruters & Groh 2012).

Moreover, the inferior colliculi are involved in the coordination of auditory reflexes, such as the startle response, by sending efferent projections to motor nuclei (Gruters & Groh 2012). These nuclei exhibit a tonotopic organisation, where different frequency ranges are represented along their anatomical axis. The external cortices of the inferior colliculus receive projections carrying low-frequency information, while the central nucleus receives projections carrying high-frequency information (Paul et al. 2019, Lee et al. 2015).

The output from the inferior colliculi is then relayed to higher auditory centres, such as the medial geniculate nucleus of the thalamus, for further processing and interpretation (Gruters & Groh 2012). They serve as convergence sites for auditory information from various sources and integrate non-auditory features into auditory processing, such as visual and somatosensory inputs (Bajo & King 2013).

1.1.1.4 The medial geniculate body of the thalamus

The medial geniculate body (MGB) is a structure located within the thalamus, which acts as a relay station for transmitting sensory information between various brain regions and the cerebral cortex (Bartlett 2013). Specifically, the MGB is involved in the processing of auditory information, receiving input from the inferior colliculus,

and relaying it to the auditory cortex for further processing and interpretation of sound (Kandler et al. 2009). The MGB is divided into several subregions, namely the ventral, dorsal, and medial divisions. The ventral division primarily receives input from the central nucleus of the inferior colliculus and is responsible for perceiving sound frequency and intensity. The dorsal division receives input from the dorsal nucleus of the inferior colliculus and analyses sound localization and spatial aspects. The medial division is connected with the limbic system and may contribute to emotional and memory-related aspects of auditory processing (Bartlett 2013, Lee 2013, Aizenberg et al. 2019). Each region is characterized by distinct neuronal cell-types, connectivity patterns, and functionalities (Bartlett 2013, Hackett, Barkat, O'Brien, Hensch & Polley 2011).

The ventral nucleus maintains the tonotopic map and projects predominantly to layer IV of the primary auditory cortex (Lee 2013). It plays a crucial role in auditory processing, preserving the organization of neurons based on their preferred frequencies. This nucleus receives input from the central nucleus of the inferior colliculus, enabling precise representation of sound frequencies in the auditory cortex. The dorsal division of the MGB, which is non-tonotopic, differs from the ventral division in terms of its information source. Unlike the ventral division, it does not receive input from the inferior colliculus. Instead, it receives input from layer 5 of the primary auditory cortex, indicating a potential alternate trans thalamic pathway for information transfer (Lee 2013, Lee & Sherman 2012). The medial MGB is a multimodal nucleus, receiving information not only from the auditory pathway but also from other sensory systems (Bartlett 2013). Subnuclear nuclei within the medial MGB have an important role in the preprocessing of auditory information, including reflex auditory information and multisensory integration (Bahmer & Gupta 2018).

1.1.2   The architecture of the AC

The auditory cortex is a complex network of neural structures located in the temporal lobe of the brain and is responsible for processing and integrating auditory information received from the ear (Graven & Browne 2008). The auditory cortex is organised hierarchically, with multiple areas that process auditory information at different levels of complexity (Rothschild et al. 2010, Read et al. 2002, Rauschecker & Scott 2009). The primary auditory cortex, also known as A1, is the first cortical area to receive input from the thalamus and is thought to be responsible for processing basic features of sound such as frequency, intensity, and duration (Graven & Browne 2008). However, several studies suggest that the computation in A1 is more specific than merely reporting auditory cues (King et al. 2018*a*, 2019). Beyond A1, multiple secondary and association areas process complex aspects of sound, such as spatial location, pitch, timbre, and speech perception (Rauschecker & Scott 2009). These areas include the posterior superior temporal gyrus, the superior temporal sulcus, and the middle temporal gyrus, among others.
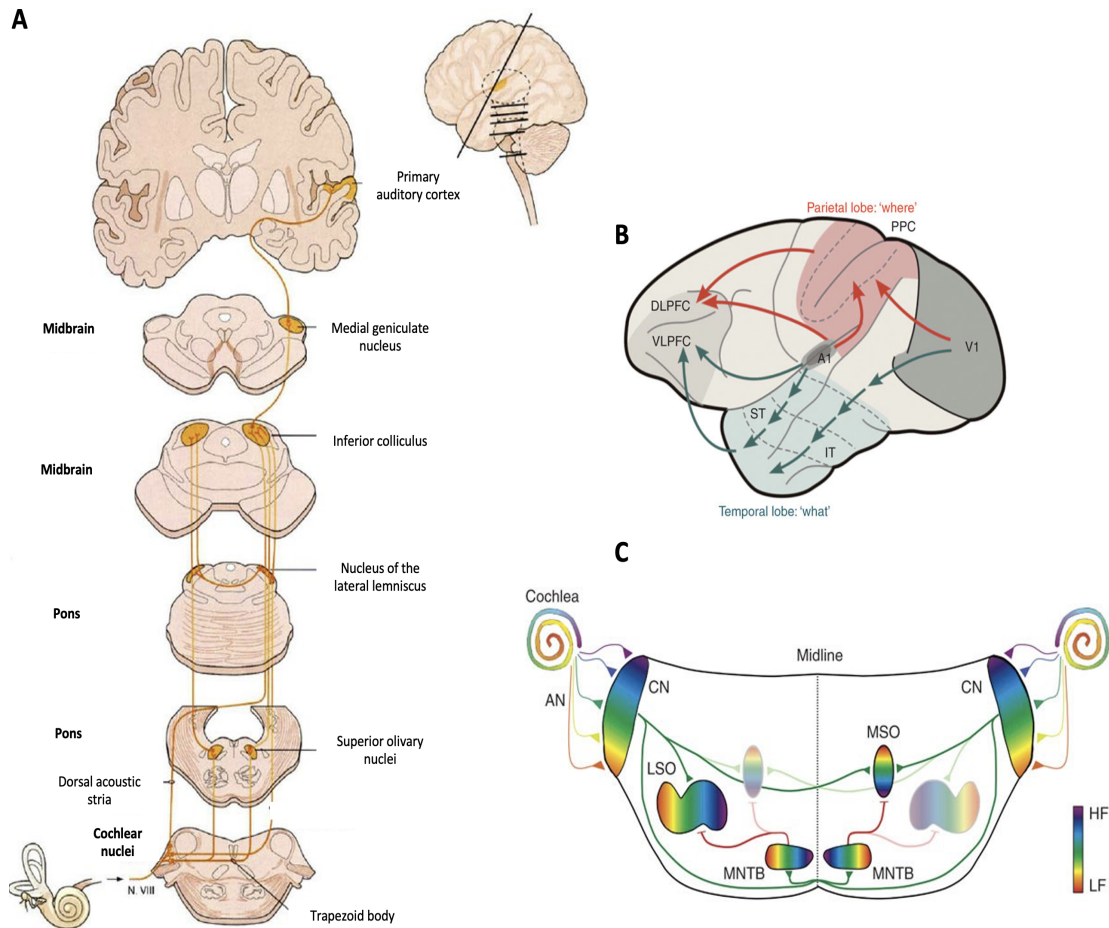
Figure 1.2: *The auditory pathway*

(A) The auditory pathway *Adapted from (Graven & Browne 2008)*, (B) Example of auditory connection from the monkey auditory cortex A1 to the other brain regions (Rauschecker & Scott 2009). (C) The tonotopic map is kept all along the auditory pathway, monkey example (Kandler et al. 2009).

1.2 The auditory cortex AC

The auditory cortex is the part of the brain responsible for processing auditory information. The human auditory cortex (AC) is situated in the temporal lobes and encompasses Heschl's gyrus (Brodmann 41/2) (Figure 1.2. A). The AC exhibits extensive connectivity with other brain regions, playing a crucial role in modulating various cognitive functions (Bizley 2017, Gage & Baars 2018, Grosso et al. 2015). In primates, two major pathways are commonly described: the "What" pathway, which connects the auditory cortex to the Wernicke area and dorsal regions involved in the semantic processing of pitch and words, and the "Where" pathway, which connects the Broca area and frontal regions associated with motor functions related to speech articulation, such as movements of the lips, jaw, tongue, and larynx (Figure 1.2. B). It is also interconnected with other brain areas such as the visual cortex, hippocampus, and basal forebrain (Aizenberg et al. 2019).

Auditory processing extends beyond the mere perception of sound and encompasses essential aspects of various life behaviour, including learning (associative and emotional), memory, attention, and emotion (Froemke & Jones 2011, Bahmer & Gupta 2018, Heilbron & Chait 2018, King et al. 2018b). This broad spectrum of activities

emphasises the significant impact of hearing and impaired audition on the autonomy and well-being of individuals and our society.

1.2.0.0.1 The tonotopic map The auditory cortex exhibits a well-organised structure characterised by the formation of tonotopic maps, which refer to the spatial arrangement of neurons based on their preferred frequency or pitch selectivity. This fundamental organizational principle was first described in the work by (Brewer & Barton 2016). Within these tonotopic maps, neurons are grouped according to their frequency-tuning properties. Neurons responsive to low frequencies are clustered in one designated area, while neurons sensitive to high frequencies are situated in another distinct area. This topographic arrangement allows for the efficient processing of different frequency components within complex auditory stimuli, such as speech and music, as highlighted in the study by (Gage & Baars 2018). The tonotopic map can be visualized as a gradient, with low frequencies represented in one region and high frequencies in another (Brewer & Barton 2016). The arrangement of the tonotopic map may differ among species (Ehret 2009, Humphries et al. 2010, Langers & van Dijk 2012, Rothschild et al. 2010), and can even vary within the same species. However, a structured anterior-posterior axis is typically observed in humans, as documented by (Ehret 2009). In mice, the auditory cortex is made up of five primary regions: the primary auditory cortex (A1), anterior auditory field (AAF), ultrasonic field (UF), secondary auditory cortex (A2), and dorsoposterior field (DP). Notably, A1 and AAF in mice demonstrate distinct tonotopic organization. In A1, neurons primarily located in the posterior part of the area are responsive to low frequencies, while those in the anterior region are attuned to high frequencies. Conversely, AAF exhibits an inverted tonotopic organization, where the anterior portion shows sensitivity to low frequencies and the posterior region responds to high frequencies (Stiebler et al. 1997). However, this tonotopic map has been challenged since (Hackett, Rinaldi Barkat, O'Brien, Hensch & Polley 2011, Guo et al. 2012), suggesting that it primarily represents a rostrocaudal axis (Hackett, Rinaldi Barkat, O'Brien, Hensch & Polley 2011).

1.2.0.0.2 Layers Like other sensory cortices, the auditory cortex is structured into a succession of layers, each composed of a unique organization of neurons (sparse/compact density, cell type) within a thickness of only a few millimetres (ranging from 1-4.5 mm in humans) (Figure 1.3. ABD) (Fischl & Dale 2000). These layers exhibit high interconnectivity among themselves and with other brain areas. The specific nature and connectivity of neurons define the characteristics of each layer (Figure 1.3. C). Layer I, the most dorsal or top layer, is sparsely populated with a predominance of inhibitory neuron types (Linden & Schreiner 2003). Layers II and III are densely populated and comprise a mixture of inhibitory and excitatory neurons. They exhibit extensive interconnections and house major cortico-cortical connections. Layer IV, also known as the granular layer, serves as the primary input site for the thalamic input. Layer V consists of large pyramidal neurons with axons projecting to subcortical areas (MGB and IC) for feedback. Unlike other sensory cortices, the dominant spiny stellate cell are absent in this layer of the auditory cortex, being replaced by small pyramidal cell (Smith & Populin 2001). Finally, layer VI predominantly consists of smaller cell bodies and primarily functions by providing feedback to the thalamus (Linden & Schreiner 2003). Ascending fibres from the MGB form synapse with the cell of layer IV, which then project to the pyramidal neurons in layer III. From there, information is distributed to the other layers (I, II, IV, and V) as well as to the

contralateral auditory cortex via the corpus callosum (distinct from other sensory cortices). Layer I neurons project to layer II, which, in turn, connects layers V and VI. Pyramidal neurons in layers V and VI have efferent axons that provide feedback to the MGB and the inferior colliculus (Linden & Schreiner 2003, Rothschild et al. 2013).
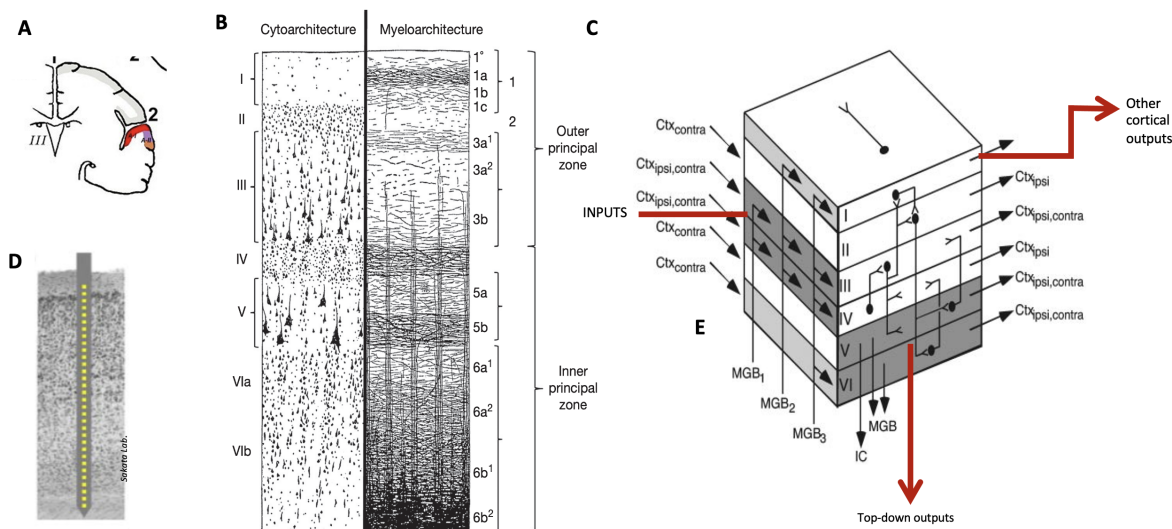
Figure 1.3: *The auditory cortex architecture.*
(A) The auditory cortex is located on the superior temporal gyrus of the temporal lobe. *Adapted from (Palomero-Gallagher & Zilles 2019)* (B) Generalized scheme of cortical layers comparing between cytoarchitectonic and myeloarchitectonic lamination patterns in the isocortex *Adapted from (Palomero-Gallagher & Zilles 2019)*. Note that this is not the auditory cortex but a representation of the isocortex. (C) Auditory cortex laminar architecture and organisation. The red arrows represent the direction of the information flux *Adapted from (Linden & Schreiner 2003)*. (D) Representation of the probe insertion into the auditory cortex (Sakata & Harris 2009).

1.2.1 Cellular specificities in the AC

Diverse cell-types have been characterised in the auditory cortex (AC) based on various criteria, including neurotransmitter expression, morphological features, and patterns of connectivity (Studer & Barkat 2022, Edeline et al. 2001, Atencio & Schreiner 2008).

As a quick reminder, neurons are polarised cell, with a difference in ion concentration between their intracellular and extracellular environments, resulting in a negative membrane potential (typically around -70mV). This resting membrane potential is maintained by the selective permeability of the neuronal membrane to different ions, such as potassium (K+), sodium (Na+), and chloride (Cl-) (Pivovarov et al. 2019). When a neuron receives inputs from afferent neurons, these inputs can either depolarise or hyperpolarise the membrane potential. The integration of excitatory postsynaptic potentials (EPSPs) and inhibitory postsynaptic potentials (IPSPs) at the soma adheres to the principle known as the "all-or-nothing" law, as elucidated by Nishi et al. (1973) in their intracellular studies (Nishi & North 1973). According to this principle, depolarisation must surpass a specific threshold to elicit an action potential. Depolarization occurs when excitatory inputs increase the membrane potential, bringing it closer to the threshold for generating an action potential. On the other hand, hyperpolarisation happens when inhibitory inputs decrease the membrane potential, making it more negative and further from the threshold (Llinás 2014, Bean 2007). This process of synaptic transmission occurs at the synapses, which are specialized junctions between

neurons. At the synaptic terminals, the action potential triggers the release of neurotransmitters, and chemical messengers, into the synaptic cleft. These neurotransmitters then bind to receptors on the postsynaptic membrane of the next neuron (Südhof & Malenka 2008). This binding triggers a cascade of cellular events, including the opening of ion channels and the generation of postsynaptic potentials (Südhof & Malenka 2008).

One way to classify auditory cortical neurons is based on their neurotransmitter profile. GABAergic neurons, which release inhibitory neurotransmitters, such as gamma-aminobutyric acid (GABA), constitute an important cell type in the AC. These inhibitory neurons play a crucial role in regulating the excitability and information processing within the auditory circuitry (Llinás 2014, Tremblay et al. 2016). They exert inhibitory control over neighbouring neurons, shaping their responses, and contributing to the precise temporal and spatial processing of auditory signals (Figure 1.4. ACD) (Studer & Barkat 2022, Tremblay et al. 2016). Excitatory neurons release excitatory neurotransmitters, glutamate, which activate postsynaptic receptors in target neurons, thereby promoting the transmission of signals. Excitatory neurons can exhibit diverse morphological features, including pyramidal cell, with their characteristic pyramid-shaped soma, which are the predominant cell type for excitatory signal transmission in mammalian brains (Douglas & Martin 2004). Excitatory cell are around 75% of the cortical cell population and are mostly pyramidal cell (soma that presents a pyramidal shape), these pyramidal cell are particularly abundant in the AC and are considered a fundamental component of the cortical circuitry (Alreja et al. 2022). In addition to neurotransmitter and morphology, the connectivity patterns of auditory cortical neurons also contribute to their classification (Blackwell & Geffen 2017, Upadhyay et al. 2008). Neurons in the AC exhibit intricate synaptic connections, forming local microcircuits and establishing long-range projections with other brain regions involved in auditory processing,(Blackwell & Geffen 2017). These connectivity patterns enable the integration and transformation of auditory information across different hierarchical levels of the auditory system.

The activity modulation of AC neurons is manifested through the spectro-temporal receptive field (STRF), a quantitative representation that delineates the temporal dynamics and optimal frequency response of neurons in response to specific stimuli. The STRF serves as a crucial instrument for investigating the frequency selectivity of auditory cortex neurons, offering valuable insights into their receptive properties and functional characteristics. (Atencio & Schreiner 2008, Atencio et al. 2009). It characterizes the spatiotemporal pattern of neural responses to different frequencies of sound over time and describes the specific timing and frequency components that elicit the strongest responses from individual neurons. By examining the STRF of a neuron, insights can be gained into its preferred frequency range, and temporal integration windows. Moreover, the STRF is not static and can be modified through experience and learning (Eggermont 2006). Plasticity in the auditory cortex allows the STRF to adapt and refine its selectivity based on the specific auditory inputs it receives over time. This plasticity contributes to the brain's ability to recognize and discriminate between different sounds, including speech, music, and environmental sounds,(Eggermont 2006, Atencio et al. 2009).

In essence, the STRF provides a quantitative representation of how neurons in the auditory cortex are tuned to different frequencies and how their responses vary with changes in the temporal dynamics of the stimuli (Eggermont 2006). Notably, inhibitory neurons play a crucial role in shaping the boundaries of the excitatory receptive field (Figure 1.4. A) (Tremblay et al. 2016). During the developmental stages, the presence and proper functioning

of inhibitory neurons are essential for refining the STRF of excitatory neurons. Studies have shown that the absence or reduced activity of inhibitory neurons can lead to a broadening of the STRF of excitatory neurons (Froemke & Jones 2011, Pernia et al. 2020, Nishimura et al. 1999). Inhibitory neurons contribute to the establishment of tonotopy and the narrowness of excitatory STRF, which determines their selectivity and specificity. Additionally, the balance between excitatory and inhibitory activity plays a crucial role in regulating the duration of the critical period for plasticity (Froemke & Jones 2011).

1.2.1.0.1 Inhibitory neurons in the auditory cortex Advances in experimental technology are starting to shed new light on the mechanisms underlying the inhibitory auditory spectro-temporal receptive field (STRF) (Moore & Wehr 2013, Sadagopan et al. 2023). Optogenetic manipulation of parvalbumin (PV) neurons in adult mice have provided insights into how inhibitory neurons continue to narrow and control the borders of receptive fields in adult auditory cortex (AC) neurons (Moore & Wehr 2013). Activation of PV neurons using ChR2 increases the signal-to-noise ratio of excitatory sound-evoked responses, reduces spontaneous excitatory activity, and results in a narrower STRF (Blackwell & Geffen 2017). These findings suggest that inhibitory neurons in adult individuals shape the selectivity and acuity of excitatory neurons' STRF (Hamilton et al. 2013a). Furthermore, the role of inhibitory neurons extends to animal behaviour , as the accuracy of successful behaviour in response to specific frequency sound presentations is correlated with the magnitude of PV tone-evoked responses rather than excitatory responses (Aizenberg et al. 2015). Inhibitory neurons exhibit several dimensions of connectivity, including inter-columnar and interlayer connections, which affect the excitation of pyramidal cell in different ways (Figure 1.4. A-C). These important connectivity patterns, combined with their numerous subtypes and distinct morphologies, (Figure 1.4. E), inhibitory neurons as key contributors to network shaping and circuit computation. Based on molecular markers, three major subtypes of inhibitory neurons have been identified: the calcium-binding protein parvalbumin (PV) group, the neuropeptide somatostatin (SOM or sst) group, and the ionotropic serotonin receptor (5HT3aR). Each subgroup contains multiple subgroups within itself (Tremblay et al. 2016). While the relationship between these markers and neuron functionality lacks clear causality, the three groups do not overlap and exhibit specific localisation and morphology (Figure 1.4. B).

In the auditory cortex, these inhibitory neurons are predominantly localized in layers IV and V for PV cell, and in layers V and VI for SOM cell (Tremblay et al. 2016) (Figure 1.4. B). PV neurons appear to play a crucial role in narrowing down specific sensory inputs into the cortex (bottom-up processing). They receive more connections from the medial geniculate body ventral division (MGBv) compared to excitatory neurons ((Hamilton et al. 2013a)). Optogenetic activation of PV neurons increases the connectivity between MGBv and Layer IV as well as columnar connectivity. However, PV neurons do not seem to have an impact on sensory expectation (top-down processing) since they do not alter interlayer connections or feedback connectivity (Hamilton et al. 2013a). This emphasises the role of PV neurons in the specificity of neuronal responses and neural selectivity (Hamilton et al. 2013a).

SOM inhibitory cell also influence the spectro-temporal receptive field (STRF) and excitatory responses. Studies on the neocortex and other sensory cortices provide insights into the distinct inhibitory behaviour of SOM and PV neurons. PV neurons predominantly target the axon initial segment of neurons, while SOM neurons exhibit

more dendritic targeting (Li et al. 2015, Wang et al. 2004, Tremblay et al. 2016). The temporal response is a major difference between these neuron types: PV neurons, especially basket cell types, exhibit fast conduction, inducing postsynaptic inhibition currents approximately 0.7ms after an action potential, and they have a narrow refractory period ((Tremblay et al. 2016)). This allows PV neurons to function as coincidence detectors (Rossignol et al. 2013, Tremblay et al. 2016). In contrast, SOM response is longer with two interesting features: prolonged spiking and the induction of short-term memory (facilitation) in targeted neurons, enabling them to facilitate summation and decrease the weight of required inputs (Tremblay et al. 2016), (Figure 1.4. C). However, the distinct effects of SOM and PV neurons on the auditory cortex are still unclear (Ekdale 2016, Rozycka & Liguz-Lecznar 2017).

Overall, the complete description of the auditory canonical cortical circuit is still in debate (Sadagopan et al. 2023). Several reviews aim to enhance understanding and develop neurocomputational models by incorporating a vast amount of data, neuronal sub-types, and connectivity (Rozycka & Liguz-Lecznar 2017) (Tremblay et al. 2016) present three working areas: anatomical tracing to improve understanding of connections, cortical slice preparations to highlight connectivity features, and optogenetic methods to selectively target specific cell types and observe their impact on global circuit activity. They discuss the laminar distribution of inhibitory neurons in coding, with sparse coding observed in layer (L) 2/3 of pyramidal cell (PCs) and dense coding in larger L5 PCs. Top-down feedback from the cortex to the thalamus can increase the spiking probability of individual cortical neurons and/or increase the number of neurons responding to a stimulus (Linden & Schreiner 2003). This facilitates specific responses by enhancing efficiency and reducing noise. Recurrent excitation can also prolong sensory responses and increase the temporal windows for various interactions. These properties can give rise to complex sound analysis or be associated with other cognitive functions such as attention or memory (Ohyama et al. 2020, Nelken et al. 1999a, Kerlin et al. 2010).
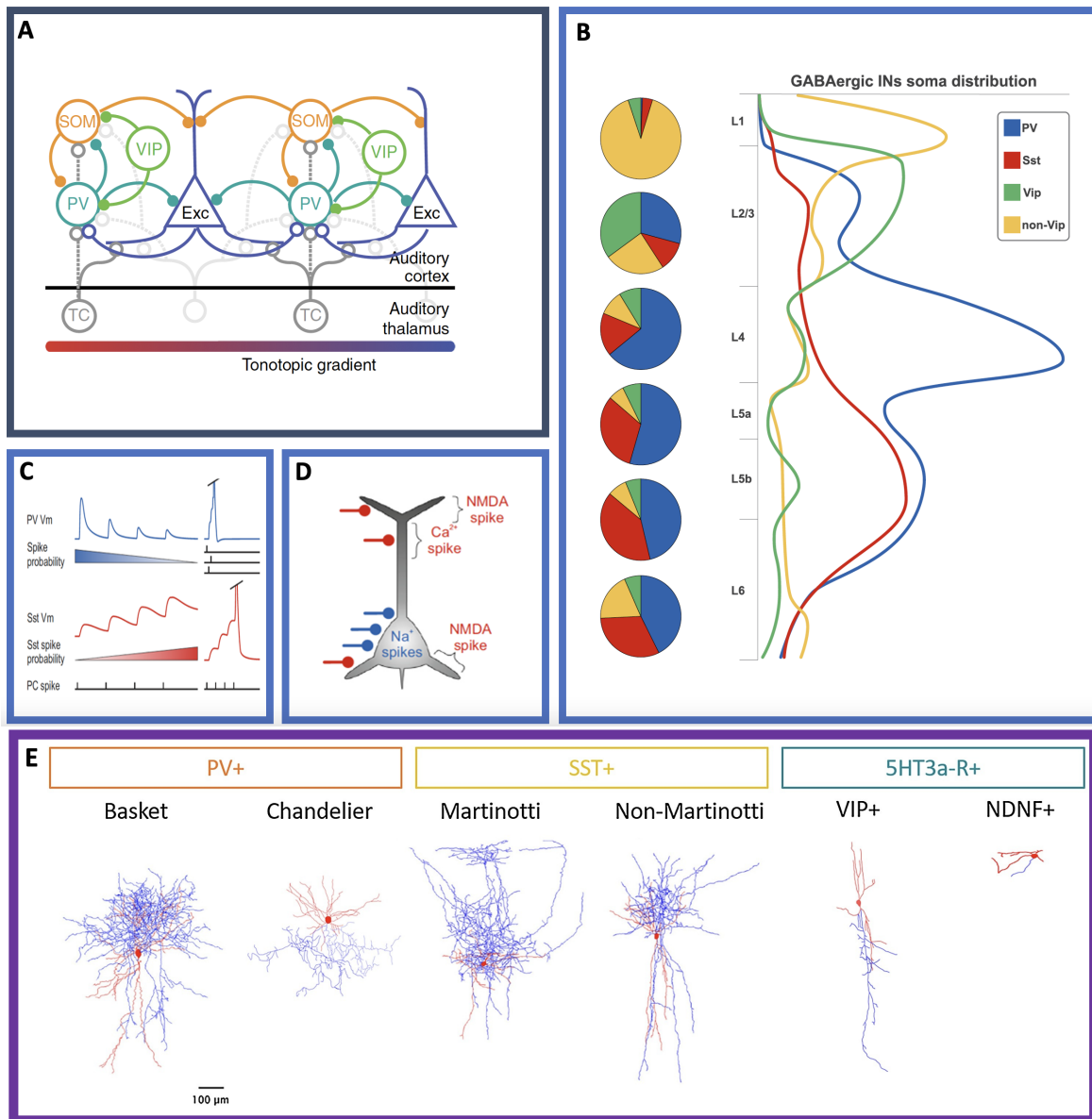
Figure 1.4: *Inhibitory neurons*
(A) Schema of the auditory network along the AC tonotopic gradient. Inhibitory cell narrow the excitatory cell activity to respond to a particular auditory stimulation. (B) The laminar distribution of the inhibitory cell types along the auditory cortex depth. (C) Differences in the membrane potential and the spiking probability of the PV and the SOM (SST) neurons to the excitatory cell (PC) activity. (D) Schema representing the different synaptic points between the excitatory cell and inhibitory major cell types. PV neurons (blue) contact the soma of the PC cell where the SOM contacts the tree. (E) Representation of the majors inhibitory sub-types morphology. *Adapted from (Tremblay et al. 2016, Studer & Barkat 2022)*

1.2.2   Representation of sounds in the auditory cortex

1.2.2.1   Pure tones and natural sounds

Natural sounds and pure tones stimulate the auditory system in different ways, resulting in different neural responses in the brain (Theunissen & Elie 2014). Natural sounds, such as speech or music, have complex, non-

uniform waveforms that contain multiple frequencies and temporal patterns (Feng & Wang 2017, Nelken et al. 1999*a*, Bielczyk et al. 2020, Destexhe et al. 1999). These complex sounds are processed differently in the auditory cortex compared to pure tones (Theunissen & Elie 2014). Neurons in the auditory system demonstrate selective responses to distinct acoustic features present in natural sounds (Montes-Lourido et al. 2021). When a complex sound is presented, different neurons in the auditory cortex respond selectively to different frequency components of the sound (Gage & Baars 2018). These features include specific frequencies, harmonics, and temporal modulations. The timing of the action potentials in the auditory neurons can also encode important temporal features of natural sounds, such as the duration and onset of different sounds. The precise timing of the action potentials can be used to distinguish between different sounds that have similar frequency content, such as different musical instruments playing the same note. This selective response allows the auditory cortex to encode and analyse the different acoustic features of the natural sound, such as pitch, timbre, and rhythm, which are important for speech and music perception (Leaver & Rauschecker 2010). Several types of activity can occur in the auditory cortex, depending on the nature of the stimulation and/or the cognitive processing of the brain. For example, when we listen to music, different parts of the brain become active depending on the pitch, timbre, and rhythm of the music, and different cognitive states could be involved such as memory and emotions (Sanju & Kumar 2016, Gage & Baars 2018). Similarly, when we attend a conversation in a noisy room, the activity in the auditory cortex needs to adapt and be focused and selective to the information of interest (Haykin & Chen 2005).

1.2.2.2 Noisy background and attention

Noisy background refers to the presence of unwanted sounds or interferences that can mask or distort the desired auditory signals. These noises can come from various sources, such as other people talking, traffic, machinery, or even internal body sounds. The auditory system has evolved to be remarkably adept at filtering out irrelevant noise and focusing on relevant sounds. The auditory cortex employs several mechanisms to encode and process auditory information in the presence of noisy backgrounds (Haines & Mihailoff 2017). For example, spectral and temporal filter processing is used by the auditory cortex to analyse the spectral content (different frequencies) and temporal patterns (timing) of sounds to change their sensitivity to sounds (Young 2008, Willmore et al. 2014). This information allows us to distinguish between different sound sources and extract meaningful auditory features, even in the presence of noise (Bizley & Cohen 2013). By selectively attending to specific frequency ranges or temporal cues, the cortex can enhance the perception of desired sounds.

In a noisy environment, our brains need also to extract relevant auditory information from the background, such as the sound of someone's voice (Willmore et al. 2014). When we attend to a particular sound in a noisy environment, such as a conversation, the activity in the auditory cortex becomes more focused and selective,(Willmore et al. 2014). This implies that neurons in the auditory cortex are specifically tuned to the sound of the individual's voice, whereas neurons tuned to other sounds in the surrounding environment undergo decreased activity,(Bizley & Cohen 2013, Willmore et al. 2014). Several hypotheses claim that this is permitted by the temporal structure difference between pitch or music compared to the noisy environment (Laffere et al. 2020*a*). Or by the release of neuromodulators, such as dopamine and norepinephrine, which can increase the sensitivity of neurons in the

auditory cortex to the attended sound (Noudoost & Moore 2011). Another mechanism is the suppression of the neural response to irrelevant sounds. This can occur through inhibitory connections between neurons in the auditory cortex, which can reduce the activity of neurons that are tuned to irrelevant sound (Studer & Barkat 2022, Zhang et al. 2018). Overall, the increased focus and selectivity of auditory cortex activity during selective attention is a critical component of our ability to communicate in noisy environments. It allows us to better extract the relevant information from complex auditory scenes and is an important aspect of our ability to understand speech and engage in conversation.

At the cellular level, the challenge of hearing or extracting sound from a noisy environment due to hearing loss results from damage to the hair cell (Jeng et al. 2020, Herrmann & Butler 2021, Spongr et al. 1997). These damaged cell disrupt the quality of the pattern of activity sent to the brain, affecting our ability to perceive speech in noisy surroundings. For example, in addition to linearly encoding frequency information, the OHC play a crucial role in amplifying or suppressing the activity of other frequency-sensitive cell (Lesica 2018). This distortion in signalling is vital for accurate speech perception in noisy environments (Moore 2016).

1.2.2.3   Top-down effect on hearing

As previously mentioned, the activity in the auditory cortex can be modulated by bottom-up processes, specifically the physical characteristics of the sound stimulus (Hamilton et al. 2013b). The auditory cortex plays a significant role in fundamental auditory processing tasks, including the detection of tones and discrimination of frequencies (Atencio et al. 2009, Bitterman et al. 2008, Carcea et al. 2017). For instance, factors like the loudness and duration of a sound shape the AC neuronal activity, resulting in variations in the perception of the sound (Thwaites et al. 2016). Another important aspect of auditory cortex activity is how it is influenced by top-down processes, such as attention, expectation, and memory (Axelrod et al. 2022). Anticipatory expectations can shape the sensitivity of neurons in the auditory cortex to particular auditory stimuli. For instance, when we expect to hear a specific sound, such as a particular word in a sentence, the neurons representing that sound in the auditory cortex may exhibit increased sensitivity, resulting in decreased reaction time (Chait et al. 2010) Attentional mechanisms also play a significant role in modulating auditory cortical activity. When we selectively attend to one sound while disregarding others, the activity in the auditory cortex becomes more focused on the attended sound, enhancing its representation and processing (Jaramillo & Zador 2011). These cognitive factors contribute to the dynamic modulation of neuronal responses in the auditory cortex, allowing for efficient auditory perception and cognitive processing.

1.2.2.4   Effect of peripheral impairments on the central auditory processing

Peripheral impairment, such as dysfunction of the hair cell, has a significant impact on central auditory processing (Michalski & Petit 2022). The altered signals that reach the brain due to deficits in the peripheral auditory system result in changes in how the auditory cortex processes sound (Michalski & Petit 2022, Lesicko & Llano 2017). A common consequence of peripheral impairment is a reduction in neural responses to sound, leading to a decreased ability to discriminate between similar sounds, particularly those with high-frequency components (Ichimiya et al.

2000, Khullar & Babbar 2011, Del Campo et al. 2012). It could induce distortion in the sent signal from the cochlea to the brain (Lesica 2018). In addition, peripheral impairment can also impact the temporal processing of auditory information. Timing cues, such as the ability to detect rapid changes in sound and perceive the temporal order of auditory events, may be compromised in individuals with peripheral hearing loss (Ichimiya et al. 2000, Harris & Shepherd 2015). This can lead to difficulties in speech perception and the perception of complex auditory stimuli. Presbycusis, associated with age-related hearing loss, can also affect sound localisation and speech understanding in noisy environments (Mazelová et al. 2003, McFadden & Willott 1994).

Furthermore, peripheral impairment can impact the cortical architecture itself, as observed in deaf cats with reduced grey matter and thicker layer 4 (Grégoire et al. 2022). To compensate for the reduced peripheral input, the central auditory system undergoes plastic changes, such as an increase in the size and number of receptive fields in the auditory cortex and modifications in the tuning properties of auditory neurons (Willmore & King 2023, Jiang et al. 2017, Jeng et al. 2020). These changes aim to enhance the remaining sensory input and improve auditory information processing. However, they can also contribute to the development of abnormal neural activity patterns associated with conditions like tinnitus, hyperacusis, and other auditory perceptual disorders (Chen et al. 2015).

Moreover, the effects of peripheral impairment are not limited to the auditory system alone but affect other brain processing such as visual and somatosensory inputs, through cross-modal plasticity (Meredith & Lomber 2011, Kral & Sharma 2023). Individuals with hearing loss may exhibit alterations in visual processing (Chia 2006), including heightened sensitivity to visual motion or improved visual attention, as the brain compensates for reduced auditory input (Opoku-Baah et al. 2021). Research has shown that hearing loss can have wide-ranging consequences on cognitive function and overall brain health (Wang et al. 2022). It has been associated with an increased risk of cognitive decline, dementia, and cognitive impairment in older adults (Akiguchi et al. 2017). The mechanisms underlying this relationship are still being investigated, but it is believed that the sensory deprivation caused by hearing loss may contribute to cognitive decline through reduced cognitive stimulation and increased cognitive load during speech comprehension (Powell et al. 2022).

Overall, the impact of peripheral impairment on central auditory processing extends beyond the immediate effects on sound perception. It encompasses alterations in spatial localisation, speech understanding, cortical architecture, cross-modal plasticity, temporal processing, and cognitive function. Understanding these complex interactions is crucial for developing effective interventions and rehabilitation strategies for individuals with auditory impairment.

1.3 The ageing brain and audition

1.3.1 The ageing brain

Ageing is an inevitable process that leads to deficits in various brain functions. As the brain ages, cognitive functions become impaired. Ageing is associated with brain atrophy, an increase in the accumulation of oxidative molecules, a decrease in adaptive stress responses, deregulation of calcium homeostasis, inflammation, metabolic perturbations, and loss of synaptic connectivity (Markocsan et al. 2009, Altena et al. 2010, Price et al. 2017, Wang et al. 2011, Morrison & Baxter 2012, Rozycka & Liguz-Lecznar 2017, Jayakody et al. 2018, Mattson & Arumugam

2018, Herrmann et al. 2019). The brain undergoes atrophy and accumulates small lesions. Both white and grey matter are affected (Blinkouskaya et al. 2021). With ageing, various cognitive functions decline, such as working memory, inhibitory function, and long-term memory (Pelvig et al. 2008, Henry et al. 2017, Jayakody et al. 2018, Murman 2015). Performance on related tasks progressively declines with age, while response timing increases (Woods et al. 2015). However, not all functions are equally affected by ageing, as simple tasks and semantic memory tend to remain stable with age (Murman 2015). The white matter, which surrounds certain neurons and enables rapid action potential conduction, is particularly affected. The degradation of this lipid membrane has been identified as a major contributor to temporal impairment in neural networks (Hirrlinger & Nave 2014). This degradation affects the temporal signalling between neurons, which is a crucial component of neural communication (Mattson & Magnus 2006, Zimmerman et al. 2021). Neuronal timing operates on a millisecond scale. If neuron A receives information from neurons B and C within a specific time window to relay signal X, the transmission of the signal may be hindered if the reception from B or C is delayed. This principle is known as coincidence (Murman 2015). Sensory perception and processing speed are then affected. However, not only with matter is affected by ageing, but grey matter too (Price et al. 2017). The neurons' proprieties and integration of the signal are highly affected in age-related diseases and healthy patients (Mattson & Magnus 2006). For example, the amplitude and latency of auditory evoked responses change with age (Clinard & Cotter 2015, Henry et al. 2017, McNair et al. 2019), an increase in stereotype response has also been observed (Henry et al. 2017), and alterations in the frequency spectrum of brain states are linked to ageing (Waschke et al. 2017, Al Zoubi et al. 2018). These suggest a potential systematic age-related change in brain state that affect underlying perceptual processes.

1.3.1.1 The ageing brain and the auditory pathway

The ageing process affects the anatomical and chemical features of the auditory pathway. At each specific step of the auditory pathway, different age- related processes are occurring (Jayakody et al. 2018). In the cochlea, the hair cell are generated during the first trimester of development and are required to survive for the lifetime of the person. Regeneration does not occur after the loss of hair cell in the mammalian auditory system (Kwan et al. 2009). With age, the cochlea undergoes structural and functional changes. These changes include the loss of sensory hair cell, which are crucial for detecting sound, and a decrease in the number of neurons in the auditory nerve. These changes can result in a reduction in the sensitivity to high-frequency sounds. At the subcortical level, the levels of GABA in the inferior colliculus and superior olivary complex decrease with ageing, particularly in cases of presbycusis pathology (Caspary et al. 2008, Ouda & Syka 2012, Caspary et al. 1995). The measurement of auditory subcortical signals, known as auditory brainstem responses (ABRs), demonstrates impaired temporal processing of rapid acoustic stimuli in older adults (Walton et al. 1999, Burkard & Sims 2001, Anderson et al. 2013, McKay et al. 2013).

In the auditory cortex, there is also a decrease in the number of parvalbumin (PV) positive neurons (Rogalla & Hildebrandt 2020). While subcortical areas are affected by slowness, the auditory cortex plays a crucial role in processing temporally structured stimuli, particularly in frequency-modulated (FM) sweep discrimination (Ohlemiller et al. 2016, Mendelson & Ricketts 2001). The selectivity of auditory cortex neurons for fast FM sweeps decreases

with age, whereas such changes are not observed in the thalamus or midbrain. Changes in the central auditory system may be attributable to the effects of the loss or attenuation of neural input from an impaired peripheral auditory system (Howarth & Shone 2006). Individuals worldwide follow a "hearing health trajectory" from birth, influenced by environmental conditions and experiences that shape their biological systems, including the auditory system, with ongoing exposures and genetic factors determining diverse outcomes in hearing health even when initial audiometric thresholds appear similar (Davis et al. 2016). Despite pioneering research on the ageing auditory system, we did not find a lot of papers describing how ageing affects the auditory pathway but rather how age-related hearing loss diseases affect it.

1.3.2 Age-related hearing loss

1.3.2.1 The presbycusis

Age-related hearing loss, also known as presbycusis, is a significant public health issue, affecting approximately one-third of the global population over the age of 65 (Khullar & Babbar 2011). It is characterised by a gradual loss of hearing, particularly in the ability to discriminate high frequencies, and weak sounds, and extract sound from a noisy background. This decline in auditory discrimination can lead to misunderstandings, social isolation, and in severe cases, hallucinations, and dementia (Lomber 2017, Jayakody et al. 2018). People with the disorder experience difficulties in conversation, music appreciation, orientation to alarms, and participating in social activities (Mazelová et al. 2003). The major complaint of patients with presbycusis is not the incapacity to hear but rather the difficulty in understanding what is being said (Gates & Mills 2005).

Presbycusis is influenced by a combination of genetic and environmental factors, such as exposure to noise over time and certain medications (Holley 2005). Several risk factors for presbycusis were reported such as noise exposure, smoking, medication, hypertension, and family history (Gates & Mills 2005). Individuals who have significant exposure to workplace noise, recreational noise, and firearms are more prone to experiencing high-frequency hearing loss. The widespread occurrence of presbycusis has made hearing difficulties a prevalent concern in both social and health contexts (Mazelová et al. 2003). The severity of hearing problems can vary considerably at any age and among individuals based on socioeconomic factors and genetic factors (Wang & Puel 2020). Industrialized societies generally exhibit poorer hearing levels compared to isolated or agrarian societies (Gates & Mills 2005). Consequently, presbycusis can be understood as a complex interplay between auditory stresses, otological diseases, and the intrinsic, genetically regulated ageing process.

It can be characterised by the degeneration of the organ of Corti (sensory presbycusis), the spiral ganglion (neural presbycusis), and/or the stria vascularis (metabolic presbycusis) (Mazelová et al. 2003). The most significant age-related hearing changes occur in the cochlea, where a decline in the population of OHC and IHC leads to peripheral changes. Both OHC and IHC are affected by the presbycusis (Wu et al. 2020), where the IHC sensibility decreases affecting the encoding of sounds and the OHC amplification of sound is impaired (Peelle & Wingfield 2016, Spongr et al. 1997). As individuals age, there is a specific loss of OHC at the basal end of the basilar membrane, which is responsible for processing high-frequency sounds (Oghalai 2004). In addition to hair cell loss, both age-related changes and exposure to loud noise can weaken cochlear afferent nerve terminals, even without

the loss of hair cell or a long-term shift in hearing threshold (Liberman 2017, Kujawa & Liberman 2015, Peelle & Wingfield 2016). This type of cochlear dysfunction is commonly known as "hidden hearing loss" because it cannot be detected through standard pure-tone audiometry. Hidden hearing loss has been linked to difficulties in encoding near-threshold sounds (Valderrama et al. 2022, Plack et al. 2014) and auditory attention (Peelle & Wingfield 2016, Plack et al. 2014).

In addition to the cochlea, age-related alterations occur in multiple components of the auditory system, including spiral ganglion neurons (Elliott et al. 2022, Bao & Ohlemiller 2010), cochlear nuclei (Dublin 1982, Gray et al. 2014), the superior olivary complex (Vicencio-Jimenez et al. 2021), and other midbrain structures extending to the inferior colliculus (Engle et al. 2014, Caspary et al. 1995, McFadden & Willott 1994). These changes in the auditory brainstem have an impact on the ability to process temporal information (Walton et al. 2002, Peelle & Wingfield 2016, Strouse et al. 1998). These age-related differences in temporal processing are closely linked to impaired speech perception (Walton 2010) and contribute significantly to the challenges faced in understanding speech during older adulthood (Pichora-Fuller & Singh 2006).

The effects of presbycusis on the cortex and how the cortex adapts to these disturbances are not well understood. This difficulty may arise from age-related changes in both peripheral and central auditory processes (Clinard et al. 2010, Anderson et al. 2013, Harris & Dubno 2017, Clinard & Cotter 2015), which can originate from a merge in the central and peripheral auditory structures (He et al. 2007, Jayakody et al. 2018). Changes in central cognitive could be due to age-related impacting the performance of older adults through top-down feedback mechanisms (Henry et al. 2017), involving impaired auditory cortex processing and reduced attention (Zanto & Gazzaley 2014, Schröger et al. 2015, Fuglsang et al. 2020). One commonly described effect of hearing loss is a decrease in inhibition, caused by changes in GABAergic and glycinergic neurotransmission throughout the brain (Tremblay & Miller 2014), with a particular decrease in the PV neurons number (De Villers-Sidani et al. 2010). Additionally, the plasticity resulting from hearing loss can impact the perception of speech in other ways, such as increasing the excitability borders (Kral & Sharma 2023) or reorganising tonotopic maps in the brain due to variations in hearing loss across frequencies (Koops et al. 2020).

The treatment of presbycusis, or age-related hearing loss, is of great importance due to its impact on individuals' quality of life. Despite the advancements and positive impact of hearing aids for patients, the currently available hearing aids are insufficient in fully restoring natural hearing and speech comprehension for patients (Lesica 2018). Therefore, it is crucial to investigate how the auditory pathway changes, also in the cortex as he is sharing connections with other brain areas creating the auditory scene understanding. Presbycusis affects various components of the auditory system, and understanding these changes can provide valuable insights into developing more effective interventions. Exploring the alterations in the cortex is essential for improving our understanding of the underlying mechanisms of presbycusis. By gaining insights into these changes, we may help to develop targeted approaches to enhance speech comprehension and restore natural hearing for affected individuals.

1.3.3 The ageing brain and brain oscillation

One particular impairment in the ageing neural system is the decline in temporal activity, which leads to a communication problem due to slower processing. However, a study suggests that the slowness observed in the

auditory cortex, unlike the visual cortex, is due to an unknown phenomenon in the grey matter rather than the white matter (Price et al. 2017). In addition to the slowness, the aged brain exhibits a widespread pattern of activity compared to young adults (Poulisse et al. 2020, Cabeza 2002). One hypothesis is that this diffuse, activity reflects the decline in neural efficiency and dedifferentiation of brain areas in the aged population (Lindenberger & Baltes 1997, Wingfield & Grossman 2006). Another hypothesis is that the aged brain requires the increased engagement of brain regions to compensate for the neurocognitive decline (Grossman et al. 2002, Wingfield & Grossman 2006, Shafto & Tyler 2014).

Brain oscillatory activity is also impaired with ageing, typically characterised by an overall flattening of the EEG signal frequency spectrum (McNair et al. 2019). EEG components show smaller amplitudes and increased latency of sentence comprehension in older adults. The global power spectrum (PSD) amplitude at stimulus presentation, which describes the dominant frequency, is smaller in older participants compared to younger adults (1-30 Hz and 30-60 Hz) (Federmeier & Kutas 2005, Federmeier et al. 2010, Wlotko et al. 2010). Beese et al. in 2019 observed age-related differences in the lower alpha-band (8-10Hz) during sentence encoding, with a shift in alpha-band power between young and older adults. Relative alpha band decreases were associated with incorrect remembrance of an encoded sentence in younger participants, while older participants showed an increase in correct remembrance (Beese et al. 2019). The authors hypothesized that this shift may represent cortical processing that recruits more inhibitory neurons and inhibition with ageing. Inhibitory neurons are believed to play a role in triggering oscillatory frequencies in some cases (Atencio & Schreiner 2008, Hamilton et al. 2013a, Henry et al. 2017).

The ageing process appears to induce impairments in the GABAergic system, leading to an imbalance between inhibitory and excitatory neurotransmission (Morrison & Baxter 2012). However, in contrast, the prefrontal cortex shows an increase in inhibitory activity with ageing (Luebke et al. 2004, Bories et al. 2013). Inhibitory neurons' function and number appear to decrease with age in sensory cortices, as observed by a decrease in the number of inhibitory postsynaptic potentials (IPSPs) and GABA-mediated current receptors (Rozycka & Liguz-Lecznar 2017). The number of fast-spiking PV neurons has been observed to decrease with age in the somatosensory, motor, and hippocampal regions (Miettinen et al. 1993). The expression of PV neurons can also differ across cortical layers, with a significant decrease in PV expression in layers I-IV over time, while an increase is observed in layers V-VI (Del Campo et al. 2012). A decrease in PV neurons has been associated with impaired gamma activity and has been implicated in various brain-related disorders such as Alzheimer's disease, autism, depression, and others (Rossignol 2011, Rossignol et al. 2013, Byron et al. 2021, Wilson et al. 2020, Van Lier et al. 2018). Regarding SOM neurons, their number has been reported to decrease in the somatosensory and motor cortices of aged rats (Miettinen et al. 1993).

1.3.4 Hearing loss and brain rhythms

In addition to showing reduced activity in specific EEG frequency bands, individuals with hearing loss may also exhibit changes in the way their brain processes auditory information. For example, studies have found that individuals with hearing loss have altered patterns of neural synchronization and reduced neural connectivity in the auditory cortex (Yang et al. 2021, Zhang et al. 2018). These changes may reflect the brain's attempt to

compensate for the loss of sensory input, but they, on the contrary, contribute to difficulties in speech perception and communication. By analysing EEG frequency bands, changes in neural activity in the auditory processing in ageing individuals have been observed (Al Zoubi et al. 2018). analysing EEG frequency bands can provide valuable information about the impact of hearing loss on the brain and can help researchers develop new interventions to improve auditory processing and communication in individuals with hearing loss (Brewer & Barton 2016).

Changes in EEG frequency bands in response to auditory stimuli can provide information about the impact of hearing loss on the brain (Beese et al. 2019, Clinard et al. 2010, Crowell et al. 2020). Here are some of the changes that have been observed in individuals with hearing loss. Reduced activity in the delta and theta frequency bands has been noted, which are associated with early sensory processing and attention to auditory stimuli (Beese et al. 2019, Crowell et al. 2020). These findings suggest that individuals with hearing loss may have difficulties processing and attending to certain types of auditory information. Conversely, increased activity in the alpha and beta frequency bands, which are associated with cognitive processes such as attention, working memory, and executive function, has also been observed (Beese et al. 2019, Crowell et al. 2020). Two contrasting hypotheses exist regarding these increases. The first hypothesis suggests that individuals with hearing loss may exhibit heightened activity in low-frequency bands, indicating a wider brain connection but impaired dissociated network necessary for memory and attention (Crowell et al. 2020). Conversely, another hypothesis proposes that with age, an increase in high frequencies may occur, potentially affecting brain connections and the integration of information between different brain areas (Beese et al. 2019). Additionally, individuals with hearing loss may exhibit reduced neural synchronization in the auditory cortex, indicating difficulties in integrating auditory information from different sources (Clinard et al. 2010, Crowell et al. 2020). Overall, these changes in EEG frequency bands and neural activity suggest that hearing loss can impact the brain's ability to process and integrate auditory information. By analysing these changes, researchers can develop new interventions to improve auditory processing and communication in individuals with hearing loss.

1.3.5 Hearing loss and mice models

1.3.5.0.1 Mice model Mice serve as an advantageous model for studying human physiology due to several reasons (Ohlemiller et al. 2016). They reach sexual maturity early, typically around 6 weeks, allowing researchers to study developmental processes relatively quickly. Moreover, many commercial mouse strains exhibit high reproductive rates, enabling the generation of large numbers of offspring within a short period. The relatively short lifespan of mice, lasting 2 to 3 years, facilitates longitudinal studies and investigations into age-related processes. Additionally, housing large numbers of mice is cost-effective and requires less space compared to other model species, allowing for larger-scale experiments and statistical analyses. From a genetic standpoint, mice share approximately 99% of their genes with humans, making them valuable for studying human health and disease. Extensive literature and established methodologies further contribute to the utility of the mouse model in experimental procedures, including studies involving the cortex and targeted investigations using probes (Flurkey et al. 2007).

While there may be some differences between mouse and human deafness genes, recent studies indicate that

these discrepancies primarily stem from variations in gene expression rather than coding differences (Ohlemiller et al. 2016, Ingham et al. 2019). Therefore, it is important to consider species-specific gene expression patterns when studying deafness and other phenotype. In summary, mice offer advantages of early sexual maturity, high reproductive rates, short lifespan, cost-effectiveness, genetic similarity to humans, and established experimental techniques. These factors make mice a valuable and widely utilized model organism in biomedical research.

1.3.5.0.2 Mouse model for audition and age-related hearing loss studies Mouse models have emerged as valuable tools for studying age-related hearing loss (presbycusis) in humans. These models exhibit similar cochlear cell pathologies to humans, including the presbycusis and as ageing models without hearing loss (Park et al. 2010, Menardo et al. 2012, Rogalla & Hildebrandt 2020). Hair cell loss, resembling sensory presbycusis in humans, significantly contributes to age-related cochlear pathology in mice. While the genetic predisposition to neural presbycusis in humans is not well understood, mouse models with specific mutations or insults can successfully replicate this type of hearing loss. Numerous genes that influence age-related and noise-induced hearing loss have been identified in mice, some of which may play comparable roles in humans (Ohlemiller 2009). However, further research is needed to fully understand the implications of these models for human hearing and presbycusis. Humans and mice share a well-defined relationship regarding metabolic rate and lifespan, Efforts have been made to align their ages for experimental purposes, although aligning developmental stages poses challenges due to the distinct nature of mouse (altricial) and human (precocial) early development (Ohlemiller et al. 2016).

1.3.5.0.3 The C57BL/6J mouse strain as a model of age-related hearing loss The C57BL/6J mouse strain is widely used in research due to its well-characterised genetics and behaviour. These mice have a mutation which causes delayed-onset deafness. The strain originated from breeding female 57 with male 52 from Lathrop's stock in 1921, resulting in various sub-strains, including the sub-strain B6 (Ohlemiller et al. 2016). Early studies on C57BL/6 mice focused on age-related hearing loss, which begins with normal hearing in early life but gradually progresses to high-frequency hearing loss, extending to lower frequencies (Henry 1982, Li 1992). The specific genetic mutation responsible for deafness in C57BL/6J mice is a deletion of the cadherin 23 gene (Cdh23). This gene encodes a protein crucial for the proper functioning of hair cell in the inner ear, which is responsible for converting sound vibrations into neural signals processed by the brain (Noben-Trauth et al. 2003).

The absence of the *Cdh23* gene disrupts the transmission of sound information from the hair cell to the brain, resulting in hearing loss. Consequently, C57BL/6J mice serve as valuable models for studying the genetic and molecular mechanisms involved in hearing loss and for developing and testing potential treatments for hearing disorders (Noben-Trauth et al. 2003). The primary cause of high-frequency hearing loss in these mice is the hypomorphic Cdh23753A allele, which they possess in a homozygous state. This allele is also present in other inbred strains. It affects the hair cell stereociliary tip-link apparatus and is associated with accelerated loss of outer hair cell and susceptibility to noise-induced hearing loss (Ohlemiller et al. 2016). The Cdh23 protein encoded by the Cdh23753A allele interacts with calcium ions, amplifying the influence of other deafness genes that encode proteins involved in calcium binding or transport, as well as other components of the hair bundle. C57BL/6 mice are frequently used as an accelerated ageing model to study age-related hearing loss (Noben-Trauth et al. 2003).

Despite their accelerated hearing loss, C57BL/6 mice do not exhibit significant loss of canal or gravity receptor function. The reasons for their preserved vestibular function are not fully understood, although several hypotheses have been proposed. In contrast to their delicate outer hair cell, C57BL/6 mice show relative resistance to hearing loss induced by aminoglycoside drugs. Additionally, their cochlear lateral wall and endocochlear potential are less susceptible to damage from noise exposure compared to other mouse strains (Ohlemiller 2002).

C57BL/6J mice exhibit a characteristic feature of the human spiral ganglion, where the soma of radial afferent neurons forms unmyelinated aggregates that may be electrically connected. This feature potentially contributes to the survival and responsiveness of neurons that have lost connections with their hair cell targets. In older C57BL/6 mice, these aggregates tend to contain the surviving neurons, suggesting their role in preserving neurons in the absence of the Cdh23753A mutation. The exact reasons behind the formation of these aggregates in C57BL/6 mice remain unclear but are enhanced in congenic strains carrying a specific variant of the Ly5 (Ptprc or CD45) gene. These characteristics of C57BL/6 mice suggest the presence of compensatory mechanisms or adaptations in the auditory pathway to compensate for outer hair cell dysfunction (Riva et al. 2007, Ohlemiller 2002).

The C57BL/6J mouse strain is frequently utilized for comparative studies on presbycusis, an age-related hearing loss condition, alongside the CBA/J strain. The CBA/ca mouse strain is commonly employed as a control to assess normal hearing in this research field (Willott 1991). Previous investigations have focused on the distinctions in auditory circuitry between CBA and C57 mice, particularly during early developmental stages (Grothe & Park 2000, Spongr et al. 1997). The CBA strain demonstrates relatively preserved auditory sensitivity and moderate hair cell loss in advanced age (Willott 1991, Spongr et al. 1997, Sha et al. 2008). The CBA strain exhibits a gradual, progressive hearing loss that mirrors the experience of many individuals when considering the differing lifespans of mice and humans (Frisina & Walton 2001*a*, Ohlemiller et al. 2008, Frisina & Walton 2001*b*). The F1 Hybrid CBA x C57 is also a good candidate to study age-related changes, as this mice strain observes even better performance compared to the CBA mice strain (Frisina et al. 2011, Bowen et al. 2020). Several studies described that the auditory pathway between the CBA and C57 mice differ along ageing (Spongr et al. 1997), describing an important loss of hair cell with ageing compared to the CBA, or changes in the AC neurons proprieties at the single unit level (Bowen et al. 2020). However, there remains a notable scarcity of comprehensive studies evaluating and comparing the activity of the auditory cortex (AC) throughout the ageing process, particularly in awake mice. Consequently, the specific alterations in AC activity during ageing at close time points remain undisclosed.

1.4 Brain states

After providing an overview of the auditory cortex, its functional units, and connectivity, we aimed to explore how ongoing experiences could impact auditory processing. To accomplish this, we will delve into the brain state, encompassing the overall rhythms of the brain, as recorded by scalp electrodes (EEG), as well as the rhythms observed within specific layers, (LFP), (Figure 1.5. AC). These techniques enable us to observe both the global brain rhythms and the local rhythms, both of which have the potential to influence auditory processing, with the hypothesis that cognitive states may affect the reception, integration, and output commands of neural networks as the temporal spiking activity of individual cell.

The term "brain states" refers to different patterns of activity that occur in the brain over time. These patterns of activity can be characterised by changes in the level of electrical activity, blood flow, and metabolic activity in different regions of the brain (Raichle 1998, Greene et al. 2023). Brain states encompass various conditions of behavioural states and can be assessed using multiple methods.

Various wave frequencies can be captured using both invasive methods like EEG and LFP involving electrode insertion, as well as non-invasive approaches such as magnetoencephalography (MEG) and electrocorticography (ECoG) to record different brain rhythms, (Buzsáki et al. 2012). In our review, we will focus on waveform analysis. The waves may represent the extracellular flow of ions (Buzsáki et al. 2012) (Figure 1.5. B). These potentials are detected by the electrodes and displayed as waves. Low-frequency waves are reflected by the synchronous activity of neurons. Conversely, if the activity of the recorded cell is asynchronous, the wave frequencies can be high (Buzsáki et al. 2012) (Figure 1.5.D). However, it is interesting to mention that a high-frequency wave may also represent the synchrony of high-frequency cell activity (Ray et al. 2008). Here, we will first describe the different common observed waveforms frequencies (Buzsáki et al. 2012), their corresponding cognitive states, and cortical activities, as well as review brain oscillations and sensory cortex areas. Additionally, we will discuss the relationship between brain waves and spikes, and how this connection impacts auditory perception.

1.4.1 Neural oscillation and wakefulness

The history of neural oscillations began with Hans Berger, who conducted pioneering experiments in the 1920s. He observed an 8-12Hz rhythm by amplifying the signal from scalp electrodes using an electroencephalograph (EEG) electrode (Jung & Berger 1979). EEG is a non-invasive tool to record brain activity. Electrodes are placed on the scalp, and the summation of ionic currents in the cortex is measured. This provides good temporal resolution of the signal (in milliseconds), but poor spatial resolution. Oscillations, by inducing fluctuations in neuronal membrane potential, can periodically bring the voltage closer to or farther from the neuron's action potential threshold (Buzsáki 2004). This phenomenon may act as a coincidence mechanism, linking the membrane potential and the arrival of inputs to either facilitate or decrease the probability of spiking. The temporal coupling between different neuronal circuits can orchestrate responses to complex tasks by integrating different pathways (Bastos et al. 2012, Engel et al. 2001, Fries 2009).

1.4.2 Oscillation and neural code

During this decade, several studies have focused on understanding the relationship between spiking activity and oscillatory behaviour (Buzsáki 2010). During wakefulness, there is a correlation between the negative peaks of the LFP and an increase in firing activity (McGinley et al. 2015). On the other hand, during the slow-wave sleep (SWS) state, the negative peaks are associated with a significant decrease in firing activity in the units, followed by an activity rebound at the positive peaks (UP states) (Destexhe et al. 1999, Zerlaut & Destexhe 2017). The close relationship between slow waves, UP and DOWN states, and firing rate, FR, has been demonstrated through intracellular recordings during natural slow-wave sleep in cats (Steriade et al. 2001, Steriade & Timofeev 2003).

Although the specific frequency ranges slightly between individuals and species, five main brainwave traces have been identified (Buzsáki et al. 2013): delta (1-4 Hz), theta (4-7 Hz), alpha (8-15 Hz), beta (16-31 Hz), and

gamma (35-80 Hz) (Figure 1.5. EF). These frequency bands have been linked to different task behaviours and pathologies (Poulet & Crochet 2019). For example, the anaesthesia state, associated with loss of consciousness, is characterised by the dominance of slow oscillation frequencies (Curto et al. 2009*a*). High concentration and meditation are associated with gamma bands, while a drowsy but awake state is associated with alpha bands. The Yerkes-Dodson U-shaped curve illustrates the relationship between arousal and performance, suggesting that moderate levels of arousal enhance task performance, while both low and high levels can impair it. describes that optimal performance is linked to middle-frequency bands, (Yerkes & Dodson 1908). The underlying hypothesis is that the participant is relaxed enough to receive inputs, yet sufficiently concentrated and awake to process them.
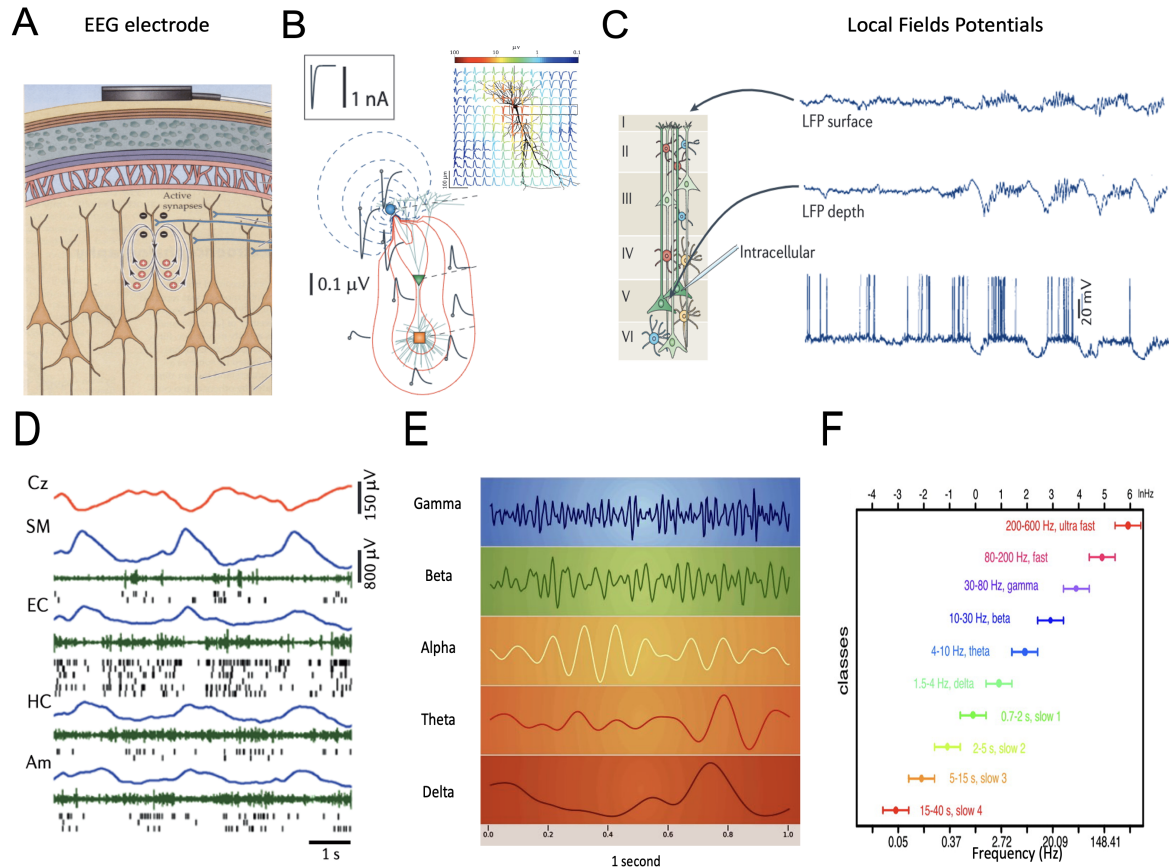
Figure 1.5: *Brain rhythms*

(A) Schema of potential pyramidal cells recording by an EEG electrode placed on the scalp *Adapted from (Van Putten 2020).* (B) Representation of the occurring potentials around the active neuron, *Adapted from (Buzsáki et al. 2012),* the bottom schema represents the simulation to an injection of current in the injection site (blue), at the mid-apical dendrite (green trace) and soma (orange trace) zones. Red and blue contour lines correspond to positive and negative values for the LFP amplitude, respectively. The top represents the LFP in response to a spike. (C) Representation of the LFP simultaneously recorded in different layers in the motor cortex comparison to an intracellular activity of a pyramidal cell in layer 5, *Adapted from (Buzsáki et al. 2012).* (D) 6-second example of the EEG, Cz, and LFP traces at different brain areas (motor area (SM), entorhinal cortex (EC), hippocampus (HC) and amygdala (Am)). The spiking activity of groups of neurons, multi-units, are represented in green and single unit, black *Adapted from (Buzsáki et al. 2012).* (E) Example of the frequency bands, from the lower frequencies, bottom, to the higher, top, *Adapted from (Kielan et al. 2020).* (F) Different oscillatory classes were observed in the rat cortex. The frequency classes are presented on a logarithmic scale, showcasing a linear progression. Each band is represented with its corresponding frequency range and commonly used term, *Adapted from (Buzsáki & Draguhn 2004).*

1.4.3   Frequency bands and brain states

Delta oscillations, ranging from 0.5 to 4 Hz, are prominent in EEG recordings during deep sleep and states of reduced arousal. These slow-wave patterns indicate a state of restorative rest and are characterised by high-amplitude, synchronized waves (Harmony 2013). Delta waves are typically observed in the frontal and central regions of the brain during the deepest stages of sleep. They are associated with essential physiological processes, such as tissue repair, immune system functioning, and hormone regulation (Cassidy et al. 2020, Abhang et al. 2016). In healthy individuals, a predominance of delta activity during sleep is considered crucial for maintaining optimal cognitive performance and overall well-being (Gu et al. 2023).

Theta oscillations are occurring at frequencies between 4 and 7 Hz. They can be categorized into at least two main types: cortical theta and hippocampal theta (Karakaş 2020). Hippocampal theta refers to theta oscillations originating from the hippocampus, a brain structure crucial for memory formation and spatial navigation. The hippocampal theta is closely linked to spatial navigation and memory processes, and it is believed to coordinate communication between the hippocampus and other brain regions during memory consolidation and retrieval (Nuñez & Buño 2021).

On the other hand, cortical theta refers to theta oscillations observed in the neocortex. These cortical theta rhythms are typically associated with cognitive processes such as attention, learning, and memory encoding (Karakaş 2020). These oscillations play a role in memory consolidation, creative thinking, and emotional processing, contributing to the overall regulation of cognitive and emotional functions. Theta oscillations have, also, been associated with the default mode network (DMN) processes in the brain (Das et al. 2022, Scheeringa et al. 2008). The DMN is a network of brain regions active during rest and mind-wandering, involved in self-referential thinking and memory retrieval (Menon 2023). Theta oscillations show increased power and coherence within the DMN during periods of mind-wandering and tasks requiring internal focus (Das et al. 2022, Scheeringa et al. 2008). They are believed to support the integration of information and contribute to cognitive processes related to self-reflection and introspection.

The alpha rhythm spanning the frequency range of 8 to 12 Hz, is an oscillatory pattern that corresponds to a state of relaxed wakefulness (Cantero et al. 2002). It is commonly observed in individuals who are awake but in a state of relaxed mental engagement or when the eyes are closed (Vago & Zeidan 2016). Some hypotheses claim that the alpha rhythm is indicative of a neural state characterised by decreased cortical excitability and enhanced inhibitory processes (Jensen & Mazaheri 2010), or linked to attention (Klimesch 2012, Jensen & Mazaheri 2010).

Beta waves are oscillatory waves between the frequency range of 13 to 30 Hz observed during episodes of heightened mental activity (Kropotov 2009). These oscillations are frequently detected during cognitive processes involving problem-solving, decision-making, and focused attention (Eggermont 2021). They reflect a state of increased cortical activation and are indicative of active engagement in mental tasks requiring sustained concentration (Chen et al. 2017). However, it is important to note that beta waves are not exclusive to productive mental activity, they can also manifest in states of anxiety or stress (Diaz et al. 2019). Consequently, the presence of beta waves serves as a valuable measure in the investigation of cognitive processes, as well as in the assessment of emotional states associated with anxiety or stress.

Gamma waves reflect synchronized neural activity across multiple brain regions and are believed to play a crucial role in information integration and binding (Buzsáki & Wang 2012). The presence of gamma wave activity indicates enhanced communication and coordination among different cortical areas, facilitating the integration of sensory information and the formation of coherent perceptual experiences (Buzsáki & Wang 2012). Additionally, gamma waves have been implicated in higher-order cognitive processes such as working memory, learning, and the generation of conscious awareness (Jia & Kohn 2011). Gamma rhythms are observed in various brain regions during waking and sleep states, but their functions and mechanisms remain debated. Gamma-band rhythmogenesis is tied to perisomatic inhibition (Buzsáki & Wang 2012), and their oscillations result from the interplay of excitation and inhibition.

There is also a distinction between low gamma and high gamma waves that lies in their respective frequency ranges and functional implications (Catanese et al. 2016, Jia & Kohn 2011). Low gamma waves typically refer to oscillations within the lower end of the gamma frequency range, around 30 to 50 Hz. They are involved in sensory perception and integration, facilitating the binding of different sensory inputs into a coherent perception. They synchronise neural activity across brain regions and play a role in creating a unified representation of the environment (Buzsáki & Wang 2012). On the other hand, high gamma waves encompass the higher end of the gamma frequency spectrum, typically ranging from 70 to 100 Hz or even beyond. They are associated with complex cognitive processes and higher-order cortical functions, such, as attention, memory formation, and the integration of information across brain regions. High gamma activity is observed during tasks that require working memory and the manipulation of information (Catanese et al. 2016). Interestingly, the frequency bands can also interact with each other in complex ways (Buzsáki et al. 2012), where the coupling between different frequency bands are supporting cognitive of-state functions. For example, alpha oscillations are thought to represent inhibited sensory processing, while gamma oscillations are thought to enhance it (Seymour et al. 2017). By studying the interactions between different frequency bands, researchers can gain insights into the underlying neural mechanisms of cognitive and behavioural processes.

1.4.4 Cell synchronization and auditory perception

The synchronization of neuronal activity in the auditory cortex provides several advantages. Firstly, it enables the neurons to collaborate more efficiently in processing the attended sound (Henao et al. 2020, Fuglsang et al. 2020). Through coordinated activity, the neurons enhance their sensitivity to specific characteristics of the sound, such as pitch, timbre, or temporal patterns. This heightened sensitivity promotes accurate and efficient processing of the attended sound, thereby improving our ability to perceive and comprehend it. The synchronization of neuronal activity in the auditory cortex plays an important role in enhancing our ability to perceive and understand the attended sound (Poulet & Crochet 2019). It is thought to arise from the synaptic interactions between neurons and can be influenced by top-down processes originating from higher-level brain regions associated with attention and cognitive control. Additionally, the synchronization of neuronal activity assists in suppressing irrelevant or distracting information present in the auditory environment (Zanto & Gazzaley 2009). In a noisy environment, like a conversation in a crowded room, synchronized activity in the auditory cortex plays a crucial role in helping us filter out background noise. This synchronization allows our brain to focus on and better understand the speech sounds

in the ongoing conversation. The coordinated activity essentially acts as a mechanism that enhances our ability to concentrate on relevant auditory information and improves our comprehension amidst a noisy background, (Sohal et al. 2009). Specifically, the synchronized firing of neurons in the auditory cortex helps emphasize the signals associated with speech, making it easier for our brain to distinguish and process the meaningful sounds while minimizing the impact of distracting background noise.

The effects of attention could be to increase synchronization and coordination of firing patterns among neurons in the auditory cortex. This synchronization is hypothesized to facilitate a comprehensive understanding of the auditory stimulus (Fuglsang et al. 2020, Harris & Thiele 2011). Attention affects aspects of neuronal activity in the auditory cortex. It reduces trial-to-trial variability and firing rate correlations between neurons. Variability and noise correlations, which typically reduce the information encoded by neuronal populations, are decreased when attention is directed to the receptive field. Moreover, attention reduces the adaptation of auditory cortex responses to repeatedly presented stimuli (Harris & Thiele 2011). Selective attention can influence the level of cortical desynchronization at a local level. Rather than a global effect, attention may cause maximum desynchronization in a small patch of cortical tissue representing the attended stimulus, while non-attended parts of the sensory world may remain in a more synchronized state. This local modulation of cortical state by attention can explain various findings related to attention-induced changes in neuronal activity (Steinmetz et al. 2000). Attention directed to the receptive field of recorded neurons in the auditory cortex leads to decreased low-frequency LFP power compared to attention directed outside the receptive field (Laffere et al. 2020*b*). This suggests that attention modulates the size of low-frequency fluctuations locally.

In summary, the synchronization of neuronal activity within the auditory cortex plays a crucial role in enhancing our capacity to perceive and comprehend the attended sound. By coordinating their activity, the neurons can effectively collaborate in extracting pertinent information from the sound signal while attenuating irrelevant or distracting auditory stimuli in the environment. Preceding activity before stimulus processing can greatly impact auditory processing. Recent studies and technological advancements, particularly in vivo invasive electrophysiology, have revealed that "brain states" encompass different spatial and temporal components (Harris & Thiele 2011, Buzsáki 2010, Buzsáki et al. 2012). Single neurons are capable of oscillating at different frequencies, neighbouring neurons can synchronise with each other, long-distance brain areas can exhibit synchronization, different layers within the same cortical area may display different oscillatory behaviour, and oscillations can propagate and assume different directions (Gold et al. 2006, Curto et al. 2009*a*, Buzsáki 2010). This underscores the importance of oscillations in shaping brain activity. This result suggests that brain oscillation may have several roles in integration and brain computation.

1.5 Spontaneous activity

1.5.1 The spontaneous activity in the brain

Spontaneous or ongoing brain activity refers to the neural activity that occurs in the absence of any external stimuli or task demands (Sadaghiani et al. 2010). More evidence suggests that the spontaneous brain activity cannot be simply described as background noise, disconnected from the system's response (Tozzi et al. 2016). Rather,

it manifests during unconstrained resting states in the awake state and englobes the resting mode state and active ongoing activities (Harris & Thiele 2011). The detection and recording of spontaneous signals through various imaging techniques such as fMRI, EEG, and MEG provide compelling evidence supporting the notion that these fluctuations constitute the fundamental framework of functional brain organization (Meyer-Baese et al. 2022).

This spontaneous activity is often characterised by the presence of rhythmic oscillations in different frequency bands. For example, the alpha (8-12 Hz) and beta (13-30 Hz) bands are often observed during resting-state EEG recordings, while the default mode network (DMN) in the brain is characterised by low-frequency (0.01-0.1 Hz) fluctuations in BOLD signal during fMRI recordings (Meyer-Baese et al. 2022). As a sight note, spontaneous activity encompasses the broader concept of intrinsic neural activity that occurs during rest and task-free conditions, while the default mode specifically refers to the pattern of activation within the default mode network observed during rest periods.

However, it is thought that spontaneous activity is important for various aspects of brain function, including sensory processing, perception, attention, and cognition (Mitra et al. 2018, Poulet & Crochet 2019), but also for cell-types spiking activity integration (Chen et al. 2017). The spontaneous activity preceding the reception of a signal appears to influence how the brain receives and processes information. In this context, the spontaneous activity or state could have an impact on the coding of information within the brain. These fluctuations in cortical excitability exert a noteworthy impact on the overall field potential activity and the spiking patterns of individual neurons. And as the coupling or nesting of numerous spikes serves a vital coordinating role, endowing a logical structure for the integration of functional activity (Gold et al. 2006, Buzsáki 2006). Recent findings further illustrate that gamma-band activity in alert primates predominantly emerges as a property of the cortex from resting-state waves (Bastos et al. 2014). Remarkably, spontaneous cortical electrical activity is already observed in the human foetal stage (Krueger & Garvan 2014), resembling the pulsations exhibited by the spontaneously contracting heart during the same period. Moreover, immature synapses display a higher propensity for spontaneous fluctuations compared to their more mature counterparts (Kavalali 2014). And spontaneous activity seems to be important for the maturation of the network, in particular the formation of GABAergic synapses (Colin-Le Brun et al. 2004). Taken together, this research suggests that spontaneous activity may potentially be linked to neural network maturation. Abnormalities in spontaneous activity have also been linked to a variety of neurological and psychiatric disorders, including Alzheimer's disease, Parkinson's disease, schizophrenia, and depression (Wen et al. 2013, Li et al. 2020). For example, individuals with Alzheimer's disease may show reduced power and coherence of alpha oscillations during spontaneous activity, "awake resting state", indicating altered cortical function and connectivity (Lejko et al. 2020). Abnormal spontaneous activity- (increase and decrease depending on the regions), has also been reported in several mental health diseases such as schizophrenia (Gong et al. 2020) and depression (Wang et al. 2019, Tabak et al. 2001), usually affecting the spontaneous activity in the prefrontal cortex, amygdala, and hippocampus regions. Overall, the study of spontaneous activity is an important area of neuroscience research, as it provides insights into the fundamental organization and function of the brain.

1.5.2 Spontaneous activity in the auditory cortex

Spontaneous activity is also present in the auditory cortex when there is no external sound input (Eggermont 2006, 2015, Luczak et al. 2009). This ongoing activity has been found to play an important role in auditory processing and perception (Eggermont 2015, Arieli et al. 1996, Ribeiro & Castelo-Branco 2022, Bartlett 2013). Studies have shown that the spontaneous activity preceding an auditory stimulation in the auditory cortex can affect the processing of incoming sound stimuli (Harris & Thiele 2011, Luczak et al. 2009). For example, the strength and timing of the ongoing activity can influence the response of auditory neurons to sound, shaping their sensitivity to specific sound frequencies and temporal patterns (Stringer et al. 2019, Eggermont 2015), or even represent the spontaneous behaviour activity (Figure 1.6. B) (Stringer et al. 2019). This may suggest that the ongoing activity in the auditory cortex may serve as a "baseline" that affects the processing of incoming sound information. The auditory cortex shows a subset of correlated neurons assemblies responding to sounds compared to wider assemblies and desynchronization in neural activity during silence (Filipchuk et al. 2022), and this is observed mostly with complex sounds (Eggermont 2006).

Some data suggest that the neuron assemblies active during spontaneous activity and evoked-response state could be the same or overlapped (Eggermont 2006). Moreover, the findings from the Basset paper (Betzel et al. 2019), indicate that although spontaneous neural activity varies across different sessions on different days, there is a subset of neurons that exhibit stable correlations. In other words, while the overall patterns of spontaneous activity may differ from session to session, certain neurons consistently show synchronized or coordinated behaviour. Furthermore, the spontaneous activity seems to be the same pre and post-stimuli (Eggermont 2015), and the spontaneous activity and evoked-response activity show different propagation pathways across layers differ (Sakata & Harris 2009). The underlying question is whether the variability in cortical responses to an identical sensory stimulus is primarily influenced by stochastic noise (Faisal et al. 2008), or if the interactions between sensory responses and spontaneous activity also contribute to this variance (Curto et al. 2009*b*, Stringer et al. 2019, Arieli et al. 1996). This question raises the possibility that the evoked activity may be either linearly or non-linearly integrated with the ongoing spontaneous activity.

This topic has been studied by the Kenneth Harris group, where they found that the dynamics of auditory cortical population in urethane-anaesthetized rats can be effectively described by a family of low-dimensional dynamical system models (Curto et al. 2009*b*). These models parameterized using spontaneous activity preceding a stimulus, accurately predict the structure of subsequent sensory responses. Consequently, the observed trial-to-trial variability can be explained as a natural outcome of sensory responses evolving according to the same dynamics governing previous spontaneous activity. By applying the model, they were able to characterise cortical dynamics with brain state. They found that the synchronized state corresponds to a nonlinear, self-exciting system, whereas the desynchronized state exhibits predominantly linear dynamics. In their 2009 publication (Luczak et al. 2009) they provide evidence that population activity shows a broad degree of consistency across diverse sensory stimuli and spontaneous events. Although individual neurons may exhibit variations in timing between stimuli, these variances do not significantly disrupt the overall sequential organization observed at the population level. This organization remains stable for approximately 100ms, with the reliability of spiking gradually declining after

the onset of an event. The firing rates of groups of neurons are limited and follow specific patterns, even when responding to different stimuli. These patterns form distinct areas within a larger constrained space, which is defined by the set of spontaneous events. These findings indicate that population spike patterns originate from a limited "vocabulary," extensively sampled by spontaneous events but more narrowly represented by sensory responses (Figure 1.6. A).
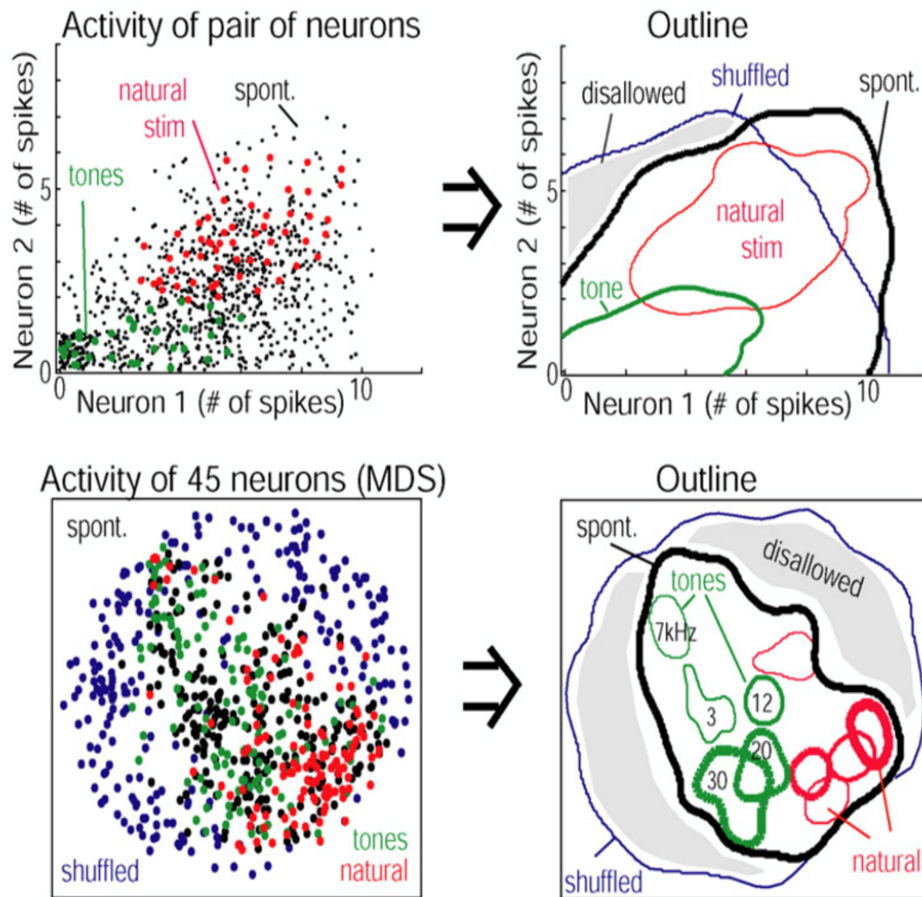
Figure 1.6: *Comparing Spontaneous and Evoked Neural Activity: Insights from Spike Count Analysis and Multidimensional Scaling*
(A) Top left represents the pike counts of two neurons, recorded from separate tetrodes, are depicted during the first 100 ms of spontaneous upstates (black), responses to a tone (green), and responses to a natural sound (magenta). Data points are jittered for visibility, revealing distinct regions occupied by responses to sensory stimuli, both contained within the realm outlined by spontaneous patterns.Top left represents a contour plot illustrating the regions occupied by points from top left, with a blue outline computed from spike counts shuffled between upstates, indicating the expected region in the absence of spike count correlations. bottom left, firing rate vectors of the entire neuron population are visualized using multidimensional scaling (MDS), where each dot represents the activity of 45 neurons nonlinearly projected into 2D space. bottom right shows a contour plot derived from MDS data shows sensory-evoked responses once again lying within the realm outlined by spontaneous events.*Adapted from (Luczak et al. 2009)*

1.5.3 Spontaneous activity, evoked responses, and brain states

Analysing the spontaneous activity of the cortex provides insights into the fundamental processes and organization of cortical activity. Spontaneous activity refers to the ongoing computations of the brain in the absence of

external stimulation or a specific task. Research in this field is continually expanding, investigating the implication of spontaneous activity implications on the brain's structural and functional architecture, (Tozzi et al. 2016).

One important question is what the cortical spontaneous activity reflects and whether it represents internal processing. The structure of cortical spontaneous activity varies across different brain states (Fairhall 2019). In the auditory cortex of urethane-anaesthetized rats, population responses to click stimuli can be accurately predicted on a trial-by-trial basis using a simple dynamical system model based on the spontaneous activity immediately preceding the stimulus presentation (Luczak et al. 2009). Changes in the cortical state consistently correspond to changes in the model dynamics, indicating a nonlinear, self-exciting system during synchronized states and an approximately linear system during desynchronized states. The variability in cortical responses to the same stimulus may arise from stochastic noise or be influenced by the spontaneous activity preceding the stimulus (Faisal et al. 2008).

In summary, if the pre-stimulus neural circuit state influences neural coding, perception is not solely determined by the qualities of the sensory signal but also by the state of the brain before the stimulus (Keller & Mrsic-Flogel 2018, Podvalny et al. 2019, Henao et al. 2020). Many studies have demonstrated that the state (power or phase) of pre-stimulus rhythmic brain activity can predict perceptual performance in various tasks (Henry et al. 2017), supporting the notion that perception is closely linked to rhythmic neural processing (Schroeder et al. 2010, VanRullen 2016). Additionally, changes in top-down influences driven by attention and cognitive strategies are also reflected in rhythmic brain activity, particularly in the alpha and beta frequency bands (Strauß et al. 2015, Henry et al. 2017, Wöstmann et al. 2017). These findings shed light on why better performance in auditory tasks can occur at an intermediate level of task difficulty, following a U-shaped curve. Recent research also indicates that the cocktail-party effect, which involves the ability to selectively attend to a specific speaker in a noisy environment, depends on the synchronization of low-frequency neural oscillations (Ding & Simon 2012, Horton et al. 2013, Golumbic et al. 2013, Kerlin et al. 2010). Age-related auditory impairment, a symptom of ageing-related hearing loss, can lead to difficulties in extracting relevant auditory information in noisy backgrounds, potentially related to disruptions in brain state and neural coding. This will be further discussed in the final part, focusing on the ageing brain, ageing-related hearing loss, brain state, and neural coding.

1.5.4 Pupillometry

Pupillometry has demonstrated the ability to reflect an arousal state and serve as a marker of brain states (Larsen & Waters 2018, Hess & Polt 1964). A dilated pupil is indicative of high frequencies, while a constricted pupil corresponds to low frequencies and sleep. Pupil diameter has been found to predict various cortical dynamics related to task performance (Stringer et al. 2019, McGinley et al. 2015, McNair et al. 2019). The detection of brain states involves both reliable spiking activity and oscillatory rhythms (Larsen & Waters 2018, Hess & Polt 1964, McGinley et al. 2015). In this section, we examined the relationship between cell synchronization measured through LFP analysis, brain state assessed by EEG, and pupil dynamics. Our goal is to introduce a metric for state assessment, known as pupillometry.

1.5.4.1 Pupillometry and brain states

There is a well-established link between changes in pupil size and changes in brain states. Pupil size is controlled by the autonomic nervous system, which is responsible for regulating involuntary bodily functions such as heart rate, breathing, and digestion. The autonomic nervous system is also involved in regulating arousal, attention, and other aspects of cognitive processing (Larsen & Waters 2018). Changes in pupil size are commonly used as a non-invasive measure of changes in cognitive processing and brain states. Specifically, the pupil tends to dilate (i.e., get larger) in response to increased arousal and cognitive effort, and constrict (i.e., get smaller) in response to decreased arousal and cognitive effort (Hess & Polt 1964, Larsen & Waters 2018, Yuzgeç et al. 2018, Reimer et al. 2014). Similarly, changes in pupil size have been used to measure changes in brain states during various cognitive tasks, such as attention, working memory, and decision-making (Reimer et al. 2014, Yuzgeç et al. 2018, Larsen & Waters 2018). The measurement of changes in pupil size in response to diverse cognitive tasks provides valuable insights into the underlying neural mechanisms of cognitive processing, thereby facilitating the development of novel interventions aimed at enhancing cognitive function.

1.5.4.2 Pupil and spiking activities

There is growing evidence to suggest that changes in pupil size are linked to changes in neural spiking activity in the brain. Specifically, pupil dilation is associated with increased firing rates of neurons in the locus coeruleus (LC), a small cluster of neurons in the brainstem that is involved in regulating arousal, attention, and other aspects of cognitive processing (Joshi et al. 2016). The LC is known to release the neurotransmitter norepinephrine, which plays a key role in modulating neural activity in various regions of the brain (Joshi et al. 2016). Studies have found that when the LC is activated, either through external stimulation (such as a stressful or emotionally charged situation) or through internal cognitive processes (such as attention or decision-making), it leads to increased firing rates of LC neurons and release of norepinephrine (He et al. 2023). This increase in norepinephrine release is thought to be responsible for the associated increase in neural spiking activity and pupil dilation. In other words, when the brain is engaged in a task that requires increased attention or cognitive effort, the LC is activated, leading to increased release of norepinephrine, increased neural spiking activity, and dilation of the pupil. Overall, the link between pupil dilation and neural spiking activity provides a valuable tool for measuring changes in cognitive processing and brain states. By analysing changes in pupil size and neural activity in response to different cognitive tasks and stimuli, researchers can gain insights into the underlying neural mechanisms of cognitive processing and develop new interventions to improve cognitive function.

1.5.4.3 Pupil and auditory cortex

There is some evidence to suggest that changes in pupil size are also linked to changes in spiking activity in the auditory cortex (Larsen & Waters 2018, Matthew et al. 2015). The J. McGinley and all paper (Matthew et al. 2015), examines the intricate relationship between arousal, behavioural performance, and neural activity, specifically in the context of a tone-in-noise detection task (Figure 1.7. AB). An inverted-U relationship, between brain states and pupil diameter have been described (Figure 1.7. B). Whereby both insufficient and excessive arousal levels detri-

mentally affect performance, while intermediate levels yield optimal outcomes (Matthew et al. 2015). Intermediate arousal levels correspond to a cortical state characterised by low noise, thereby facilitating superior behavioural performance and eliciting optimal sensory responses in the auditory cortex. During this state, sensory responses are notably amplified and reliable, while cortical membrane potentials remain consistently hyperpolarised. Consequently, the signal-to-noise ratio of evoked cortical responses is significantly heightened. Conversely, heightened arousal levels are associated with diminished amplitude/reliability of cortical sensory responses and compromised behavioural performance. This decline in sensory-evoked responses may disrupt the precise spatiotemporal interactions of cortical circuits crucial for optimal functioning (Matthew et al. 2015). The proposed mechanisms underlying arousal-related changes in cortical responsiveness likely involve the engagement of multiple neurotransmitter systems, including adrenergic and cholinergic pathways (Bennett et al. 2013). Activation of these pathways may modulate cortical excitability and the delicate balance between excitation and inhibition, thereby influencing the sensory responsiveness of cortical circuits. In essence, unravelling the neural mechanisms governing arousal and its impact on performance holds great potential in enhancing our comprehension of optimal neural network function, while concurrently mitigating trial-to-trial variability in sensory responses.
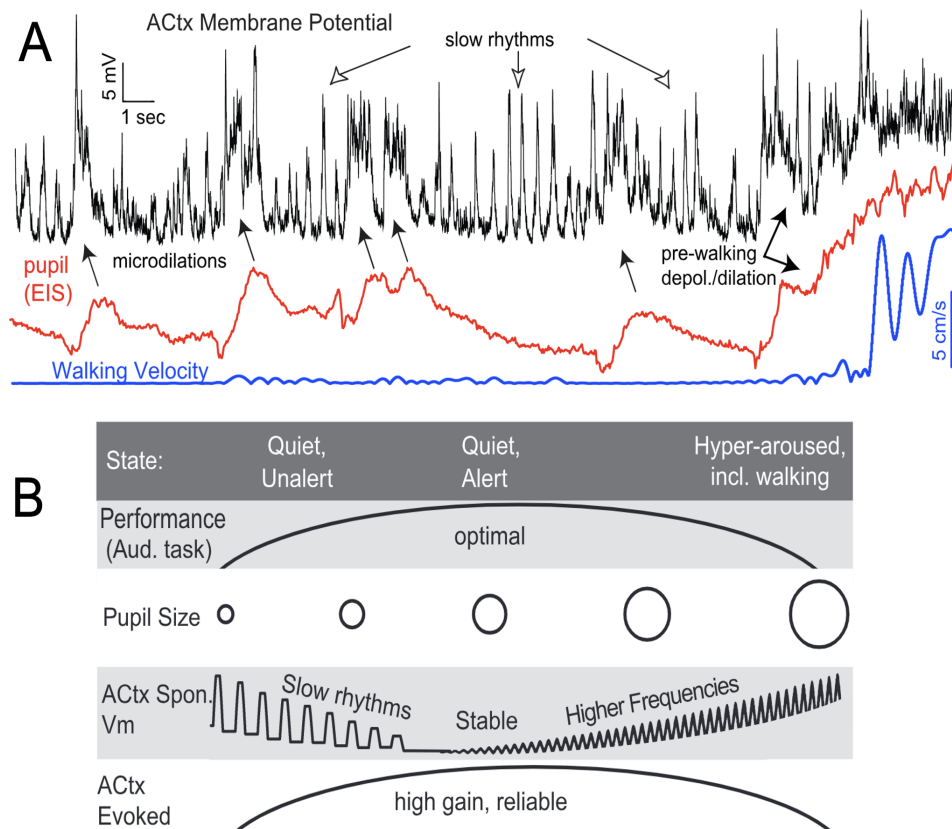
Figure 1.7: *Pupil and auditory cortex activity*
(A) The relationship between AC neurons membrane potential, pupil diameter, and behaviour in mice is expanded over time. (B) The relationship between state, behavioural performance, and auditory cortex responsiveness observed by *Both adapted from (Matthew et al. 2015).*

1.6 Investigating the neuronal activity

The comprehension of neuronal coding depends on the methodologies utilized for its investigation and the metrics employed for extracting relevant information. The selection of techniques is dictated by the specific spatiotemporal scale of analysis involved in the study. Investigating the information received by the auditory cortex can be achieved by simultaneously recording the activity of a large number of neurons while presenting various sound features. Comparing the evoked activity to the spontaneous activity can provide insights into auditory processing (Rees 2009, Bahmer & Gupta 2018).

1.6.1 Neuronal complexity and technological advances in brain research

The human brain exhibits a remarkable level of cellular complexity and organization. It is estimated that the brain contains approximately 10^{11} neurons, each establishing connections with a vast network of 21-26 billion neurons within the cerebral cortex (Herculano-Houzel 2009, Pelvig et al. 2008). This intricate interplay of neuronal connections forms the basis for the brain's functionality and allows for complex cognitive processes to occur. The high-density arrangement of neurons and their extensive connectivity contribute to the brain's capacity to process and integrate information, enabling the intricate operations underlying human cognition. The role of the brain has been hypothesized to be significant since ancient times, with early thinkers such as the Egyptians (Fanous & Couldwell 2012), and Greek philosophers like Aristotle (Gross 1995), recognizing its importance. The study of the brain's function became more prominent in the 17th century. François Pourfour du Petit observed a correlation between the area of motor cortex injury and the resulting handicap in soldiers, establishing the principle of contralateral motor action (Tacik et al. 2012). Thomas Willis and Descartes debated the significance of the cortex (Caron 2015). In the field of electrophysiology, the story began with Luigi Galvani in the 1760s, who conducted a famous experiment involving a frog and observed muscle contractions when the nerve was in contact with a metal compound (Verkhratsky et al. 2006). In the 19th century, the German physiologist Emil du Bois-Reymond continued this work and demonstrated the electrical nature of nerve signals. He is considered the father of electrophysiology due to his research on action potentials and resting potentials (Verkhratsky et al. 2006, Finkelstein 2015). In the 19th, Lord Edgar Adrian described the "all or none" property of action potentials and their specific response to stimuli. He shared the 1932 Nobel Prize in Physiology with Sir Charles Sherrington for their discoveries regarding the functions of neurons (Grant 2006, Verkhratsky et al. 2006). The effects of action potentials were further established by L. Hodgkin and A. Huxley, who developed the voltage clamp technique using the squid giant axon. They proposed the existence of two distinct independent conductances, one selective for sodium ions and the other for potassium ions (Hodgkin & Huxley 1952, Verkhratsky et al. 2006).

Together with J. Carew Eccles, they expanded these observations from nerves to neurons and characterised synaptic connections by measuring excitatory postsynaptic potentials (EPSPs) and inhibitory postsynaptic potentials (IPSPs) in the stretch reflex model. In this model, when the sensory neuron is stimulated, an EPSP is recorded in the motoneuron that innervates the muscle, while an IPSP is recorded in the motoneuron that innervates the opposing muscle. They also observed that a single EPSP is not sufficient to activate the motoneuron; instead, it is the summation of multiple sensory stimuli that leads to the generation of an action potential. Their ground-

breaking studies earned them the Nobel Prize in Physiology or Medicine in 1963 (Schwiening 2012, Caron 2015). After 20 years and a meeting with K. Popper, Eccles and Katz elucidated that synaptic transmission is chemical rather than electric and described the role of acetylcholine as a neurotransmitter (Stahnisch 2017). In the 1970s, E. Neher and B. Sakmann introduced the patch-clamp technique, a single-cell electrophysiological method in which a micropipette filled with an electrolyte solution is used as a recording electrode to amplify the membrane potential (Verkhratsky et al. 2006). This technique allows researchers to control the current or voltage and observe the resulting voltage or current of the cell. Typically, the resting membrane potential varies between -60 mV and -80 mV. Several variations of the patch-clamp technique have been developed. For example, the inside-out and outside-out configurations involve excising the main body of the cell, enabling the observation of individual channel behaviour. The patch-clamp technique earned Neher and Sakmann the 1991 Nobel Prize in Physiology or Medicine and remains one of the most widely used intracellular recording methods (Neher & Sakmann 1976). These advancements encouraged scientists to directly insert invasive electrodes into the brain and record neuronal activity in vivo. The original studies by Renshaw, Forbes, and Morrison (1940) on the cat's hippocampus demonstrated that unitary discharge of pyramidal cell could be recorded with microelectrodes when they were placed within the stratum pyramidal (Renshaw et al. 1940).

Hubel and Wiesel, recipients of the 1981 Nobel Prize in Physiology or Medicine, demonstrated a link between visual sensory input and neuronal activity. They inserted a microelectrode into the primary visual cortex of an anaesthetized cat and observed the response of neurons to light and dark patterns projected onto a screen. They found that certain neurons fired in response to specific lines at a particular angle, which they termed "simple cell." Other neurons, known as "complex cell," responded to multiple edges and exhibited a preference for motion in specific directions (Hubel & Wiesel 1962). At the time, the cat's visual system was relatively understudied, and the use of invasive microelectrodes became more prevalent. Results were discussed in terms of intracellular or extracellular recordings depending on the sign of the recorded potential (Renshaw et al. 1940, Li & Jasper 1953). The emergence of large neural population studies was facilitated by the ability to simultaneously record from large populations of cell.

In our modern times, technological advancements in neural interfaces have led to the development of better neural interfaces with improved designs, components, and integrated devices. The field of neuroscience has expanded significantly, with substantial progress and an ever-growing body of knowledge. Approximately 25,000 papers were published annually between 2015 and 2020 that included the term "neuron" in their titles or abstracts (online PubMed, September 2021). Various aspects such as the role of glia, microenvironment, dendritic integration, cell types, brain organization, connectivity, white matter, and genetics serve as essential building blocks that contribute to our understanding of how neurons function and thrive.

To encompass the broad field of neuroscience studies, these interfaces should enable the recording and/or stimulation of multiple discrete neurons during specific periods. Additionally, for translational and clinical applications, additional requirements such as safety, reliability, acceptance, and cost-effectiveness need to be addressed. Microfabricated electrode arrays, known as neural probes, consist of thin layers of conductors and insulators, such as silicon or polymer substrates, and offer the advantage of being designed to meet specific experimental needs

(Figure 1.8 A) (Kipke et al. 2008, Schjetnan & Luczak 2011). Silicon-based microfabrication technology allows for the creation of high-density two-dimensional shapes with single or multiple shanks (Hong & Lieber 2019). Various stimulating techniques can be employed. For instance, deep brain stimulation (DBS) involves surgically implanting electrodes into specific brain regions. These electrodes, also known as leads, generate electrical impulses to modulate abnormal brain activity. While this technique has applications in both research and clinical settings, it is commonly used in the clinic to treat patients with conditions such as Parkinson's disease or epilepsy who do not respond well to medication (Bragin et al. 2000, Lozano et al. 2019).

Another cutting-edge technical tool for stimulation is optogenetics. Optogenetics allows for the selective activation of neurons through genetic manipulation, involving the transgenic expression of photon-gated ion channels, known as opsins, into the membranes of neurons. By illuminating these cell with a specific wavelength, the ion channels in the neurons can be opened, inducing either depolarization (e.g., Channelrhodopsin-2, ChR2) or hyperpolarization (e.g., Arch). This approach enables researchers to selectively observe the effects of neuron activity, its impact on brain activity and animal behaviour, and even the circuit patterns of nearby neurons (Yizhar et al. 2011, Airan et al. 2009). Optogenetics provides temporal precision at the millisecond scale, allowing scientists to study rapid biological information processing, such as action potentials. In 2010, optogenetics was recognized as the "Method of the Year" by the journal Nature Methods (Editorial, 2011).
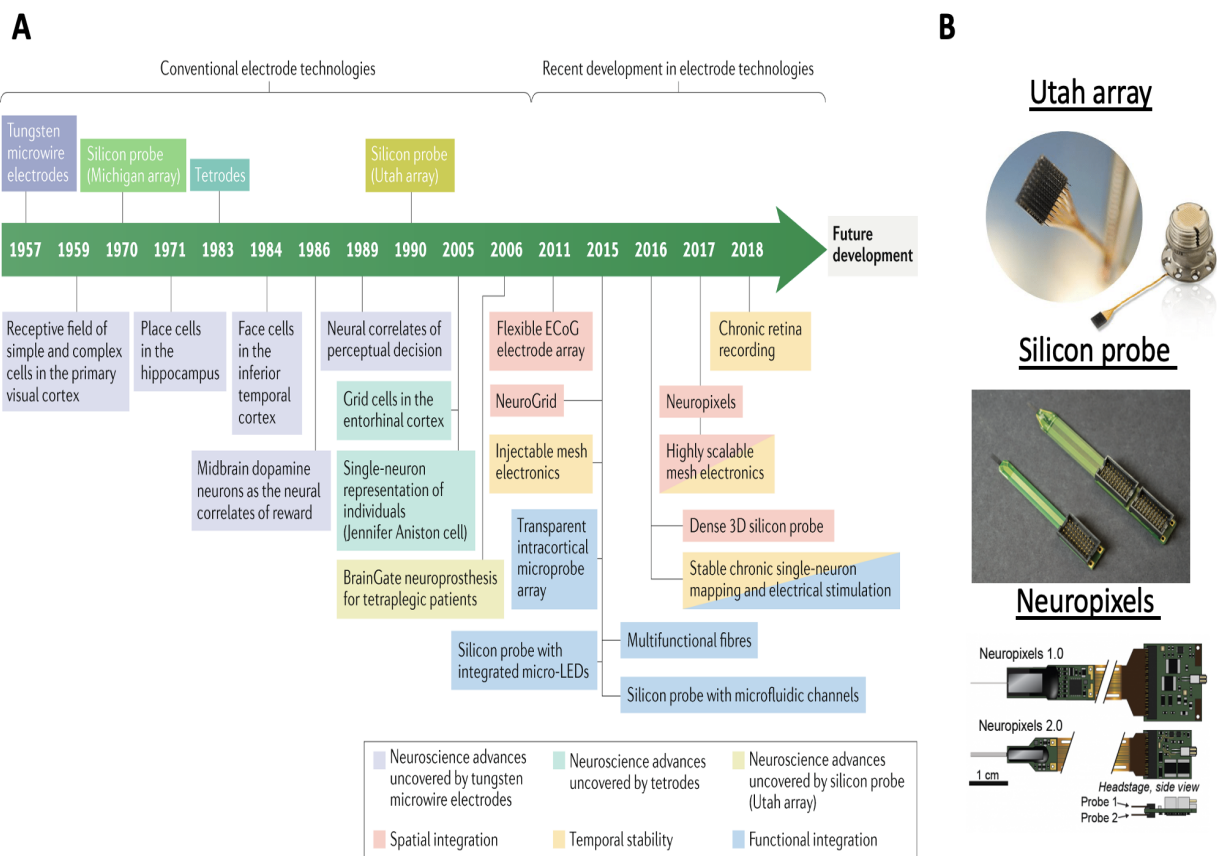
Figure 1.8: *Neural probes technologies*

A) Evolution of the probes technologies during the last century. B) With the design of the major known probes: the Silicon probes (1970) middle, the Utah array (1990), top, and the Neuropixels (2017), bottom. *Adapted from (Hong & Lieber 2019)*

1.6.2   Spike train measures

The study of neuronal activity entails the examination of diverse electrophysiological measures. In this section, we will explore several metrics, underlines electrophysiological recordings, that provide valuable insights into neuronal dynamics. When an electrode array is inserted into a specific region of the brain, such as the auditory cortex, it enables the acquisition of valuable data regarding neuronal activity. The inserted probe captures extracellular currents, which represent the collective electrical signals generated by the neurons in that particular area. These extracellular voltages result from the summation of individual neuronal action potentials and synaptic potentials. By reading and analysing these extracellular currents, we can gain insights into the patterns, timing, and overall dynamics of neuronal firing.

Spike sorting techniques utilize the similarities in spike shapes to group neurons into clusters. Generally, spike sorting algorithms involve four major steps, starting from the raw data and concluding with classified spike shapes. The initial step involves filtering the raw data by applying a band-pass filter to eliminate low-frequency activity and enhance spike visualization. Next, spikes are typically detected from the filtered data using an amplitude threshold, which can be manually set as a multiple of the standard deviation of the signal or automatically determined (Pouzat et al. 2002, Rey et al. 2015). The third step entails extracting features from the spike shapes, which reduces the dimensionality of the data points per spike. These features enable the separation of waveforms into distinct clusters representing different spiking neurons. Finally, in the last step, spikes with similar features are grouped into clusters corresponding to different neurons (Rey et al. 2015). These detected spikes are further analysed for various spike parameters such as the firing rate or the entropy of the spike train. This is based on the principle that each neuron tends to generate spikes with a distinct shape (Gold et al. 2006, Pachitariu et al. 2016).

Independently, the filtered data is used to calculate the local field potential (LFP) by extracting the low-frequency components of the signal. This LFP represents the summation of synaptic potentials and other collective neuronal activities in the recorded area. LFPs can be used to investigate, neuronal rhythms. After analysing the spike activity of various neurons, the question arises as to what metrics we can extract from this data to characterise neuronal behaviour.

1.6.2.0.1   Firing rate   The firing rate refers to the rate at which a neuron generates action potentials or "fire". It is one of the fundamental measures used to understand and quantify neural activity (Tomar 2019). Neurons communicate with each other through AP. When a neuron receives inputs from other neurons, it integrates those inputs and, if the accumulated electrical potential reaches a certain threshold, it generates an action potential (Gerstner et al. 1997). The firing rate of a neuron is the average number of action potentials it produces per unit of time, typically measured in spikes per second (or Hz) (Tomar 2019). The firing rate of a neuron can be influenced by various factors such as the strength and timing of inputs from other neurons, the summation of different inputs, the presence of neurotransmitters, and the neuron's intrinsic properties. Neurons can exhibit a wide range of firing rates, from a few spikes per second to hundreds of spikes per second (Vonderschen & Chacron 2011). Different firing rate patterns could represent different aspects of sensory stimuli or cognitive processes. For example, in the auditory system, the firing rate could encode for frequency, intensity, orientation, or motion direction of the sounds

stimuli (Kral & Sharma 2023, Phillips et al. 2002, Bitterman et al. 2008, Gold et al. 2006, Pachitariu et al. 2016). These measurements provide insights into how neural circuits process information and how changes in firing rates contribute to various brain functions and behaviour. In many cases, an increase in firing rate can be associated with the presence of a stimulus or the engagement of a specific cognitive process (Matthews 1999). For example, in sensory systems, neurons often respond with increased firing rates when they are presented with a preferred stimulus (Cooke et al. 2020). However, it's important to note that the interpretation of firing rates can vary depending on the context and the specific neuronal population being studied. Additionally, the firing rate is just one aspect of neural coding, and other measures such as spike timing, population activity, and synaptic connectivity also play significant roles in understanding neural information processing. Similarly, in cognitive tasks or decision-making processes, firing rates can reflect the encoding of relevant information or the involvement of specific neural circuits. Neurons involved in memory formation or attention, for instance, increased firing rates during the task compared to baseline levels (Lim et al. 2015). On the other hand, a decrease or cessation of firing can also carry information. In some cases, neurons may exhibit decreased firing rates in response to specific stimuli or as part of an inhibitory mechanism (Revill & Fuglevand 2017). Inhibition can be crucial for regulating the activity of neural circuits, preventing excessive firing, or shaping the overall response patterns. It's worth noting that firing rates alone might not provide a complete understanding of neuronal activity. Other factors such as the precise timing and pattern of spikes, as well as the synchronization of activity across multiple neurons, can also contribute to the neural code. Additionally, the relationship between firing rate and information processing can be complex and context-dependent, requiring careful experimental design and analysis to extract meaningful insights. In summary, while higher firing rates often indicate more active neurons and can be associated with stimulus detection or cognitive processes, the interpretation of firing rates depends on the specific experimental context and the properties of the neurons being studied.

1.6.2.0.2 Analysing the spiking pattern Since neurons exhibit variable responses to the same stimulus (Einevoll et al. 2012), averaging the neural responses across multiple stimulus presentations provides a more representative picture of natural brain processing and reduces spiking variability (Cooke et al. 2020). Several techniques are used to describe the spiking pattern of activity. The time to the first spike in response to a stimulus, known as latency, is another measure used (Chase & Young 2007). It provides insights into the speed and efficiency of neural processing, offering valuable information about sensory perception, motor control, and cognitive functions. Latency measurements are crucial for understanding the timing and coordination of neural activity, contributing to our understanding of brain function. These measures serve as valuable tools for studying neuronal dynamics. The interval spiking, also known as the inter-spike interval (ISI), refers to the time duration between consecutive spikes or action potentials generated by a neuron (Reich et al. 2000). ISI analysis is a valuable tool to examine the temporal patterns and regularity of neuronal firing. The ISI could give insight into the firing rate pattern. ISI analysis plays a role in understanding the coding and communication processes within neuronal populations and holds the potential for advancing our knowledge of various neurological disorders and their treatment. To observe possible system-level activity, correlations and synchronicity can be measured among pairs or groups of neurons that are thought to be functionally related. These measures can reveal special events and convey information that is

not captured by the firing rate of individual neurons alone (Malsburg 1994). Temporal pulse correlations can also be examined to determine if a pattern represents a meaningful event. For instance, in the case of a spike pattern involving three neurons, if neuron 1 fires at time t1, followed by neuron 2 at time t1+d, and then by neuron 3 at t1+da+db, where da and db are constants, it might signify a specific stimulus condition (Abeles 1991, Cessac et al. 2010).

1.6.2.0.3 Entropy Information theory offers a framework to quantify the information content in a signal or system by considering the probabilities of different outcomes or events (Shannon 1948). The entropy, a fundamental concept in information theory, represents the degree of uncertainty associated with the state of a continuous, discrete system or a collection of data. The idea of information theory is to assess the information transmitted from a source to a receiver (Figure 1.9) (Reinagel 2000). The information transmission is based on a binary representation, responding the response: 1, 'yes', or, 0, 'no'. For instance, if we consider the example of coin tosses (n), with 1 choosing a particular face, n repetition gives the $N=2^n$ formula. By then, 2^n combination is $\log2(2^n)$ =n bits of information (Reinagel 2000). This binary logarithm captures the binary nature of Shannon's information theory. However, unlike coins tonnes, the probability of an event occurring is not equal (Borst & Theunissen 1999).

The Shannon entropy equation provides, then, a means to estimate the minimum average number of bits, considering the probabilities of those events. In the equation, H represents entropy, and pi denotes the probability of an event, (Figure 1.9. A). The entropy is a dimensionless measure, and it is widely applicable to various types of data. Its utility has been extensively recognized in the neuroscience fields (Borst & Theunissen 1999, Timme & Lapish 2018, Piasini & Panzeri 2019), giving insights into statistical measures of the information contained in neurons, the brain, or fibres, concerning different stimuli and conditions. However, measuring entropy can be challenging due to potential sampling biases resulting from the signal size, quantization levels, and sampling methods, and this aspect needs to be assessed in the study (Piasini & Panzeri 2019). The information theory application to the neurosciences was widely investigated at the end of the 20th Century, soon after the publication of the Shannon paper (Bialek et al. 1991, Rubio & Holden 1975, Mackay & McCulloch 1952, Eckhorn & Pöpel 1974), where the main goal was to adapt the entropy formula to the neural analysis. MacKay and McCulloch (1952) were among the first to apply the concept of information to explore the transmission capacity of nerve cell (Mackay & McCulloch 1952). The (Attneave 1954), and (Barlow 1961), research proposed that the neural structure, particularly in sensory systems, matches the statistical structure of the sensory environment, optimizing the information transmission (Dimitrov et al. 2011). See (Dimitrov et al. 2011) for an intensive historical review of the information theory in neurosciences.

However, after the first investigation efforts in the 60-90s, the information theory in the neurosciences field decreased until the push to new technologies with the increase of recorded neurons. By then, the information theory was used to investigate single unit spike train (Keshmiri 2020, Pryluk et al. 2019), EEG signals (Waschke et al. 2017), or fMRI (Saxe et al. 2018). Changes in the entropy of neuronal activity have been associated with cognitive state and behaviour (Keshmiri 2020). Changes in the entropy of neuronal activity have been linked to more sensitive (Waschke et al. 2017), efficient (Pryluk et al. 2019) coding strategies, or ageing (Saxe et al. 2018) and the entropy seems to be modulated by brain regions (Pryluk et al. 2019) or age groups (Waschke et al. 2017).

Even though most metrics use information theory as their inspiration to compute entropy, we have not observed a specific pipeline or sufficient control over the diversity of potentially sent information to enable a comparison of entropy results between brain areas, cell types, or papers, nor particular clear conclusion on how the neurons entropy change along age. The paper by Pryluk et al. (2019) is interesting in that it normalizes the computed entropy by an analytical entropy that represents the maximum information a particular signal could hold. This approach allows for the comparison of results between cell and brain areas that may have different capabilities (Pryluk et al. 2019). Overall, the entropy of neuronal activity could be an interesting measure of the underlying dynamics of the neural system and can provide insights into how the brain processes and responds to sensory information.

A

Shannon entropy formula:

$$\sum_{i=1}^{n} P_i \log_b \left(\frac{1}{P_i} \right) = -\sum_{i=1}^{n} P_i \log_b P_i$$

B

—Entropy in the case of two possibilities with probabilities p and $(1-p)$.
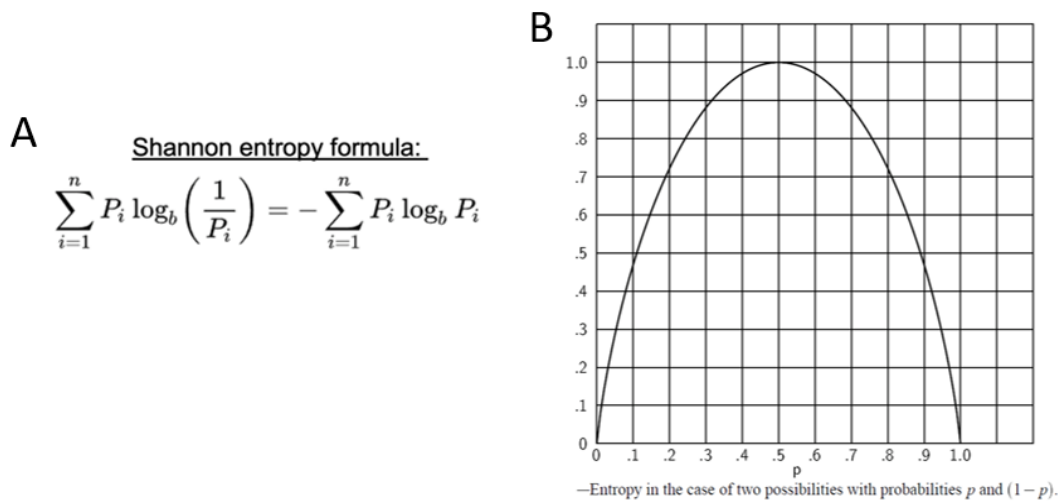
Figure 1.9: *The Shannon information theory*

The entropy is calculated based on the probabilities to observe a particular pattern. The Shannon entropy formula is given by the formula (A), where H(X) is the entropy of the discrete random variable, P(i) is the probability of event i, n is the number of distinct events in the sample space, logb is the logarithm to the base b. Common choices for the base of the logarithm 2 (for bits). The choice of the base determines the unit of entropy. (B) In the case of two possible state of information, an entropy of zero represents a probability to observe one of the two information, and an entropy of 1 represents the probability to observe both of the information. A higher entropy represents a higher unexpectedness *Adapted from (Shannon 1948)*

1.7 Hypothesis and specific aims

Age-related hearing loss is a prevalent condition that affects a significant portion of the population, especially as the population continues to age. Typically characterized as a peripheral auditory impairment, the presbycusis has received limited research attention regarding its effects on auditory cortex (AC) (Jayakody et al. 2018, Fuksa et al. 2022, Gates & Mills 2005). However, given the crucial role of the auditory cortex in auditory integration, it is imperative to investigate how it adapts to these peripheral impairments, as it may provide novel insights into potential therapeutic strategies. The auditory cortex is composed of a complex network of excitatory and inhibitory cell, each playing a crucial role in auditory information processing. The balance between excitatory and inhibitory activity is vital for proper information processing and maintaining the integrity of auditory perception. Disruptions in this delicate balance, which may occur as a result of age-related hearing loss, can lead to altered cortical

responses and impaired auditory function. In addition to age-related changes in peripheral auditory function, ageing also affects the biophysical properties of the brain and cognitive functions. Based on this understanding, we formulated the hypothesis that changes would be observed in the activity of the auditory cortex during the ageing process, we aimed to compare the presbycusis aging model to a non-pathological one. We hypothesise that changes in auditory cortex activity will be observed in the ageing process, and comparing mouse models with different auditory peripheral integrity will help differentiate the effects of peripheral and central ageing on auditory processing. Instigating three axes: -Age-related hearing loss is an important condition that requires further research on its impact on auditory cortex activity. -Understanding how the auditory cortex adapts to peripheral impairments can provide valuable insights into potential therapeutic strategies. -The comparison between mouse models with different auditory peripheral integrity allows for differentiation of the effects of peripheral and central ageing on auditory processing.

To address this hypothesis, we conducted a comparative analysis using two mouse models that exhibit different levels of auditory peripheral integrity. Specifically, we explored the differences in ageing between mice known to carry a mutation affecting the peripheral system and mice without this mutation. By comparing these mouse strains, we aimed to uncover differences in the ageing process within the auditory cortex and differentiate the effects of peripheral and central ageing on auditory processing. The first model is the C57 mice, which carry a specific mutation in the *cdh23* gene, resulting in early-onset hearing loss that progressively worsens with age (Lyngholm & Sakata 2019). The second model is a congenic mouse line obtained by crossing C57 mice with CBA, F1 Hybrid mice, referred to as Hybrid mice, which restore the *cdh23* mutation and display age-related hearing loss without the early onset (Li & Hultcrantz 1994, Lyngholm & Sakata 2019). Moreover, the mice model lifespan permits us to explore these age-related changes and allows us to add our results to the understanding building of auditory processing. To achieve our aims, we analysed the data of a designed experimental procedure (Lyngholm & Sakata 2019) exploring the AC single-unit activity in awake, head-fixed mice presented to silence or natural sounds at different age groups.

The experiment was conducted on awake mice to minimize the potential effects of anaesthesia on brain oscillation, synchrony, and spike train activities. Head-fixed setup facilitates the experiment procedure and permits to minimisation of the effects of other cognitive functions on the spike train, such as running or exploring. To monitor the states of the mice during the experiment, we utilized EEG and pupil tracking. These measures allowed us to assess the behavioural states of the mice. A large number of single-unit activities in the AC were captured by using silicon probes. The wide range of AC possible activities we explore by analysing both spontaneous and evoked-response during the presentation of natural sounds and silence periods to the mice isoloated in an acoustic chamber.

To comprehensively assess the auditory cortex's adaptive changes, we employed natural sounds as stimuli. Natural sounds offer a more ecologically valid representation of auditory inputs compared to synthetic or simple tones. They encompass a wide range of acoustic features, such as temporal dynamics, spectral complexity, and spatial cues, which are essential for auditory perception and higher-level processing. By presenting natural sounds, we aimed to gain a deeper understanding of how age-related hearing loss affects the processing of complex auditory

information. Furthermore, exploring the role of spontaneous activity in the auditory cortex is of great interest. Spontaneous activity refers to the neural firing patterns that occur in the absence of external stimuli. It is thought to play a crucial role in shaping the receptive fields of auditory neurons and maintaining the overall excitability and plasticity of the auditory cortex. By investigating spontaneous activity, we can gain insights into the intrinsic dynamics and functional organization of the auditory cortex. For that purpose, we analysed spiking train metrics as the the firing rate, (FR), the contrast entropy (CE), the mutual information (MI) and the variation of spikes intervals (CV). We hypothesized that these metrics would be complementary, with reflecting the excitability of the AC, and providing information about the amount of information transmitted per spike train.

Age-related hearing loss poses a significant challenge to auditory perception and communication abilities. Understanding the impact of peripheral impairments on the auditory cortex is crucial for developing effective therapeutic interventions. Our comparative analysis of mouse models and exploration of the role of excitatory and inhibitory cell, spontaneous activity, and responses to natural sounds will shed light on the adaptive changes in the auditory cortex during the ageing process. These findings may provide valuable insights into the underlying mechanisms of age-related hearing loss and inform the development of targeted therapeutic strategies to mitigate its effects.

2 Materials and Methods

2.1 Animals and experimental setup

2.1.1 Surgery

All animal experiments were performed in accordance with the United Kingdom Animals (Scientific Procedures) Act of 1986 Home Office regulations and approved by the Home Office (PPL 70/8883). The C57BL/6 background ("C57") and the F1 hybrid of C57BL/6 and CBA/Ca backgrounds ("Hybrid") have been used, respectively, as model of early age-related hearing loss and as a non-pathologic age-related hearing loss model. The C57 X CBA F1 Hybrid restore the cdh23 gene mutation (Lyngholm & Sakata 2019, Frisina et al. 2011) (Figure 2.1 A-C). As our study focused on age-related changes, mice were kept for up to 2 years within the local animal facility. To maintain their body weight, low-calorie diet was given from 3 months of age.

Mice express the ChR2-EYFP in parvalbumin cell (PV-Cre) or in somatostatin cell (SOM-Cre) (PV-Crec57::Ai32c57; SOMCrec57::Ai32c57; PV-Crec57::Ai32cba; SOM-Crec57::Ai32cba). In the present study, a total of 95 mice (39 PV-Crec57::Ai32c57; 28 PV-Crec57::Ai32cba/ca; 17 SOM-Crec57::Ai32c57; 16 SOM-Crec57::Ai32cba/ca) were used. Their age and gender are summarized in table 2.1. For the remainder of the thesis, 'PV-Crec57::Ai32c57 and SOMCrec57::Ai32c57 will be reported using 'C57' and PV-Crec57::Ai32cba and SOM-Crec57::Ai32cba 'Hybrid'.
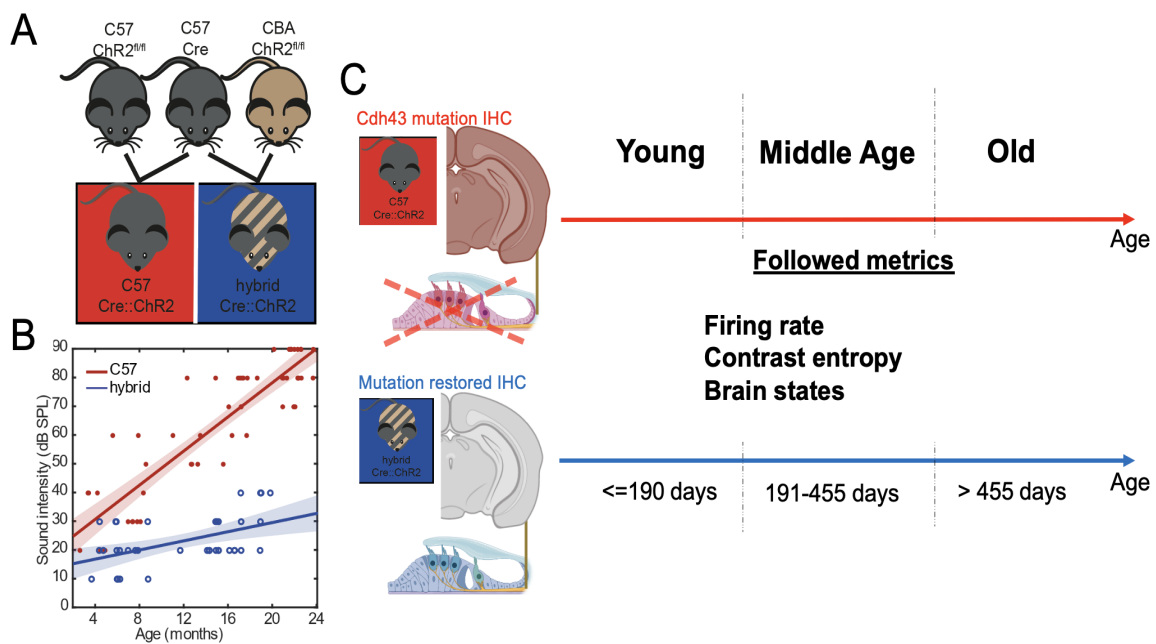
Figure 2.1: *Animals*
A. The crossing between a Cre-driver mice on a C57BL/6J background (top middle) with a Cre-dependent channelrhodopsin2 (ChR2) mice on CBA/Ca background (top right) restore the hearing deficit in the F1 Hybrid (bottom right). B. Sound intensity threshold as a function of age. C57 present a linear hearing loss during ageing compared to Hybrid *Adapted from (Lyngholm & Sakata 2019)*. C. Measurements monitored on C57 and Hybrid, across age-groups to investigate strain age-related changes.

Lyngholm and Sakata (2019) performed and described all experiments in (Lyngholm & Sakata 2019, Yague et al. 2017). Briefly, an initial surgery was performed to attach a head-post to the skull for cortical electroencephalogram (EEG) recording and two screws over the cerebellum for ground and reference. Animals recover for at least 5 days and placed in a head-fixed apparatus (SR-8N-S, Narishige) in a custom made in an acrylic tube. This habituation phased extended gradually from 15 to 60 min. Simultaneously, animals were habituated to sound exposure in the same manner as the electrophysiological recording, see Lyngholm and Sakata, 2019 and Josue G. Yague, 2017 for details (Lyngholm & Sakata 2019, Yague et al. 2017).

Animals were then anesthetized with isoflurane and a craniotomy was performed to insert the recording electrodes into the primary auditory cortex (2 mm × 2 mm at 2.3 mm posterior and 4.2 mm lateral to bregma). The cranial window is protected with a biocompatible sealant (Kwik-Sil, World Precision Instruments). Animals were placed, awake, into the head-fixed setup for testing along with electrophysiological recording. In addition to neuronal signals, a camera (acA1920-25mm, Basler Ace) with a zoom lens (M0814-MP2, Computar) and an IR filter (FGL780,Thorlabs) was placed 10 cm in front of the mouse eye to record the pupil dynamic (Tsunematsu et al. 2020), and the EEG signals were monitored to evaluate brain states. Electrophysiological activities were measured across cortical layers with 32 or 64 channels silicon probes (NeuroNexus, A1x32-10mm-25 s-177-A32 or A4x16-10mm-50 s-177-A64). A day after the accumulation period, the mice were anesthetized with isoflurane and their primary auditory cortex was exposed through a craniotomy (2 mm × 2 mm at 2.3 mm posterior and 4.2 mm lateral to bregma). The cranial window was protected with a biocompatible sealant (Kwik-Sil, World Precision Instruments). An electrophysiological recording experiment was then performed at the desired age for the mice.

2.1.2 *In vivo* electrophysiology

All experiments have been performed by Lyngholm and Sakata, 2019, and are the same as those described in previous works (McAlinden et al. 2015, Scharf et al. 2016, Yague et al. 2017). Briefly, a 32 or 64-channel silicon probe (A1 × 32–10 mm–25 s–177-A32 or A4 × 16–10 mm-50 s-177-A64, respectively, NeuroNexus Technologies) was inserted into the cranial window using a manual micromanipulator (SM-25A, Narishige). The probes were inserted at an angle of $40°–50°$ to be perpendicular to the cortical surface ($800\,\mu m$ to $1000\,\mu m$ depth from the cortical surface), and the recording session was initiated > 30 min after the probe was inserted to its target depth for signal stabilization. Local field potential (LFP) and multiunit activities (MUA) were used to evaluate the AC localization in response to white noise auditory stimulation. The signals were amplified relative to the ground (RHD2132, Intan Technologies, LLC) and digitized at 20 kHz (RHD2132 and RHD2000, Intan Technologies, LLC). Lastly, a typical recording session consisted of an optical stimulation, > 15 min baseline recording of spontaneous activity, followed by different sound types of presentation. This thesis analyzes data during silence and natural sound presentations (Figure 2.2, Figure 2.3. A).

2.1.3 Sound stimulation

Briefly, the recordings were performed in a single-walled acoustic chamber lined coated by three inches of acoustic absorption foam (MAC-3, IAC Acoustics). The sound was digitally generated (sampling rate 97.7 kHz, RZ6, Tucker-Davis Technologies) and delivered through a calibrated electrostatic loudspeaker (ES1) located ∼15

cm in front of the animal. A silence period with no sounds or optical stimulation was used to assess the spontaneous activity in the auditory cortex. Natural sound exposure was used to test the auditory cortex ageing of both mouse strains. The natural sound presentation periods consisted of 10 seconds of stimulation with 1-second intervals at 65, 70, or 80 dB SPL for 30, 50, or 100 repetitions. The number of repetitions, decibel, and type of natural sound presentation did not follow a particular order. The structure of natural sound stimulation was a concatenation of digital natural auditory cues such as bird songs and door closings.
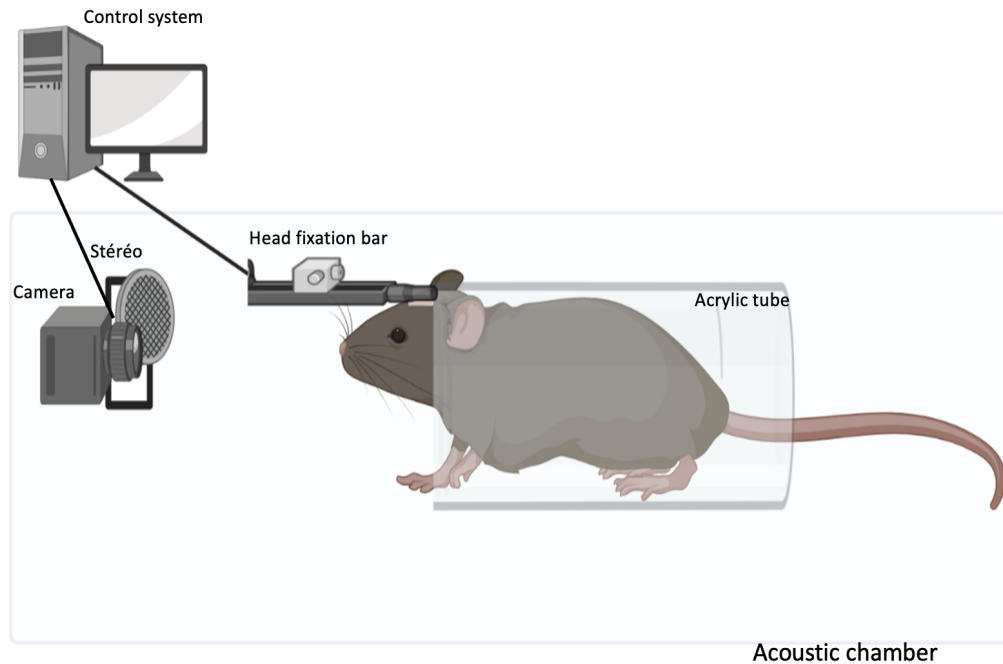
Figure 2.2: *Experimental setup*

Animals were placed, awake, into the head-fixed setup in an acoustic chamber for testing along with electrophysiological recording. Electrophysiological activities were measured across cortical layers with 32 or 64 channels silicon probes, signals were amplified and collected by the computer. The EEG, EMG and ground were connected to an adaptor and amplifier and collected by the computer. Sounds were generated digitally and transmitted to the speaker and camera was connected to the computer.

2.2 Electrophysiological analyses

Spike detection and spike sorting were done by Dr Lyngholm offline using freely available software (Klusta package) (Rossant et al. 2016) or Kilosort (Pachitariu et al. 2016), and data was used to explore the spike train and pupillometry (Figure 2.3).

2.2.1 Single-cell extraction and cell-type identification

Following spike sorting, the inclusion criteria of an isolation distance of > 20 (Schmitzer-Torbert et al. 2005) was used. For each cluster of neurons, the spike waveform was averaged (Figure 2.4. A), and the trough-to-peak duration, width at 20%, and 50% of spike amplitude were calculated (Madisen et al. 2012, Sakata 2016) (Figure 2.4. B-C). These measures present a bimodal distribution, and a trough-to-peak of 0.5 ms was enough to discriminate between broad (> 0.5) and narrow spiking cell (< 0.5).
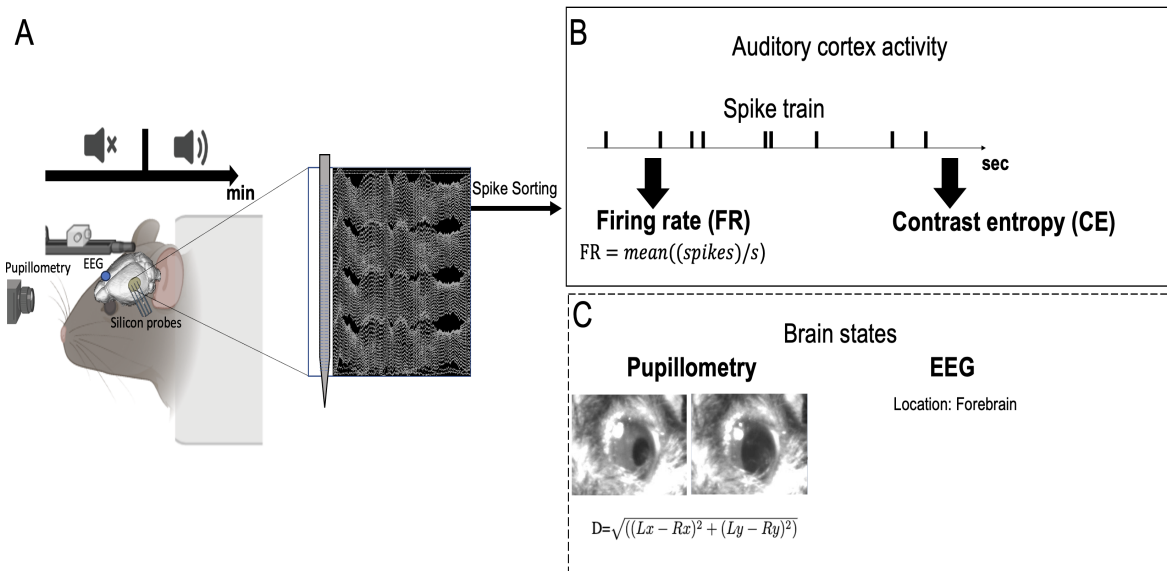
Figure 2.3: *Data Analysis*

A. Awake head-fixed mice were exposed to sound stimulation and silence, see (Lyngholm & Sakata 2019, Yague et al. 2017). Electrophysiological activities were measured across cortical layers with silicon probes inserted in the auditory cortex (AC). A camera recording the pupil dynamic was placed in front of the mouse eyes. The spike sorted data (by Daniel Lyngholm) have been used to characterize auditory cortex activity. B. The spike train of each sorted neuron is used to compute the firing rate measure (FR) or converted to a binary vector for the contrast entropy (CE) calculation. C. Brain states have been investigated using pupillometry and frontal EEG traces. See each related materials and methods sections for formulas and details
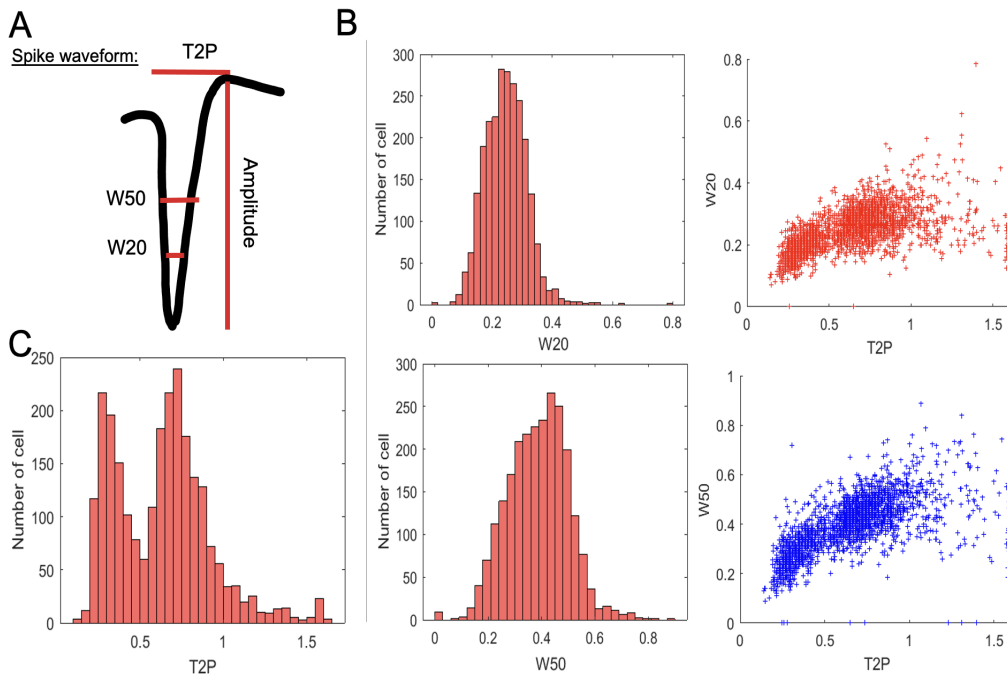
Figure 2.4: *NS and BS cell-type identification, waveform features*

A. Spike waveform example. Discrimination markers 20% and 50% width (W20, W50) and the trough to peak (T2P). B. Histograms of the W20, W50 of all recorded cell (merged strain and age). And their scatter plot vs the T2P. C. T2P histogram of all recorded cell.

2.2.2 Responsiveness to sound

During the experiment, natural sounds lasting 10 seconds were repeated at least 30 times with 1-second intervals between presentations. The number of spikes occurring in bins of 50ms was counted and converted to a firing frequency. The firing rate during the 250ms preceding the stimulus onset (the baseline period) was then averaged. The 10 seconds of sound presentation and the 250ms following it were defined as the evoked-response period, this to include the offset response. A cell was considered responding if its firing rate during the evoked-response period was greater than the baseline firing rate plus three times the standard deviation, otherwise the cell was labelled as non-responding. Same protocol have been followed for noise, with a widows of 50ms for baseline.

2.3 Firing rate calculation

For each cluster of neurons, spike timings were extracted depending on the onsets and offsets of silence and natural sounds. The firing rate of a neuron was then calculated by counting the number of spikes during the silence or sound stimulation period divided by the respective stimulation time length (spikes/seconds). This gives the mean firing rate per second of a particular neurons during silence or natural sound exposure.

2.4 Contrast entropy computation

To assess the efficiency of each neuron, we computed the contrast entropy as described in the (Pryluk et al. 2019) paper. This measure represents the amount of information transmitted within the spike train of a neuron. To do this, we created a time vector with the same onsets and offsets as the sound and silence recording periods. We discretized the vector into bins of length Δt (1, 4, 6, 8 or 16ms) and counted the number of spikes occurring during each bin. If more than one spike occurred, the bin was recorded as a 1, otherwise it was recorded as a 0. This resulted in a binary vector. Next, we read the binary vector from left to right, grouping it into words. For example, the word 1100 indicates that at least one spike occurred in the first two bins, and no spike was counted in the last two bins. We tested words of 4, 6, and 8 letters with Δt bins. We quantified the occurrence of each word, pi, by counting the number of possible words (15 words for 4-letter words) and dividing by the total number of words.
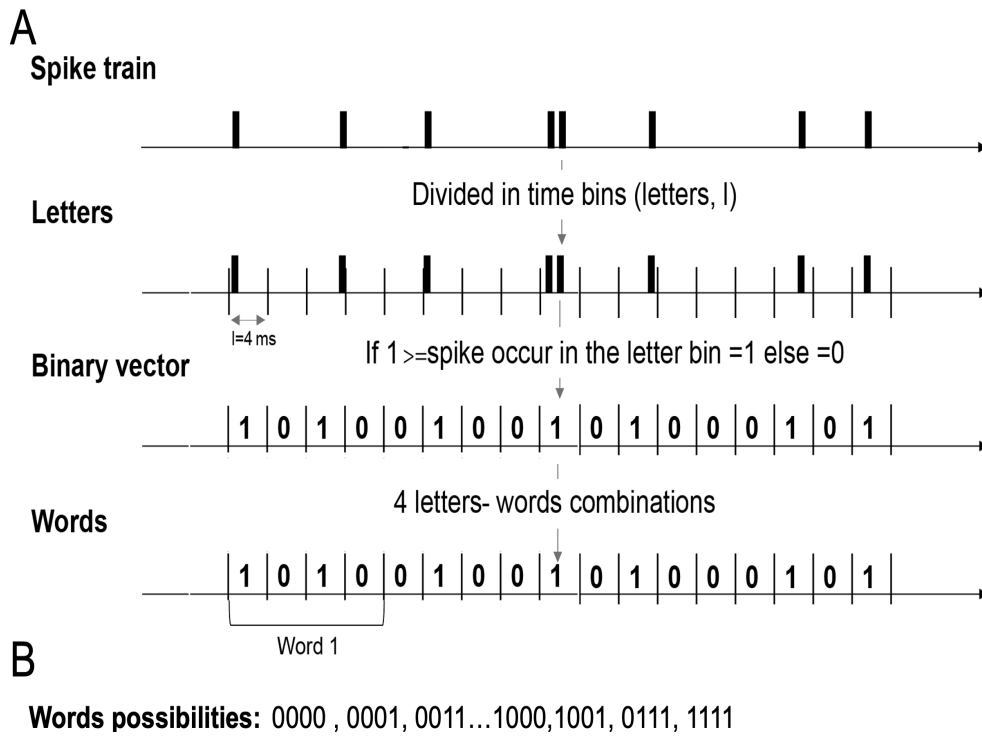
Figure 2.5: *Contrast entropy*
(A) The spike train of each sorted neuron is converted to a binary vector to compute the contrast entropy (Pryluk et al. 2019). The binary vector was done with letters of 1, 2, 4, 6, and 16 ms. The words length were 4, 8 and 16 letters per words. (B) Example of possible words with 4 letters. .

To calculate the contrast entropy, we first computed the Shannon entropy from information theory (Shannon 1948). This involved summing the binary logarithm of each probability to assess the entropy of the signal. Then this entropy is divided by the total length of the words (T, in ms, sot the product of word length and bin size) to give the entropy rate. (Figure 2.5. AB) (Rieke et al. 1999).

To compare different cell types and strains, we divided the entropy rate by the analytic entropy (Pryluk et al. 2019). The analytic entropy describes the theoretical maximum entropy that a neuron's spike rate can hold. It is calculated by assuming that each spike is a random event and follows the Poisson theory. In a random vector, the spikes are indeterminate, and therefore the entropy is maximal. We calculated the probability of a spike occurring in one bin as pr = Δt × FR, where FR is the firing rate. The analytic entropy is then calculated using the following formula:

$$(1) \qquad \mathrm{ER} = \frac{-\sum_i p_i log_2 p_i}{T}$$

$$(2) \qquad \mathrm{EA} = \frac{-\sum_{i-0}^{W} C_i^W p_s^i (1-p_s)^{W-i} log_2 (p_s^i (1-p_s)^{W-i})}{T}$$

$$(3) \qquad ContrastEntropy = \frac{Entropy_R}{Entropy_A}$$

For example, the word 1100 indicates that at least one spike occurred in the two firsts bins, and no spike was occurred in the two last bins (Figure 2.5 B). We tested words of 4, 6, and 8 letters with each Δt bins.

To confirm that the contrast entropy is independent of the firing rate, we calculated the contrast entropy for neurons with matching firing rates. We discretized the neurons into groups based on their firing rate, with each group having a width of 0.1 Hz. The first group contained neurons firing from 0.1 to 0.2 Hz, the second group contained neurons firing from 0.2 to 0.3 Hz, and so on up to the maximum firing rate of 92.8 Hz, for spontaneous analyses, and 81.1 Hz, for the natural sound exposure.

2.5 Mutual Information

The Mutual information between the natural sound presentation and the neurons response have been computed using the information theory toolbox on MATLAB, (Magri et al. 2009). The natural sound envelope of the natural sound is determined using the magnitude of its analytic signal computed by filtering the natural sound signal with a Hilbert FIR filter of 4ms length. The neurons spike trains were discretized in bins of 4ms, to be consistent with the CE study, and the matrix of discretized spike train across trials was used for the MI calculation, performed using the direct method with a quadratic extrapolation (Magri et al. 2009). Neurons with a difference between the MI computed using all the spike train trials is different than the MI computed using only half of the trials is higher than 5 percent, were discretized (Pachitariu et al. 2015).

2.6 Spontaneous and evoked-response comparison

2.6.1 Database

In the spontaneous and evoked-response comparison analyses, only matching mice and cell were used to compare the two conditions. As the experimental protocol for each mouse differed, some mice were not exposed to natural sound stimulation. These mice were therefore excluded from our analyses. See table 2.1 for a summary of the mouse and cell population numbers. To compare the firing rate (FR) and contrast entropy (CE) between the two sound exposure conditions, a normalization index was calculated using the following formula. This allowed us to center all the values around zero. When the value is negative, the FR/CE decreases during the sound presentation period, and conversely, if it is positive, it increases during the sound presentation period.

2.6.2 Fraction of changes index

To compare the activity of the auditory cortex (AC) during periods of silence and natural sound presentation, we employed a computational approach to determine the fraction of changes in firing rate (FR, equation (1)) and contrast entropy (CE, equation (2)) between spontaneous and evoked-response activity .

(1)
$$Index\ FR = \frac{EvkFR - SpontFR}{EvkFR + SpontFR}$$

(2)
$$Index\ CE = \frac{EvkCE - SpontCE}{EvkCE + SpontCE}$$

The computed result is expressed on a scale ranging from -1 to 1, where a value of 0 indicates no discernible difference. A positive value signifies an increase in FR/CE from the spontaneous state to sound presentation, while a negative value indicates a decrease in FR/CE.

2.7 Pupillometry

2.7.1 Pupil dynamic computation

Recorded videos of the pupil (25 Hz) were used to track the pupil diameter for each mouse. A subset of video frames at equal intervals was manually labelled at the left and right pupil edges and used to train the DeepLabCut software (Figure 2.6. A) (Mathis et al. 2018). The software then performed a training phase using the labelled 50 frames per video, after which the pupil edges for all recording sessions were automatically tracked by DeepLab-Cut. This process took several hours (around 6h) and was performed for a total of 45 mice (*see* Table 2.1). Using custom MATLAB scripts, the pupil diameter was calculated using the following formula, where L and R are the left and right pupil edges, respectively, and (x,y) are the label coordinates of the pupil edges per frame.

$$(1) \qquad \qquad D=\sqrt{((Lx-Rx)^2+(Ly-Ry)^2)}$$

To minimize noise errors and experimental artifacts (such as closing eyes or light interference), the pupil dynamics (pupil diameter per frame) were filtered using the movemean function with a smoothing factor of 0.05 at a 0.5 Hz sampling rate (MATLAB signal analyzer app) (Figure 2.6. B).

To analyse the pupil dynamics signal, the distribution of the pupil diameter was evaluated using pupil distribution histograms (with 40 bins, where the peaks represent the number of frames in a particular pupil diameter value) and the first derivative histogram (which is the subtraction between each pupil diameter time point). Four arbitrary pupil states were then established using the following boundaries: median, maximum, and minimum diameter and the average between the median and the maximum/minimum values median+maximum/2 and median+minimum/2. The pupil states maximally dilated (MD), dilated (D), constricted (C), and maximally constricted (MC) were defined as follows: MD corresponds to the frames where the pupil size is between the maximum and maximum+median/2, D between maximum+median/2 and median, C between median and minimum-median/2, and MC between minimum-median/2 and minimum.

Pupil states were then used for statistical analysis to compare the total fraction of time spent in each state (time in one state/ total time), the number of transitions between states, and the mean duration of each state (time spent in one state) across age and mouse strains.

2.7.2 Pupil dynamics and firing rate cross-correlation

To determine the correlation between the pupil dynamics and the spike train, we counted the number of spikes that occurred during bins of 0.04s throughout the spontaneous recording. The histogram of firing activity was aligned with the pupil's dynamic signal, by then at a 25 Hz frequency. Each pupil diameter value was aligned with the bins that occurred during the -0.02 s before to the +0.02 s after. The peri-stimulus time histogram (PSTH) was then transformed into a single vector using a Gaussian filter function in MATLAB. To quantify the correlation, we calculated the Pearson correlation coefficient and the cross-correlation between these two signals over a period of 30 seconds moving window using MATLAB functions corrcoef and xcorr (MathWorks).
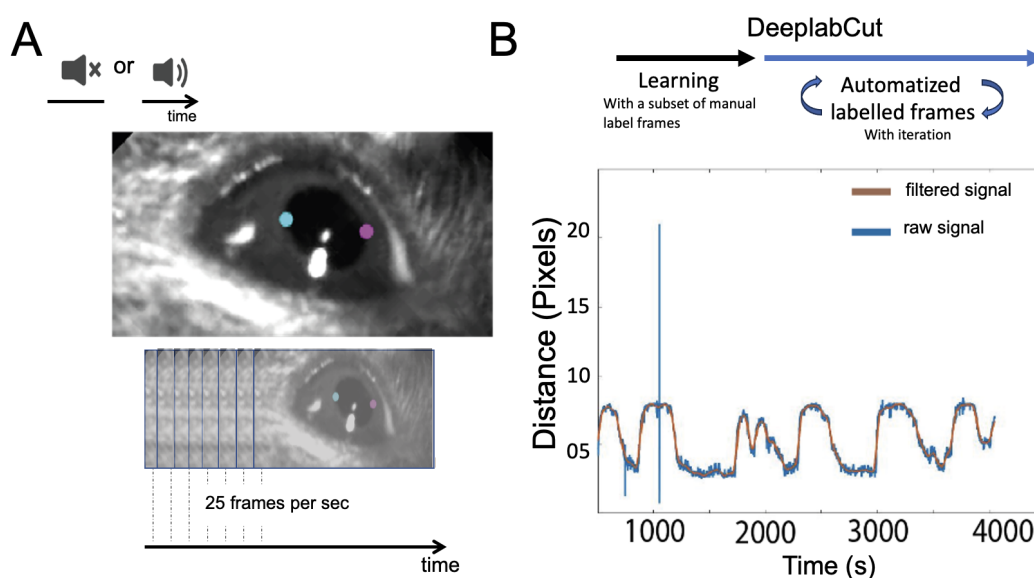
Figure 2.6: *The pupil analysis*
A) The pupil edges are labeled manually using the software Deeplabcut (Mathis et al. 2018). The labeled frames are used to train the deep learning algorithm to automatically label the remaining frames. The diameter of the pupil is calculated using MATLAB and the dynamic of the pupil is observed along the frames converted to time in seconds. B) This signal is then filtered to exclude technical or experimental artifacts.

2.8 EEG analysis

2.8.1 Frequency bands relative power determination

To assess the changes in the mice' brain states, we compute the power spectral density (PSD) using the Pwelch function in MATLAB (MathWorks). This function divides the signal into segments with an overlap of around 50%, deletes the white noise, and applies the Fourier transformation (DFT). In our analysis, we used 1024 as the length of the windows vector and as the number of points in the DFT, 512 is the number of overlapped samples. The signal is sampled at 1000 frames per second (Fs). The function used is pwelch(signal, 1024, 512, 1024, Fs). As most of our recording contains experimental artifacts, the frequency band between 45 and 60 Hz was removed and we ended our analysis at 90Hz. We then extracted the PSD of the most common frequency bands (delta: 0.5 to 4 Hz, theta: 4.5 to 8 Hz, alpha: 8.5 to 13 Hz, beta: 15 to 25 Hz, low-gamma: 30 to 45 Hz; high-gamma: 60 to 90 Hz) to calculate their relative power by normalizing their power spectral density with the total power spectral density.

2.8.2 EEG and pupil dynamics cross-correlation

A correlation between pupil dynamics and EEG activity was determined by cross-correlating pupil diameter for 1 ms and frequency bands' power spectral density (PSD) for a 1-second window, using a 30-second moving window (xcorr, MathWorks). PSDs of each frequency band were calculated for each second of the EEG signal, which was divided into one-second bins. As a final step, we computed the pwelch function for each pupil state episode to assess the correspondence between the pupil states and EEG power. The purpose of this analysis was to determine whether a specific frequency band or pattern of frequency bands predominated during a certain pupil

state.

2.9 Statistical analysis

Age groups have been established using the Jackson library (Flurkey et al. 2007), where young mice have been defined as those younger than 190 days old, middle-aged (adults) between 191 and 449 days old, and old from 450 days old. Data analyses were performed using custom-written MATLAB scripts (MathWorks). The Pearson's correlation analysis between the firing rate (FR) and the contrast entropy (CE) or entropy rate (ER) was done using the corrcoef MATLAB function (MathWorks). The cross-correlation between pupil dynamics and power spectral densities (PSDs) or spike trains was performed using the xcorr function (MathWorks). The linearity regression between the spontaneous and natural sound FR or CE or the frequency PSD along ageing was tested with the fitlm function (MathWorks). Statistical analyses were performed using R-studio software (R core team, 2022). Comparisons between multiple groups and variables were investigated using 2-way ANOVA and Tukey post-hoc tests after testing for normality and homogeneity of variance. In the case of non-homogeneity, data were transformed using their logarithmic function (in the firing rate analysis) or the Scheirer-Ray-Hare test, and the Dunn test with Bonferroni correction as a post-hoc test or the ANOVA and Tukey post-hoc with 999 permutations were performed. Two variables were compared using a t-test or Wilcoxon Mann-Whitney test if the data distribution was not homogeneous. Normality and homogeneity were tested using the Shapiro and Bartlett tests. Proportions of responding and non-responding cell were tested using the prop.test function (R Core Team 2022). The CE figures were computed using the ggplot2 package (Hadley Wickham,(R Core Team 2022)), and the Rmisc, readxl, dplyr, and vegan packages were used to optimize the coding (Ryan M. Hope, Hadley Wickham, Jari Oksanen, (R Core Team 2022)).

Table 2.1: Table of mice and single unit used in the electrophysiology and pupillometry analysis

		Strain	N mice female | male	Young female | male	Adult female | male	Old female | male	N cells	Young BS|NS	Adult BS|NS	Old BS|NS
Electrophysiology	Silence	Hybrid	19 | 21	5 | 5	6 | 7	8 | 9	1361	124 | 56	267 | 183	367 | 232
		C57	29 | 39	6 | 3	10 | 7	13 | 29	1497	189 | 123	218 | 136	649 | 314
	Sound	Hybrid	20 | 15	5 | 5	1 | 6	9 | 9	1317	211 | 132	118 | 133	444 | 264
		C57	8 | 19	3 | 1	3 | 7	2 | 11	832	105 | 42	162 | 92	272 | 142
Pupillometry	Silence	Hybrid	8 | 10	1 | 2	4 | 3	3 | 5				
		C57	7 | 16	3 | 1	3 | 3	1 | 12				
	Sound	Hybrid	6 | 9	1 | 2	1 | 3	4 | 4				
		C57	6 | 13	2 | 3	3 | 2	1 | 10				

3 The spontaneous activity of the auditory cortex during silence

I. Spontaneous activity ▶ **II. Natural evoked-response activity** ▶ **III. Comparison Spontaneous and Evoked activities**
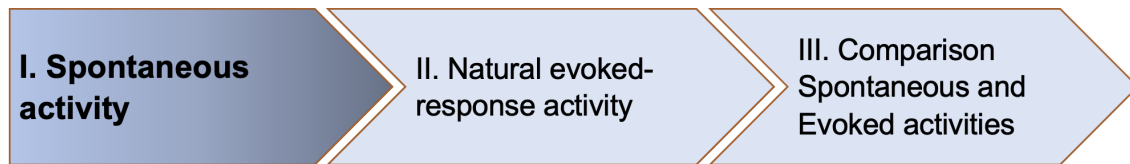
The AC plays a crucial role in processing and interpreting auditory information, contributing to our ability to perceive and understand sounds. One important aspect of AC function is its spontaneous activity, which refers to the ongoing neural patterns in the absence of external stimuli. Spontaneous activity in the AC is thought to be involved in various physiological processes, including sensory processing, maintenance of receptive fields, and the establishment of functional connectivity (Harris & Thiele 2011, Meyer-Baese et al. 2022, Eggermont 2015).

As individuals age, there are changes in the auditory system that can lead to hearing loss, known as presbycusis (Gates & Mills 2005). Presbycusis is a complex condition influenced by both peripheral and central factors. While the peripheral components involve the loss of sensory hair cell and damage to the cochlea, the central components involve alterations in neural processing along the auditory pathway. However, all these changes may be closely intricate. Currently, it remains unclear whether the spontaneous activity differs between healthy age-related hearing loss and presbycusis models. It is plausible to expect that the presbycusis model may exhibit distinct spontaneous activity patterns, potentially representing different ongoing processes within the AC.

In this study, we aim to investigate the effects of ageing on auditory cortical processing using two mouse models: the Hybrid mice mouse strain, which serves as a model of central age-related changes with minimal peripheral impairment, and the C57 mouse strain, which serves as a model of age-related hearing loss with significant peripheral impairment in addition to central ageing. By examining these models, we can gain insights into how age-related hearing loss affects the spontaneous activity in the AC ageing, how the AC adapts and potentially identify specific alterations associated with presbycusis.

To achieve our research objectives, we conducted experiments on awake, head-fixed mice, a setup that minimizes the influence of other cognitive functions on the neural spike trains. Building upon a designed experimental procedure previously utilized by Lyngholm et al. (2019), we analysed the single-unit activity of the AC in response to silence at different age groups (Lyngholm & Sakata 2019). We analysed data from a total of 95 mice at different ages (Table 2.1). This allowed us to observe the activity of a large number of cell and cross-sectionally track the changes in AC activity over time. We specifically focused on two spike train metrics : the firing rate (FR) and the contrast entropy (CE). We hypothesized that these metrics would provide complementary information, with the FR reflecting the excitability of the AC cells, while the CE would offer insights into the amount of information transmitted within the neural network. By examining the spontaneous activity and its age-related changes in these mouse models, we aim to shed light on the neural mechanisms underlying age-related hearing loss and the role

of the AC in this process. Understanding these mechanisms could contribute to the development of interventions and strategies for preventing or mitigating the effects of presbycusis, ultimately improving the quality of life for individuals affected by age-related hearing loss.

3.1 Cell-types identification

We were initially interested in describing the AC cell-types and excitability, (Figure 2.4), for that we classified recorded cell into two types, namely Broad-Spiking cell (BS) and Narrow-Spiking cell (NS), by analysing their spike waveforms. Cell types were classified using a trough-to-peak threshold of 0.55ms (Figure 3.1 A), as outlined in the Materials and Methods section. These cell types are commonly described as putative excitatory and inhibitory fast-spiking cell, respectively (Figure 3.1 C) (McCormick et al. 1985, Connors & Gutnick 1990, Frank et al. 2001), although there is ongoing debate about their exclusive identification (Lee et al. 2021). A total of 1705 cell from C57 mice and 1543 cell from Hybrid mice were analysed, with proportions of 34% and 39% NS in C57 and Hybrid mice, respectively (Figure 3.1 AB). This proportion was generally consistent across our mice with some exceptions (Figure 3.1 C).

The literature describes an average of 25% inhibitory cell and 75% excitatory cell in the cortex (Tremblay et al. 2016). The slight variation in the ratio of cell types may be attributed to factors such as sampling variation, spike sorting analysis, and inclusion criteria. We further analysed the firing rates and contrast entropy of the identified cell to investigate changes associated with ageing. (Table 2.1) presents information on the total number of mice and cell used in our study.
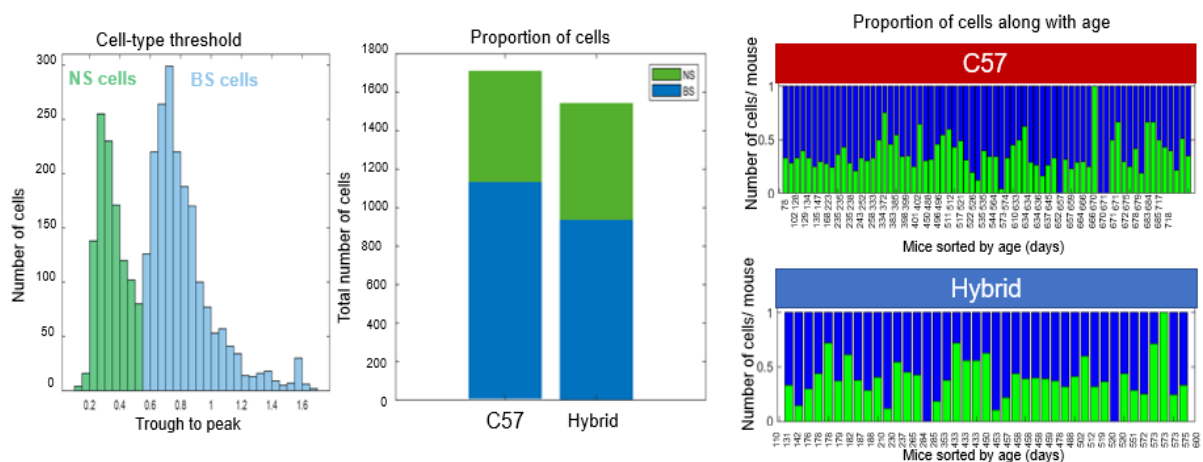
Figure 3.1: *Identification of Broad-Spiking (BS) and Narrow-Spiking cell (NS)*
(A) Histogram of trough-to-peak, T2P, distribution per cell. The threshold for the T2P duration was set at 0.55 to differentiate between NS (green) and BS (cyan). (B) The proportion of recorded cell in C57 and Hybrid mice: C57, n=1705 cell with 577 NS and 1128 BS; Hybrid mice, n=1543 cell with 607 NS and 936 BS. (C) The proportion of cell per mouse across different ages for C57 (top) and Hybrid mice (bottom), the mice are sorted by age.

3.2 Decrease in the spontaneous FR of BS and NS in Hybrid mice with age

We, then, aimed to observe the excitability of the cells. For that, we investigate the spike rate of the AC cell by computing the Firing Rate (FR), which is the average number of spikes per second of each cell. We

will, first, describe the spontaneous activity of the model of central age-related changes with minimal peripheral impairment, Hybrid mice (3.0.2), and then compared it with the age-related hearing loss, C57 mice model (3.0.3). We examined whether FR in Hybrid mice changes as they age (Figure 3.2. A-C) and observed a slight decrease in the FR in both BS and NS (Figure 3.2. A). The same trend was observed when plotting the mean FR per mouse (Figure 3.2. B). To quantify this trend, we grouped the mice into three age groups based on the criteria of Jackson Lab (Jackson library 2017, Fox & Amsterdam): young (>190 days old), middle-age (called "adult") (190 - 450 days old), and old (>450 days old). We found that the FR of BS and NS decrease significantly across age groups (BS, $F_{(2)}$=12.43, $p < e-3$; NS, $F_{(2)}$=6.57, p=.0015, one-way ANOVA with post-hoc Tukey HSD test) (Figure 3.2. C). On the other hand, there was no significant difference in the FR between the two cell types at any age group nor an interaction effect of age groups and cell types (Hybrid mice BS vs NS: $F_{(2, 1)}$ = 101.7, p = .1, two-way ANOVA). Thus, in Hybrid mice, spontaneous activity decreases in both BS and NS as they age.

3.3 Increase in the spontaneous FR of BS C57 with age

We tested the FR activity in the C57 mice strain in the same way as we tested Hybrid mice FR. We found that the BS FR increased their activity with age (Figure 3.2 DEF). This increase was observed progressively along age groups, with an increase from young to adult and from young to old ($F_{(2)}$=8.06, p=.0003, one-way ANOVA; p=.005 and p=.0002, respectively, Tukey HSD Post hoc). The FR activity in the C57 NS is not significantly different with age. In Hybrid mice, the FR activity in the C57 mice did not differ between cell types, and there was no interaction effect between age groups and cell types (C57 BS vs NS: $F_{(2, 1)}$ = 13, p = .24, two-way ANOVA).

3.4 Age-related difference in the BS spontaneous FR between young and old Hybrid and C57 mice

We compared the FR between Hybrid and C57 of all recorded cell in the AC (All), as well as BS and NS subgroups (Figure 3.3. A). We found no significant difference in the FR between the two strains in either cell type (Figure 3.3. A). However, along the age-groups, we observed a significant interaction between age-groups and strain effect, (All cell: $F_{(2, 1)}$=20.53, p=1.4e-9, two-way ANOVA), reflecting the previous observed results, with an increase in FR between young and adult and young to old in C57 (All cell: p=.01, p=.002, Tukey HSD post hoc) and a decrease between young to old, adult to old in Hybrid mice (All cell: $p>e-5$, p=.0005, Tukey HSD post hoc). These results confirm the results observed in Figure 3.2. Cell-types analysis revealed that this increase in FR was primarily due to the BS (Figure 3.3. B), which exhibited a significant increase in FR from young to adult and young to old age in C57 mice (Figure 3.3. C, $F_{(2, 1)}$=16.75, p=6.18e-8, two-way ANOVA, young to adult p=.008, young to old p=.001, Tukey HSD post hoc), while the FR decreases between young to old and adult to old in Hybrid mice (p=.0007, p=.0005 Tukey HSD post hoc). In the NS group, we observed and effect of the age-groups and strain interaction ($F_{(2, 1)}$=4.01, p=.01, two-way ANOVA), but no significant difference is observed instead of the decreases in the Hybrid mice FR from young to old, as observed in Figure 3.2. C (Figure 3.3. C, p=.007, Tukey HSD post hoc).
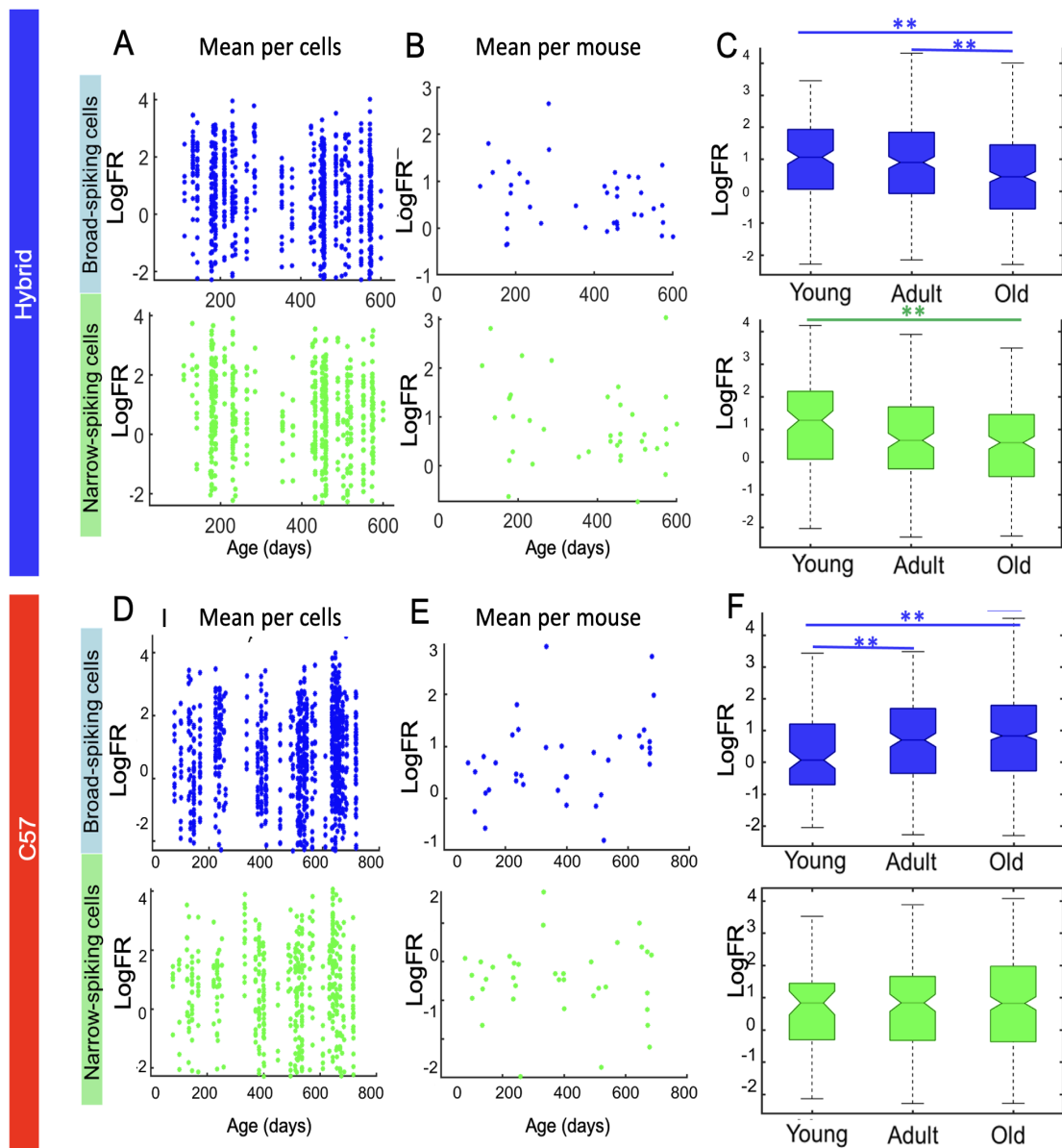
Figure 3.2: *Age-related decrease in FR during spontaneous activity in Hybrid mice auditory cortex and increases in BS C57*
(A) FR along with ageing. The logarithmic mean FR (Log FR) of BS (top, blue) and NS (bottom, green) of all cell decreases with ageing. Each dot represents the cell Log FR. (B) Log FR per mouse along with ageing. Each dot represents the mean Log FR of all recorded cell per mouse. (C) Boxplots of the Log FR per age-groups. BS Log FR decreases significantly from young to adult and from adult to old ($F(2)=12.43$ $p=4.8$-06, one-way ANOVA, both $p<e$-3, Tukey HSD Post hoc). In NS it decreased from young to old ($F(2)=6.57$ $p=.0015$, one-way ANOVA, $p<e$-3, Tukey HSD Post hoc). (D) Same as in (A) for C57. (F) Same as in (B) for C57. (F) Same as in (C) for C57. The BS Log FR increases from young to adult and from young to old ($F(2)=8.06$, $p=.0003$, one-way ANOVA; $p=.005$ and $p=.0002$, respectively, Tukey HSD Post hoc)..

Differences in the FR between C57 and Hybrid mice strains were observed in BS in both young and old age groups (Figure 3.3. B). The FR of young C57 was found to be significantly lower compared to that of Hybrid mice ($F(2,1)=16.75$, two-way ANOVA, $p=.0001$, Tukey HSD Post hoc). Conversely, in old animals, an increase in the C57 FR was observed alongside a decrease in the Hybrid mice FR, resulting in a higher C57 FR in the old group (Figure 3.3. B, $F(2,1)=16.75$, two-way ANOVA, $p=.004$, 2-way ANOVA, Tukey HSD Post hoc). These findings

suggest that age-related changes in the AC FR may vary across the mouse strains and support the need for further investigations into the underlying mechanisms driving these differences.

Here, we observed differences in the spontaneous mean FR between the two strains from a young age. They followed divergent kinetic trajectories as they aged, eventually converging at adult age, and differing again at old age. In C57, the FR increased, while in Hybrid mice, it decreased. In both strains, we observed cell-types specificity in ageing, with Hybrid mice and C57 showing inverse changes in BS spontaneous mean FR and a constant mean FR in C57 contrasting with a decrease in Hybrid mice. These findings suggest that peripheral impairment in C57 may impact spontaneous activity in an age-dependent manner in the auditory cortex.
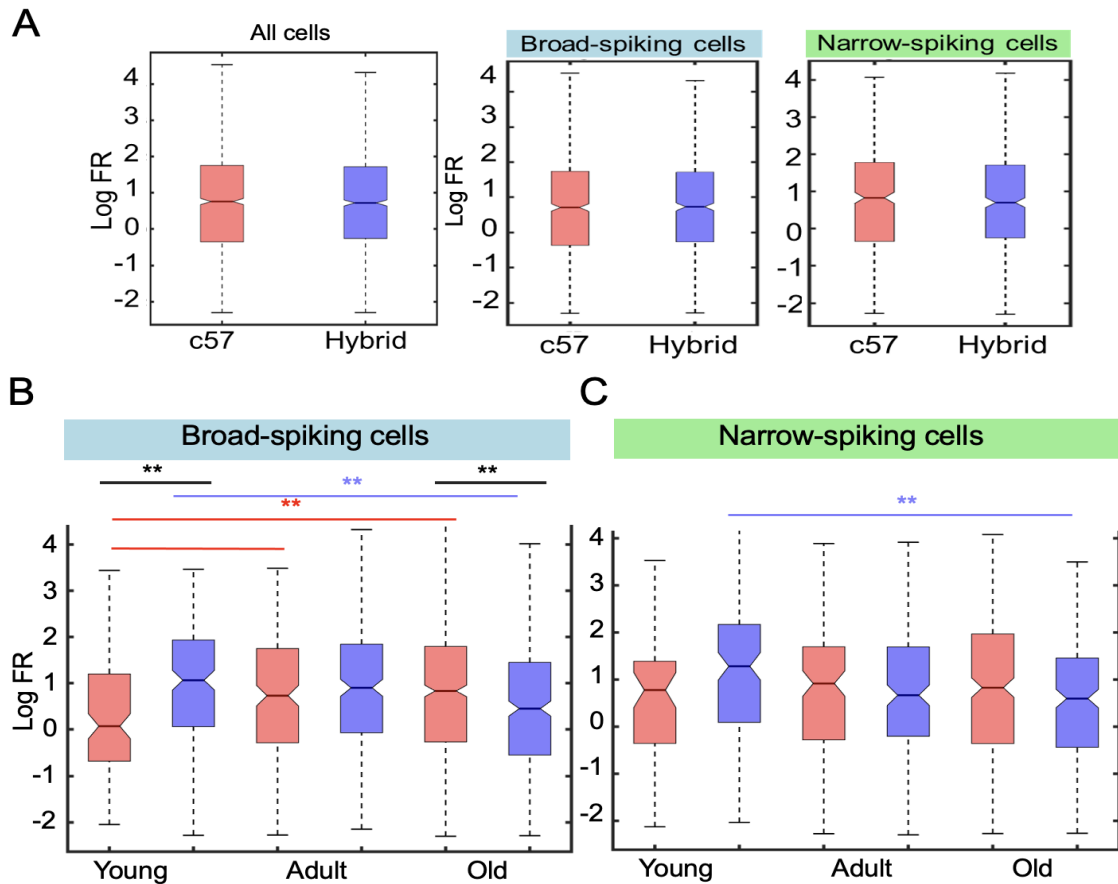
Figure 3.3: *Age-related difference in the BS spontaneous FR between young and old Hybrid mice and C57.*
(A) All cell Log FR comparison between Hybrid mice and C57 (left panel), with respective medians of 0.7205 and 0.7586. BS (middle panel) with median CE of 0.7283 and 0.7082 for Hybrid mice and C57 and for NS (right panel) with median CE of 0.7037 and 0.8318 for Hybrid mice and C57. (B) Age-related changes in Hybrid mice and C57 BS Log FR. In BS, the Log FR C57 increased from young to adult and from young to old (F(2,1)=16.75, two-way ANOVA, young to adult p=.008, young to old p=.001, Tukey HSD post hoc) and decreases from young to old (F(2,1)=16.75, two-way ANOVA, p=.0007, Tukey HSD post hoc). The Log FR of C57 is lower than Hybrid mice in both young and old age groups (F(2,1)=16.75, two-way ANOVA, young p=.0001, old: p=.004, Tukey HSD Post hoc). (C) Age-related changes in Hybrid mice and C57 NS Log FR. Significant interaction effect between strain and age-groups (F(2,1)=8.20, two-way ANOVA, p=.01) is observed. Note that Hybrid mice Log FR decreased as previously observed in Figure 3.2 C (young to old p=.0007, Tukey HSD post hoc).

3.5 The contrast entropy metric

Since the firing rate does not take into account the structure of the spike train, we wanted to assess how the spiking patterns of individual neurons are changed by ageing. To this end, we computed the contrast Entropy (CE), which is defined as the proportion between the observed entropy rate of a neuron and the theoretically maximum entropy rate, given a certain FR (Pryluk et al. 2019, Rieke et al. 1999). The CE measure converts the neuron's spike train into a binary vector of words and assesses whether the neuron utilizes a significant proportion of its total number of possible words. A high contrast entropy value indicates that the neuron is utilizing a large portion of its possible words, while a low contrast entropy value indicates the opposite. Then, the CE of the neuron is not influenced by the firing rate, thereby providing a more nuanced understanding of the spike train. In essence, the CE provides a measure of the information efficiency of a neuron, (Rieke et al. 1999).

If the CE along ageing is different between the C57 and Hybrid mice strains, this could represent the difference in neurons capability in the utilization of the possible range of possible words and underlie difference in the AC computation in case of impairment of the peripheral auditory system. If that is the case, different hypotheses can be proposed regarding the relationship between CE and ageing (Figure 3.4. A). If the CE increases with age, this represents a wider utilisation of the possible words and could reflect a) a compensatory mechanism of the auditory cortex to convey information, b)or the coding specificity is altered. If the CE decreases along age, this represents a more systematic vocabulary utilisation that could reflect a)an effect of ageing on the coding efficiency, with the capability to transmit less information per spike train or b) a compensatory mechanism where the neuron's vocabulary needs to be robust. Finally, if the CE is maintained along with ageing, it could reflect that the efficiency of the neurons is not affected by ageing, even if the FR is, or that underlying mechanisms are put in to maintain the spike train capability as a function of ageing.

It is worth noting that when we discuss "the transmission capability", the analysis only pertains to the transmitter of information, the neuron spike train, and does not reflect the receiver's capacity to receive the information, the post-synaptic neuron. In addition, the CE value only assesses the ability of the neuron to utilize the available words in its vocabulary and does not provide information about the size of the vocabulary or how it changes across age-groups. Since we do not have any specific hypothesis regarding the optimal size of the vocabulary across different strains, age-groups, cell-types, and even within the same cell-type of neurons, the CE appears to be the most suitable measure to gain insights into the pattern of spike trains. Finally, a difference in the CE between Hybrid mice and C57 could reflect how the AC convey differently the information. Again, three hypotheses are possible . If the CE in Hybrid mice and C57 is similar, the information transmission capability of the neurons spike train is not affected even if the FR is different. If the CE is higher in Hybrid mice /C57 than C57/Hybrid mice, the Hybrid mice neurons are more efficient, and they present more variability in their spike train. This could represent a) more sent commands, and b) less robust spike trains. If the CE is lower this could represent, inversely a)a more restricted number of sent commands and b) a more robust pattern of spike trains.

3.6 Calculation of the contrast entropy during spontaneous acitivity period

We started with the examination of the AC CE during the spontaneous activity. In this study, we investigated 2,830 neurons comprising 1,469 cell from the C57 strain and 1,361 cell from the Hybrid mice strain. We first calculated the Entropy Rate (ER), this measurement based on the Shannon entropy metric (Pryluk et al. 2019), represents the sum of words probabilities of the neurons, (Materials and Methods-Contrast entropy computation). To minimize the impact of arbitrary choices in defining letter and word sizes, we evaluated the entropy rate using 15 different combinations of letter bins and word lengths (letter bins: 1, 2, 4, 8, and 16 ms; word lengths: 4, 8, and 16 letters/words). Next, we compared the ER to the analytic entropy (EA), which represents the probability of all possible words that could be spoken by the neuron. To calculate this, each spike is defined as a random event and the Poisson law is applied to compute all possible outcomes. Upon comparing the values of EA and ER, we observed that their range of values is similar, which validates our calculations (Figure 3.4. B). This finding is consistent with the pioneering research on CE by Pryluk et al., 2019 (Pryluk et al. 2019).
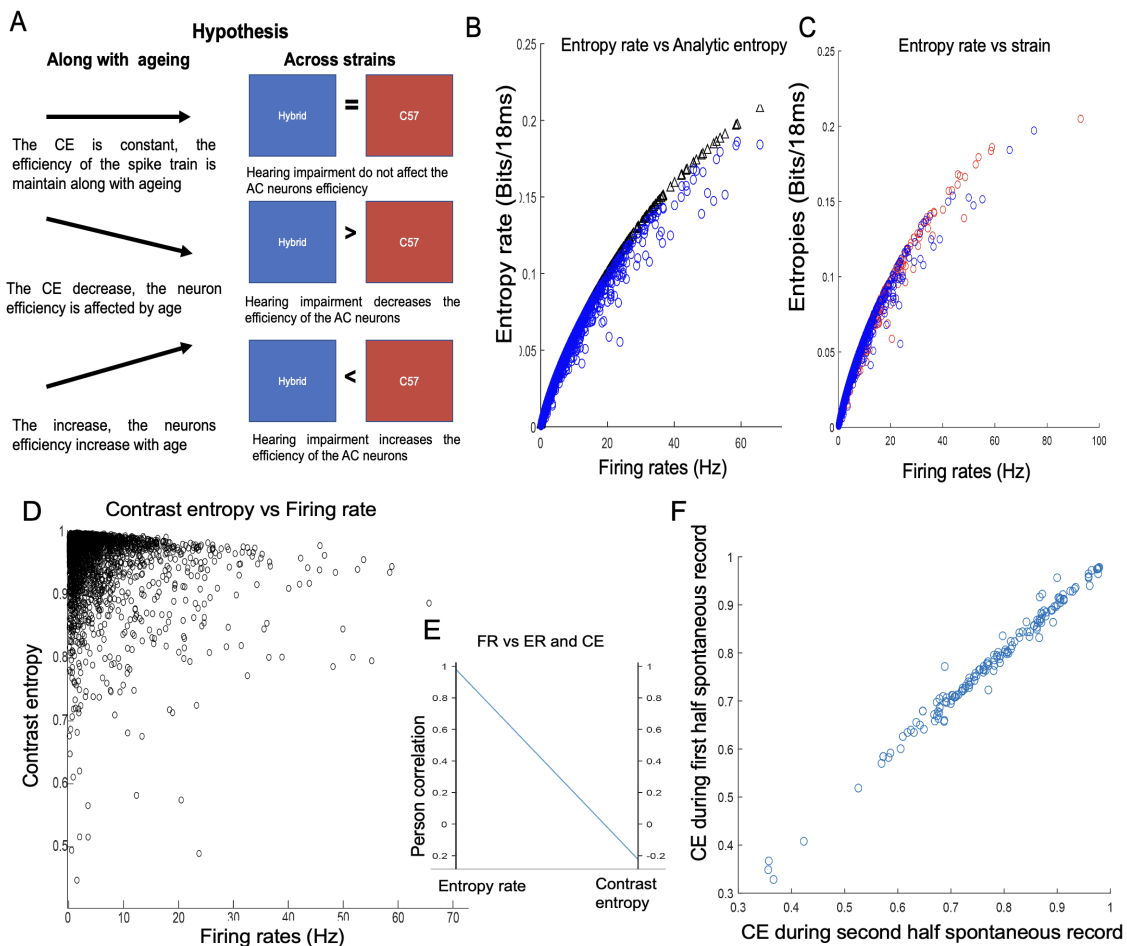
Figure 3.4: *Spontaneous contrast entropy computation 1*
(A) Hypothesis of the study along ageing and across strains. (B) Comparison between the analytical (EA, black triangles) and observed entropy (ER, blue circles). (C) ER, comparison between the C57, red, and Hybrid mice, blue. No significant differences. (D) Cells contrast entropy, (CE), vs FR. The CE computation minimizes the relation between the ER and the FR. (E) Pearson correlation coefficient between the FR and the ER (R^2=0.98) or CE (R^2=-0.8). (F) Comparison of the CE computed for the first and second half of the record duration.

As depicted in Figure 3.4 BC, an increase in the neurons FR leads to higher entropy, which is in line with previous studies including the pioneering work by Pryluk et al. (2019) and a recent study by Ohyama et al. (2020) (Pryluk et al. 2019, Ohyama et al. 2020). Moreover, we observed no difference in the ER between the Hybrid mice and C57 (Figure 3.4. C, p>.05, Wilcoxon Mann-Whitney test).

Dividing the ER by the EA leads to the CE to limit the FR, age groups, cell type, or strain influence on the word probability analysed (Figure 3.4 DE). After calculating the CE, our observations showed that the values were found to fluctuate around 1, a finding consistent with prior studies (Pryluk et al. 2019, Ohyama et al. 2020). A value of 1 signifies that the spike trains were capable of generating all possible words with maximum probability, implying that the neurons conveyed information efficiently. Therefore, a higher contrast entropy value is indicative of a neuron using a more diverse range of vocabulary during its activity. In Figure 3.4. DE, we observed that the CE per cell distribution is no longer affected by the FR, and the correlation between ER and FR, (R^2=0.98, Pearson correlation), is abolished while comparing the CE with the FR (R^2=-0.8). The length of the silent period, which we studied, was approximately 20 minutes. To verify that the number of words was not affected by sampling size, we compared the observed probability of words with the theoretical one during the spontaneous period and during the all recording, (Figure 3.5. G Figure 3.5. H). We found that spontaneous recordings contained most possible words, and their occurrences were consistent with the theoretic predictions (Figure 3.5. G). Notably, neurons with high CE overlapped with the analytical maxima more narrowly than those with low CE, as previously reported (Pryluk et al. 2019, Ohyama et al. 2020). When we analysed the probability of words for longer recordings, approximately two hours, we found an overlap mismatch (Figure 3.5. H). Consequently, increasing the length of the recording did not increase the overlap between recorded words and theoretical probabilities. Thus, the 20-minute spontaneous recording is sufficient for analysing the contrast entropy. Finally, we analysed the CE for the first half and the second half of the record by cross-validating the estimation of CE (Figure 3.4. F).

3.7 CE follows a U-shaped trend across aging in Hybrid mice BS while it stable in NS during the spontaneous activity

As for the analysis of FR ageing, we first characterized the ageing CE of the non-pathological hearing loss model, Hybrid mice (Figure 3.6. A-C). Quantifying across age-groups (Figure 3.6. C), we observed a U-shaped trend with ageing in the BS CE of Hybrid mice. With a decrease in the CE from young to adult and an increase from adult to old (Chi-squared (2)=11.52, p=0.003, Kruskal-Wallis test; p=.001 and p=.003, respectively, Dunn test post hoc), while it remains constant in Hybrid mice NS. Comparing between the two cell-types, we observed age-groups (H(2)=15.89, SRH test, p=.0003) and cell-type effects (H(1)=23.27, SRH test, p<e-6) effects, with the BS showing higher CE than NS, but no significant interaction effect. This suggests that inhibitory neurons in the Hybrid mice AC maintain their spontaneous vocabulary regardless of age, in contrast to excitatory neurons which have a more limited vocabulary during adulthood.
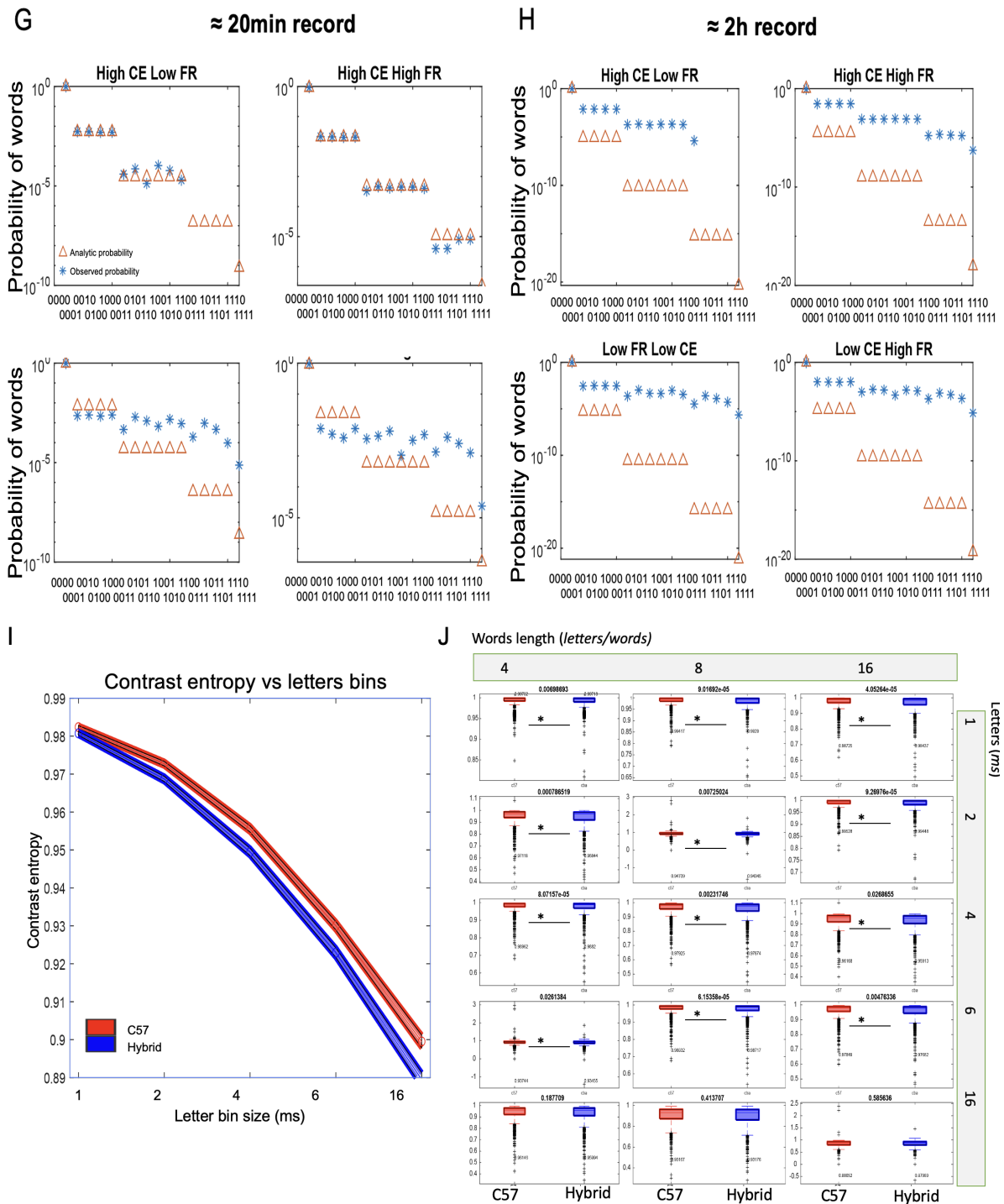
Figure 3.5: *Spontaneous contrast entropy computation 2*

(G) Accuracy between analytical and observed words probabilities. The graph shows the expected probability of words (red triangles) and the recorded neurons' word probability (blue asterisk) for four types of neurons (high and low contrast entropy/firing rate activity) for the spontaneous time record of around 20 minutes. From left to right and bottom to top: CE=0.99 FR=1.79, CE=0.99 FR=10.63, CE=0.7 FR=23.73, CE=0.86 FR=23.74. (H) Same as (G) for the entire recording length of around 2 hours. Note the poorer overlap. Same neurons than in (G). (I) CE vs letter bin size. The blue (Hybrid mice) and red (C57) lines represent the mean of the contrast entropy and its standard deviation for the different letter bin sizes for words of 8 letters. (J) Comparison of the CE values for the 15 combinations of letter and word length. All p are significant except for words with 16ms letters. From A to I-results are presented for 4ms letters with 4 letters per word.

3.8 The CE pattern in C57 is stable across ageing during the spontaneous activity

In C57, we found that the CE remained stable across age and in both cell-types (Figure 3.6. D-F). Comparing the CE between the two cell-types with ageing, we observed no effect of ageing or interaction between the two variables. However, as with the Hybrid mice group, the NS CE is lower than the BS (H(1)=27.55, p=1.52e-7, one-way ANOVA).
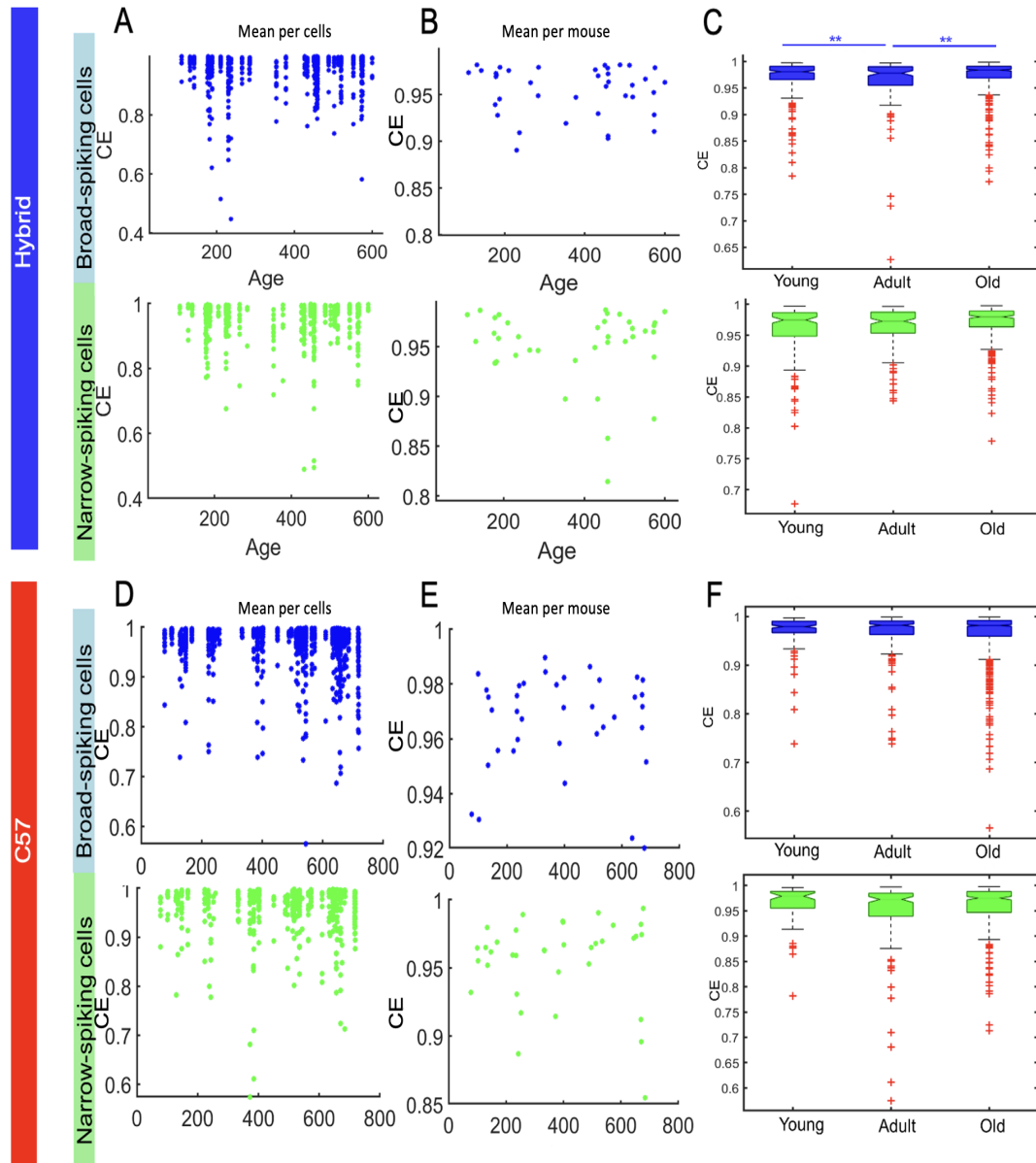
Figure 3.6: *U-Shaped CE pattern of Hybrid mice BS neurons with a stable CE pattern in NS and in BS and NS C57 during spontaneous ageing*
(A) Hybrid mice cell CE in both BS (top) and NS (bottom) along age. (B) Hybrid mice CE along age. Each dot represent the mean CE per mouse. (C) Hybrid mice CE across cell types and age groups. In BS the CE follow a U-shape (Chi-squared (2)=11.52, p=.003, Kruskal-Wallis test; p=.001 and p=.003, respectively, Dunn test post hoc). NS CE is stable along with ageing. (D) as in (A) for C57. (E) as in (B) for C57. (F) as in (C) for C57. No significant effect has been observed. The CE is computed for 4ms letter with 8 letters per word..

3.9 C57 neurons show a higher CE than Hybrid mice neurons during spontaneous activity

Comparing the cell CE between strains reveal that the C57 shows a higher CE than Hybrid mice during spontaneous activity (p=.0023, Wilcoxon Mann-Whitney test (Figure 3.7. A). This difference is not attributed to variations in the ER or EA calculation between the two strains, as shown in Figure 3.4. C. Furthermore, grouping the neurons based on their FR range (+/- .1 HZ) reveals that the C57 neurons exhibit qualitatively a higher CE than the Hybrid mice neurons in most of the FR groups (Figure 3.7. B). Consistently, the C57 neurons demonstrate higher CE than the Hybrid mice for all letter and word combinations, except for 16ms bin size (Figure 3.5. IJ). These findings align with previous studies that have demonstrated that CE decreases with coarse bin discretization for various species and brain regions (Pryluk et al. 2019, Rieke et al. 1999). In summary, our results indicate that during spontaneous activity, the AC cell exhibit higher spike train efficiency in C57 mice compared to Hybrid mice, providing support for hypothesis 3, Figure 3.4. A.

Comparing strains CE between cell-types (Figure 3.6. C), we observed that the BS CE was lower in Hybrid mice (p=.048, Wilcoxon Mann-Whitney test) while NS CE level did not differ between Hybrid mice and C57 mice. The CE in BS was higher than in NS for both mice strains (Figure 3.6. D, C57 p=1.57e-7, Hybrid mice p=1.41e-6, Wilcoxon Mann-Whitney test). This result suggests that inhibitory cell have more robust spike trains than excitatory cell during spontaneous activity, in both mice strains. Upon comparing between age-groups, we observed that the CE of C57 mice remains stable with age in both cell-types (Figure 3.7. E) at the same level as young Hybrid mice. However, the CE is affected by ageing in Hybrid mice, while it decreases in adulthood resulting in a significant difference between adult C57 and Hybrid mice CE, a difference attributed to the activity of BS (Figure 3.7. E, H(2,1)=6.09, SRH test, p=.04, adult C57 vs Hybrid mice p=.025, Dunn test Post hoc with Bonferroni correction). The CE of NS remains constant along with ageing in both mice strains.

In this Chapter III of the thesis, we investigated the activity of the auditory cortex during spontaneous activity in Hybrid mice and C57 mice, with a focus on ageing. Our findings indicate that while the FR decreases in both Hybrid mice cell types, the CE follows a U-shaped pattern in adulthood, suggesting that neurons become more robust or less efficient in adulthood compared to younger and older ages. In C57 mice, the FR increases in BS with ageing and remains constant in NS, while the CE is stable with ageing in both cell types. Overall, the CE and FR are similar between strains, but they show age-group and cell-type specificities. The NS mean FR is similar between the two strains but is higher in BS in young and lower in old Hybrid mice compared to C57 mice. Where the efficiency of the neurons is similar in NS and BS but lower in adult Hybrid mice BS. This suggests that peripheral impairments affect the spontaneous FR of excitatory cell from a young age. These results suggest, also, that the AC of C57 mice has similar capabilities as that of Hybrid mice. This makes sense as only the peripheral auditory system is initially affected in C57 mice. However, these findings also indicate that peripheral impairment affects the functional architecture of the cortex and its spontaneous activity with ageing.
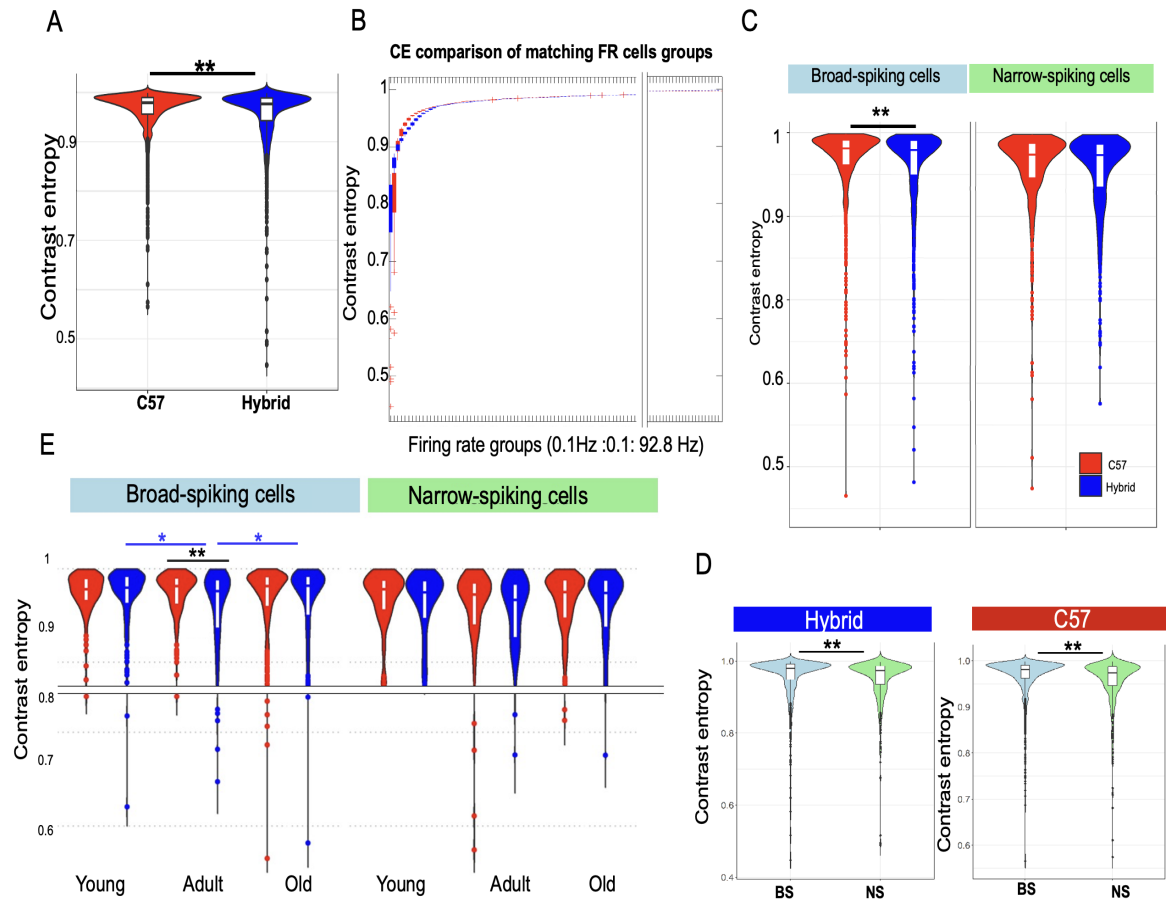
Figure 3.7: *The CE is higher in C57 BS compared to Hybrid mice*

(A) CE vs mice strain. Hybrid mice show a lower CE than C57 (p=.0023, Wilcoxon Mann-Whitney test), median CE Hybrid mice =0.977, n Hybrid mice =1361 cell; CE C57=0.979, nC57=1469 cell. (B) CE of neurons grouped by FR in Hybrid mice and C57. Each FR group contain cell with the same FR +/- 0.1Hz/bin. The range of FR was from 0.1Hz to 92.8Hz. (C) CE per cell-types. Hybrid mice show a lower CE than C57 in the BS (cyan) (p=.04, Wilcoxon Mann-Whitney test), medians CE Hybrid mice =0.979, CE C57=0.981. There is no significant difference in the NS CE (green), medians CE Hybrid mice =0.974, C57=0.973. (D) Cell-types CE within strains, The BS showed a higher CE than NS in both Hybrid mice (left, blue) (p=1.41e-6, Wilcoxon Mann-Whitney test) and C57 (right, red) (p=1.53e-7, Wilcoxon Mann-Whitney test). (E) CE ins BS (cyan, left) and NS (green, right) along age-groups and across strains. In BS, left and NS, right. The C57 CE is higher than Hybrid mice in the adult age group (F(2,1)=6.09, SRH test, p=.04, adult C57 vs Hybrid mice p=.025, Dunn test Post hoc with Bonferroni correction). Note that the Hybrid mice BS CE follow a U-shaped (H(2,1)=6.09, SRH test, p=.04, young vs adult p=.01, adult vs old p=.03, Dunn test Post hoc with Bonferroni correction)..

> **Key findings**:
>
> ❖ As mice age, the spontaneous firing rate decreases in both cell types in Hybrid mice, while it increases in the BS of C57 mice and remains stable in the NS.
>
> ❖ The CE during spontaneous activity follows a U-shaped pattern with aging in Hybrid mice (BS), while it remains constant in C57 mice.
>
> ❖ The CE during spontaneous activity is higher in C57 mice than in Hybrid mice (BS), particularly at adult age.

The evoked-response activity of the auditory cortex during natural sound presentation

| I. Spontaneous activity | **II. Natural evoked-response activity** | III. Comparison Spontaneous and Evoked activities |

Ageing is associated with changes in auditory function, including alterations in the AC's evoked-response activity (Price et al. 2017). Age-related hearing loss, known as presbycusis, involves both peripheral and central components. While peripheral factors such as the loss of sensory hair cell contribute to presbycusis (Gates & Mills 2005), the central components involve age-related changes in neural processing within the AC. Investigating the evoked-response activity of the AC in age-related hearing loss models can provide insights into the neural mechanisms underlying this condition. When presented with sounds, the AC generates a characteristic pattern of neural responses that reflect the encoding and analysis of various acoustic features (Theunissen & Elie 2014). Analysing the AC's response to sound is essential for understanding the mechanisms underlying auditory perception and the effects of ageing on auditory processing.

In this study, we aim to investigate whether the evoked response to natural sounds differs between a healthy age-related hearing loss model and a presbycusis model. It is of particular interest to examine the response to natural sounds, as they represent complex auditory stimuli that encompass a wide range of spectral and temporal features (Theunissen & Elie 2014, Nelken et al. 1999*a*, Theunissen et al. 2000, Rieke et al. 1995). By focusing on natural sounds, we can gain a more comprehensive understanding of how the AC processes and represents ecologically relevant auditory information. Therefore, this type of stimulus is more likely to resemble real-life auditory stimulation (Theunissen & Elie 2014). Moreover, several studies support that natural sounds elicit more robust and complex neural responses in the AC compared to pure tones (Nelken et al. 1999*a*, Rieke et al. 1995, Theunissen et al. 2000). To the best of our knowledge, there is currently limited research comparing the evoked-response activity of the AC to natural sounds across different age groups and between healthy and presbycusis models. This knowledge gap highlights the importance of our study, as it can provide novel insights into the alterations in evoked-response activity associated with ageing and presbycusis. By comparing the evoked responses in these models, we can determine whether there are distinct patterns of AC activity related to the different hearing profiles and explore potential differences in the neural coding of natural sounds.

To investigate these questions, we conducted experiments utilizing a well-established experimental protocol to assess the evoked responses of the AC in both healthy age-related hearing loss and presbycusis models. We analysed the neural responses elicited by natural sounds across different age groups, focusing on specific metrics such as response magnitude, latency, and selectivity to different sound features. By elucidating the age-related changes in the evoked-response activity of the AC during the natural sound presentation, we aim to enhance our

understanding of the mechanisms underlying age-related hearing loss and the specific alterations in neural processing associated with presbycusis. This knowledge can contribute to the development of targeted interventions and therapies for individuals affected by age-related hearing loss, ultimately improving their auditory perception and quality of life. We presented natural sounds to awake, head-fixed mice during the same experimental session as the spontaneous analysis. The natural sound stimulation consisted of a succession of natural sounds (such as bird songs and door closings) presented for 10 seconds, followed by a 1-second interval, and repeated 30, 50 and 100 times (Figure 4.1. A). In this Chapter IV, we will first investigate the responsiveness of the mice AC to natural sound presentation across age groups and strains. This will enable us to quantify the percentage of cell that respond to such stimuli. Subsequently, we will analyse the FR and CE of the AC during natural sound-evoked responses, focusing on age-related changes.

4.1 Responding (R) and non-responding (NR) cell identification

As the C57 mice become deaf over time (Lyngholm & Sakata 2019, Ison et al. 2007), due to the peripheral impairment, we wanted to investigate how the AC is activated by sound during ageing. To measure the responsiveness of AC cell, we counted the number of spikes occurring during the 10-second natural presentation over the repetitions and compared it with the number of spikes occurring in the 250-ms preceding window, baseline (Figure 4.1. B-D, Materials and Methods Identifying Cell Responsiveness). Briefly, the peri-stimuli histogram (PSTH), aligns all the sound stimulation spike trains and counts the number of events in a 50ms bins length. Then the PSTH, converted to Hz, was then used to detect responding (R) and non-responding (NR) cell. A neuron was considered an R cell if at least a one-time bin during sound presentation crossed a threshold of mean FR plus 3 standard deviations (Figure 4.1. D).

Figure 4.1. E shows examples of R and NR cell PSTH. We observed distinct types of responses, ranging from sparse to dense. These different response types could reflect the neuron's sensitivity to different sound structures and/or components, Figure 4.1. B , such as onset, offset, and harmonics) (Solyga & Barkat 2021, Nelken et al. 1999*b*). This could also represent different strategies of coding (sparse or dense), as various signal coding schemes, in particular the sparse coding have been described in the literature (Beyeler et al. 2019).

4.2 Proportion of responding cells to natural sound stimulation across strains and age-groups

We first determined whether the proportion of responding cell is maintained across ageing and different mouse strains. The proportion of R and NR cell is the fraction of R and NR on the total number of cell per mouse. We presented the proportion of R and NR per mouse sorted by age for Hybrid mice and C57, as well as across age groups (Figure 4.2. A-D). We observed a tendency for a decrease with age in both Hybrid mice and C57 mice, particularly in Hybrid mice NS and in both BS and NS in C57.
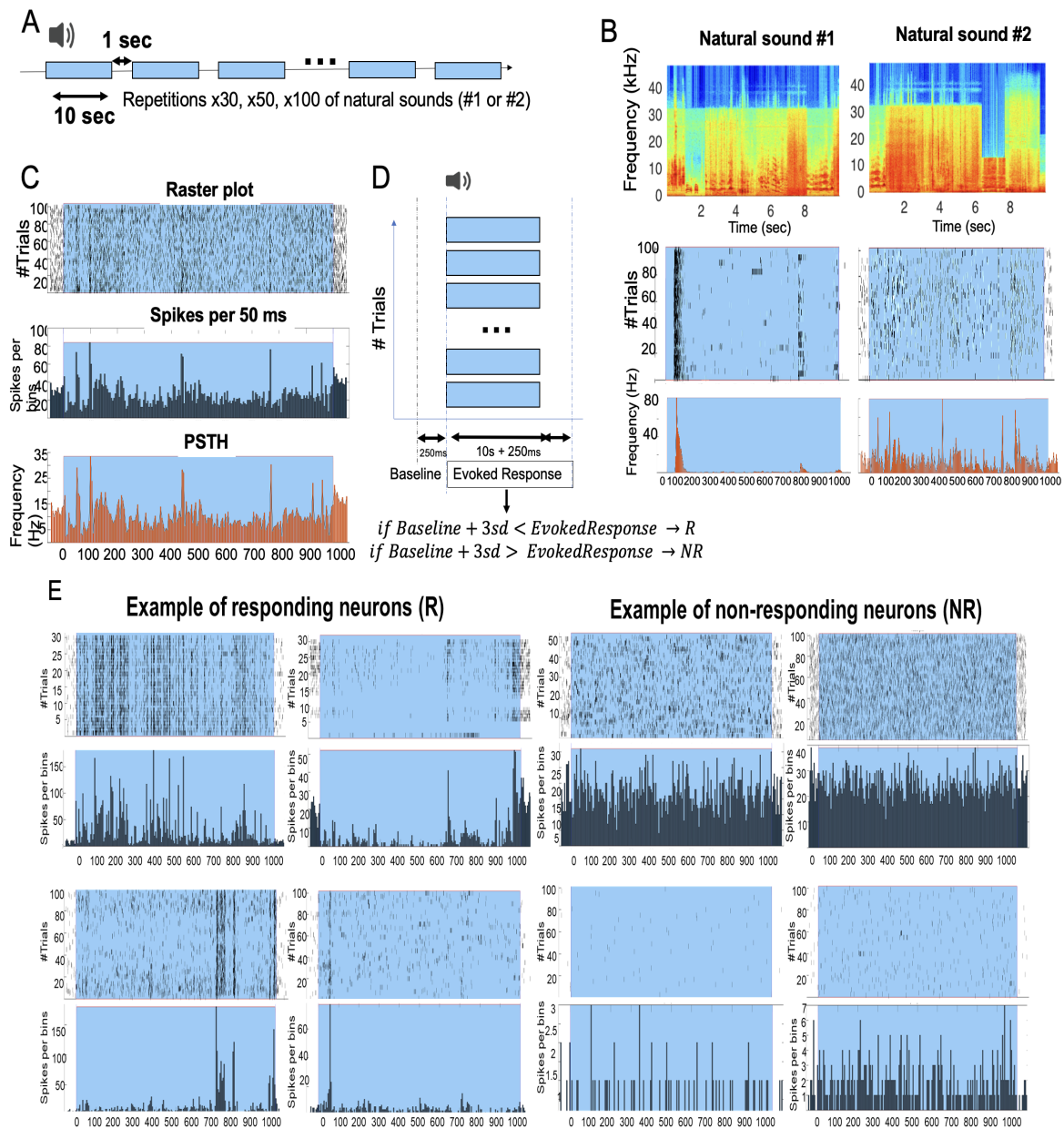
Figure 4.1: *Identification of responding (R) and non-responding (NR) cell types*

(A) Natural sounds presentation protocol. The protocol consisted of repeated ten-second natural sound stimulation with a 1-second interval repeated 30, 50, or 100 times to awake head-fixed mice. Sounds with different dB levels of 60, 70, and 75 dB were presented. Two types of natural sounds have been presented to the mice. No particular order has been followed for the dB, number of repetitions or natural sound type presentation. Blue colour rectangles represent sound exposure times. (B) The structure of both used types of natural stimuli with related neuron responses examples. The blue areas represent the exposure time, the middle panels are the raster plot and the bottom panel is the PSTH. (C) Procedure to identify responding (R) and non-responding (NR) cell. See Materials and Methods-Identifying Cell Responsiveness for more details. From top to bottom, the neuronal response for each repetition is aligned, and the number of spikes within 50 ms is counted in a histogram. The number of spikes per histogram is converted to firing frequency (Hz), the PSTH. (D) The mean FR during the baseline period, 250ms, plus three standard deviations (sd) was used as a threshold to label the cell as R if one bin crosses the threshold,3 or NR otherwise. (E) Example of responding (left) and non-responding cell (right). The blue ribbon represents the 10-second sound presentation window.

69
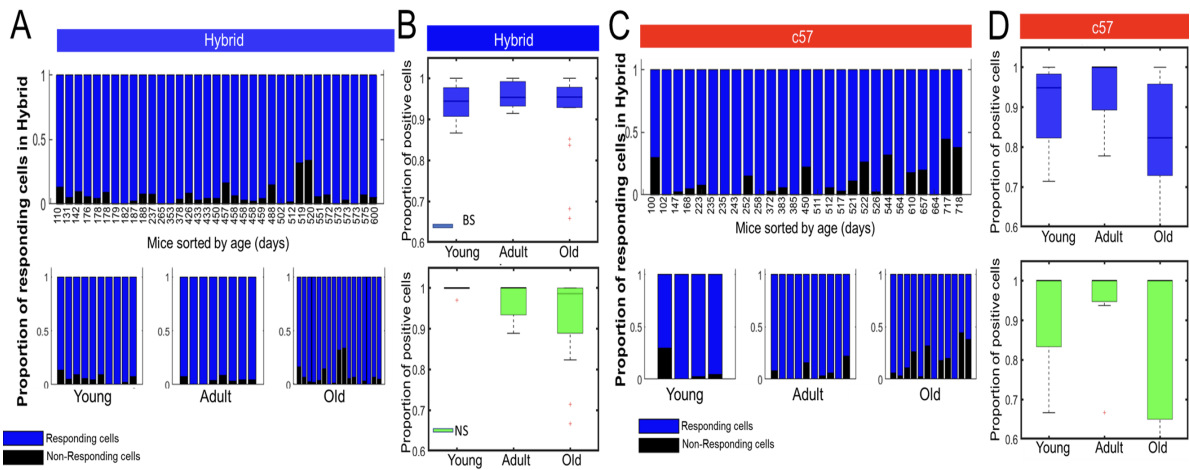
Figure 4.2: *Proportion of responding cell per mouse*
(A) Proportion of responding cell along with ageing in the Hybrid mice strain. (B) Boxplot of the age-groups proportion of R per mouse in the BS (blue, top) and NS (green, bottom) in Hybrid mice. (C) The proportion of R along with ageing in the C57 strain. (D) Boxplot of the age-groups proportion of R per mouse in the BS (blue, top) and NS (green, bottom), in C57.

Comparing between strain (Figure 4.3), we computed the mean proportion of responding cell per mouse and we observed the same tendency of decreasing in the number of R and a tendency to a lower proportion of R in C57 than in Hybrid mice, (Figure 4.3. C-D). The analysis of the mean proportion of R per mouse can be biased by the number of cell that were recorded per mouse, see the Materials and Methods chapter. This is because some mouse might have only one recorded neuron, which could impact the observed proportion of responsiveness. To address this issue, similar to the FR and CE analysis, we opted to compare the mean proportion of cell across groups of mice rather than across the mean per mouse followed by the mean age-group. We found that the proportion of NR was higher in C57 (Figure 4.3. E, p=6.35e-5, proportion test). In both cell types, the proportion of R was lower in the old group of C57 than in Hybrid mice (Figure 4.3. F, BS p=.003, NSC p=.002, proportion test). In addition, the responsiveness decreased in the Hybrid mice NS (Figure 4.3. G, young to old p=.02, proportion test) as well as in both cell types in C57 mice (Figure 4.3. G, BS p=1.29e-5 and NS p=.002, proportion test).

4.3 Decrease with age in the natural sound evoked-response FR of both cell types in Hybrid mice

Similar to the previous section, we investigated age-related changes in FR in Hybrid mice during sound presentation, (Figure 4.4. A-C). We computed the FR during all the sound-presentation protocol, including the 10 sec sound exposure repetitions and the 1 sec intervals (Figure 4.1. A). Our analysis revealed that FR tended to decrease with age in both BS and NS, as observed by analysing cell FR (Figure 4.4. A) and mean FR per mouse (Figure 4.4. B). We found that the Hybrid mice FR decreases from young to adult and from too old in the two cell-types (Figure 4.4 C, BS: F(2)=9.2, p=.0001, one-way ANOVA; p=.002 and p=.0001, respectively, Tukey HSD Post hoc, NS: F(2)=9.59, p=8.13e-5, one-way ANOVA; p=.0001 and p=.0013, respectively, Tukey HSD Post hoc). While comparing the cell types we observed an age-groups effect (F(2)=16.81, p<e-5) and a cell-types effect,

(F(2)=24.31, p=.0001, two-way ANOVA), where the FR of NS is higher than BS but no interaction effect with age groups.
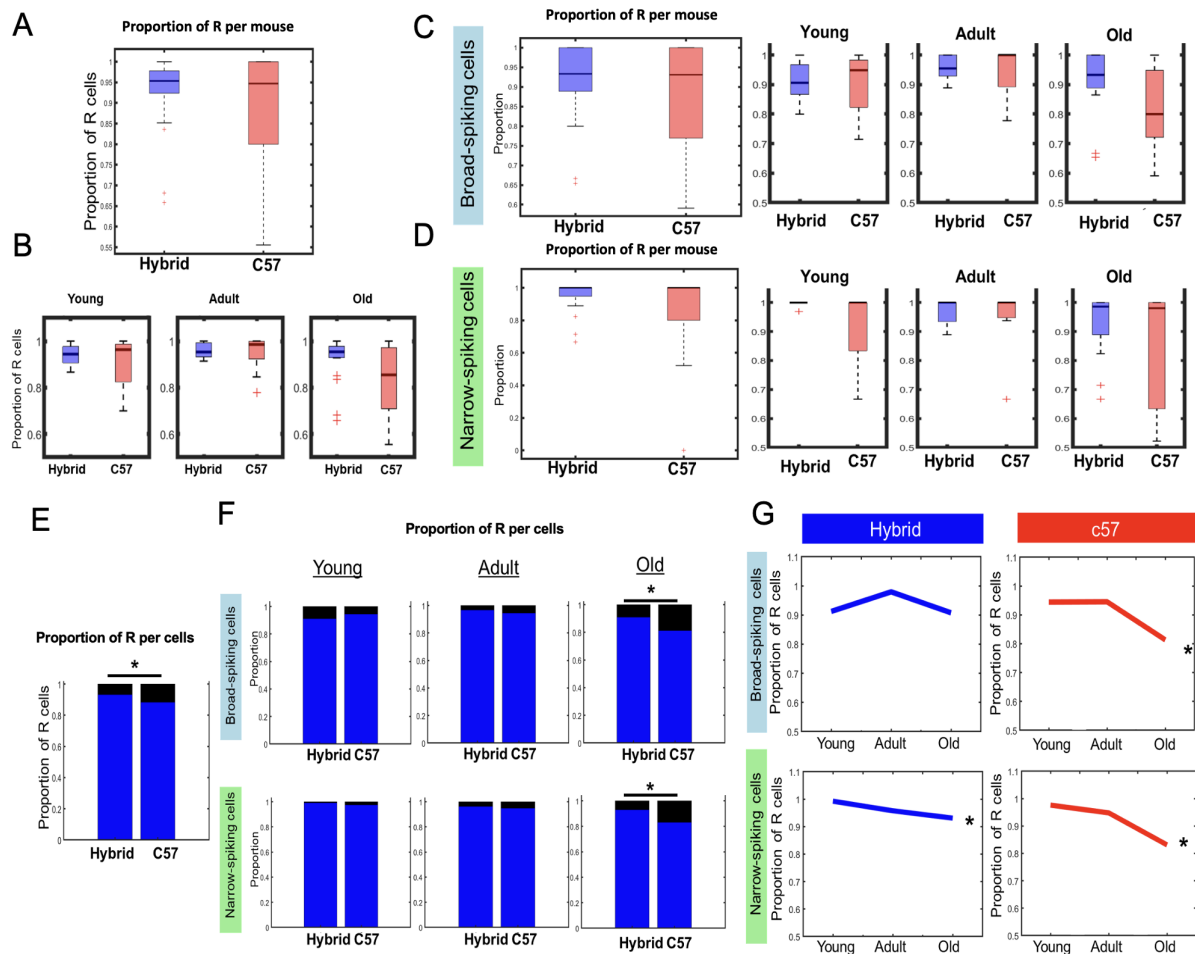
Figure 4.3: *Proportion of responding cell*

(A) Boxplot of the mean proportion of responsiveness per mouse. Note the tendency to a lower proportion of responsiveness in C57 than Hybrid mice, but with no significance. (B) Boxplot of the mean R proportion per mouse across age groups. Note the tendency of a lower proportion of responsiveness in old C57, but with no significance. (C) The proportion of the mean responsiveness in BS per mouse and per age group on the right. (D) The proportion of the mean responsiveness in NS per mouse and per age group on the right. (E) The proportion of responding cell in blue and the proportion of non-responding cell in black per strain (p=6.35e-5, proportion test). (F) The proportion of responsive BS, top, and NS, bottom, per age groups and strain. Significantly higher proportion of NR in C57 than in Hybrid mice in old BS (p=.003, proportion test) and NS (p=.002, proportion test). (G) Changes in the proportion of responsiveness in BS, top, and in NS, bottom, along with ageing across strain. Asterisks represent changes from young to old. Significant decrease is observed in Hybrid mice NS proportion of responding cell (p=.02, proportion test) and in both C57 BS proportion of responding cell (p=1.29e-5, proportion test) and NS (p=.002, proportion test).

4.4 Decrease with age in the natural sound evoked-response FR of NS in C57

In the C57 mice, we observed a decrease in the FR of NS (Figure 4.4. D-F). This difference is significant between young and old age, (F(2)=3.5, p=.03, one-way ANOVA, p=.02, Tukey HSD Post hoc). In BS, there is a slight tendency to increase in panel E, however, no significant difference in FR is observed. When comparing the FR ageing between the two cell-types, we observed a significant cell-type effect, (F(1)=5.78, p=.01, two-way

ANOVA) and an interaction effect between cell-types and age-groups, (F(1,2)=3.22, p=.04, two-way ANOVA). The analysis shows that the NS FR was higher than the BS in young C57 mice, (p=.05, Tukey HSD Post hoc).
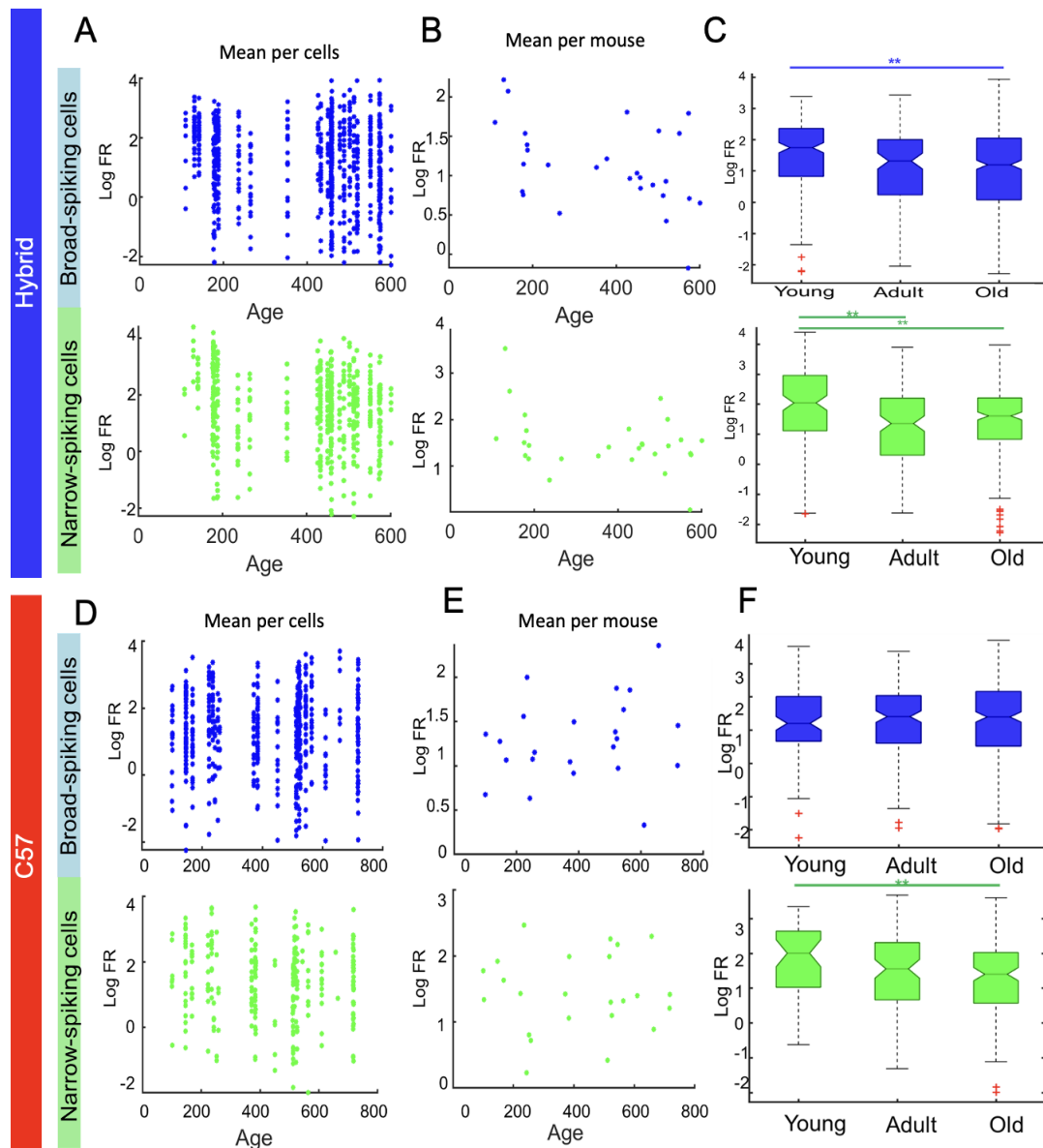
Figure 4.4: *Age-related decrease in FR during sound presentation in BS and NS of Hybrid mice and decreases in NS C57* (A) Logarithmic firing rate (Log FR) per cell of Hybrid mice BS (top) and NS (bottom) along with ageing. (B) Mean Log FR per mouse of Hybrid mice along with ageing. (C) Log FR of Hybrid mice cell across the three age groups. The Log FR of BS decreases significantly from young to old (BS: F(2)=9.2, p=.0001, one-way ANOVA; p=.002 and p=.0001, respectively, Tukey HSD Post hoc), and from young to adult and from young to old in NS (F(2)=9.59, p=8.13e-5, one-way ANOVA; p=.0001 and p=.0013, respectively, Tukey HSD Post hoc). (D) as is (A) for C57. (E) as in (B) for C57. (F) As in (C) for C57. The Log FR in NS decreases from young to old age (F(2)=3.5, p=.03, one-way ANOVA, p=.02, Tukey HSD Post hoc).

4.5 Age-related difference in BS natural sound evoked-response FR between Hybrid and C57 mice

When comparing the Hybrid mice to C57, we did not observe any significant differences in the FR of All cell (Figure 4.5. A) or in BS and NS (Figure 4.5. B). As a reminder, the term "All cell" refers to all recorded cell, without distinguishing between their cell type. Comparing along ageing (Figure 4.5. C), we observed a significant effect of the age-groups and strain interaction on the FR of BS, ($F_{(2,1)}=4.73$, p=.006, two-way ANOVA), where the BS of Hybrid mice decreases from young to old (p=.0001, Tukey HSD post hoc). In the NS we observed no strain effect whereas we observed age-groups effects ($F_{(2)}=11.8$, p=9e-6, two-way ANOVA), the FR decreases between young to adult and between young to old (p=.00006 and p.00003 respectively, Tukey HSD post hoc).
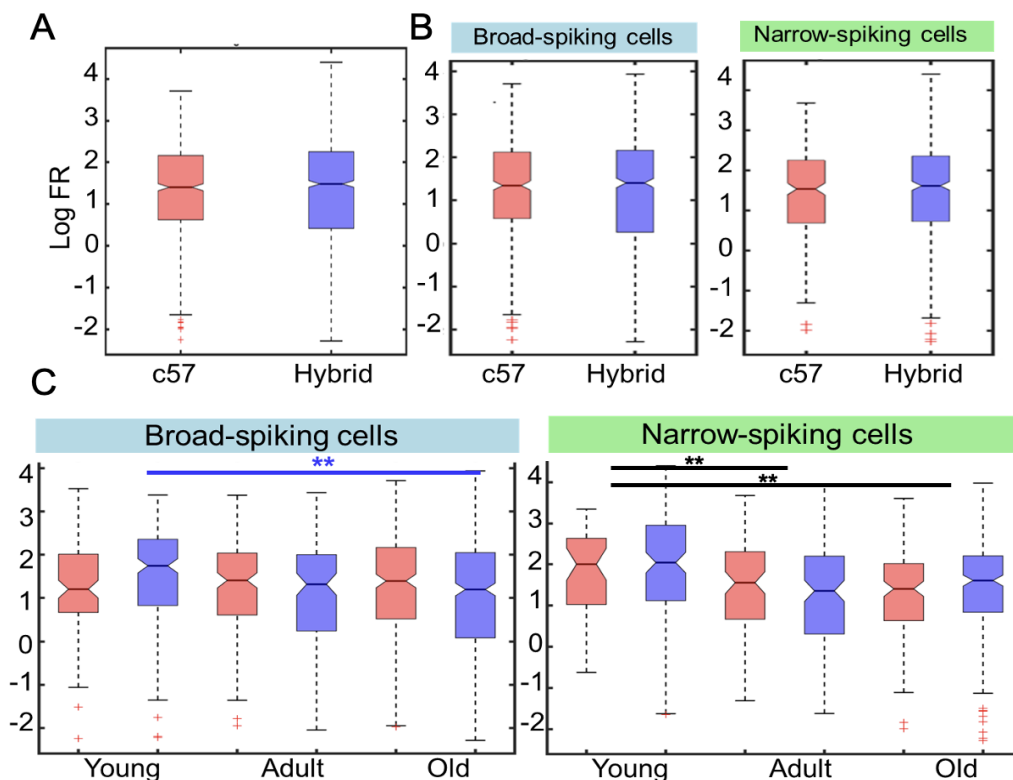
Figure 4.5: *During the natural sound presentation, the BS ageing is different between Hybrid mice and C57* (A) All cell Log FR between Hybrid mice, blue, and C57, red. (B) As in (A) for BS (left panel) and in NS (right panel). (C) BS Log FR changes along age across strain. The BS is affected by age groups ($F_{(2)}=5$, two-way ANOVA, p=.005, Tukey HSD post hoc), and it is affected by the interaction effect of age groups and strain ($F_{(2,1)}=4.73$, p=.006, two-way ANOVA), where the BS of Hybrid mice decreases from young to old (p=.0001, Tukey HSD post hoc). In NS, the Log FR is only affected by age-groups ($F_{(2)}=11.8$, p=9e-6, two-way ANOVA), the FR decreases between young to adult and between young to old (p=.00006 and p=.00003 respectively, Tukey HSD post hoc).

4.6 Comparison of the FR between R and NR to natural sound stimulation

We were surprised by the stable BS FR that we observed in C57 as they age, given that C57 mice are typically known to experience hearing loss with age. To investigate this finding further, we aimed to determine whether our FR metrics could have influenced the results. We compared the FR during all sound-presentation exposure times,

including the repetitions of ten-second sound presentations and the one-second intervals, to the FR only during the ten-second sound presentation excluding the intervals (Figure 4.1. A). We found that the FR is not significantly different between the two FR metrics for both mice strains (Figure 4.6. A). Additionally, we examined whether the FR during the 10-second stimulus exposure also exhibited similar changes with age (Figure 4.6. B). We obtained similar results to those in Figure 4.5. C, where the FR of Hybrid mice BS decreased with age while that of C57 remained stable in both cell types, (F(2,1)=4.73, p=.009, two-way ANOVA, p=.002, Tukey HSD post hoc).

We then classified cell into two groups based on their responsiveness label, as shown in Figure 4.1.D and compared their FR with the hypothesis that if the neurons are responding cell, (R), their FR should increase during the sound presentation. We compared the FR of R and NR cell (Figure 4.6.CD). The analysis revealed that, in both strains, the FR of R was higher than that of NR during the entire sound presentation protocol recording (Figure 4.6.C, F(1,1)=7.13, p=.0007, two-way ANOVA, Hybrid p=.0007, C57 p=.0014, Tukey HSD post hoc) and also during the ten-second stimulation period (Figure 4.6.D, F(1,1)=7.53, p=.0006, two-way ANOVA, Hybrid mice p=.0002, C57 p=.0002, Tukey HSD post hoc). Additionally, the NR of C57 was found to be higher than that of the Hybrid mice (10-sec stimuli: p=.02, Tukey HSD post hoc, All record: p=.03, Tukey HSD post hoc).

To further investigate the FR, we compare the FR during the 500ms before sound exposure, 'pre-stimuli', and during the ten-second sound-presentation, 'stimuli' (Figure 4.6. EF). The hypothesis is that the FR of R cell should increase from the pre-stimuli period to the stimuli period, whereas the FR of NR should not show such a change. Our results show that in both strains of mice, the FR of NR cell did not change between the pre-stimuli and stimuli period (Figure 4.6. G), while the FR of R cell increased during the sound presentation period, (Hybrid mice: F(1,1)=15.07, p=.002, two-way ANOVA, p=.0006, Tukey HSD post hoc, C57: F(1,1)=10.42, p<e-6, two-way ANOVA, p<e-6, Tukey HSD post hoc). These findings support the notion that R are responding to sound stimuli. Notably, in the Hybrid mice strain, the FR of R was higher than that of NR cell during the stimuli period (p=.0006, Tukey HSD post hoc), and there was no difference between the two cell types during the pre-stimuli period. However, in the C57 strain, the FR of NR was higher than that of R during the pre-stimuli period at the level of R (p=.003, Tukey HSD post hoc). This result suggests that in C57, NR are highly active during the sound presentation, but this does not necessarily indicate a direct response to the sound stimulus. We found that the FR metric was not affected by the length of the analysed spike train and was stable across the metric investigation. We also observed that the FR of R increased during the sound presentation period, while that of NR cell remained unchanged. These findings support the notion that R are responsive to sound stimuli. Interestingly, the NR of the C57 strain was found to be higher than that of the Hybrid mice strain. These results suggest that NR cell may have a role in sound information training or represent other task computations.

In this section, we observed that the proportion of responding cell differed between the two strains of mice. With ageing, Hybrid mice exhibited a decrease in the number of NS R, whereas in C57 mice, both the BS and NS R populations decreased, and this difference become significant compared to Hybrid mice at an advanced age. Moreover, the FR activity during sound presentation varied between Hybrid and C57 mice, with the FR of both BS and NS declining with age in Hybrid mice but remaining stable in the BS and decreasing in NS C57.
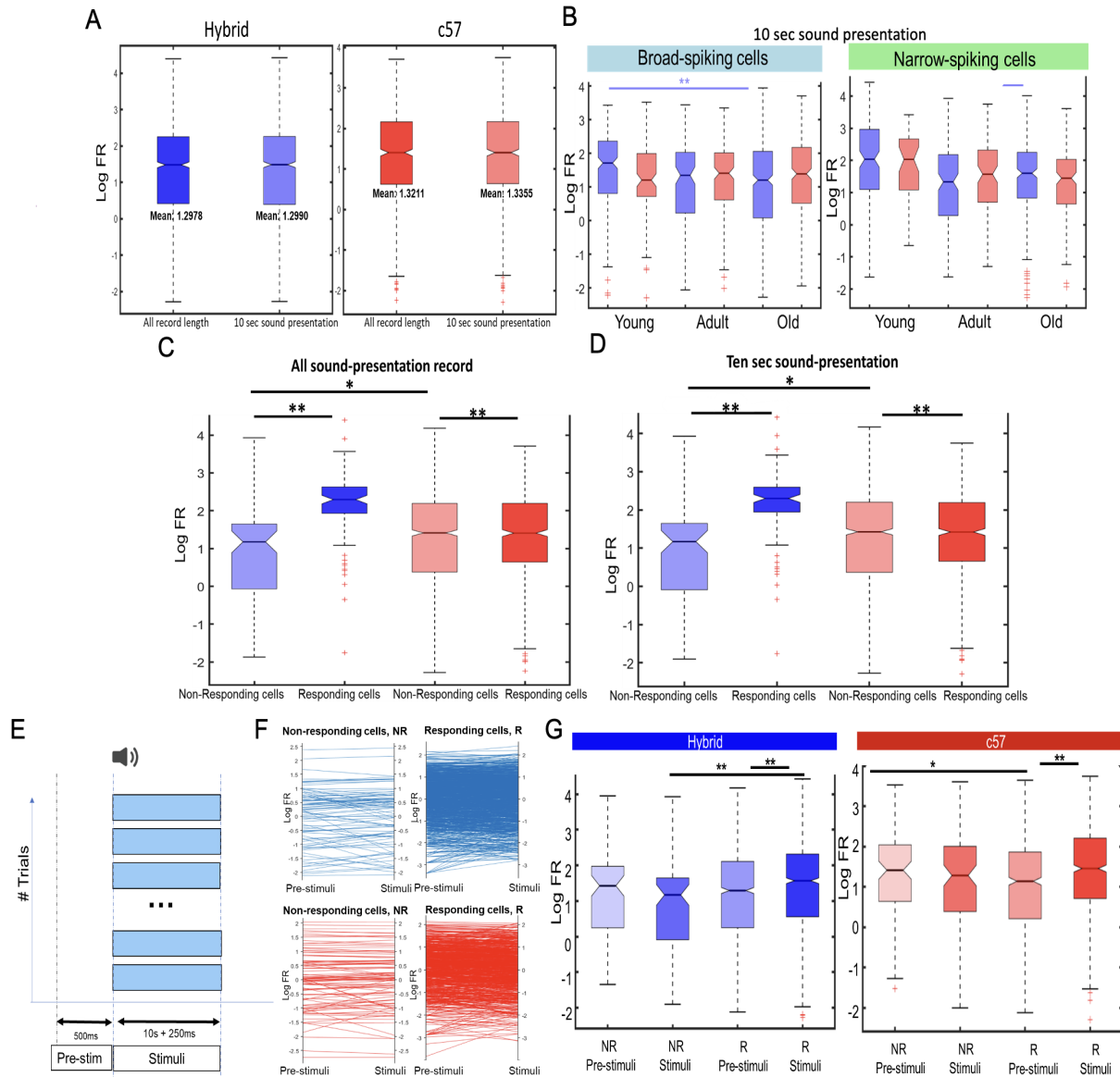
Figure 4.6: *FR metric investigation during sound-presentation*

(A) Comparison between all record mean FR and only 10sec sound presentation mean FR in Hybrid mice (blue, left panel) and C57 (red, right panel). The FR calculated during the entire sound stimulation (all record length), includes the repetitions of the 10-second sound and the 1-second intervals (as described in Figure 4.1. A). (B) The mean FR during the 10-second sound presentation only along age-groups in BS, and NS. As observed in Figure 4.4. F, the FR in Hybrid mice decreases with age in Hybrid mice BS ($F(2,1)=4.73$, p=.009, two-way ANOVA, p=.002, Tukey HSD post hoc). (C) Comparison of the FR between R and NR cell during the entire sound stimulation length in Hybrid mice (blue) and C57 (red) ($F(1,1)=7.53$, p=.0006, two-way ANOVA, Hybrid mice p=.0002, C57 p=.0002, NR p=.03, Tukey HSD post hoc). (D) As in (C) during the ten seconds sound presentation ($F(1,1)=7.13$, p=.0007, two-way ANOVA, Hybrid mice p=.0007, C57 p=.0014, NR p=.02, Tukey HSD post hoc). (E) FR changes between pre and stimuli period protocol schema. The FR during the 10-second sound stimulation period with the offset period (250ms) ('stimuli', light blue) is compared with the FR during the 500ms 'pre-stimulus' period to determine whether the FR has increased. (F) FR between pre-stimulus and stimuli periods in non-responding cell (left) and responding cell (right) for Hybrid mice (blue, top) and C57 (red, bottom) mice. Each line represents a cell. (G) FR changes of NR and R cell from pre-stimulus to stimuli periods for Hybrid mice (blue) and C57 (red) mice. In both strains, R cell exhibit an increase in FR from pre-stimulus to stimuli periods, while NR cell exhibit a constant FR. (Hybrid mice : $F(1,1)=15.07$, p=.002, two-way ANOVA, p=.0006, NR vs R p=.0006 Tukey HSD post hoc, C57: $F(1,1)=10.42$, p<e-6, two-way ANOVA, p<e-6, NR vs R p=.003 Tukey HSD post hoc).

4.7 Calculation of the contrast entropy during natural sound presentation

To further investigate AC computation, we examined the CE of AC cell during natural sound exposure, following the same methodology as for the spontaneous activity analysis. The CE of the AC was computed during the natural sound presentation to investigate how the central information carrying is affected by ageing in both mouse strains and by peripheral impairment in the C57 strain. The underlying hypotheses are the same as for the investigation of spontaneous activity, as shown in Figure 3.4. A. However, in the case of sound exposure, the CE is closely linked to how the auditory cortex processes sound. For example, changes in the CE could suggest that the neural population is becoming more selective in response to the sound, that the quality or characteristics of the sound are changing over time, or that there are changes in the way that information is being encoded or processed by the auditory system. The CE was computed for the natural sound length of recording, which was approximately 18 minutes and included the 10-second repetitions and intervals to maximize the sample size.
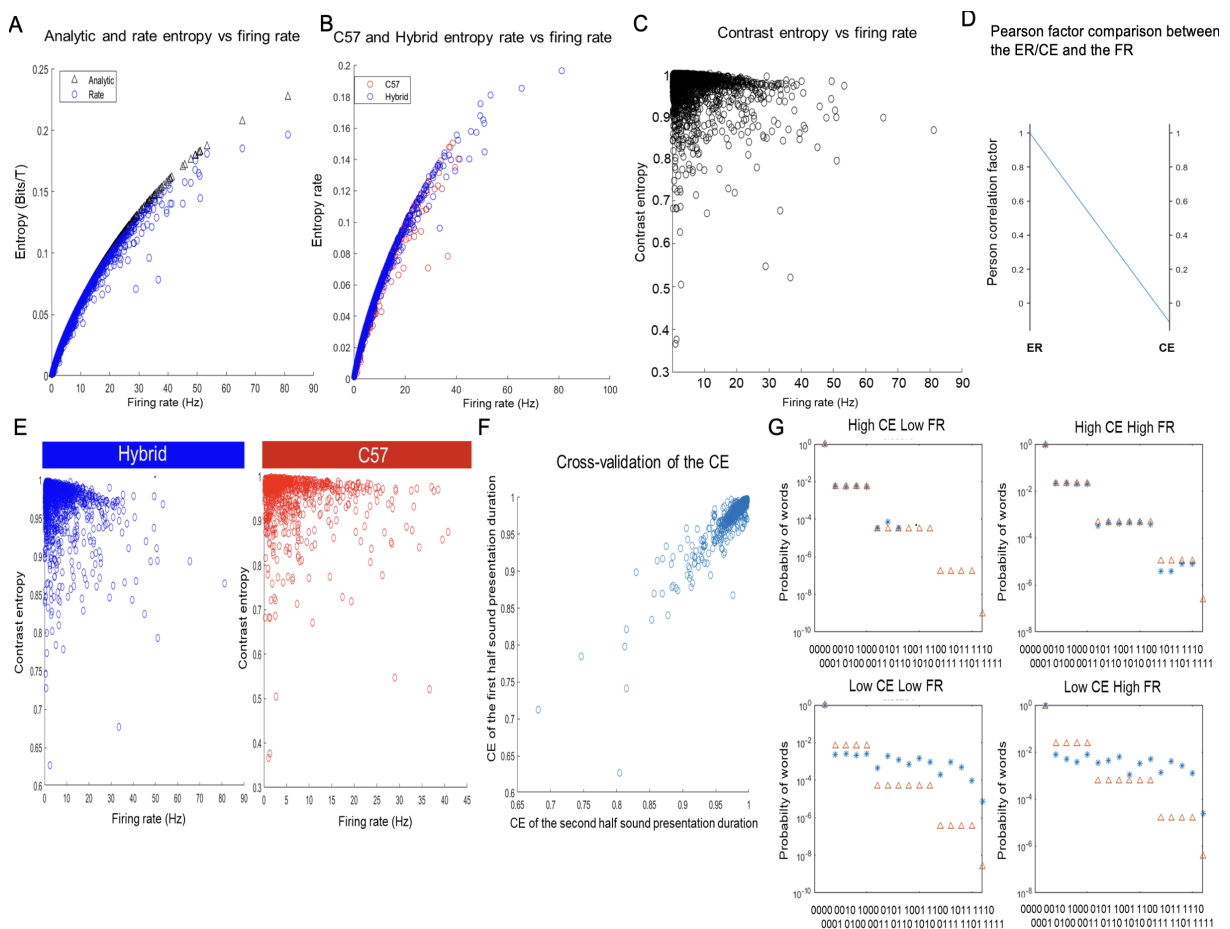
Figure 4.7: *Evoked-response contrast entropy computation*
(A) Comparison between analytical (EA, dark triangles) and observed entropy rate (ER, blue circles) along FR. (B) Comparison of the ER and FR in C57 (red) and Hybrid mice (blue). (C) Contrast entropy (CE) vs. FR, black circles are cell. (D) Person correlation between FR and ER (R2=0.97) or CE (R2=-0.15). (E) As in (C) for C57, red, and Hybrid mice, blue. (F) CE cross-correlation of first half and second half of the natural sound presentation recording. (G) Accuracy between analytical (red triangles) and observed words probabilities (blue asterisk) for 4 types of neurons (high and low contrast entropy/firing rate activity) during sound presentation. From left to right and bottom right: CE=0.97, FR=1.79; CE=0.99, FR=10.63; CE=9.0, FR=23.73; CE=0.86, FR=23.74.

As for the CE during spontaneous activity, the observed entropy (ER) follows the same trend as the analytical entropy (EA) (Figure 4.7. A, p<.05, Pearson correlation test) and the ER of Hybrid and C57 mice are similar (Figure 4.7. B, p<.05, Wilcoxon Mann-Whitney test). Both ER and EA are increasing with the FR as observed in Figure 3.4. C or Pryluk and al. 2018 (Pryluk et al. 2019) and normalizing the ER by the EA (CE) eliminates the relationship between the FR (Figure 4.7. C-E).

To validate that the CE is independent of the sample length, we computed the CE of the first half and second half periods of the natural sound presentation time (Figure 4.7. F). We found that the values tend to be a linear distribution (no statistical tests have been performed). However, this distribution was broader than the one found in the spontaneous analysis (Figure 3.4. F). This could be explained by the different evoked responses of auditory neurons to natural sounds. As, some neurons respond to onset, offset, or cues of the auditory stimuli (Solyga & Barkat 2021, Nelken et al. 1999*b*), which was also found in our dataset (Figure 4.1. E). Thus, the CE of onset-responding neurons, for example, could be higher or lower during the first half of the stimulation period compared to the second half. Finally, as for the spontaneous record, we compared the occurrence of words during evoked-responses activity with their expected probabilities (Figure 4.7. G). We found a match between the observed and expected measurements, which validated our CE calculation, with a narrower overlap in neurons presenting a higher CE (Pryluk et al. 2019, Ohyama et al. 2020). Therefore, we conclude that CE can be calculated using the length of our natural sound stimulus.

4.8 The CE of Hybrid mice neurons increases slightly with age, while it decreases in C57 during natural sound evoked-response activity

The CE was computed in Hybrid mice and C57 for all cell (Figure 4.8. AD) or mean CE per mouse (Figure 4.8. BE) along ageing. In Hybrid mice, the CE showed a slight increase for both BS and NS cell types from young to old (Figure 4.8. C, BS: Chi-squared(2)=6.53, p=.04, Kruskal-Wallis test, p=.006, Dunn test Post hoc, NS: Chi-squared(2)=7.85, p=.02, Kruskal-Wallis test, p=.005, Dunn test Post hoc with Bonferroni correction). In contrast, C57 showed a consistent decrease in CE with ageing in both cell-types (Figure 4.8. D-F). We found that the CE of both cell-types decreases from young to adult (BS: Chi-squared(2)=17.13, p=.0002, Kruskal-Wallis test, p<e-5, Dunn test Post hoc, NS: Chi-squared(2)=7.85, p<e-11, Kruskal-Wallis test, p<e-5, Dunn test Post hoc) and from young to old, (BS: p=.0002, Dunn test Post hoc with Bonferroni correction, NS: p<e-5, Dunn test Post hoc with Bonferroni correction). In contrast to the previous analysis of spontaneous CE or FR, we observed an effect of age-group and cell-type on the CE during natural sound presentation in Hybrid mice (H(2)=20, p=7e-6, SRH, H(1)=12, p=.003, SRH, respectively). Although no interaction effect gave been observed, post-hoc analyses shows that NS CE is lower than BS in young Hybrid mice, (H(2,1)=2, p=,4, SRH, p=.01, Dunn test Post hoc with Bonferroni correction).

In C57, we found that the CE decreased with age in both cell types, starting at the adult age. In the BS, the CE decreased from young to adult and from young to old, (H(2,1)=13.13, p=.0014, SRH, p=8e-4 and p=.005, Dunn test Post hoc with Bonferroni correction). A similar pattern was observed in the NS, with the CE decreasing from young to adult and from young to old, (p=5e-9 and p=1.8e-10, Dunn test Post hoc with Bonferroni correction).

Moreover, starting from adult age and old age, the CE became lower in NS than BS (p=2.2e-4 and p=3.5e-5, Dunn test Post hoc with Bonferroni correction).
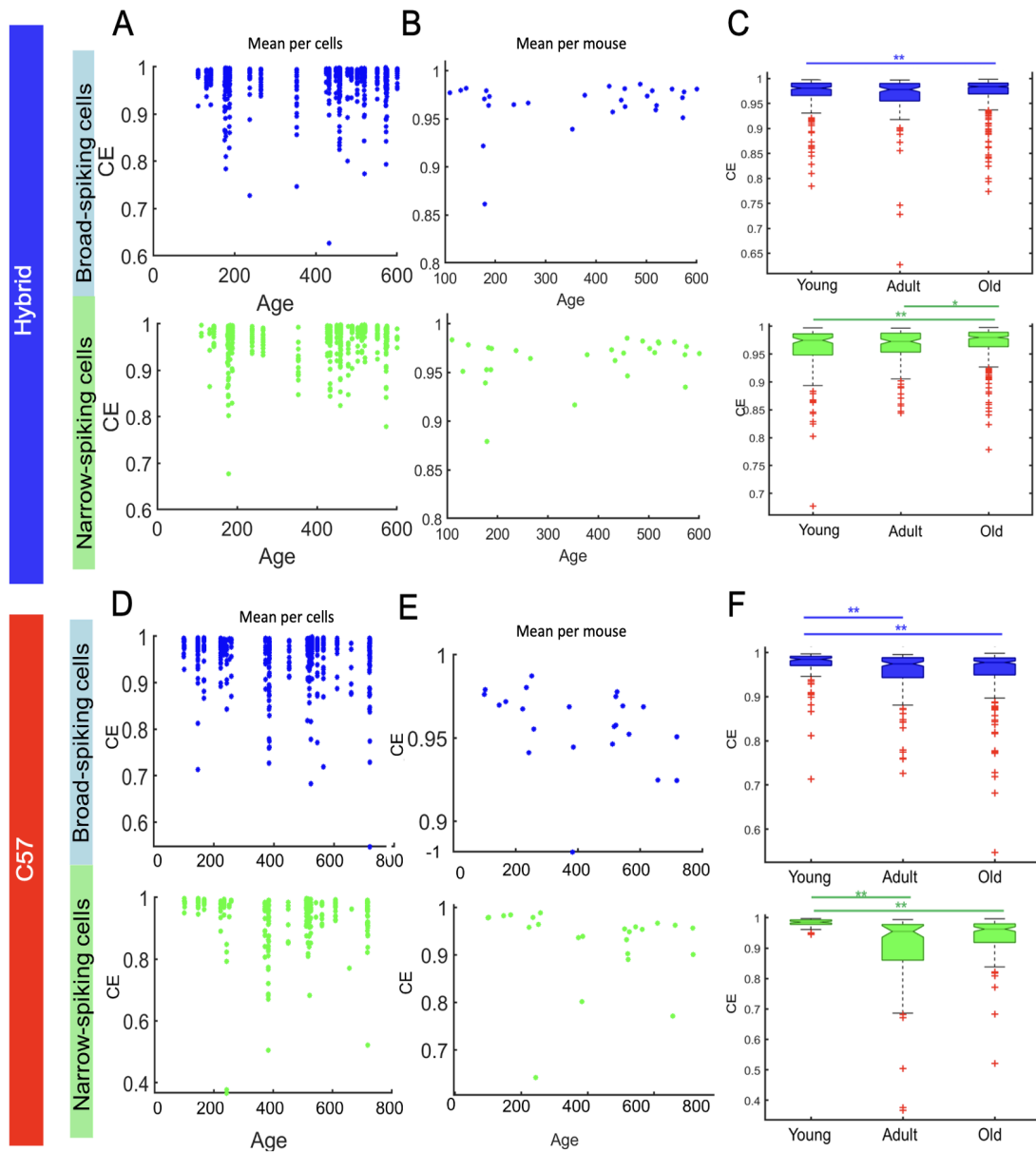
Figure 4.8: *Increases with the age of the CE in Hybrid mice while it decreases in C57, during natural sound-presentation* (A) Hybrid mice CE per cell in BS, top, and NS, bottom, along with ageing. (B) Hybrid mice Mean CE per mouse, along with age in BS, top, and NS, bottom, along with ageing. (C) Boxplot of the Hybrid mice CE cell in the three age groups. The CE increases in both cell-types (BS: Chi-squared(2)=6.53, p=.04, Kruskal-Wallis test, p=.006, Dunn test Post hoc, NS: Chi-squared(2)=7.85, p=.02, Kruskal-Wallis test, p=.005, Dunn test Post hoc with Bonferroni correction). (D) As in (A) for C57. (E) As in (B) for C57. (F) As in (C) for C57. The CE increases along with ageing (BS: Chi-squared(2)=17.13, young p=.0002, Kruskal-Wallis test, young adult p<e-5, young to old p=.0002 Dunn test Post hoc, NS: Chi-squared(2)=7.85, p<e-11, Kruskal-Wallis test, young adult p<e-5, young to old p>e-5, Dunn test Post hoc).

4.9 C57 show a lower CE than Hybrid mice during natural sound evoked-response activity

When comparing the CE of natural sound presentation between the Hybrid mice and C57 mice strains, we observed that Hybrid mice exhibited a significantly higher CE compared to C57 mice (Figure 4.9. A, p=2.58e-11, Wilcoxon Mann-Whitney test). This difference was not explained by variations in the ER or FR (Figure 4.7. B, Figure 4.9. B) and is observed in all of the letters-words combinations tested except word4 letters of 1ms, (Data not shown, all letters/words p<e-3). The result is consistent across both BS and NS (Figure 4.9. C, p=6.83e-6 and p=4.2e-9, respectively, Wilcoxon Mann-Whitney test). These findings suggest that the CE of the Hybrid mice is higher during the natural sound presentation and that the BS are more efficient compared to NS in both strains. Furthermore, we found that the BS were more efficient than the NS in both mouse strains (Figure 4.9.D, Hybrid mice p=1.41e-6, C57 p=1.53e-7, Wilcoxon Mann-Whitney test).

When comparing across age-groups, we observed that both the mouse strain and age groups affected the CE in both BS and NS (Figure 4.9. E). Consistent with the previous section, we found that the CE in C57 mice decreased from young to adult and too old in both BS, (H(2,1)=13.45, p=.001, SRH test, p=.002, p=3e-4, Dunn test post hoc with Bonferroni correction) and NS (H(2,1)=47.59, p=4e-11, SRH test, p=2e-9, p=8e-11, Dunn test post hoc with Bonferroni correction). Furthermore, we found that the CE in BS was different between the two strains in the old age group (p=8.56e-6, Dunn test post hoc with Bonferroni correction), whereas in NS, it was different in all age-groups (young p=6.6e-4, adult p=2.4e-5, old p=1.5e-9, Dunn test post hoc with Bonferroni correction).

In conclusion, our study demonstrates that there are significant differences in the contrast entropy of natural sound presentation between the Hybrid mice and C57 mice strains. The Hybrid mice exhibited a significantly higher CE compared to the C57; a difference observed in both cell-types. Moreover, we found that the CE of C57 mice decreased significantly with age in both cell types, starting at the transition between young to adult age, whereas in Hybrid mice, the CE remain mostly stable along age or exhibits a slight increase. Finally, we observed that the CE ageing kinetic is different between Hybrid mice and C57, whereas in NS, the CE is different in all age-groups and becomes different at old age in BS. Our findings suggest that there are complex interactions between age groups and cell types that influence the CE during natural sound presentation differently between Hybrid mice and C57. The AC neuron vocabulary is importantly affected by the peripheral impairment, even the FR seems to be stable.

Figure 4.9: *During the sound presentation the CE of Hybrid mice is higher than C57*
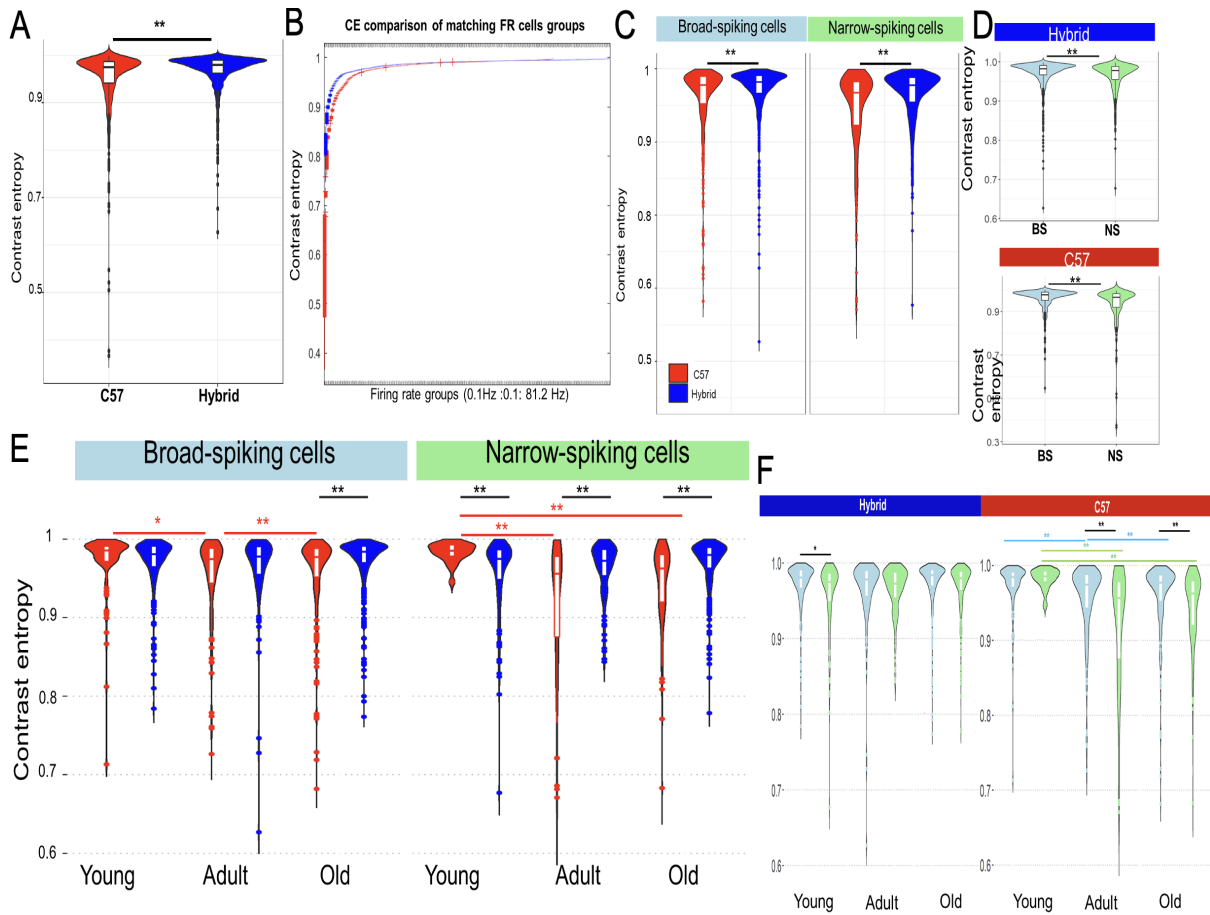
(A) CE comparison between strain. Hybrid mice, blue, CE is higher than C57, red, (p= 2.58e-11, Wilcoxon Mann-Whitney test). Median CE for Hybrid mice = 0.981 (n= 825 cell), and for C57= 0.975 (n= 1317 cell). (B) CE values per FR groups between Hybrid mice and C57. Each boxplot contains cell within the same FR group of 0.1 Hz. FR group edges range from 0.1 Hz to 81.2 Hz with +/- 0.1 Hz/bin. (C) In both cell types, Hybrid mice CE is higher than C57. BS (left, blue) (p=6.83e-6, Wilcoxon Mann-Whitney test), median CE for Hybrid mice = 0.977 (n= 535 cell), and for C57= 0.982 (n= 773 cell). NS (right, green) (p=4.2e-9, Wilcoxon Mann-Whitney test), median CE for Hybrid mice = 0.978 (n= 273 cell), and for C57= 0.966 (n= 529 cell). (D) BS (cyan) CE is higher than NS (green) in both strains (Hybrid mice p=7.8e-6, Wilcoxon Mann-Whitney test), C57 p=2.6e-8, Wilcoxon Mann-Whitney test). (E) CE vs cell types and age groups. In BS (left), C57 CE shows a U-shaped trend (H(1,2)=13.45, SRH test, p=.001, young to adult p=.002, adult to old p=9.75e-4, Dunn test Post hoc with Bonferroni correction). This kinetic is not observed in the Hybrid mice. The CE is higher in old Hybrid mice than in old C57 (SRH test, p=1.3e-5, Dunn test Post hoc with Bonferroni correction). In NS (right), the C57 CE decreases from young to adult (H(1,2)=47.6, SRH test, ANOVA, p=2.4e-10, Tukey HSD Post-hoc) and from young to old (p=1.12e-8, Dunn test Post hoc with Bonferroni correction). NS CE is different between C57 and Hybrid mice in all age-groups. It is higher in C57 than in Hybrid mice in young age (p=6.5e-4, Dunn test Post hoc with Bonferroni correction) and lower in adults (p=8.2e-5, Dunn test Post hoc with Bonferroni correction) and old (p=1.1e-8, Dunn test Post hoc with Bonferroni correction). (F) Cell types CE within strain along age-groups. In Hybrid mice, BS CE is higher than NS in young age (H(1)=20, p=7e-6, SRH test). In C57, the CE is affected by cell-types and ageing. In both cell types, CE decreases along ageing (H(1,2)=13.13, p=.001, SRH test, BS young to adult p=.0008, young to old p=.005; NS young to adult p=1e-10, adult to old p=5.9e-9, Dunn test Post hoc with Bonferroni correction). BS present a higher CE than NS in adult and old age groups (adult p=.0002, old p=3.5e-5, Dunn test Post hoc with Bonferroni correction).

Overall, our findings suggest that in the non-pathological model of hearing loss, there is a decrease in the number of NS-responding cell, while BS responsiveness remains constant with age. Regarding coding, the FR of AC BS and NS decreases while their CE remains stable or increases slightly. In the pathological hearing loss model, we observed that the number of responding cell decreases with age in both NS and BS, and the proportion of NR is higher than in the non-pathological model. Interestingly, the FR of BS is not decreased in this model, and the proportion of NR shows a higher FR during the sound presentation. However, the CE of NS and BS is significantly affected by ageing, with levels lower than in Hybrid mice. Overall, our study provides novel insights into the mechanisms underlying auditory processing in mice and may have important implications for understanding age-related changes in auditory function.

> **Key findings:**
> ❖ The percentage of responding cells decreases with age in putative excitatory cells of AC Hybrid mice, and in putative excitatory and inhibitory cells in C57 mice.
>
> ❖ The FR decreases in both cell types of the AC in Hybrid mice and only in the BS in C57 mice, while the NS remains stable.
>
> ❖ During natural sound presentation, the CE increases in Hybrid mice, while it decreases in C57 mice.
>
> ❖ During natural sound presentation, the CE is lower in C57 mice than in Hybrid mice.

5
Comparative Analysis of Auditory Cortex Activity during Sound Presentation and Silent Periods

| I. Spontaneous activity | II. Natural evoked-response activity | III. Comparison Spontaneous and Evoked activities |
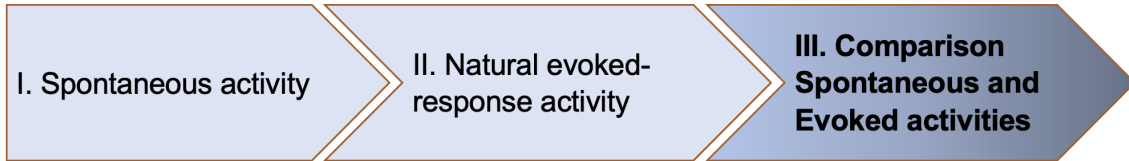
In this chapter, we aim to investigate whether the differences between spontaneous activity and evoked responses to natural sounds vary in a healthy age-related hearing loss model and a presbycusis model. Understanding these differences can provide a comprehensive understanding of how the AC functions in response to auditory stimuli in both normal ageing and pathological conditions. We expect to observe differences in the spontaneous activity and evoked response changes between the two mouse strains, reflecting distinct changes in auditory cortical processing of sound, due to different spontaneous states and/or cell activity recruitment.

To explore these questions, we used the data of the neural activity in the AC during both silent periods and sound presentation. By comparing the neural responses during silent periods to the evoked responses during the sound presentation, we can elucidate the differences in spontaneous and stimulus-driven activity patterns. We focused on the used metrics FR and CE, and the ratio of changes between both silent and sound conditions. This includes examining the FR and CE of 832 C57 cell and 1317 Hybrid mice cell across 62 mice while presenting natural sounds and periods of silence. We will also distinguish the FR and CE activity of responding cell, (R), and non-responding cell, (NR), to get insight into their role in sound processing. In our initial exploration, we will delve into a comprehensive investigation of the effect sizes on the FR and CE metrics. This analysis will be augmented by the inclusion of additional effect size metrics such as tailratio, U3, and Auroc in our statistical tests, providing a nuanced and thorough understanding of the underlying neural activity patterns. We will, then, focused on the FR comparison followed by the CE one.

5.1 Effect size analysis

In the pursuit of a nuanced understanding of neural dynamics, this chapter subsection delves into the exploration of effect size effects. Acknowledging that even subtle differences, such as those in FR ad CE, may achieve statistical significance with a sufficiently large sample of neurons, our focus shifts towards unravelling the practical significance and implications of these seemingly modest variations in neural activity. To achieve this aim, we incorporated a comprehensive suite of effect size metrics, including tailratio, U3, and Auroc, into our statistical tests. This addition enables a more nuanced examination of neural dynamics, allowing us to discern meaningful patterns and implications even in cases where statistical significance might hinge on the subtleties of a large neuronal sample.

5.1.1 Effect size metrics

Tailratio: This metric assesses the tail behaviour of the distributions, aiding in understanding the extent of deviation from a null hypothesis. A Tailratio $>$ or $<$ 1: Indicates a distribution with a heavier or longer tail than the reference distribution. This suggests that there are pronounced differences in the tails of the compared distributions, signifying a notable departure from the null hypothesis. A Tailratio $=$ 1: Suggests that the tails of the distributions are similar, implying no substantial deviation from the null hypothesis in terms of tail behaviour. In our results, higher Tailratio values would suggest a more pronounced deviation from the null hypothesis, indicating significant differences in the tail behaviour of the compared distributions. Conversely, values closer to 1 or below 1 suggest a milder or no significant deviation in tail behaviour.

The U3 represents the probability that a randomly selected score from one group will exceed a randomly selected score from another group. It is often used as an effect size measure in nonparametric statistical tests, such as the Wilcoxon-Mann-Whitney U test.

A U3 $=$ 0.5: Indicates no difference between the groups, as there is an equal probability that a randomly selected score from one group will exceed a randomly selected score from the other group. A $0 < U3 < 0.5$: Suggests a higher probability that a randomly selected score from the first group will exceed a randomly selected score from the second group, indicating a positive effect size. A $0.5 < U3 < 1$: Suggests a higher probability that a randomly selected score from the second group will exceed a randomly selected score from the first group, indicating a negative effect size. In general, the closer the U3 value is to 0 or 1, the stronger the effect size, indicating a greater probability that scores from one group are higher than scores from the other group. The interpretation of U3 should be considered in conjunction with other effect size and pvalues.

Auroc: (Area Under the Receiver Operating Characteristic Curve) is metric that assesses the discriminatory power of a diagnostic test, offering insights into the precision of our observed effects. The Area Under the Receiver Operating Characteristic Curve (Auroc) values typically range from 0.5 to 1, where: Auroc $=$ 0.5: Indicates a classifier with no discriminatory power; it performs no better than random chance. An Auroc $=$ 1: Represents a perfect classifier with complete discriminatory power, achieving optimal precision in distinguishing between groups. Therefore, in the context of our results, Auroc values closer to 1 suggest a better ability of the diagnostic test to precisely discern observed effects, while values closer to 0.5 indicate a weaker discriminatory power, approaching random chance.

5.1.2 Effect size metrics investigation

We initiated a thorough investigation to unravel and analyse the underlying patterns of FR and CE differences between C57 and Hybird mice and insights it holds. Turning, first, our attention to FR, Figure 5.1.A, the Wilcoxon-man-Withney tests (WMU), for yielded p-values indicating non-significant differences between groups. Effect size metrics, revealed minor deviations from the null hypothesis, suggesting poor distinctions in FR distributions. Here, we presented below is the report and discussion on our findings related to effect sizes:

FR spontaenous activity

All cells: **WMU Test:** p-value=0.8151 **Tailratio:** 1.0787 suggests a moderate extent of deviation from the null

hypothesis. **U3:** 0.4901, there is a balanced probability that a randomly selected firing rate from one group will the same that of a randomly selected firing rate from another group. **Auroc:** 0.4975, The Auroc indicates a marginal discriminatory power of the diagnostic test.

BS cells: **WMU Test:** p-value=0.9174 **Tailratio:** 1.0286 denotes a relatively minor extent of deviation from the null hypothesis. **U3:** 0.505 there is a balanced probability that a randomly selected firing rate from one group will be the same that of a randomly selected firing rate from another group. **Auroc:** 0.5014 suggests a marginal improvement in the discriminatory power of the diagnostic test.

NS cells: **WMU Test:** p-value=0.5694 **Tailratio:** 1.1092 indicates a moderate extent of deviation from the null hypothesis. **U3:** 0.462 there is a moderate probability that a randomly selected firing rate from one group will lower that of a randomly selected firing rate from another group. **Auroc:** 0.4898 suggests a modest discriminatory power of the diagnostic test.

FR natural sound evoked-response activity

All cells WMU Test: p-value=0.7783 **Tailratio:** 0.8882 denotes a minor extent of deviation from the null hypothesis. **U3:** 0.528 there is a balanced probability that a randomly selected firing rate from one group will exceed that of a randomly selected firing rate from another group. **Auroc:** 0.5036 indicates a marginal improvement in the discriminatory power of the diagnostic test.

BS cells: **WMU Test:** p-value=0.4511 **Tailratio:** 0.8719 suggests a relatively small deviation from the null hypothesis. There is no strong evidence of a substantial difference in the distributions between the compared groups. **U3:** 0.5215 indicates a moderate probability that a randomly selected CE from one group will exceed that of another group. However, this effect is not pronounced enough to be considered significant. **Auroc:** 0.4878 is below 0.5, suggesting a weak discriminatory power of the diagnostic test. This indicates a limited precision in capturing the observed effects.

NS cells: **WMU Test:** p-value=0.5694 **Tailratio:** 1.1092 indicates a moderate extent of deviation from the null hypothesis. **U3:** 0.462, there is a moderate probability that a randomly selected firing rate from one group will exceed that of a randomly selected firing rate from another group. **Auroc:** 0.4898, The Auroc value of 0.4898 suggests a modest discriminatory power of the diagnostic test.

In the case of CE, we followed a similar approach, presenting detailed information on WMU test results and effect size calculations in Figure 5.1.B. The notable significance and effect sizes varying from weak to substantial effects underscore the robustness and relevance of our findings. Here an explaining for All-cells CE during sound presentation results. We conducted a similar analysis for CE across age groups.

CE spontaenous activity

All cells WMU Test: p-value=0.0023 **Tailratio:** 1.1321 signifies a considerable deviation from the null hypothesis, suggesting a pronounced difference in CE distributions between the compared groups. **U3:** 0.4568, there is a probability that a randomly selected CE from one group will exceed that of a randomly selected CE from another group, contributing substantially to the overall effect size estimation. **Auroc:** 0.4669 indicates a moderate discriminatory power of the diagnostic test, revealing a discernible precision in capturing the observed effects.

BS cells WMU Test: p-value=0.048 **Tailratio:** 1.0655 denotes a moderate extent of deviation from the null

hypothesis, implying a discernible difference in CE distributions between the compared groups. **U3:** 0.4599, there is a moderate probability that a randomly selected CE from one group will exceed that of a randomly selected CE from another group. **Auroc** :0.4730 suggests a weak discriminatory power of the diagnostic test, indicating a moderate precision in discerning the observed effects.

NS cells: WMU Test: p-value=0.0941 **Tailratio:** 1.1672 indicates a substantial deviation from the null hypothesis, signifying a notable difference in CE distributions between the compared groups. **U3:** 0.4769, there is a moderate probability that a randomly selected CE from one group will exceed that of a randomly selected CE from another group, contributing significantly to the overall effect size estimation. **Auroc:** 0.4699, suggests no discernible discriminatory power of the diagnostic test, indicating a limited precision in capturing the observed effects.

CE natural sound evoked-response activity

All cells: WMU Test: p-value=2.5816e-11 **Tailratio:** 0.7145 denotes a moderate extent of deviation from the null hypothesis. **U3:** 0.6121, there is a substantial probability that a randomly selected CE from one group will exceed that of a randomly selected CE from another group. **Auroc:** 0.5855 indicates a discriminatory power of the diagnostic test.

BS cells: WMU Test: p-value=6.8380e-06 **Tailratio:** 0.7658 denotes a moderate extent of deviation from the null hypothesis, suggesting a discernible difference in CE distributions between the compared groups. **U3:** 0.5944, there is a substantial probability that a randomly selected CE from one group will exceed that of a randomly selected CE from another group. **Auroc:** 0.5731 suggests a considerable discriminatory power of the diagnostic test.

NS cells: WMU Test: p-value=4.2162e-09 **Tailratio:** 0.5342 denotes a substantial deviation from the null hypothesis. **U3:** 0.6447 there is a substantial probability that a randomly selected CE from one group will exceed that of a randomly selected CE from another group. **Auroc:** 0.6265 indicates a considerable discriminatory power of the diagnostic test, revealing a precision in capturing the observed effects.

These interpretations provide a nuanced understanding of the functional relevance of FR and CE differences, considering both statistical significance and effect size metrics. Furthermore, despite a considerable sample size, the number per samples is the same in CE and FR analyses however there is no consistent effects in CE and FR across similar age groups and strains nor inverse effects, suggesting that the statistical observations are not due to the variance or the samples.
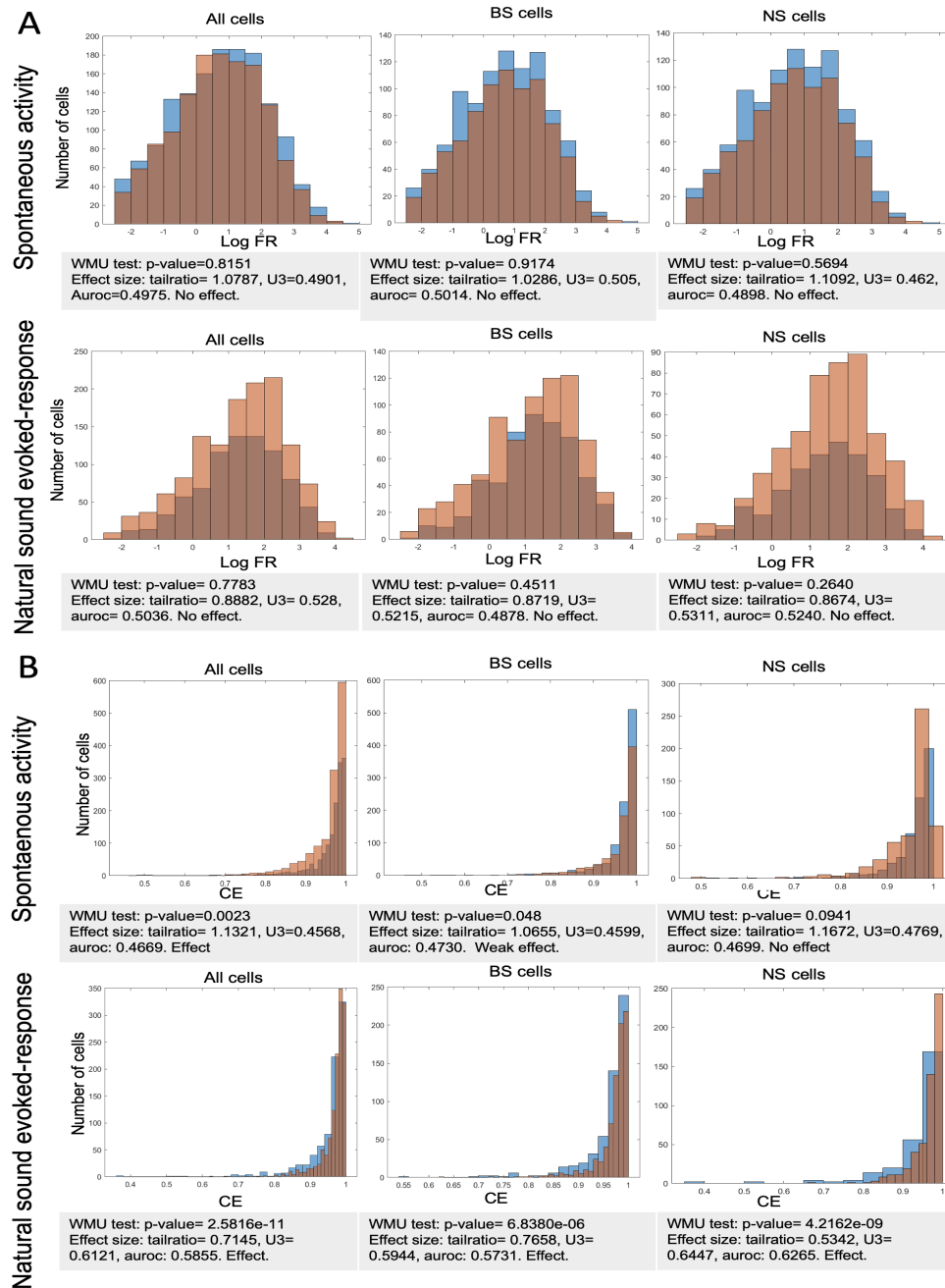
Figure 5.1: *CE, FR and effect size.*
(A) Comparison of the cell LogFR distribution in All, BS and NS cells between Hybrid, blue, and C57, red, mice strains, and their relative p values and effect size. (B) Same than (A) for the CE.

5.2 Natural sound presentation leads to higher FR in R compare to silence

We conducted a comparison between the spontaneous and evoked-response FR of the R cell. As expected, R cell exhibit a significantly higher FR during sound presentation compared to silence in both mouse strains and all cell types (Figure 5.2. BEH, All cell: F(1)=379, p<e-16, two-way ANOVA, BS: F(1)=177, p<e-16, two-way ANOVA, NS: F(1)=200, p<e-16, two-way ANOVA).
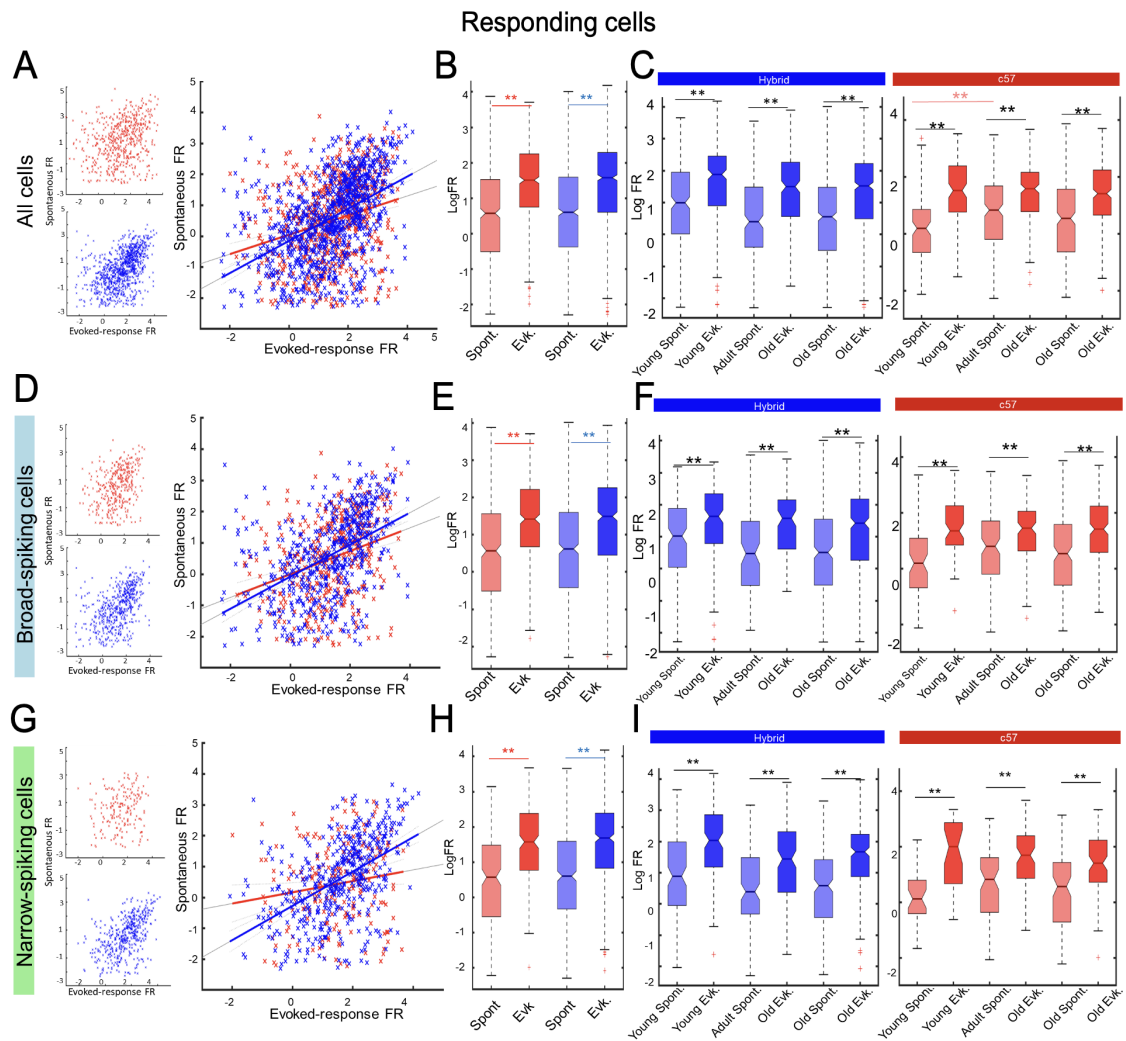
Figure 5.2: *Comparison between the spontaneous and evoked-response FR in R*

(A) Log FR during spontaneous, spont, and, evoked-resepose, evk in All cell show a linear relationship in Hybrid mice cell, blue, (p=1.88e-16, linear regression) and C57 cell, red, (p=8e-16, linear regression). (B) Log FR during spont and evk activity comparison in All cell. Higher FR during evk than spont activity is observable (F(1)=379, p<e-16, two-way ANOVA, all p<e-7, Tukey HSD Post hoc). (C) Log FR is a spont and evk across age groups and strains. In Hybrid mice, Log FR is higher during evk than spont (F(1)=220, p<e-16, two-way ANOVA). In both auditory stimulation the Log FR decreases with age (F(2)=15, p=3e-7, two-way ANOVA, young to adult p=.0001, young to old p=e-6, Tukey HSD Post hoc), no significance of the interaction between auditory stimuli and age groups. In C57, the Log FR is affected by auditory stimulation (F(1)=164, p<e-16, two-way ANOVA, all stimulation p<e-7,) and auditory stimulation and age groups effect, where the Log FR increases from young to adult during spont activity (F(1,2)=5.7, p=.02, two-way ANOVA, young to adult spont p=.01, Tukey HSD Post hoc). (D) as in (A) for BS. Hybrid mice (p=2e-37, linear regression) and C57 (p=2e-14, linear regression). Log FR show a linear relationship between evk and spont activity. (E) Same as (B) for BS, (F(1)=177, p<e-16, two-way ANOVA, all p<e-7, Tukey HSD Post hoc). (F) Same as (C) for BS. In Hybrid mice, Log FR is higher during evk than spont (F(1)=95, p<e-16, two-way ANOVA, all p<e-3, Tukey HSD Post hoc), with no significance of the interaction between auditory stimuli and age groups. In C57, the Log FR is affected by auditory stimulation (F(1)=87, p<e-16, two-way ANOVA, all p<e-6, Tukey HSD Post hoc). (G) as in (A) for NS in Hybrid mice (p=7e-32, linear regression) and C57 (p=.006, linear regression). Log FR show a linear relationship between evk and spont activity. (H) Same as (B) for NS, (F(1)=200, p<e-16, two-way ANOVA, all p<e-7, Tukey HSD Post hoc). (I) Same as (C) for NS. In Hybrid mice, Log FR is higher during evk than spont (F(1)=137, p<e-16, two-way ANOVA, all p<e-6, Tukey HSD Post hoc), Log FR decreases with age (F(2)=10, p=3e-5, two-way ANOVA, young to adult p=.00009, young to old p=.0003, Tukey HSD Post hoc), no significance of the interaction between auditory stimuli and age groups is observed. In C57, the Log FR is affected by auditory stimulation (F(1)=65, p<e-16, two-way ANOVA), and no age or interaction effects are significant.

The higher FR during sound-presentation than silence remained consistent across mice ageing in Hybrid mice (Figure 5.2.CFI, Hybrid mice All cell: $F(1)=220$, $p=2e-16$, two-way ANOVA, all $p<e-8$, Tukey HSD Post hoc, Hybrid mice BS: $F(1)=95$, $p=2e-16$, two-way ANOVA, young $p=.001$, adult $p<e-6$, old $p<e-8$, NS: $F(1)=137$, $p=2e-16$, two-way ANOVA, young $p<e-8$, adult $p<e-7$, old $p<e-8$, Tukey HSD Post hoc).Although the effect of auditory stimulation on FR was significant in Hybrid mice All cell, BS and NS ($F(2)=15$, $p=3e-7$, $F(2)=6$, $p=.003$, $F(2)=10$, $p=3e-5$, two-way ANOVA, respectively), there was no interaction between auditory stimulation and age in All, BS, and NS. In C57, the FR was also higher during sound presentation than silence in All, BS, and NS (All: $F(1)=164$, $p=2e-16$, two-way ANOVA, BS: $F(1)=87$, $p=2e-16$, two-way ANOVA, NS: $F(1)=65$, $p=7e-15$, two-way ANOVA) with the FR higher during sound than silence (All: all $p<e-8$, BS: young $p=e-7$, adult $p=.0004$, old $p<e-8$, NS: young $p=5e-4$, adult $p=.0001$, old $p<e-7$, Tukey HSD Post hoc). The All cell C57, the FR is affected by the interaction of the auditory stimulation and age groups (Figure 5.2.C, $F(1,2)=164$, $p<2e-16$, two-way ANOVA, $p=.02$, Tukey HSD Post hoc), but no interaction effect between auditory stimulation and age was observed in BS and NS Hybrid mice and C57 (Figure 5.2.FI).

When comparing the FR across age groups and strains, we found that the evoked-response FR is consistently higher than the spontaneous FR in both mouse strains and all cell types across all age groups (Figure 5.3). Comparing the FR during spontaneous and evoked-response activity showed a significant main effect of auditory stimulation on FR (Figure 5.3.BDF, All cell: $F(1)=98$, $p<e-16$, BS: $F(1)=41$, $p<e-10$, NS: $F(1)=61$, $p<e-14$, two-way ANOVAs). Interestingly, we observed an interaction effect between auditory stimulation and strain in the BS at the young age group (Figure 5.3.B, middle panel, $F(1,1)=7$, $p=.01$, two-way ANOVA). The spontaneous FR was significantly higher in Hybrid mice than in C57 mice (Figure 5.3.B, $p=.0006$, Tukey HSD Post hoc). Conversely, in the adult age group, we observed an inverse result in All cell (Figure 5.3.D, top panel, $F(1,1)=6.5$, $p=.01$, two-way ANOVA, $p<e-5$, Tukey HSD Post hoc).

To further investigate the relationship between the FR during silence and sound presentation, we compared the FR value of the same cell during spontaneous and evoked response via scatterplots (Figure 5.2.ADG and 5.3.ACE). Our results showed that there is a linear relationship between the two types of activity in all cell types (All, BS, and NS) in the Hybrid mice and C57 strains, as demonstrated by linear regression analysis (Figure 5.2.ADG, All cell Hybrid mice $p=e-59$, C57 $p=e-12$, BS Hybrid mice: $p=e-33$, C57 $p=e-10$, NS Hybrid mice: $p=e-30$, C57 $p=.01$, linear regression). This relationship in different along age-group, the linear relationship between the spontaneous and evoked-response FR is abolished in all young C57 cell types and old NS, where it is conserved in all age groups in Hybrid mice (Figure 5.3.ACE, young Hybrid mice: All cell: $p=e-28$, BS: $e-15$, NS: $e-15$, adult Hybrid mice: All cell: $p=e-15$, BS: $p<e-10$, NS: $p<e-7$, C57: All cell: $p<e-7$, BS: $p=.0003$, NS: $p=.0007$, linear regression) and in all adult and old C57 cell-types (adult C57: All cell $p=1.4e-7$, BS $p=.0003$, NS $p=.0007$, old C57: All cell $p=1.19e-7$, BS $p=1.6e-7$, linear regression linear regression). These results support the previous results the FR is lower than Hybrid mice in young C57 mice during spontaneous activity and not different during sound-presentation.
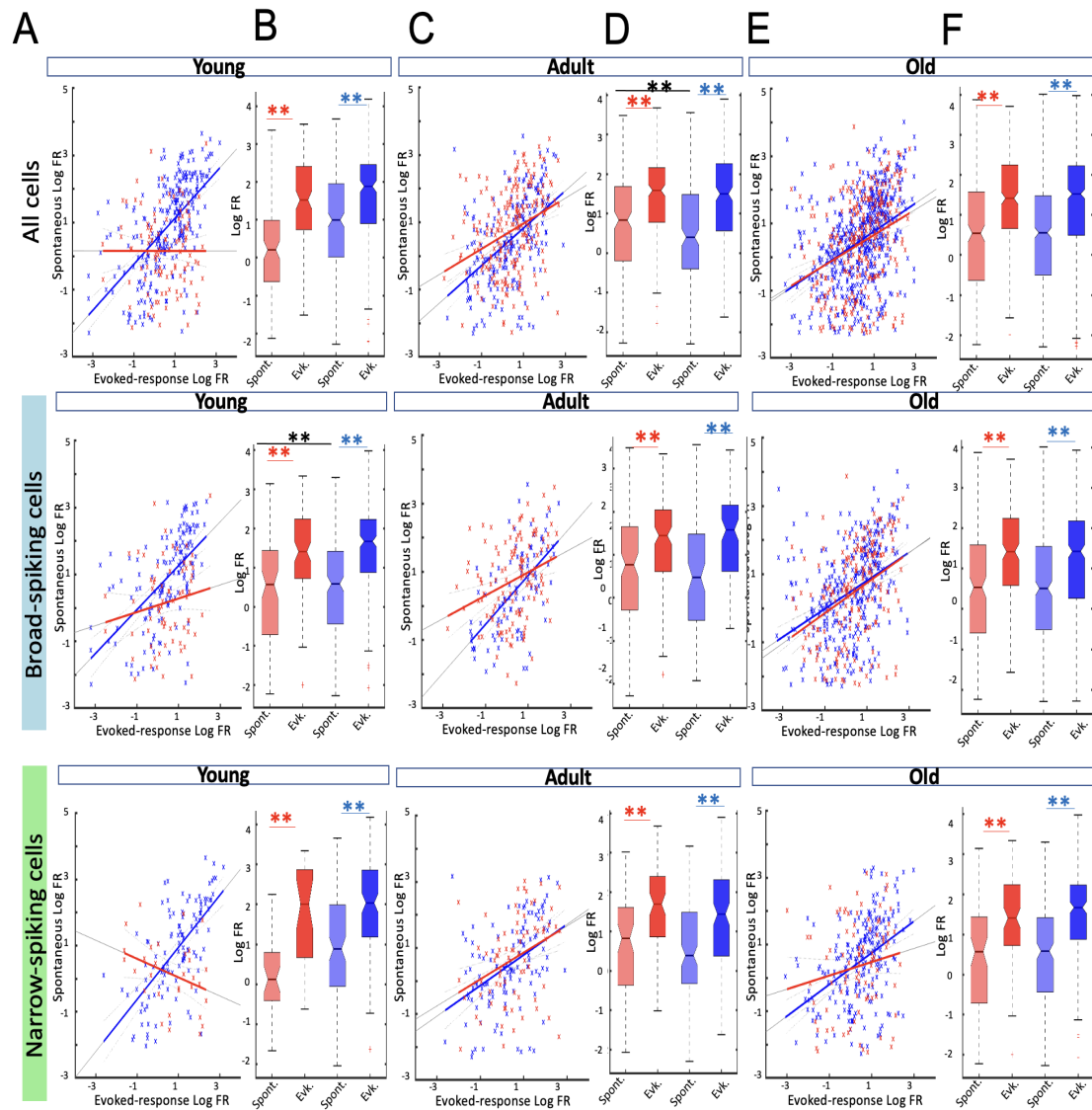
Figure 5.3: *Comparison of R FR during spontaneous and evoked activity across age groups, strains, and cell types*
(A) Log FR during spont and evk in Young All (top panel), BS (middle panel) and NS (bottom panel). A linear relationship is found in young Hybrid mice, blue, (All cell: p=9.55e-28, BS p=6.7e-15, NS p=1.12e-15, linear regression) and not in C57, red. (B) Log FR during spont and evk activity comparison in All cell. Higher FR during the evk than spont activity is observable (F(1)=144, p<e-16, two-way ANOVA, all p<e-7, Tukey HSD Post hoc). (C) Same as (A) in adults. A linear relationship is observed in Hybrid mice (All cell, p=3e-10, BS p=2.33e-10, NS p=6.17e-7, linear regression) and C57, (All cell p=1.4e-7, BS p=.0003, NS p=.0007, linear regression). (D) Same as (B) in adults. In All cell, the Log FR is higher during evk than spont (F(1)=101, p<e-16, two-way ANOVA, all p<e-7, Tukey HSD Post hoc), with an effect of strain (F(1)=19, p<1e-5, two-way ANOVA) and interaction effect (F(1,1)=7, p=.01, two-way ANOVA). The Log FR is higher in spont C57 than in Hybrid mice (p<e-6, Tukey HSD Post hoc). Only auditory stimulation affects BS and NS (BS: F(1)=48, p<e-11, two-way ANOVA, p<e-5, Tukey HSD Post hoc, NS: F(1)=46, p<e-11, two-way ANOVA, p<e-4, Tukey HSD Post hoc). (E) Same as (A) in old. A linear relationship is found in old Hybrid mice, (All cell p=4.1e-22, BS p=4.74e-14, NS p=5.07e-11, linear regression) and C57, (All cell p=1.19e-7, BS p=1.6e-7, linear regression). The old C57 NS do not present this linear relationship. (F) Same as (B) in old. (Hybrid mice and C57: All: F(1)=205, p<e-16, two-way ANOVA, p<e-8, Tukey HSD Post hoc, BS: F(1)=205, p<e-16, two-way ANOVA, p<e-8, Tukey HSD Post hoc, NS: F(1)=90, p<e-16, two-way ANOVA, p<e-8, Tukey HSD Post hoc).

Finally, to quantify changes in the FR from spontaneous activity to natural sound presentation evoked-responses, we computed a modulation index (Figure 5.4).A modulation index of zero indicates no change in the FR between the two auditory simulations, a negative value indicates a decrease in FR during the evoked response, and a positive value indicates an increase. Analysis of the FR index revealed that the strain and age-groups interaction affect the All and BS FR index (Figure 5.4, all cell: $F(1)=4.56$, $p=.01$, BS: $F(1)=6.84$, $p=.001$, two-way ANOVA). A decrease from young to adult in the C57 FR during the natural sound presentation than during spontaneous activity in All ($p=.03$, Tukey HSD Post hoc with 999 permutations), while the increased FR during the sound presentation is more important in young C57 than Hybrid mice at young age, ($p=.04$, Tukey HSD Post hoc with 999 permutations). No such difference was observed in NS.
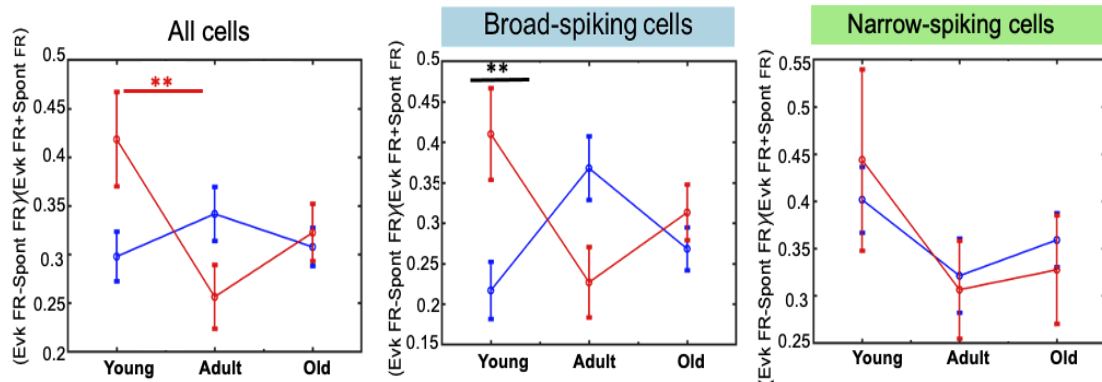
Figure 5.4: *Fraction of changes between spontaneous and evoked-responses FR*
Modulation index along with ageing in Hybrid mice, blue, and C57, red, (All cell: $F(1)=4.58$, $p=.01$, two-way ANOVA, young to adult C57 $p=.03$, Tukey HSD Post hoc 999 permutations, BS: $F(1)=4.02$, $p=.04$, two-way ANOVA, young C57 vs Hybrid mice. $p=.04$, Tukey HSD Post hoc 999 permutations)..

5.3 NR FR shows a higher FR during the natural sound presentation than silence in old mice

As a next step, we aimed to compare the NR cell activity between the natural sound presentation and the spontaneous response. Studying the NR in the AC could provide information about the processing of sensory information in the AC. NR are defined as neurons that do not show a significant change in their FR in response to the natural sound stimulus (Figure 4.6). To investigate the difference in FR between spontaneous and evoked activity in the NR, we compared the level of FR of the same cell recorded in the two auditory conditions, silence, and natural sound-presentation (Figure 5.5). We found that in All cell, the FR of NR is higher during the sound presentation than silence in both mouse strains (Figure 5.5. B, $F(1)=98$, $p=e$-16, two-way ANOVA). In BS, we observed an effect of sound stimulation and strain ($F(1)=11$, $p=.0009$, $F(1)=11$, $p=.002$, two-way ANOVA), although we did not observe an interaction effect, we found that the spontaneous firing rate in C57 mice was lower than in Hybrid mice, (Figure 5.5. B, $F(1,1)=6$, $p=.01$, two-way ANOVA, $p=.0006$, Tukey HSD Post hoc). In the NS, although we found a difference between auditory stimulation, ($F(1)=15$, $p=.0001$, two-way ANOVA), we did not observe any interaction or strain effect. In the NS we observed only an effect of stimulation, where the evoked-response FR is higher than the spontaneous ($F(1)=15$, $p=.0001$, two-way ANOVA).
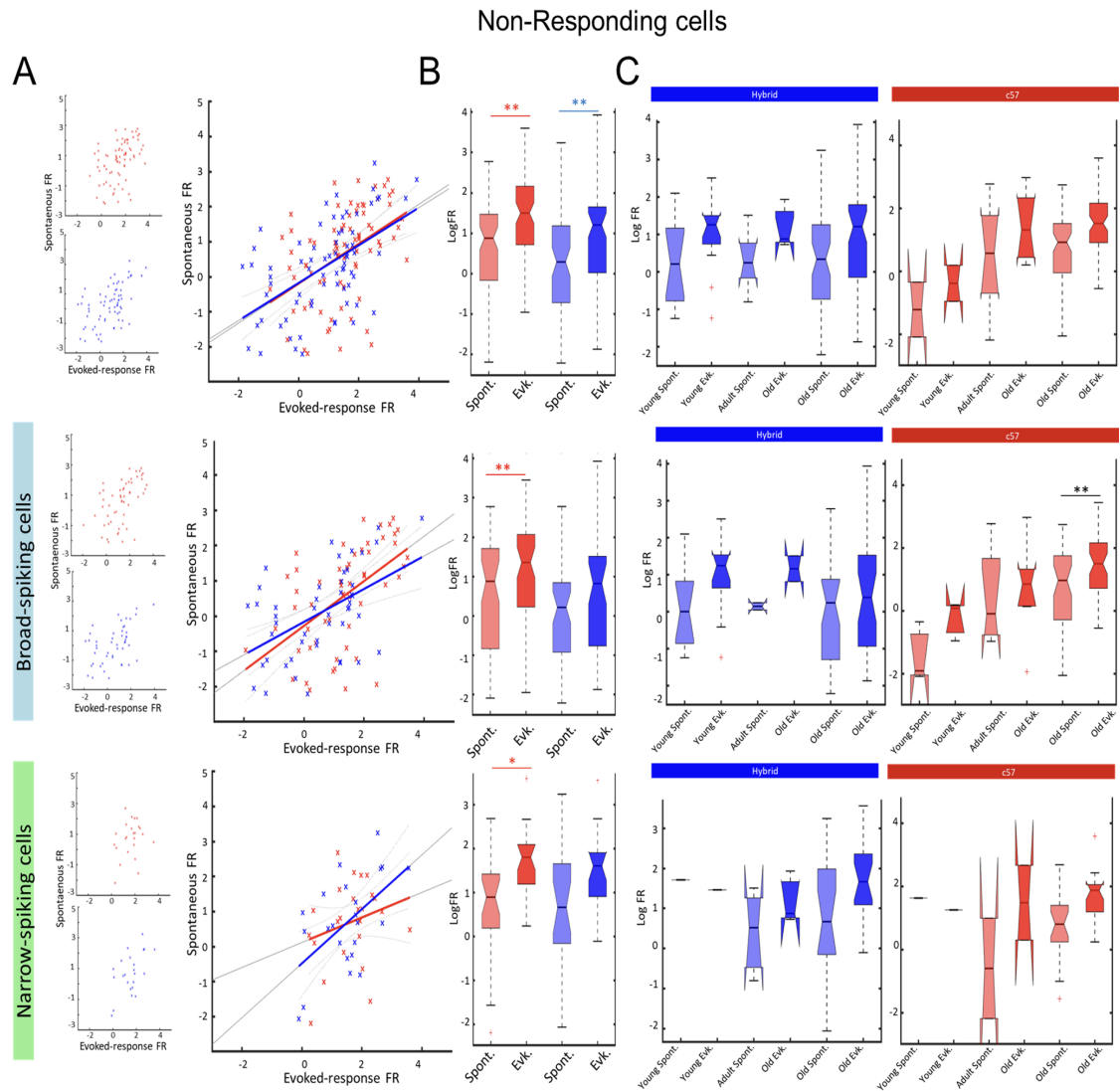
Figure 5.5: *Comparison of NR FR during spontaneous and evoked activity across age groups, strains, and cell types*
(A) Log FR during spont and evk show in All (top panel), BS (middle panel) and NS (bottom panel). A linear relationship is observed in Hybrid mice, blue, (All cell p=2.8e-6, BS p=1.32e-5, NS p=.005, linear regression), C57 cell, red, (All cell p=1.27e-6, BS p=.0003, linear regression) but not in NS. (B) Log FR during spont and evk activity comparison. Higher FR during evk than spont is observable as a strain effect in All and BS while only a stimulation effect is found in NS (All cell: $F(1)=23$, $p>e-16$, $F(1)=8$, $p=.004$, two-way ANOVA, Hybrid mice: $p=.03$, C57 $p=.0004$, Tukey HSD Post hoc, BS: $F(1)=11$, $p=.008$, $F(1)=11$, $p=.001$, two-way ANOVA, C57: $p=.01$, NS: $F(1)=15$, $p=.001$, two-way ANOVA, C57 $p=.02$). (C) Log FR in spont and evk across age groups and strains. In Hybrid mice, the Log FR is higher during evk than spont in All cell and NS ($F(1)=6$, $p=.01$, two-way ANOVA, $F(1)=5$, $p=.02$, two-way ANOVA). In C57, Log FR is higher during evk than spont (All cell: $F(1)=18$, $p=3e-5$, two-way ANOVA, BS: $F(1)=10$, $p=.002$, two-way ANOVA, NS: $F(1)=10$, $p=.002$, two-way ANOVA) and the Log FR increases with age in All and BS (All cell: $F(1)=6$, $p=.002$, two-way ANOVA, BS: $F(1)=7$, $p=.001$, two-way ANOVA).

We also observed that Hybrid mice NR cell show a significantly lower FR during spontaneous activity in All and NS (Figure 5.5.C, All $F(1)=6$, $p=.01$, two-way ANOVA, NS: $F(1)=5$, $p=.02$, two-way ANOVA). Hybrid mice BS NR cell do not present significant FR differences. In C57, we observed an effect of auditory stimulation and age groups in All and BS (Figure 5.5.C, All $F(1)=18$, $p=e-5$, $F(2)=6$, $p=.002$, two-way ANOVA, BS: $F(1)=10$,

p=.002, F(2)=7, p=.001, two-way ANOVA). In the BS, although the interaction is not significant, we observed a tendency of the spontaneous FR increases from young to old (p=.05, Tukey HSD Post hoc). In NR C57 NS, we observed an effect of auditory stimulation (Figure 5.5.C, F(1)=10, p=.002, two-way ANOVA). This result shows that the FR activity changes between spontaneous and evoked activity differ between Hybrid mice and C57 ageing. The NR FR in old age of All and BS is affected by strain and auditory stimulation conditions (Figure 5.6.A), All: F(1)=12, p=.0005, F(1)=17, p=e-5, respectively, two-way ANOVA, BS: F(1)=8, p=.006, two-way ANOVA, BS: F(1)=17, p=5e-5, F(1)=7, p=.006, respectively, two-way ANOVA). Post hoc analyses show that the C57 NR FR is higher during sound presentation than spontaneous in All and BS (All: p=.001, Tukey HSD Post hoc, BS: p=.02, Tukey HSD Post hoc) and higher in C57 than Hybrid mice during evoked-responses (All: p=.009, Tukey HSD Post hoc, BS: p=e-5, Tukey HSD Post hoc). Only old group is analysed as there were too few NR cell in the young and adult age groups. Interestingly, we found no significant difference in the modulation index in the FR of NR from spontaneous activity to natural sound presentation evoked-responses (Figure 5.6.B), shows no significance in the age groups, strains nor interaction effects.

Finally, we examined the linearity between spontaneous and evoked FR in the NR cell (Figure 5.5.A, Figure 5.6.A). The results showed that the Hybrid mice NR maintained a linear relationship between their spontaneous and evoked FR in all cell types, (All cell: p=5.7e-6, linear regression, BS: p=.001, linear regression, NS: p=.002, linear regression). However, the NS in the old C57 strain did not exhibit a significant relationship. Only All cell (p=.0008, linear regression) and BS (p=.001, linear regression) in the old C57 strain demonstrated a linear relationship between their spontaneous and evoked FR, as shown in Figure 5.5.A, Figure 5.6.A). In old Hybrid mice cell, the FR present a linear relationship in all cell types (All: p=5e-6, linear regression, BS: p=.001, linear regression, NS: p=.002, linear regression).
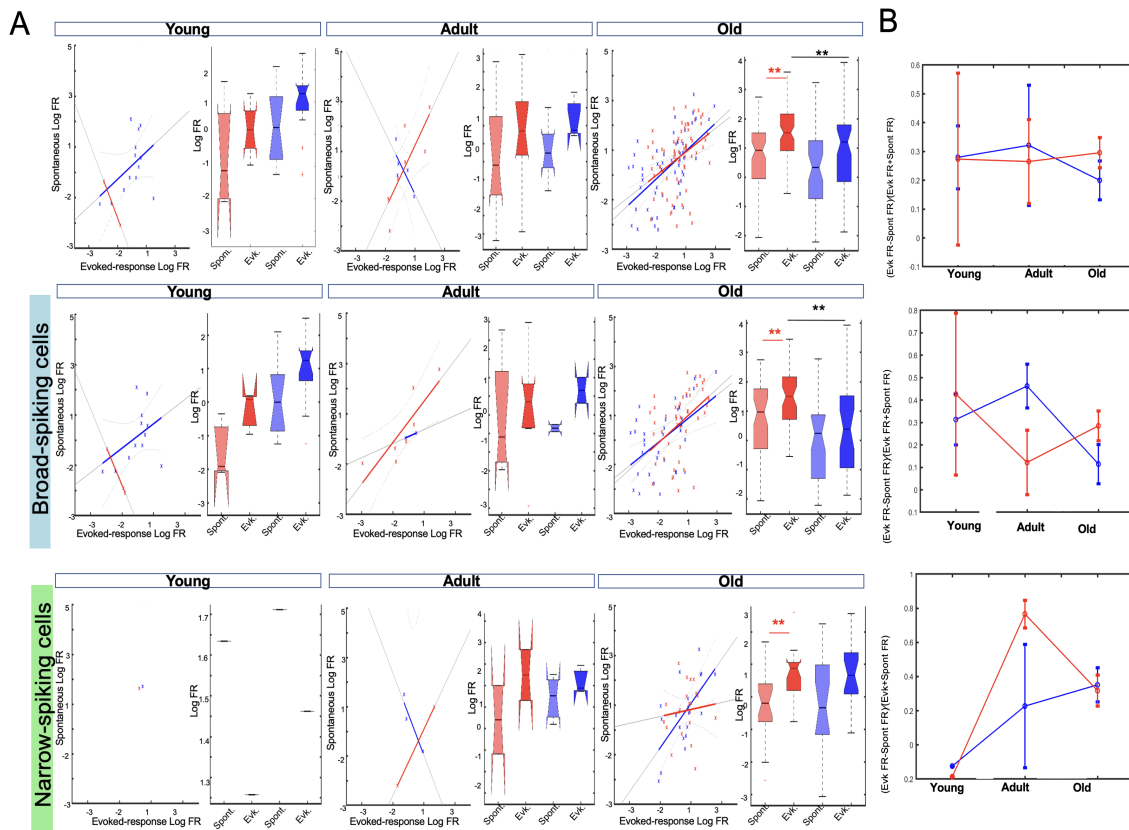
Figure 5.6: *Comparison of NR FR during spontaneous and evoked activity across age groups, strains, and cell types* (A) NR FR across age groups and strains. No statistical tests have been applied on young and adult ages because of the sample size. In old Hybrid mice, cell show a linear relationship between the spont and the evk firing activity in all cell types (All cell: p=5.7e-6, BS: p=.001, NS: p=.002, linear regression). In C57, only All cell and BS show a significant linear relationship (All cell: p=.0008, BS: p=.001, linear regression). In Hybrid mice, Log FR is higher during evk than spont all cell types (All cell: F(1)=17, p=4e-5, two-way ANOVA, BS: F(1)=8, p=.006, two-way ANOVA, NS: F(1)=13, p=.0004, two-way ANOVA). In All and BS, the Log FR increases from young to old (All cell: F(1)=20, p=.005, two-way ANOVA, BS: F(1)=17, p=5e-5, two-way ANOVA). (B) Modulation indexes of NR along with ageing in Hybrid mice and C57 shows no significant differences.

5.4 Higher responsiveness and FR to natural sound presentation compared to noise in both mice strains

To investigate age-related changes in the AC, mice were also exposed to noise at specific decibel levels, and evoked spike responses were recorded, same protocol than for natural sound presentation. Initially, we analysed the responses to multiple dB stimulation to simulate environmental conditions of natural sound presentation and we noted that the AC responses in C57 and Hybrid mice exhibited a higher FR compared to silence (Figure 5.7.C, p<e-5, two-way ANOVA) and linearity between the two variables (Figure 5.7.D, Hybrid p=8.5161e-177 and C57 p=8.4761e-167, linear regression analyses. Moreover, the FR in Hybrids compared to C57 mice was higher (Figure 5.7.AB, p=2e-23, T-test, and p=6e-23, Wilcoxon Mann-Whitney test).(Figure 5.7.AB presents the FR and LogFR along with their respective test p-values, illustrating the distribution changes. In our study, we opted to transform values using a log function to normalize the distribution, presenting a more suitable statistical approach. Transforming FR to Log FR proved to be a methodologically sound choice. We then analysed the FR between

spontaneous and noise evoked-response merged dB, observing an increase in firing during sound presentation in both strains).

Subsequently, emphasis is placed on the response to 80dB, where both strains of mice are expected to evoke a reaction even in advanced age, (Lyngholm & Sakata 2019). As for the merged dB analasis, the evoked-response FR is higher during sound presentation compared to silence and for both mice strains (Figure 5.7.E, F=49.7, both p<e-3, two-way ANOVA). A higher FR in Hybrid is found compared to C57 mice (p=0.03). We investigated the FR of R and NR (Figure 5.7.F) and found that R exhibited higher FR in Hybrid compared to C57 (p=4e-7, T test), while it was lower in NR (p=2e-12, T test). Additionally, C57 AC showed a lower proportion of R to noise compared to Hybrid (p=.0146, t-test).
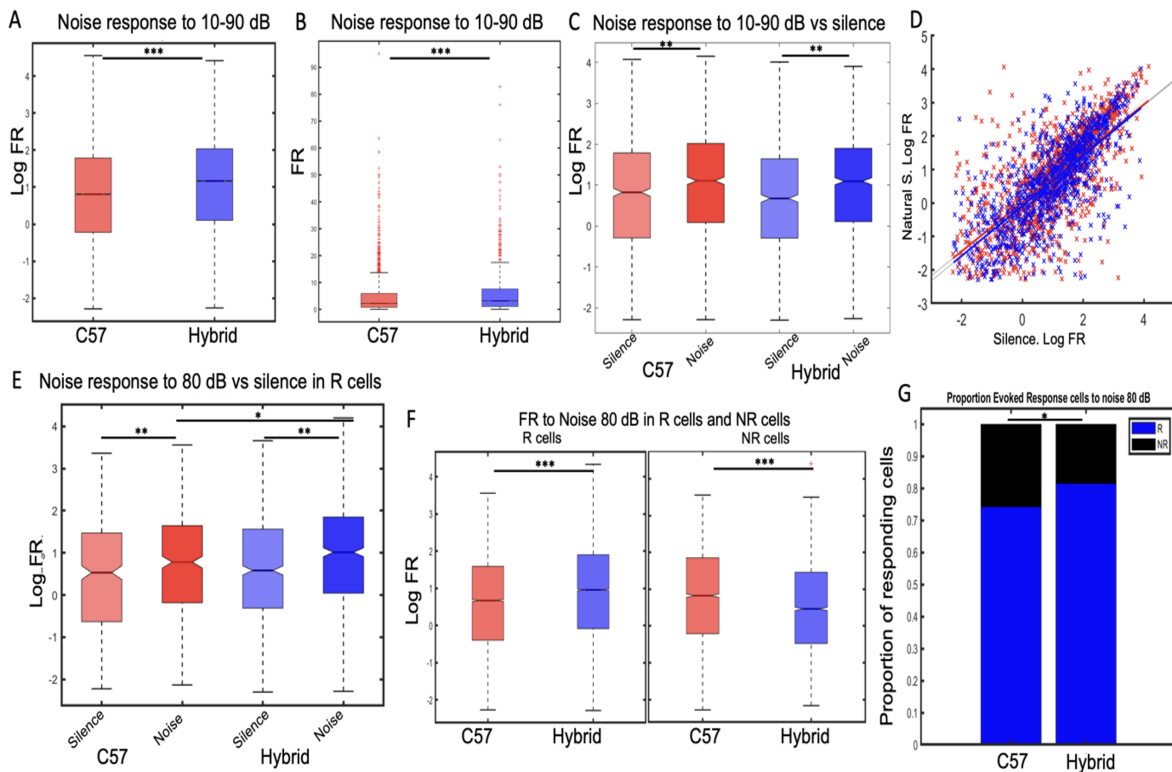
Figure 5.7: *FR activity during noise presentation across strains.*
(A) Log FR evoked-activity in response to noise range from 10 to 90 dB stimulation across strains, (p=2.e-23, t-test), C57 (red), Hybrid (blue). (B) Same as in A but with the FR before transformation (p=6e-23, Wilcoxon Mann-Whitney test). (C) LogFR changes between spontaneous to evoked-response to noise range from 10-90 dB across strains (all p<e-5, two-way ANOVA). (D) Linear relationship between spontaneous and noise evoked-response LogFR (Hybrid p=8.5161e-177 and C57 p=8.4761e-167, linear regression). (E) LogFR changes between spontaneous to evoked-response to 80dB noise presentation within strain (F=49.7, both p<e-3, two-way ANOVA two-way ANOVA), a higher FR is observed in Hybrid evoked-response compared to C57 (p=.03). (F) Higher evoked-response to 80dB FR is R Hybrid compared to C57, (p=4e-7, T test). Lower in NR Hybrid compared to C57 (p=2e-12, T test). (G) Proportion of responding cells between C57 and Hybrid (p=.0146, t-test).

In our exploration of AC response to 80dB noise presentation across ageing, we visualized the proportion of R across mice ageing (Figure 5.7.G and Figure 5.8.A). We found a lower proportion of R in old C57 compared to Hybrid (Figure 5.7.B, p=0.01, t test). These results are observed for BS and NS (BS old C57 Hybrid p=0.03,

t test, and NS p=0.01, t-test). In both mice strains, the FR evoked-response decreased with age (Figure 5.8.C), with a higher FR activity in Hybrid compared to C57 at young and old age groups (F=90, all p<e-5, two-way ANOVA). Similar results were observed in BS (F=49, all p<e-5, two-way ANOVA) and NS (F=46, all p<e-5, two-way ANOVA).
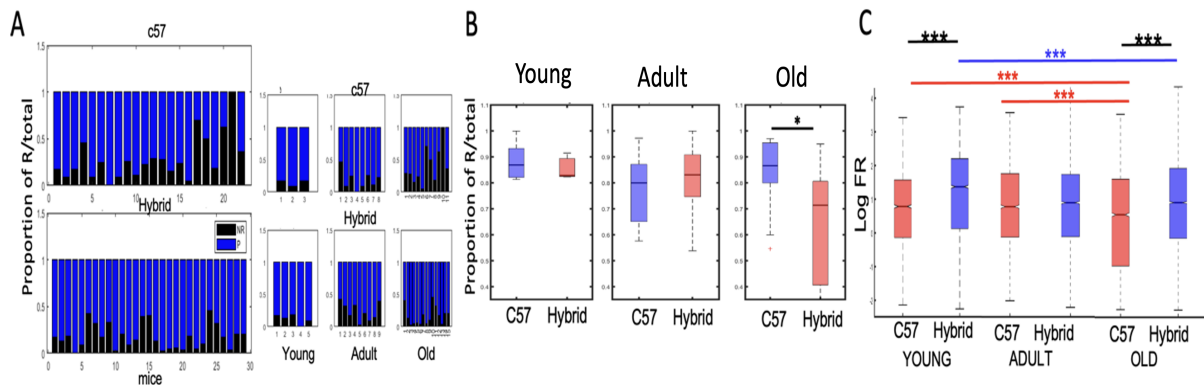
Figure 5.8: *Age-related changes in responsiveness and FR activity during noise presentation across strains.* (A)The proportion of cells across in C57 and Hybrid mice sorted by age and across young, adult, and old age-groups. (B) Proportion of R in C57 and Hybrid mice across age-groups. A lower proportion of R is observed in old C57 (p=0.01, t test). (C) LogFR changes along with ageing, the LogFR decreases between young to adult and between adult to old in C57 and between young to old in Hybrid R (F=90, all p<e-5, two-way ANOVA). Both LogFR decreases throughout ageing and Hybrid FR activity is higher than C57 in young and old groups (all p<e-5, t-test).

Integrating the analyses of noise-evoked responses with those of natural sound-evoked responses in the AC to adds a compelling layer of depth and relevance to our study. We compared the FR activity during noise at 80dB presentation and natural sound, revealing a linear relationship between noise and natural sound LogFR in both strains (Figure 5.9.A, Hybrid p=3.9548e-11, C57 p=6.1869e-06, linear regression test). With an increase in the LogFR during natural sound presentation compared to noise (Figure 5.9.BD, F=33, both p<e-4, two-way ANOVA), consistency seen in all age groups (Hybrid and C57 all p<e-5, t-tests).

We then questioned whether NR and R cells recorded during noise were the same during natural sound presentations (Figure 5.7C). Approximately 70% of labelled cells during noise were the same during natural sound presentation (R and NR). Interestingly, more neurons responded to natural sound compared to 80 dB noise presentation, in both mice strains (Hybrid: X-squared = 3161.2, p< 2.2e-16, ni proportion of R= 0.8388, ns proportion of R= 0.9468, C57: X-squared = 1904, p<2.2e-16, proportion test, ni proportion of R= 0.7264, ns proportion of R = 0.9062). Moreover, the transition between NR to R was more significant in C57 compared ton Hybrid (X-squared = 611.79, p= <2.2e-16, proportion test), especially during ageing (Figure 5.9.E).

Our results highlighted several key findings. First, Hybrid and C57 mice exhibited higher FR during natural sound presentation compared to noise, a trend consistent across age groups, with a proportion of responding cells decreasing from young to old C57 mice compared to Hybrid but are higher during natural sound presentation compared to noise.
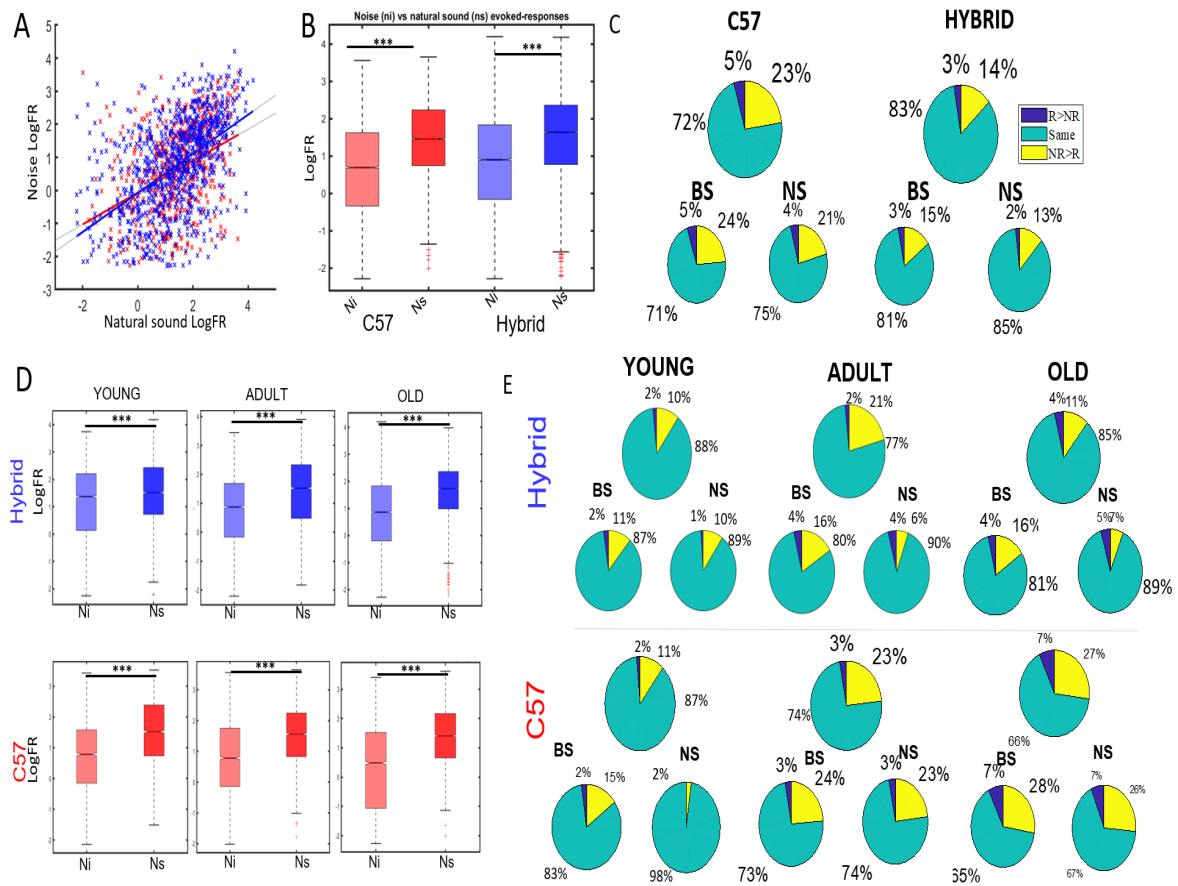
Figure 5.9: *Comparison between C57 and Hybrid FR and proportion of R cells.*
(A) Linear relationship between noise and natural sound evoked responses, LogFR in R of C57 and Hybrid mice (Hybrid p=3.9548e-11, C57 p= 6.1869e-06, linear regression test). (B) LogFR comparison between noise (ni) and natural sound evoked-response (ns) in R of C57 and Hybrid, (F=33, both p<e-4, two-way ANOVA). (C) Analysis of the consistency of R across sound stimulation. Green represents the same cells labelling between noise and natural sound auditory stimulation. Yellow represents the switching in labelling of the cells from NR in ni to R in ns and blue from R in ni to NR in ns. Top Camembert plots represent all cells in C57, left, and Hybrid mice, right. bottom Camembert plots represent changes in the cells labelling across cell-types. (D) Comparison of the LogFR of R in ni and ns across age groups and strains, Hybrid, top, and C57, bottom, (Hybrid and C57 all p<e-5, t-tests). (E) Same as in C across ageing and strains.

The intriguing aspect of these results lies in the fact that, despite potential hearing impairment in C57 mice, the AC still demonstrates a heightened ability to respond to natural sound activity, with a higher proportion of responding cells. Even in the context of potential deafness, the observed higher FR during natural sound presentation in C57 mice suggests that the AC retains a remarkable sensitivity to natural auditory stimuli.

5.5 Higher CE during natural sound evoked-response in Hybrid mice, but lower in C57, compared to spontaneous activity

To conduct a more comprehensive analysis and delve deeper into the computational disparity between spontaneous and evoked responses, we compared the CE derived from spontaneous and evoked activities. This comparison enabled us to detect any changes in the transmission of information caused by auditory stimuli and explore how such changes may differ across various age groups, cell types, and mouse strains. This information can provide

valuable insights into the AC's response to auditory input, and shed light on how alterations in the processing of sensory information may contribute to hearing loss or other auditory impairments.

We compared the CE changes between silence and sound presentation (Figure 5.10. B), we observed that the CE is affected by the interaction between the strain and auditory stimulation conditions in all cell types (All: $F(1,1)=30$, $p=4e-8$, BS: $F(1,1)=10$, $p=.001$, BS: $F(1,1)=22$, $p=3e-6$). We first observed that the CE is higher during sound-presentation than during silence in Hybrid mice (Figure 5.10. B, All: $p=2e-7$, BS: $p=.0007$, and NS: $p=.0005$, Tukey HSD Post hoc 999 permutations), whereas the CE is lower during sound-presentation in C57 in All and NS, (All: $p=.03$, SRH test, Tukey HSD Post hoc 999 permutations, NS: $p=.01$, two-way ANOVA 999 permutations). Secondly, we observed that the CE during the sound presentation was higher in Hybrid mice compared to C57 across all cell types (All: $p=e-6$, Tukey HSD Post hoc 999 permutations, BS: $p=.008$, Tukey HSD Post hoc 999 permutations, NS: $p=e-6$, Tukey HSD Post hoc 999 permutations). These results suggest that the vocabulary used during sound-presentation is broader than during silence in Hybrid mice, and inversely in C57.

To investigate the effects of age and auditory stimulation on CE changes, we examined the ageing CE changes in each strain (Figure 5.10. CD). In Hybrid mice, we observed that the CE of R is influenced by auditory stimulation conditions and age groups, but not the interaction between both variables (Figure 5.10 C). The CE is higher during sound presentation than in silence (All: $H(1)=16$, $p=e-4$, SRH, BS: $H(1)=5$, $p=.02$, SRH, NS: $H(1)=10$, $p=.001$, SRH). We also observed an age-group effect in All and BS, where the CE followed a U-shaped trend (All: $H(2)=31$, $p<e-6$, SRH, BS: $H(1)=23$, $p=.00001$, SRH). However, no age effect was observed in NS, nor was there any interaction effect between age groups and auditory stimulation conditions. Given the age and stimulation effects, post hoc analyses on All revealed that the Hybrid mice spontaneous CE followed a U-shaped trend, and the evoked-response CE increased from adult to old. Additionally, the CE was higher in evoked-response than in silence in the old age group (spontaneous: young to adult: $p=.0006$, adult to old $p=.0006$, evoked-response: adult to old $p=.0005$, old spontaneous vs evoked-response $p=.001$, Dunn test Post hoc with Bonferroni correction). The same results were observed in BS, except for the difference between spontaneous and evoked responses in the old group (spontaneous: young to adult: $p=.007$, adult to old $p=.0013$, evoked-response: adult to old $p=.01$, Dunn test Post hoc with Bonferroni correction).

In the C57 strain, we observed that the CE of R is affected by auditory stimulation and the interaction between age groups in All and BS (Figure 5.10. D, All: $H(1)=9$, $p=.01$, SRH, BS: $H(1)=8$, $p=.01$, SRH). Specifically, the CE of spontaneous activity and evoked-responses decreases with age and is higher during silence in the adult group in All (spontaneous: young to adult: $p=.006$, young to old $p=.003$, evoked-responses: young to adult: $p<e-4$, young to old $p<e-4$, adult: $p=.005$, Dunn test Post hoc with Bonferroni correction). In BS, there was no significant difference in the spontaneous CE nor between the two auditory conditions at adult age, but the CE decreased from young to adult and from young to old during the sound presentation (young to adult: $p<e-4$, young to old: $p<e-4$, adult: $p=.005$, Dunn test Post hoc with Bonferroni correction). In the NS, only an age-group effect was observed ($H(1)=60$, $p<e-6$, SRH).
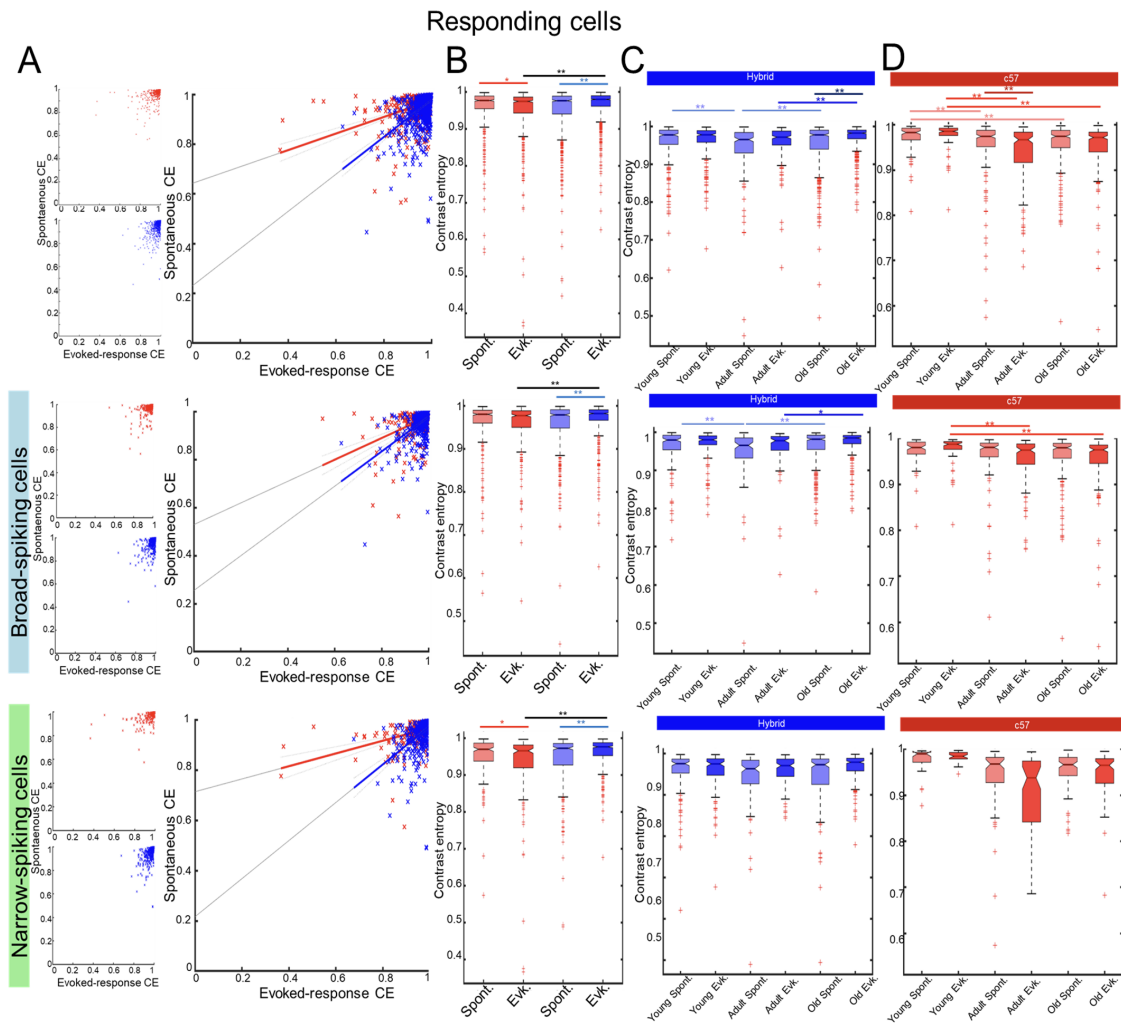
Figure 5.10: *Comparison between the spontaneous and evoked-response CE in R.*

(A) Spont and evk CE show a linear relationship in Hybrid mice and C57. Hybrid mice All cell, top, p=5.6e-71, BS, middle, p=3.9e-21, NS, bottom, p=1.9e-29, linear regression, C57 All cell p=2.18e-28, BS p=1.6e-42, NS=2.44e-10, linear regression. (B) CE during spont. and evk. between strain. The CE is higher in Hybrid mice than C57 during evk (All cell: p=e-7, Tukey HSD post hoc 999 perm, BS: p=.008, Tukey HSD post hoc 999 perm, NS: p=e-7, Tukey HSD post hoc 999 perm). In Hybrid mice, the CE is higher during evk than spont (All cell: p=.e-7, Tukey HSD post hoc 999 perm, BS: p=.0007, Tukey HSD post hoc 999 perm, NS: p=.0005, Tukey HSD post hoc 999 perm). In C57, the CE is lower during evk than spont in All cell and NS (All cell: p=.03, Tukey HSD post hoc 999 perm, NS: p=2e-6, Tukey HSD post hoc 999 perm). (C) CE in spont and evk across age groups. In Hybrid mice All cell, the CE is affected by age groups and auditory stimulation (respectively, F(2)=6, p=.002, F(1)=36, p=2e-9, two-way ANOVA 999 perm, young to adult p=.04, young to old p=.001, Tukey HSD post hoc 999 perm), where the CE is higher during evk than spont. The spont CE follow a U-shape (F(2,1)=3, p=.06, two-way ANOVA 999 perm, young to adult p=.006, adult to old p=.0006, Tukey HSD post hoc 999 perm), while the evk CE increase from adult to old (p=.04, Tukey HSD post hoc 999 perm) with higher CE in evk than spont at old age (p<e-7, Tukey HSD post hoc 999 perm). In BS, the CE is affected by age groups and auditory stimulation (respectively, F(2)=6, p=.002, F(1)=16, p=6e-5, two-way ANOVA 999 perm, old evk vs spont p=.005, Tukey HSD post hoc 999 perm). In NS, the CE is affected by auditory stimulation and the interaction between age groups and auditory stimulation (respectively, F(1)=19, p=9e-6, F(2,1)=3, p=.04, two-way ANOVA 999 perm, old spont vs evk p=.00005, Tukey HSD post hoc 999 perm). (D) CE in spont and evk across age groups and auditory stimulation. In C57 the CE is affected by auditory stimulation and its interaction with the age-groups variable in All cell and BS (All cell: H(1)=9, p=.01, SRH, BS: H(1)=8, p=.01, SRH). In All cell, the CE of spont and evk decreases with age and is higher during silence in adult (Spont: young to adult: p=.006, young to old p=.003, evk: young to adult: p<e-4, young to old p<e-4, adult: p=.005, Dunn test Post hoc with Bonferroni correction). In BS, the CE decreased from young to adult and from young to old during evk (young to adult: p<e-4, young to old p p<e-4, adult:p=.005, Dunn test Post hoc with Bonferroni correction). In the NS, only an age-group effect was observed (H(1)=60, p=<e-6, SRH).

To compare between age groups and strain, we compared the CE during silence and sound presentation between strain across young, adult, and old age groups (Figure 5.11). At the young age group, we observed a strain effect with no effect of auditory stimulation or interaction between strain and auditory stimulation (Figure 5.11. B). The C57 CE was higher than Hybrid mice, (All: H(1)=20, p=e-5, SRH, BS: F(1)=5, p=.02, SRH, NS: F(1)=12, p=.0005, SRH). In the adult group, we observed an interaction between strain and auditory stimulation (Figure 5.11. D). The CE was higher during sound presentation than silence in Hybrid mice while it was lower in C57 (All: Hybrid mice p=.03, C57 p=.005), and the CE during sound presentation was significantly lower in C57 and higher during silence (silence: p=.02, evoked-response: p=.005, Dunn test Post hoc with Bonferroni correction). In BS, only the CE during spontaneous activity was higher in C57 than in Hybrid mice (p=.003, Dunn test Post hoc with Bonferroni correction), and in NS, the evoked response of Hybrid mice was higher than C57, and the C57 CE was lower in evoked-response than during spontaneous activity (p<e-4, p=.04, Dunn test Post hoc with Bonferroni correction). Finally, in the old age group, the C57 CE was lower than Hybrid mice during evoked-response in All, BS, and NS (Figure 5.11. F, All: p<e-5, Dunn test Post hoc with Bonferroni correction, BS: p<e-5, Dunn test Post hoc with Bonferroni correction, NS: p<e-5, Dunn test Post hoc with Bonferroni correction), while the Hybrid mice evoked-response CE was higher than silence in All and NS (All: p=.0003, Dunn test Post hoc with Bonferroni correction, NS: p=.0008, Dunn test Post hoc with Bonferroni correction).

We then investigated the relationship between spontaneous and evoked-response CE values and found that they were linearly related in all cell types across all age groups (Figure 5.10. A, Figure 5.11. ACE, young Hybrid mice: All cell p=1.9e-15, BS p=1.3e-5, NS p=1.2e-10, young C57: All cell p=.01, BS p=.08, NS p=.008; adult Hybrid mice : All cell p=1.07e-15, BS p=5.42e-14, NS p=.0006, adult C57: All cell p=6.64e-13, BS p=1.6e-13, NS p=.0005; Old Hybrid mice: All cell p=1.44e-37, BS p=4e-19, NS p=8e-19, old C57: All cell p=1e-10, BS p=1.4e-37, NS p=9.7e-5, linear regression model ANOVA), except in young BS of C57 strain. This result shows that not only the FR shows a relationship between spontaneous and evoked-response activity, but the CE as well.

Finally, the modulation index of CE changes between spontaneous and evoked responses in R (Figure 5.11. G) was computed to investigate whether the neuron's efficiency changes if natural sound is present. We found a significant effect of strain on the CE modulation index level for all cell types (Figure 5.11. G, All: F(1)=47, p>e-12, two-way ANOVA with 999 permutations, BS: F(1)=16, p=6e-5, two-way ANOVA with 999 permutations, NS: F(1)=33, p>e-8, two-way ANOVA with 999 permutations), indicating a greater change in evoked-response CE compared to spontaneous CE in Hybrid mice. Furthermore, in All and NS, we observed strain and age-group interaction effect on the CE (All: F(1,2)=7, p=.0005, Tukey HSD post hoc with 999 permutations, NS: F(1,2)=7, p=.0004, Tukey HSD post hoc with 999 permutations). The CE was found to be different between Hybrid mice and C57 at adult and old age, with the CE in Hybrid mice being higher (All: adult p<e-8, old p=.0001, Tukey HSD post hoc with 999 permutations, NS: adult p<e-8, old p=.02, Tukey HSD post hoc with 999 permutations). This difference is due to the U-shaped pattern of the C57 index of CE changes, which decreases between young to adults and increases between adult to old (All: young adult p=.0036, adult old p=.0015, Tukey HSD post hoc with 999 permutations, NS: young adult p=.0038, adult old p=.0013, Tukey HSD post hoc with 999 permutations).
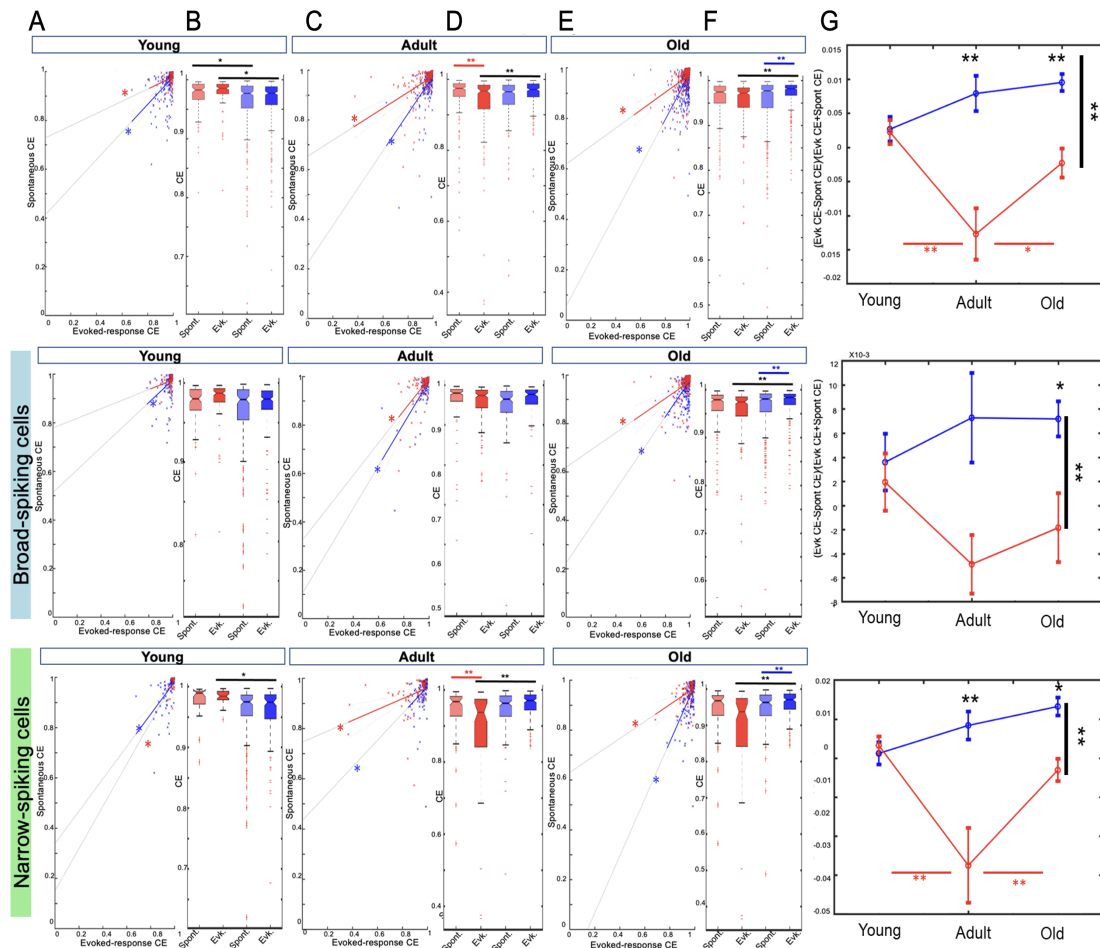
Figure 5.11: *Comparison of R CE during spontaneous and evoked activity across age groups, strains, and cell types*
(A) CE during spont and evk in young All cell (top panel), BS (middle panel) and NS (bottom panel). A linear relationship is found in All cell, BS, NS, young Hybrid mice, (All cell: p=1.9e-15, BS p=1.3e-5, NS p=1.2e-10, linear regression) and in C57 All cell and NS but not in BS (All cell p=.01, NS p=.008, linear regression). (B) Young CE during spont and evk. The C57 CE is higher than Hybrid mice (All: H(1)=20, p=e-5, SRH, BS: F(1)=5, p=.02, SRH, NS: F(1)=12, p=.0005, SRH). (C) Same as (A) in adult. A linear relationship is found in Hybrid mice (All cell p=1.07e-15, BS p=5.42e-14, NS p=.0006, linear regression) and in C57, (All cell p=6e-13, BS p=2e-13, NS p=.0005, linear regression). (D) Same as (B) in adult. Evk CE is higher than during spont in Hybrid mice while it is lower in C57 (All: Hybrid mice p=.03, C57 p=.005), and the CE during evk is lower in C57 and higher during spont (spont: p=.02, evk: p=.005, Dunn test Post hoc with Bonferroni correction). In BS, only the CE during spont is higher in C57 than in Hybrid mice (p=.003, Dunn test Post hoc with Bonferroni correction), and in NS, the evk of Hybrid mice is higher than C57, and the C57 CE is lower in evk than during spont (p>e-4, p=.04, Dunn test Post hoc with Bonferroni correction). (E) Same as (A) in old. A linear relationship is found in old Hybrid mice, (All cell p=1e-37, BS p=5e-19, NS p=6e-19, linear regression) and in C57, (All cell p=2e-10, BS p=6e-7, NS p=9e-5, linear regression). (F) Same as (B) in old. C57 CE is lower than Hybrid mice during evk in All cell, BS, and NS (All: p<e-5, Dunn test Post hoc with Bonferroni correction, BS: p>e-5, Dunn test Post hoc with Bonferroni correction, NS: p>e-5, Dunn test Post hoc with Bonferroni correction), while the Hybrid mice evk CE is higher than spont in All and NS (All: p=.0003, Dunn test Post hoc with Bonferroni correction, NS: p=.0008, Dunn test Post hoc with Bonferroni correction).(G) Modulation index along with ageing in Hybrid mice and C57 shows an effect of the strain on the CE (All: F(1)=47, p<e-12, two-way ANOVA with 999 perm, BS: F(1)=16, p=6e-5, two-way ANOVA with 999 perm, NS: F(1)=33, p<e-8, two-way ANOVA with 999 perm). In All and NS, we observed strain and age groups interaction effect on the CE (All: F(1,2)=7, p=.0005, Tukey HSD post hoc with 999 perm, NS: F(1,2)=7, p=.0004, Tukey HSD post hoc with 999 perm). The CE is higher in Hybrid mice than C57 (All: adult: p>e-8, old: p=.0001, Tukey HSD post hoc with 999 perm, NS: adult: p<e-8, old: p=.02, Tukey HSD post hoc with 999 perm). C57 CE follows a U-shaped pattern with a decrease between young to adult and increases between adult to old (All: young adult: p=.0036, adult old: p=.0015, Tukey HSD post hoc with 999 permutations, NS: young adult: p=.0038, adult old: p=.0013, Tukey HSD post hoc with 999 perm).

5.6 The CE of NR remain stable along with ageing and their natural sound voked-response CE is higher in Hybrid mice than C57

To conclude our investigation, we directed our analysis towards the CE of non-responsive cell (NR) (Figure 5.12). As for the FR, we only investigate the CE of All and All old groups as the sample size of NR is too low for statistical investigation. Our findings revealed a linear relationship between spontaneous and evoked-response CE of All NR (Figure 5.12. A, Hybrid mice p=2.62e-14, C57 p=.001, linear regression). We observed a strain effect on the CE (Figure 5.12 B, H(1)=16, p=e-4, SRH), where Hybrid mice NR CE is higher than C57. Comparing the CE within the age-groups strains (Figure 5.12. C) and found that the NR CE did not differ between the sound's stimulation conditions. Investigating between age groups and across strain, we observed that old Hybrid mice showed a higher CE during sound and silence compared to C57 (Figure 5.12. D, H(1)=19, p=.00001, SRH test). Even though no interaction effect between stimulation and strain has been observed, Post Hoc analyses revealed that the CE NR of Hybrid mice is higher than C57 in both auditory conditions (sound: p=.005, silence: p=.005, Dunn test Post hoc with Bonferroni correction). These results suggest that, inversely of a high CE value in responding cell, a higher CE in non-responding cell could represent a poorer specificity of the signal or could reflect a broad cell computation, linked or not to the sound stimulation.
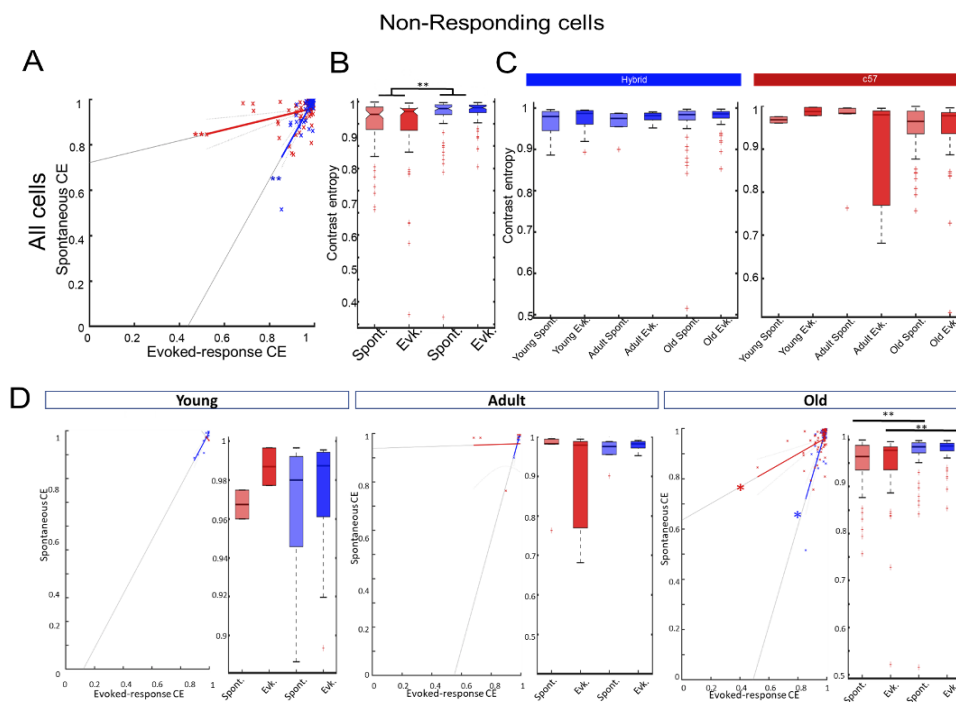
Figure 5.12: *Comparison of NR CE between spontaneous and evoked-response*
(A) Linear relationship of the NR, between the spont and evk CE, in both Hybrid mice, blue, and C57, red, (Hybrid mice p=2.62e-14, C57 p=.001, linear regression). (B) The CE of NR during evk is higher in Hybrid mice than in C57 (H(1)=16, p=e-4, SRH). (C) Boxplots comparing the CE of spont and evk along with ageing for each strain, revealed no significant differences. (D) NR CE between spont and evk across age groups and strains. Young and adult groups were not tested because of the sample size. In old age, NR CE is significantly lower in C57 than in Hybrid mice (H(1)=19, p=.00001, SRH test, sound: p=.005, silence: p=.005, Dunn test Post hoc with Bonferroni correction). Results are for All cell groups (BS and NS). NR CE also shows a linear relationship between the two auditory stimulation conditions (Hybrid mice p=.001, linear regression, C57 p=.002, linear regression).

Observing this higher CE in Hybrid mice NR, we wanted to investigate the CE of NR and R during the sound presentation. We conducted a comparison of the CE between R and NR in each strain, Figure 5.13. A, and found that the CE of NR was significantly higher during sound only in Hybrid mice, (Hybrid mice p=.006, Kruskal Wallis test). Figure 5.13. BD summarize the key finding related to changes in R and NR across ageing and between strains. The R CE is affected by the strain, stimulation condition and interaction between both variables (Strain: H(1)=27, p=2e-7, stimulation condition: H(1)=33, p=5e-8, H(1,2)=48, p=2e-11, SRH test). The CE of R decreased from young to adult and from young to old in C57, while it increased from adult to old in the Hybrid mice strain (C57: young to adult p<e-5, young to old p<e-5, Hybrid mice: adult to old p=.0002, Dunn test Post hoc with Bonferroni correction). At each age group, the CE between the two strains was significantly different, with C57 CE higher than Hybrid mice in young mice and lower in adult and old mice (young p=.0003, adult p=.03, old p<e-5, Dunn test Post hoc with Bonferroni correction). In the NR, the CE is higher in Hybrid mice than C57 (Figure 5.13. D, H(1)=12, p=.0006, SRH). These results are interesting, suggesting that the C57 NR are more robust than Hybrid mice. However, the CE of NR did not change during the sound presentation and remained constant across ageing for both mouse strains (Figure 5.13. D). These results are supported by the changes in the ratio of CE changes, shown in Figure 5.13. CE, where the ratio of CE changes was different between the two strains in R (see Results Figure 5.11. G for statistics), while it remained stable and similar in NR.
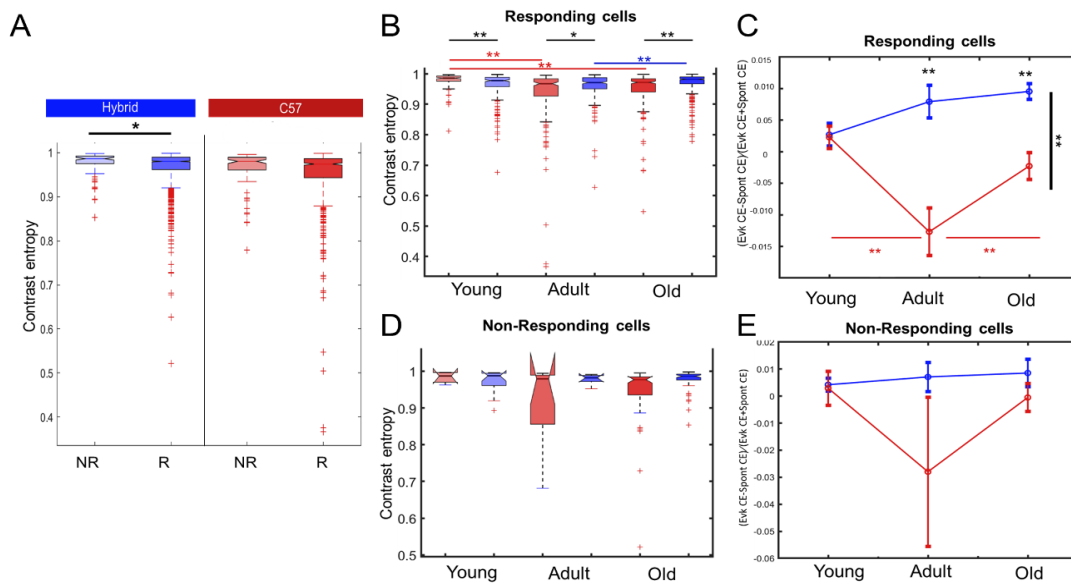
Figure 5.13: *Comparison between the R and NR CE during the sound presentation.*
(A) The CE of NR and R in Hybrid mice, and C57. The CE is lower in R than NR in Hybrid mice (p=.006, Kruskal-Wallis rank sum) and not in C57. (B) R CE comparison between Hybrid mice and C57 along with ageing, (Strain: H(1)=27, p=2e-7, auditory stimulation : H(1)=33, p=5e-8, H(1,2)=48, p=2e-11, SRH test). The CE decreases along ageing in C57 and increases from adult to old in Hybrid mice (C57: young to adult p<e-5, young to old p<e-5, Hybrid mice: adult to old p=.0002, Dunn test Post hoc with Bonferroni correction). There is a difference between Hybrid mice and C57 in the CE in each age group, lower in young and higher in adults and old (young p=.0003, adult p=.03, old p<e-5, Dunn test Post hoc with Bonferroni correction). (C) The modulation index between spont and evk CE of the R is calculated across age groups in Hybrid mice (see Figure 5.11 G for statistics). (D) Similar to B, for NR. The CE is lower in C57 than in Hybrid mice (H(1)=12, p=.0006, SRH) but no difference between age groups is observable. (E) Same as (C) in NR, no significant difference is observable.

In our study, we investigated how neurons in the AC of old mice respond to sound compared to spontaneous activity. We focused on NR that don't typically show changes in FR during sound stimulation. The findings revealed that NR in both mouse strains had a higher FR during sound presentation than during silence. Interestingly, the C57 mice had lower spontaneous FR than Hybrid mice, indicating strain differences. When examining the CE, which measures the ability of neurons to encode information, NR cell in all types showed higher CE during sound presentation in both strains. Hybrid mice exhibited higher CE during sound presentation compared to C57 mice, indicating strain-specific variations. The CE of NR cell remained consistent across ageing and strain. Additionally, comparing the CE of responding R and NR cell, Hybrid mice showed significantly higher CE in NR cell during sound presentation, while the CE of R demonstrated strain-specific changes with ageing. These findings provide valuable insights into how different mouse strains and ageing affect neural responses to sound in the AC, contributing to our understanding of auditory information processing

Based on our analysis, we found that the CE of NR is higher than responding R in both Hybrid mice and C57 strains. Additionally, we observed that the CE changes in R along with ageing are different in the two strains, with the C57 strain showing a decrease in CE, while the Hybrid mice strain showing an increase in CE. At all age groups, the CE is different between the two strains, with the C57 strain having a higher CE in young mice and a lower CE in adult and old mice compared to the Hybrid mice strain. We also calculated the modulation index between spontaneous and evoked-responses CE of the responding cell across age groups and strains and found it to be significantly different between the two strains. However, there was no significant difference in the modulation index between spontaneous and evoked responses CE of the NR across age groups and strains. Finally, at old age, we found that the Hybrid mice NR cell showed a higher CE during natural sound presentation compared to C57 NR cell. Overall, our findings suggest that the CE of auditory neurons varies across age and mouse strains and that there are differences in the CE between responding and non-responding cell.

> **Key findings**:
> ❖ Presentation of natural sounds elicits a higher FR in the AC compared to silence.
> ❖ The linear relationship between the spontaneous and the natural evoked-response FR is abolished in young C57.
> ❖ The modulation index of the FR from spontaneous to evoked-response is higher in young C57 compared to Hybrid mice.
>
> ❖ The CE is higher during natural sound presentation than silence in Hybrid mice while the inverse is observed in C57.
> ❖ The CE is lower in C57 than Hybrid (BS and NS), in all age groups in NS and in old age in BS.

The spike pattern and the CE during natural sound presentation

In our investigation into neural information processing, we delve into the relationship between neurons' spiking patterns and stimulus representation. We quantify this connection through Mutual Information (MI) measured in bits per second (bit/seconds) and Mutual Information per Spikes (MIs) in spikes per second, the coefficient of variation of the interspike interval (CV) and their relation with the CE. This analysis aims to uncover how neurons convey information about external stimuli, offering a streamlined understanding of information encoding in neural circuits.

6.1 Mutual Information (bits/seconds), MI, between neurons spike trains and natural sound stimuli

We first examined whether Mutual Information (MI) between the sound stimulus and the spike train varies between R and NR. Our findings reveal a significantly higher MI in R compared to NR (Figure 6.1.A, p= 6.6283e-23, Wilcoxon Mann-Whitney test), a distinction consistent across both C57 (p=2.1e-11) and Hybrid (p=2.7e-13) mice strains.
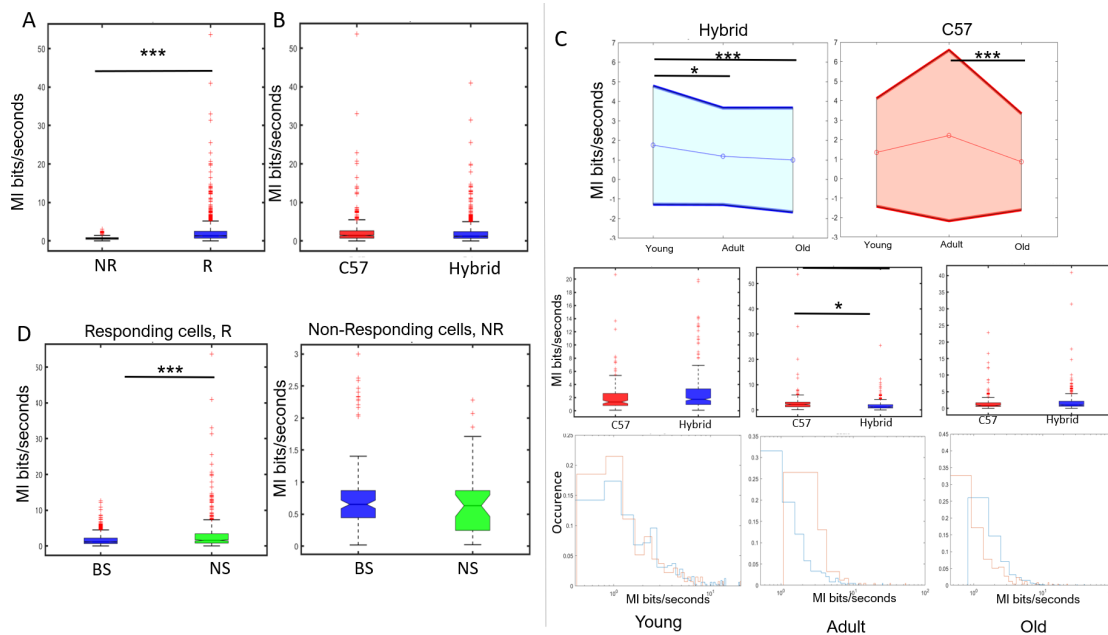
Figure 6.1: *Mutual Information, MI (bits/seconds) across strains and age-groups.*
(A) (MI (bits/seconds) and cell responsiveness, NR (black), R (blue), (p=6.6283e-23, Wilcoxon Mann-Whitney test). (B) R MI across strain, C57 (red), Hybrid (blue). (C) Age-related changes in the MI of R in Hybrid and C57. Top panels: medians and standard error of MI across young, adult, and old ages. Decrease in the MI of Hybrid R between young to adult and young to old (F= 14.33, respectively p=.01 and p<e-4 two-way ANOVA) and between adult to old in C57 R (p<e-4 two-way ANOVA). Middle panels: comparison across strains. The MI is significantly higher in C57 than Hybrid in adult mice, (p=.005, two-way ANOVA). bottom panels: Histograms of the occurrence distribution of cells MI across age-groups and strains. (D) MI is higher in NS, green, compared to BS, blue, (C57 and Hybrid merged, p=1.9e-13 Wilcoxon Mann-Whitney test).

The investigation into MI differences between R cells of Hybrid and C57 mice yielded non-significant distinctions (Figure 6.1.B, p=.7). These outcomes underscore the responsive nature of observed R cells in the C57 auditory cortex (AC). We observed a decline in MI of R with ageing in Hybrid mice starting young age, contrasting with its maintenance to adult age in C57 followed by a subsequent decrease from adult to old (Figure 6.1.C). This temporal divergence suggests a heightened information-carrying capacity in C57 adult R cells compared to Hybrid (Figure 6.1.D), revealing age-related changes in MI dynamics between auditory stimuli and neuron information encoding. Notably, across cell types, MI is higher in NS compared to BS (Figure 6.1.D, Wilcoxon Mann-Whitney test), with consistent trends observed across age groups and strains (Figure 6.1.C). The observed MI patterns underscore the nuanced influence of age and stimulus type on information encoding in the auditory cortex, emphasizing the need for comprehensive exploration to elucidate underlying mechanisms.

6.2 Mutual Information (bits/spikes), MIs, between neurons spike trains and natural sound stimuli

We subsequently delved into the analysis of Mutual Information per spikes (MIs), revealing noteworthy insights. Surprisingly, contrary to the metrics based on information per seconds, MIs per spikes did not exhibit significant differences between R and NR cells (Figure 6.2.A, p=.06, Wilcoxon Mann-Whitney test). Even, there is a tendency toward higher MIs in R cells, (Figure 6.2.A), suggesting the potential presence of stimulus-related information at the spike resolution in NR cells.

Upon comparing mouse strains, MIs showed no significant differences (Figure 6.2.B). Examining the impact of ageing on MIs (Figure 6.2.C), we identified a significant interaction effect between strains and age groups (F=2.99, p=.050, two-way ANOVA). Notably, MIs per spikes increased with age in Hybrid R cells (p=.02) while it exhibited an inverse U-shape in C57 mice (with an increase from young to adult, p=.02, and a decrease between adult to old, p=.01), emphasizing the dynamic relationship between age, cell types, and information per spikes.

Further exploration of differences between cell types and ageing patterns in Hybrid and C57 mice showed that the MIs did not differ between BS ad NS cells in Hybrid, while a significant lower MIs in BS compared to NS is observed in C57 (Figure 6.2.D, p=.03, Wilcoxon Mann-Whitney test). Comparing cell types between Hybrid and C57, BS MIs were not significantly different, whereas NS MIs were higher in C57 than Hybrid (Figure 6.2.E, p=.03, Wilcoxon Mann-Whitney test). Examining age-related changes in MIs, we observed an increase in R BS MIs with ageing only in Hybrid (Figure 6.2.F, F=3.81, p=.01, two-way ANOVA), with no changes in C57. Notably, a tendency toward higher MIs in Hybrid compared to C57 was discernible at old age, achieving significance with a Wilcoxon Mann-Whitney test (p=.04). In R NS, an inverse U shape in MIs was observed from young to adult and adult to old in C57 mice (F=3.81, p=.01 and p=.02, respectively, two-way ANOVA), while MIs remained constant in Hybrid mice. These age-related changes led to higher MIs in NS at adult age in C57 compared to Hybrid (p=.001, two-way ANOVA) (Figure 6.2.G).
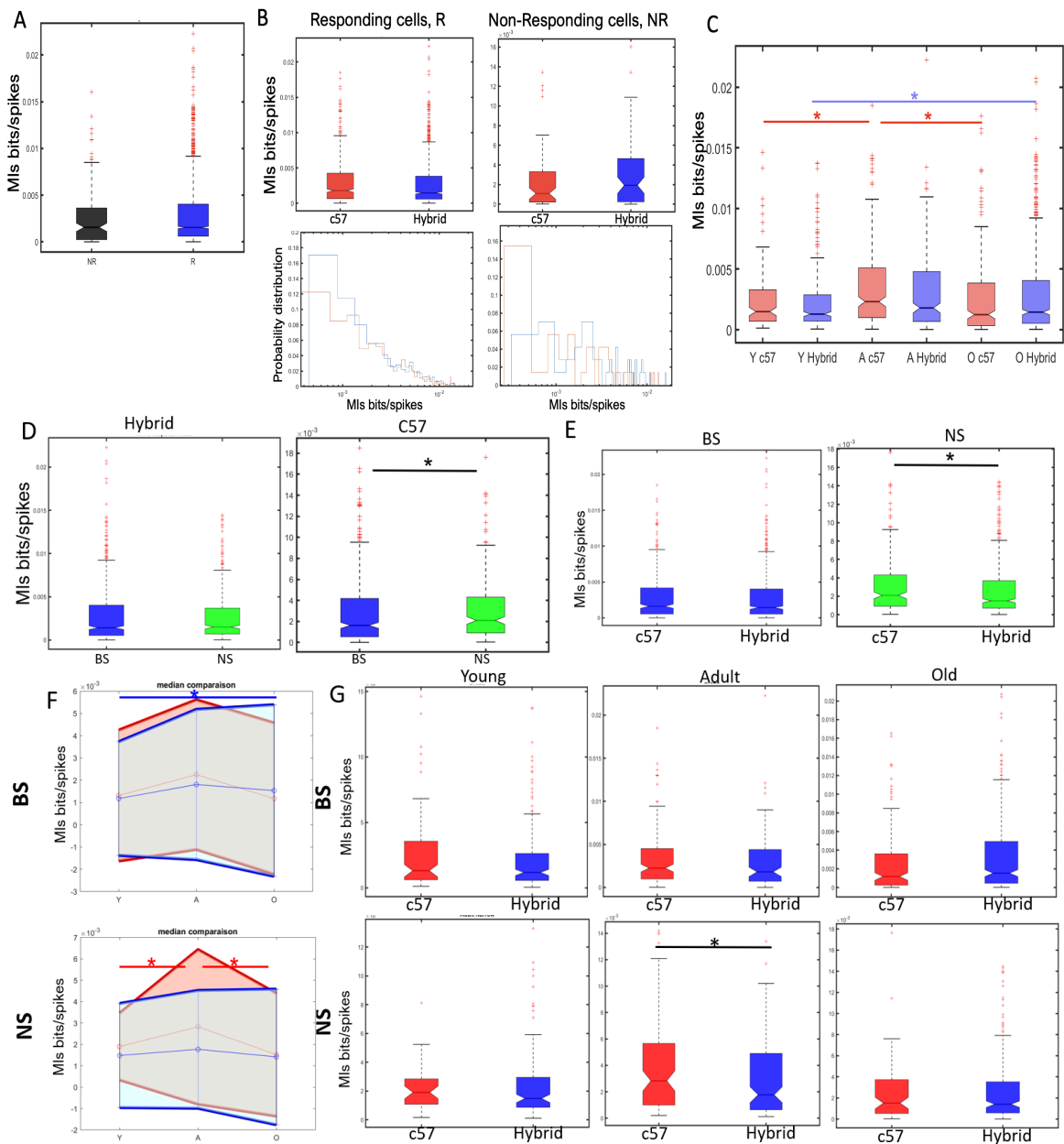
Figure 6.2: *Mutual Information, MIs (bits/spikes) across strains and age-groups.*
(A) MIs (bits/spikes) and cell responsiveness, NR (black), R (blue). (B) R and NR MIs across strain, C57 (red), Hybrid (blue) and related distribution probabilities. (C) Age changes in the MIs of R in Hybrid and C57, (F=2.99, p=.050, two-way ANOVA), where the MIs increases along ageing in Hybrid R cells (p=.02), it follows an inverse U-shape in C57 mice, with an increase from young to adult (p=.02) and a decrease from adult to old (p=.01). (D) The MIs and cell. MIs is higher in NS, green, compared to BS, blue, only in C57 (p=.0379, Wilcoxon Mann-Whitney test). (E) MIs comparison between cell across strains. The C57 MIs is higher in NS compared to Hybrid (p=.0386, Wilcoxon Mann-Whitney test). (F) Age-related changes in the MIs of R in Hybrid and C57. Hybrid MIs increase between young to old (F=3.81, p=.01, two-way ANOVA). C57 MI followed an inverse U-shape (F=3.81, respectively p=.01 and p=.02, two-way ANOVA). Medians and standard error. (G) The MIs difference between strains across age-groups shows a higher MIs in adult NS R of C57 compared to Hybrid (F=3.81, p=.001, two-way ANOVA).

6.3 Coefficient of variation of the interspike interval, CV, of the natural sound evoked-response neurons spike trains

To further investigate the AC activity along ageing, we explored the coefficient of variation of the interspike interval (CV) in our study. This metric provides valuable insights into the temporal structure of neural spike trains. We initially examined whether a disparity in the CV existed between NR and R and determined that there was no significant difference in CV in both strains. Subsequently, when comparing CV between strains, we observed a higher CV in R of C57 compared to Hybrid (Figure 6.3.A, p=3.2705e-31, Wilcoxon Mann-Whitney), while the opposite trend was noted in NR (Figure 6.3.B, p=1.9168e-04, Wilcoxon Mann-Whitney).

In the context of ageing, R in C57 exhibited an inverse U-shaped pattern in CV, with an increase from young to adult (Figure 6.3.C, F=8.3, p<e-5, two-way ANOVA) and a decrease from adult to old (p=.0001, two-way ANOVA). In contrast, Hybrid R displayed a decline in CV from adult to old age (F=8.3, p=.0038, two-way ANOVA). Furthermore, R in C57 displayed higher CV compared to Hybrid in both adult and old age groups (both p<e-5, two-way ANOVA). Across cell types, no interaction effect between strains and age groups was observed in R BS, but a significant difference between the two strains was identified (Figure 6.3.D, F=47, p<e-5, two-way ANOVA). In R NS, both strains and age groups influenced CV (Figure 6.3.E, F=14, p=e-9e-7, two-way ANOVA). Notably, the CV of Hybrid NS remained consistent across ageing, while C57 displayed a net increase in CV along ageing from young to old (p=.0006, two-way ANOVA). No interaction effect between age groups and strain was observed in NR cells for both BS and NS.

Finally, when comparing CV between BS and NS within strain ageing (Figure 6.3.F), C57 displayed a significant effect of cell types and age groups (F=7.1, p=.0009), maintaining BS CV consistency across age while NS CV increased from young to old and decreasing from adult to old (F=1.32, respectively p=.009, p=.01, two-way ANOVA), exhibiting an inverse U-shape, but with an overall increase from young to old (p<e-5). In Hybrid, no interaction effect was observed; however, higher CV was noted in R BS compared to NS (F=1.32, p<e-5, two-way ANOVA).

Integrating the CV results into our discussion, we find that the temporal structure of spike trains, as captured by CV, adds a nuanced layer to our understanding of age-related and strain-specific variations in neural activity.
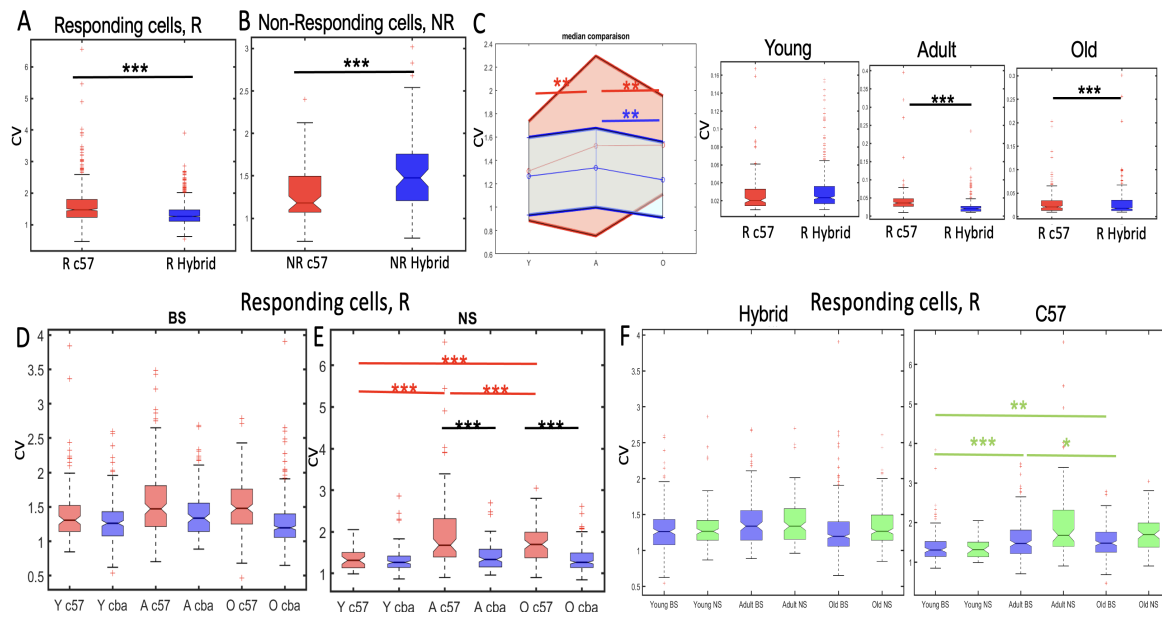
Figure 6.3: *Coefficient of variation of the interspike interval, CV, across strains and age-groups.*
A) Higher CV in R C57 compared to Hybrid mice, (p=3.2705e-31, Wilcoxon Mann-Whitney). (B) Lower CV in NR C57 compared to Hybrid mice, (p=1.9168e-04, Wilcoxon Mann-Whitney). (C) R C57 CV follows an inverse U-shape, with an increase of the CV from young to adult (F=8.3, p<e-5, two-way ANOVA) and a decrease from adult to old (p=0.0001, two-way ANOVA). Left panel: Medians and standard error. Right panels: Hybrid CV decreases from adult to old in R (F=8.3, p=0.0038, two-way ANOVA). CV is higher in R C57 compared to Hybrid in adult and old age-groups (both p<e-5, two-way ANOVA). (D) CV in BS R C57 compared to Hybrid mice across age-groups. (E) R NS CV across strains and age-groups. CV of Hybrid NS is maintained along with ageing. In C57, the CV follows an inverse U-shape, with increase from young to adult and decreases from adult to old (both p¡e-4, two-way ANOVA), and an overall increase from young to old (p=0.0006, two-way ANOVA). The CV in NS R Hybrid is lower than C57 in adult and old ages (both, p<e-5, two-way ANOVA). (F) Intra-strain comparison between the BS and NS CV along with ageing. C57 NS shows same results observed in (E) but without specific difference with BS. (young to old and young to adult p¡e-5, adult to old p=.

6.4 Correlation with the CE

We then visualised the correlation between the CE and the other computed metrics, Figure 6.4.A, we found that the CE is significantly correlated to most of the parameters, MI, MIs and CV (Figure 6.4.B). However, we observed a stronger correlation between the CV and the CE. We then tested a multiple regression of the CV, MI, MIs on the CE, selecting the variables affecting the CE value, automatically using the Akaike Information Criterion algorithm, AIC (Figure 6.4.D). We found that the variation of the CE is mostly explained by the MIs with small inverse effect of the CV and the MI (Figure 6.4.C): CE = -1.597525MIs -O.002263CV -0.002263MI + 1.071252.

The correlation analysis between CE and those various computed metrics underscores the intricate relationship between CE and critical parameters. Our findings reveal significant correlations with Mutual Information per Spikes (MIs), Coefficient of Variation of interspike intervals (CV) and Mutual Information (MI). Particularly noteworthy is the robust correlation observed between CE and MIs and CV, indicating that the CE measure may englobe the information per spikes and the structural temporal patterns of AC cells.
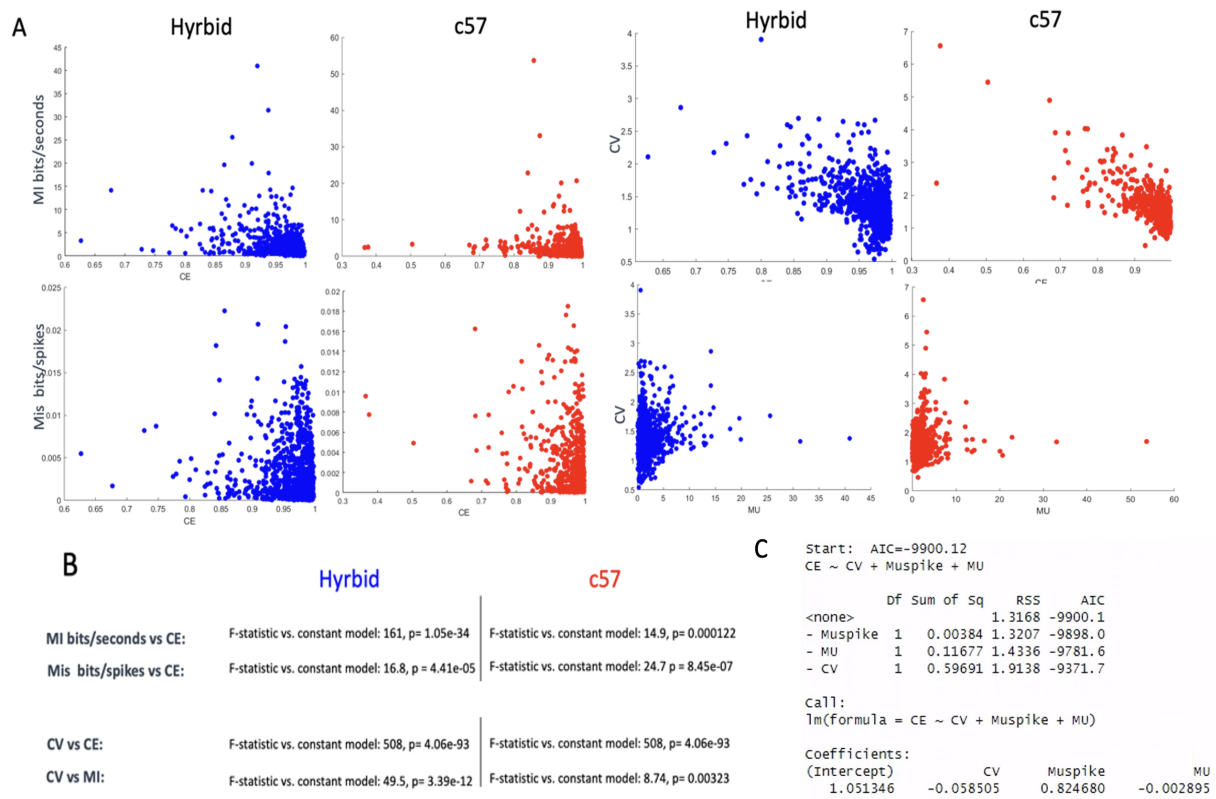
Figure 6.4: *Spike trains metrics correlation with CE.*
(A) Scatter plot between the metrics computed in our study, and their relatives p in (B). (C) represents the statistics output of the regression correlation of the CE and MI, MIs and CV. (D) Output of the Akaike Information Criterion algorithm, AIC.

7 Age-related changes in cortical states and pupil dynamics

Cortical states play a crucial role in shaping neural activity and cognitive processing (Harris & Thiele 2011). Investigating brain states provides valuable insights into the mechanisms underlying cognitive functions and age-related changes in brain activity. Pupil dynamics have emerged as a promising marker of brain states, offering a non-invasive and easily measurable indicator of cognitive and neural processes (Joshi et al. 2016, He et al. 2023, Reimer et al. 2014, Larsen & Waters 2018). Understanding the relationship between brain states and pupil dynamics can provide complementary information to the analysis of AC activity and further enhance our understanding of age-related changes in cortical processing.

Previous research has demonstrated a correlation between pupil diameter and neural activity, suggesting that pupil dynamics reflect brain states (Hess & Polt 1964, Yuzgeç et al. 2018, Ribeiro & Castelo-Branco 2022). Pupil size is controlled by the autonomic nervous system, which regulates arousal and attention, making it a suitable indicator of cognitive and neural processes (Larsen & Waters 2018). Pupil dilation corresponds to increased arousal and cognitive effort, while constriction indicates decreased arousal and cognitive demand. This link between pupil dynamics and brain activity has paved the way for using pupillometry as a non-invasive tool to investigate neural processes.

In the context of auditory processing, analysing the relationship between brain states and pupil dynamics can provide valuable insights (McGinley et al. 2015). Understanding how the brain responds to auditory stimuli and how it changes with age is critical for comprehending age-related hearing loss and optimizing auditory function. By investigating both AC activity and brain states as reflected by pupil dynamics, we can gain a more comprehensive understanding of the neural mechanisms underlying age-related changes in auditory processing.

This study aims to investigate age-related changes in cortical states in response to auditory stimuli, with a specific focus on the analysis of pupil dynamics as an indicator of brain states. We will explore the correlation between pupil dynamics and AC spiking activity, leveraging previous research that has established this relationship. Furthermore, we will examine the variations in pupil dynamics across different auditory stimuli and explore how they change with ageing in two mouse strains: the Hybrid mice strain and the C57 strain.

Our approach involves establishing the correlation between pupil diameter dynamics and AC spiking activity, examining this relationship within the context of ageing, and comparing the patterns of pupil activity across the two mouse strains. Additionally, we will establish a pipeline for automatically characterizing pupil states and investigate whether they are reflected in specific electroencephalography (EEG) frequency bands, using frontal EEG recordings.

By integrating the analysis of pupil dynamics with AC activity and age-related changes, we aim to enhance our understanding of the neural mechanisms underlying auditory processing and age-related hearing loss. This investigation will provide valuable insights into the relationship between brain states and pupil dynamics, offering a complementary perspective to the analysis of AC activity. Ultimately, this research has the potential to contribute

to the development of interventions and strategies for optimizing auditory function in ageing populations. To investigate the ageing of brain states in response to auditory stimuli, our approach involves initially exploring the measurement of pupil dynamics as an indicator of brain states. Subsequently, we aim to analyse the variations in pupil dynamics across different auditory stimuli and with the ageing process in both the Hybrid mice and C57 strains of mice.

Previous research demonstrated a correlation between pupil diameter and spike train/local field potentials, suggesting that pupil dynamics could reflect brain activity (Hess & Polt 1964, Reimer et al. 2014, Yuzgeç et al. 2018, McGinley et al. 2015). This non-invasive technique could facilitate investigations into brain activity. To investigate the relationship between brain states and pupil dynamics, we will, first, test the correlation between the pupil diameter dynamic and the auditory cortex spiking activity (Reimer et al. 2014, Yuzgeç et al. 2018). We will then explore this correlation along with ageing and across the two mice strains.

In this study, we strived to identify distinct patterns of pupil activity and determine whether they corresponded to specific brain states, utilizing frontal EEG recordings. Additionally, we established a systematic approach for automatically characterizing pupil states and examined their potential associations with particular EEG frequency bands. To minimize the influence of auditory stimuli on both pupil dynamics and AC spiking activity, we initially focused on analyzing pupil dynamics during the AC's spontaneous activity. Subsequently, we developed a pipeline for classifying pupil states and investigated their correlation with EEG traces. Finally, we examined pupil states during natural sound presentation to assess whether they underwent age-related changes and differed between the C57 and Hybrid strains. By undertaking these analyses, we aimed to gain insights into the relationship between pupil dynamics, brain states, and auditory processing across different age groups and mouse strains.

7.1 Correlations between pupil dynamics and spiking activity of the AC

First we investigated whether the pupil dynamic could correlate with spiking activity. To this end, we compared the pupil dynamic with the spiking rate distribution of 41 mice (C57, n = 23; Hybrid mice, n = 18). During the experiment, mouse pupils were tracked by a camera (see Materials and Methods- Animals and experimental setup).

For each mouse, the diameter was calculated by manually labelling the left and right edges in the video frames. All video frames were then automatically labelled (Materials and Methods- Pupil dynamic computation). The diameter was then calculated using the coordinates of the pupils' edges per frame to compute the pupil diameter along the recorded session. This will be then called the 'pupil dynamic'. The frame rate of the video was 25Hz, so the pupil dynamic represents the pupil diameter every 0.04 seconds. The signal was then filtered to remove noise introduced during the experiment, by mouse movement or eye closing for example, or by the software automatic labelling (Figure 7.1. AB). Here, we used individual cell FR of the auditory cortex activity to investigate the spiking and pupil correlation. This analysis used the same data of Chapter I to III of the theses. The spiking activity represents the spiking rate of the auditory cortex used in the previous results sections also.

This was conducted during the silent period to investigate the correlation between pupil dynamics and spiking activity. Both signals were aligned, and the spiking rate was discretised in bins of 0.04 sec (Figure 7.1. CD). We observed that the pupil dynamic and the firing dynamics signals were cross-correlated with a pick centred at zero

(Figure 7.1. D), indicating that these dynamics are correlated and occur almost simultaneously. Since this analysis uses timing alignment and smoothing methods, we cannot exclude a sequential activity, in which the spiking or pupil might precede one another. The Pearson correlation was significant between the pupil dynamic and the spike train (40 of 42 mice showed a significant p between the pupil dynamic and the firing signal, Pearson correlation test), regardless of the strain and the age of the mice (Figure 7.1 D).

The results of this section suggest that pupil dynamics correlate with internal spiking activity. This is the following paper that describes a relationship between pupil a membrane potential (McGinley et al. 2015, Reimer et al. 2014). Moreover, this relationship is preserved across ages.

Figure 7.1: *Correlation between Pupil Diameter Dynamics and Firing Rate*
(A) The pupil edges are automatically labelled using a supervised algorithm, Deeplabcut software (Mathis et al., 2018). Labelled edges are used to calculate the pupil diameter per frame during the spontaneous period (the sample rate of the video is 25 Hz). (B) The signal is then filtered to exclude technical or experimental artefacts. The blue line represents the raw signal before filtering, while the brown line represents the filtered signal. (C) Example of the spontaneous pupil (top), related spike rate (bins of 0.04 sec) (middle), and the firing distribution (smoothed histogram using a moving window Gaussian filter, sigma=825). (D) Cross-correlation between the pupil dynamic and the firing distribution for 30 seconds. The red line represents C57 mice, and the blue line represents Hybrid mice. The mice are sorted by age, from young (top left) to old (bottom right). Titles represent the mice's age.

7.2 Qualitative characterization of pupil dynamics

To determine whether ageing affects brain state and whether brain state differs between strains during sound presentation and silence (Figure 7.2). We first looked at the distribution of the pupil diameters (Figure 7.2. A).

This could give insight into how dynamic the pupil is. Each histogram represents the distribution of mouse pupil diameter in each strain at a certain age (days). We observed that in Hybrid mice, there was a tendency for a broader distribution than in C57 mice (40 pixels of difference) with multiple peaks, while C57 mice showed a narrower distribution (Figure 7.2. A). In addition to the analysis of pupil size values, we also computed the first derivative, which represents the subtraction of each pupil diameter frame. Figure 7.2. B shows the distribution of the pupil's first derivative, and we observed that Hybrid mice show a tendency for a larger distribution than C57 mice. We also observed that the distributions tend to change with age. Hybrid mice young and adult mice showed a tendency for a broader pupil dynamic distribution than C57 mice and converged to the same dynamics with ageing (Figure 7.2. B). These qualitative assessments imply that pupil dynamics may vary depending on strains and age groups. To quantify the pupil dynamic across all datasets, we defined four arbitrary pupil states: for each record, the maximum and minimum pupil diameters and the median were used as pupil state thresholds (Figure 7.2. C, see Materials and Methods section - pupil dynamic computation). Pupils were defined as maximally dilated (MD) state for larger pupil diameters, dilated (D), constricted (C), and maximally constricted (MC) for smaller pupil diameters (Figures 7.2. CD). Diameter values were discretized into these four states (Figure 7.2. CD). To support our pupil states characterization, we randomly selected four frames of the pupils based on their labelled pupil states and visually confirmed their pupil characterization (Figure 7.2. E). We can observe a good match between the expected pupil size and the observed one.

7.3 Pupil size and dynamics during silence

The three axes of work, as illustrated in Figure 7.2. C, are assessed using the pupil states. Firstly, (A) the total time spent in each state (MD, D, C, MC) is measured over the ageing period. Secondly, (B) the number of transitions between each pupil state is counted. Finally, (C) the mean episode duration of each state is calculated. These measurements provide insight information into the dynamic nature of the pupil in mice and its ageing.

7.3.1 Total duration of pupil states during silence

We first investigated the dynamics of the pupils during the silence period. Figure 7.3. A-C show the fraction of time spent in each pupil state as a function of age. We observed that in young Hybrid mice, the pupil spent more time in the extreme states (MC and MD) than young C57 mice, and less time in the middle states (C and D) (Figure 7.3. BC, young Hybrid mice vs C57: MD, $F_{(2,2)}=5.18$, $p=0.04092$; D: $F_{(2,2)}=5.18$, $p=.04091$; C: $F_{(2,2)}=4.52$, $p=.0108785$; MC: $F_{(2,2)}=4.52$, $p=.0108774$, two-way ANOVA, Post hoc Tukey HSD).

This difference is due to the Hybrid mice showing a decrease in extreme states and an increase in middle states as they age, as shown in Figure 7.3. B and 7.3. C ($F_{(6,2)}=6.98$, MC young to old: $p=.022461$; C young to old: $p=.022461$; D young to old: $p=.006560$; MD young to old: $p=.006562$, two-way ANOVA, Post-hoc Tukey HSD). Note that the p-values are symmetric because each state represents 25% of the total pupil diameter. A similar difference is not observed in the C57 strain, where the pupil spends more time in the middle stages and remains constant throughout life. These results are consistent with the previous histogram observation shown in Figure 7.2.

7.3.2 Transitions between pupil states during silence

To investigate whether the disparity in pupil states is attributable to the number of transitions or the average time spent in each state, we conducted an analysis of state transitions (Figure 7.2. D-E). Our results showed that C57 mice exhibited a pattern of oscillation between middle states from a young age, while Hybrid mice displayed a less frequent dynamic, tending to switch only between middle states with age (Figure 7.3. E). However, these differences did not reach statistical significance.

7.3.3 Episode duration of pupil states during silence

Lastly, we examined the average length of each episode, defined as the duration of time spent in one state when an episode is reached. Our analysis revealed that when young Hybrid mice and C57 mice reached an extreme state, young Hybrid mice spent more time in that state than young C57 mice (Figure 7.3. F, MD: $F(3,3)=23.25$, $p=.008$; MC: $p=2.7e-5$, two-way ANOVA, Post hoc Tukey HSD).
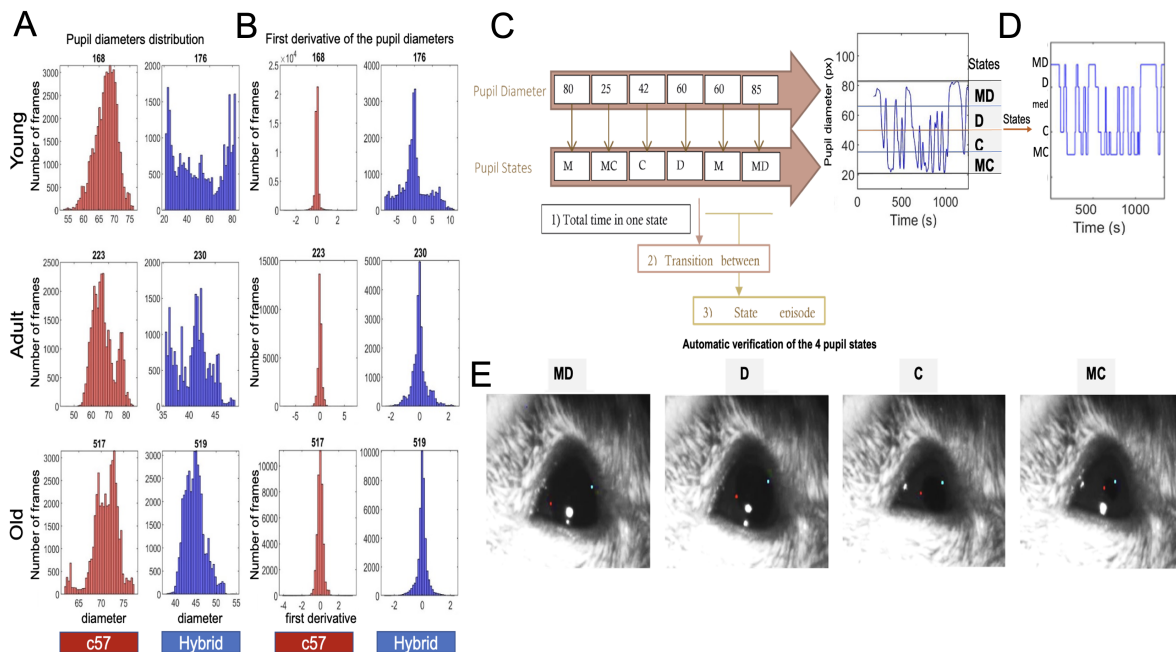
Figure 7.2: *Pupil states definition*
(A) Representative histograms of 6 mice' pupil diameter distribution in the Hybrid mice (blue) and C57 (red) strain. Mice are split into 3 groups: young (less than 190 days old), middle age 'adult' (between 190 and 450 days old), and old (more than 450 days old). Titles represent the mice's ages. The number of histogram bins = 40. The distribution represents the occurrence of pupil size during the spontaneous period. (B) Same as A for the pupil size derivative, the difference between pupil size in subsequent frames. (C) Delimitation of the 4 pupil states. C: contracted state between Median and (Median + Min/2) (blue). MC: maximum constructed in between Minimum and (Median + Min/2)-min. D: dilated between Median and (Median + Max/ 2). MD: maximum dilated between Maximum and (Median + Max/2). (D) For pupil dynamic states example, pupil diameter values are converted to the pupil states MC, C, D, MD, med: median. (E) Randomly and automatically picked frames corresponding to pupil states.
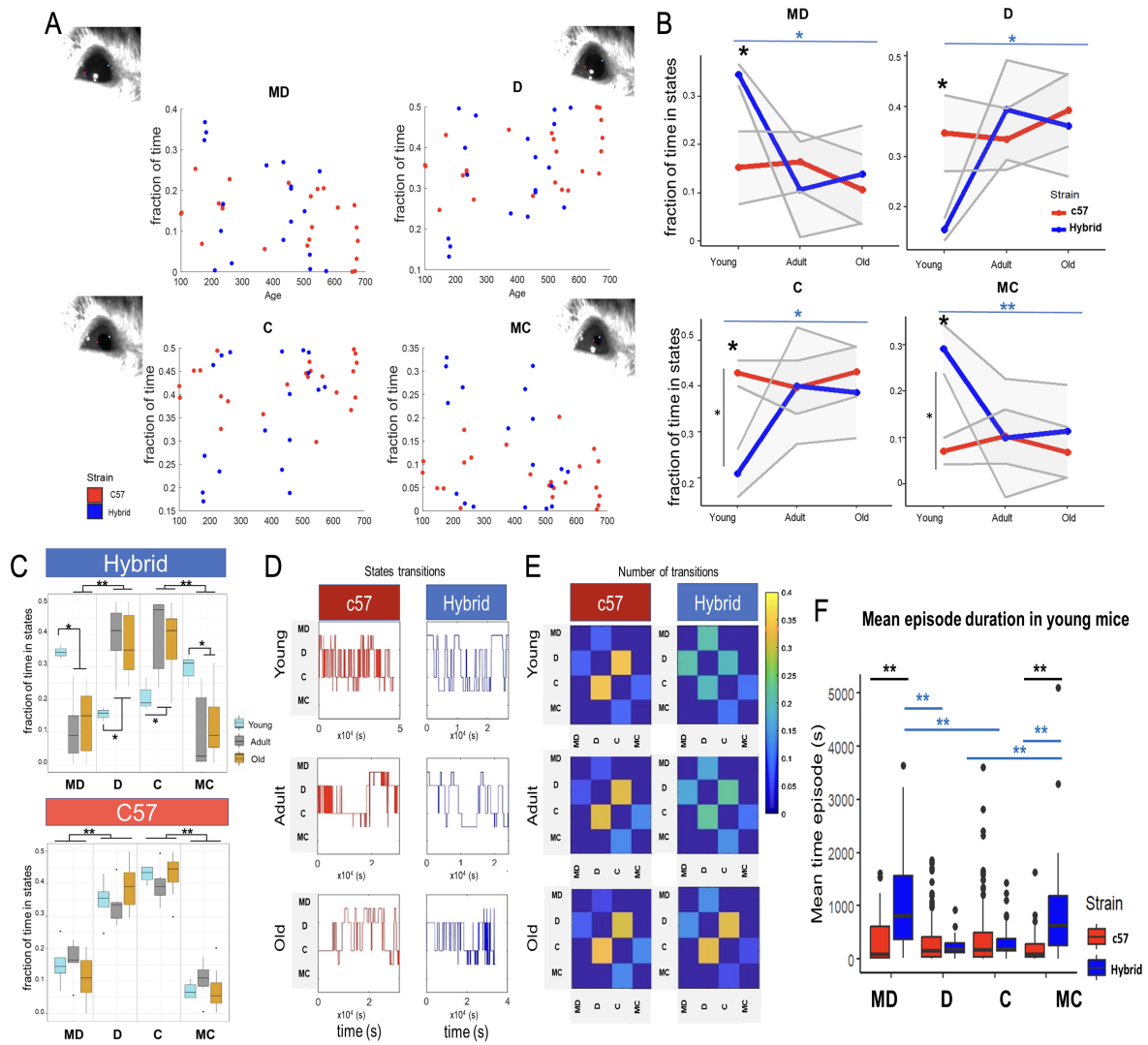
Figure 7.3: *Pupil states definition*

(A) Total fraction of time spent in each pupil state (MD, D, C, and MC) as a function of age for Hybrid mice (blue) and C57 mice (red). Each dot represent the total fraction of time spent per mouse (total time spent in the state (s) divided by the total spontaneous time (s)). (B) Interaction plots representing (A) per age group. The dots represent the means, and grey ribbons represents the standard deviation. The fraction of time spent by young Hybrid mice in MC and MD states is higher than in C57, and lower in C and D states. Young Hybrid mice vs C57: MD, $F_{(2,2)}=5.18$, $p=0.04092$; D: $F_{(2,2)}=5.18$, $p=.04091$; C: $F_{(2,2)}=4.52$, $p=.0108785$; MC: $F_{(2,2)}=4.52$, $p=.0108774$, two-way ANOVA, Post hoc Tukey HSD). (C) Total fraction of time per strain. Young Hybrid mice, cyan, spent more time in higher pupil MC and MD states, than adult and old mice, grey and brown, p as in (B), C57 spend more time in C and D states same in adult and old Hybrid mice. (D) Six mice representative pupil state plots. (E) The colour map of the number of transition of (D) pupil traces. (F) Mean episode duration in young mice. The episode duration is the mean time spent in one state when it is reached,(total episode time (s) / the number of episodes). The strain, pupil states, and the interaction between both variables are significant (strain: $F_{(1)}=13.20$, $p=.0003$; pupil states: $F_{(3)}=10.56$, $p=8.61e-7$; interaction: $F_{(3,3)}=23.25$, $p=2.54e-14$). In Hybrid mice, the MD episode duration is higher than D and C (both $p<e-8$, Post hoc Tukey HSD), and higher than in C57 ($p<e-8$). The same trend is observed for MC (with C and D in Hybrid mice: both $p<e-7$ and in C57: $p<e-8$, two-way ANOVA, Post hoc Tukey HSD). Only young age is represented.

115

7.4 Investigating the correlation between EEG and pupil activity

In this section, we aimed to establish a relationship between pupil states and brain states and to examine if ageing has an impact on the relationship. To assess brain states, we analysed cortical EEG signals.

7.4.1   Higher theta band activity in C57 mice compared to Hybrid mice

Before establishing the relationship between cortical EEG signals and pupil dynamics, we investigated how cortical EEGs change with age and across strains (Figure 7.4. A-C). We first compared cortical EEG power across distinct frequency bands (0.5-4 Hz, theta 4.5-8 Hz, alpha 8.5-13 Hz, beta 15-25 Hz, low gamma 30-45 Hz, and high gamma 60-95 Hz) irrespective of age, and found that theta power in C57 mice was significantly higher than that in Hybrid mice (Figure 7.4. C, p=.0136, Wilcoxon Mann-Whitney test).

To identify age-related changes in cortical EEG power, we examined the power spectral density (PSD) of individual animals as a function of age across frequency bands (Figure 7.4 D-F). We found that the PSD power changed along with ageing with the frequency bands. In Hybrid mice, delta relative power appeared to decrease, while theta, alpha, beta, and gamma relative power seemed to increase. In C57 mice, the relative power was relatively flat but followed the same tendency as in Hybrid mice. Applying linear regression on the relative power of ageing (Figure 7.4 E), we observed this tendency but none of these regressions was significant. Finally, we computed the mean relative power per age group and found a strain effect on theta power, with C57 mice showing higher theta relative power than Hybrid mice (Figure 7.4 F, Strain effect: $F(1)=4.8$, p=.0293 and age-group effect $F(1)= 3.7$, p=.0274, with no effect of interaction between strain and age-groups in the two-way ANOVA). In higher frequency bands, we continued to observe a tendency of higher Hybrid mice relative power than C57, particularly in old age (beta, low gamma, and high gamma). These findings indicate a significant difference in C57 theta power compared to Hybrid mice during spontaneous activity, and a tendency of higher Hybrid mice high frequencies power, particularly in old age.
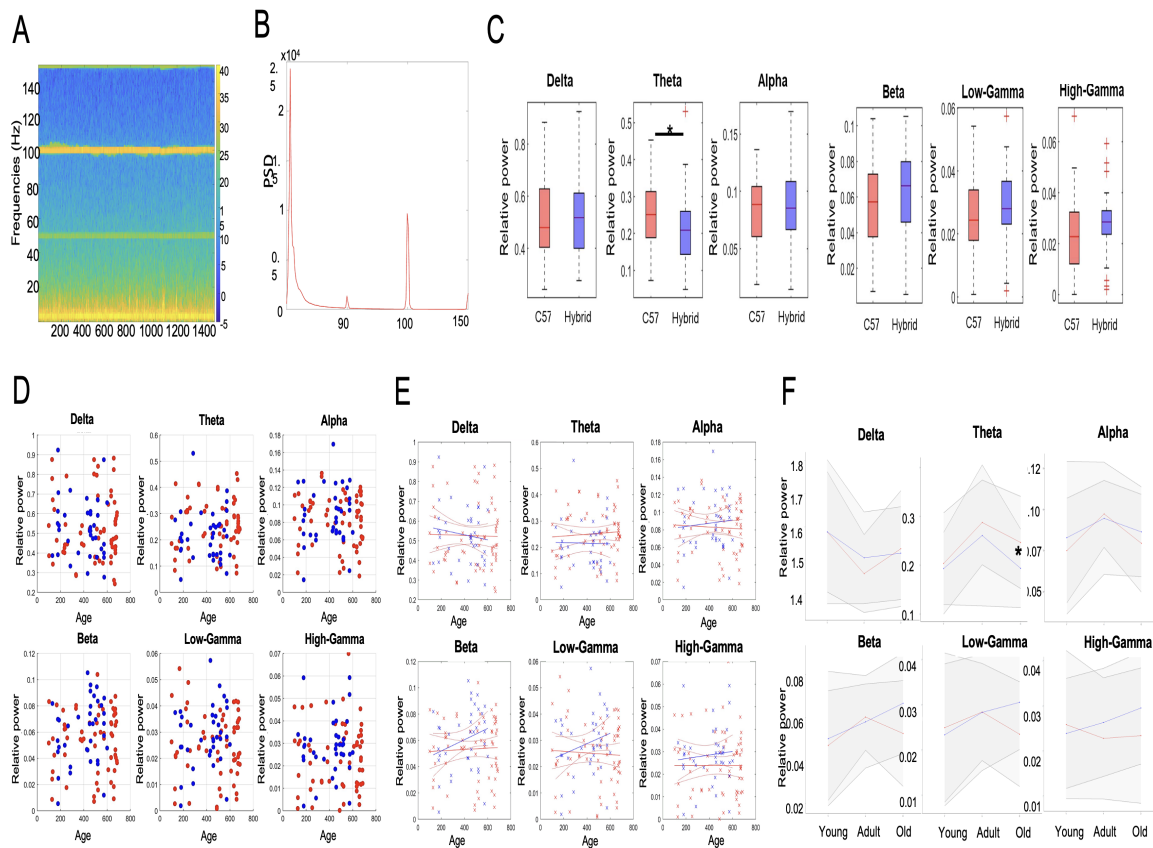
Figure 7.4: *C57 mice shows a higher theta band activity than Hybrid mice*
(A) Spectrogram of an example mouse recording's EEG Note that our recordings were noisy around 50 and 100Hz. (B) its relative power spectrum density. (C) Comparison of the frequency bands between Hybrid mice (blue) and C57 (red) mice. The theta power is higher in C57 mice (p=.042, Wilcoxon rank-sum test). (D) Scatter plot representing the relative power of each frequency over ageing and (E) their linear regression. (F) Comparison of frequency relative power across age groups. The theta power is higher in C57 mice than in Hybrid mice (Strain effect: F(1)=4.8, p=.0293, two-way ANOVA). Errors bars indicate the SEM.

7.4.2 Cross-correlation between EEG frequencies and pupil dynamics

Our aim in this study was to determine whether pupil diameter dynamics could serve as a marker of brain activity and to investigate whether these dynamics were correlated with EEG frequency bands. To determine the correlation between pupil and EEG dynamics, we first band-passed the relevant frequencies in the signal. As previously, we focused on the delta, theta, alpha, beta, low gamma, and high gamma bands. We then compared the mean firing diameter per second to the PSD power of each frequency band per second (Figure 7.5. A), finding that the PSD range of values was similar for all record PSD and PSD per second (Figure 7.5. C). We also found that the changes in the PSD power and pupil mean per second were cross-correlated (Figure 7.5. BD), although our technique needs improvements.

We further explored whether pupil states were correlated with a particular frequency band by computing the PSD for each pupil state episode (MD, D, C, MC) (Figure 7.5. E). We observed that alpha power was higher in the constricted pupil, relaxed state, and decreased with dilation, while high gamma was powerful in a highly dilated state, active state, and decreased with constriction (Figure 7.5. F). This correspondence was only observed

in these frequencies and at the young stage, not for adults and old mice. Our findings suggest that pupil dynamics may represent ongoing cortical activity and could potentially serve as a marker of brain activity. However, further experiments are needed to support our findings and perfect our pipeline.

We observed that the pupil and EEG frequency bands are cross-correlated, but there is no clear representation of the frequency bands with the established pupil states. Although the alpha and high-gamma frequency bands seem to inversely increase or decrease as the pupil is dilated, all the frequency bands are not defined by particular pupil state patterns of distribution. To validate or exclude the hypothesis that the pupil is more dynamic in young Hybrid mice during spontaneous activity than in C57 mice, complementary controls such as sleep scoring are necessary. Finally, we focused on analysing pupil dynamics during the sound presentation as the EEG traces are noisy.
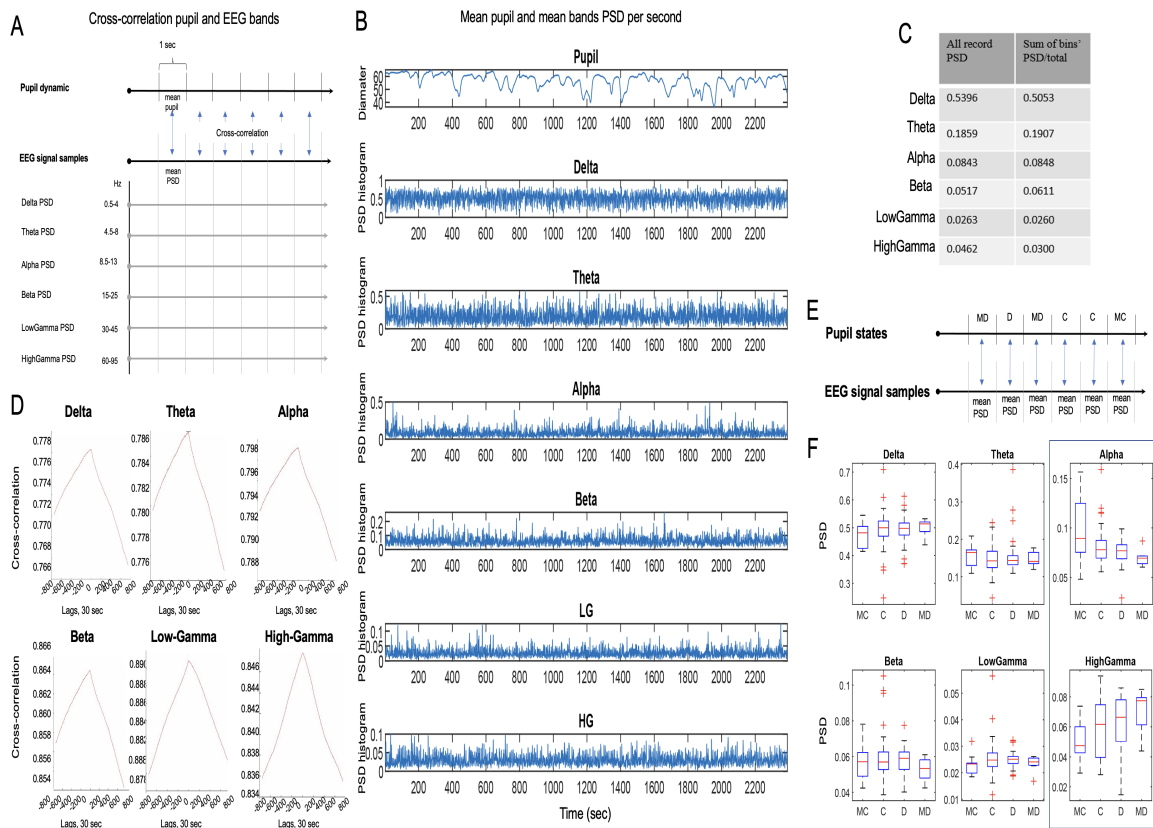
Figure 7.5: *Relationship between EEG Frequency Power and Pupil Dynamics: Cross-Correlation Analysis*
(A) Method of comparison between the EEG and pupil signals. 1 sec pupil diameter mean was cross-correlated with the aligned 1 sec EEG PSD mean (B) Example of an alignment of pupil dynamics and PSD power per second. (C) A comparison of the PSD during the spontaneous recording with the sum of the computed 1-second PSDs shows similar magnitudes. LG: low gamma, HG: high gamma (D) Cross-correlation between frequency and pupil dynamics for a duration of 30 seconds. (E) Method of the EEG power of the pupil states investigation. The mean PSD was computed for each pupil episodes. (F) The power PSD distribution of the 4 pupil states in the young mice group.

7.5 Pupil size and dynamic during sound presentation

To explore the brain states during sound presentations, we utilized the same pupil states characterization protocol. First, we examined the pupil diameter distribution and the first derivative (Figure 7.6. AB).

7.5.1 Total duration of pupil states during sound presentation

We began by examining the fraction of time spent in each pupil state (MD, D, C, MC) (Figure 7.6). Surprisingly, we found no differences in the fraction of time spent in pupil states or in changes during ageing between the two strains (Figure 7.6. C). When comparing the age groups, we observed that young Hybrid mice spent equal amounts of time in all pupil states. In both mice strains we observed an effect of pupil states (Hybrid mice: $F(3)=33.7$, $p<e-15$, two-way ANOVA, C57: $F(3)=17.01$, $p<e-7$, two-way ANOVA), where the difference is between extremes and middle states (all $p<e-4$) with no difference between D-C and MD-MC.

7.5.2 Transitions between pupil states during sound presentation

After converting the pupil diameter dynamics to pupil state phases as described in Figure 7.3), we calculated the fraction of transitions (7.6. DE). This is determined by dividing the number of transitions between two states by the total number of transitions. The fraction of transitions for both Hybrid mice and C57 mice did not vary with age. However, when comparing the strain per age groups, we observed that young Hybrid mice had a higher frequency of transitions than C57 mice (interaction between strain and type of transition: $F(1,11)=5.5$, $p=1.35e-5$, two-way ANOVA), but this interaction disappeared when the individual's reached the Adult stage.

7.5.3 Episode duration of pupil states during sound presentation

Lastly, we compared the mean time between episodes (Figure 7.6. G), which corresponds to the duration of an episode if it occurs. Unlike during spontaneous activity, the mean episode duration of young Hybrid mice and C57 mice showed no significant difference during the sound presentation (Figure 7.6. G). However, the mean episode duration varies between strains in adulthood and old age. In adults, we observed a significant interaction between strains and mean time episodes ($F(3,1)=4.1$, $p=.007$, two-way ANOVA), with C57 mice exhibiting higher mean episode duration than Hybrid mice in all pupil states. Lastly, in old age, we observed a significant difference in mean episode duration (Figure 7.6. G, $F(1,3)=5.21$, $p=.001$, two-way ANOVA), where the MC mean episode duration is higher in Hybrid mice than C57. These results suggest that C57 may have a flat pupil dynamic that was not captured by the fraction of transition analysis. As the sound presentation periods vary in length, the total number of transitions could not be accurately evaluated, and even when the fraction of transitions is similar, Hybrid mice could have more total transitions than C57, for example.
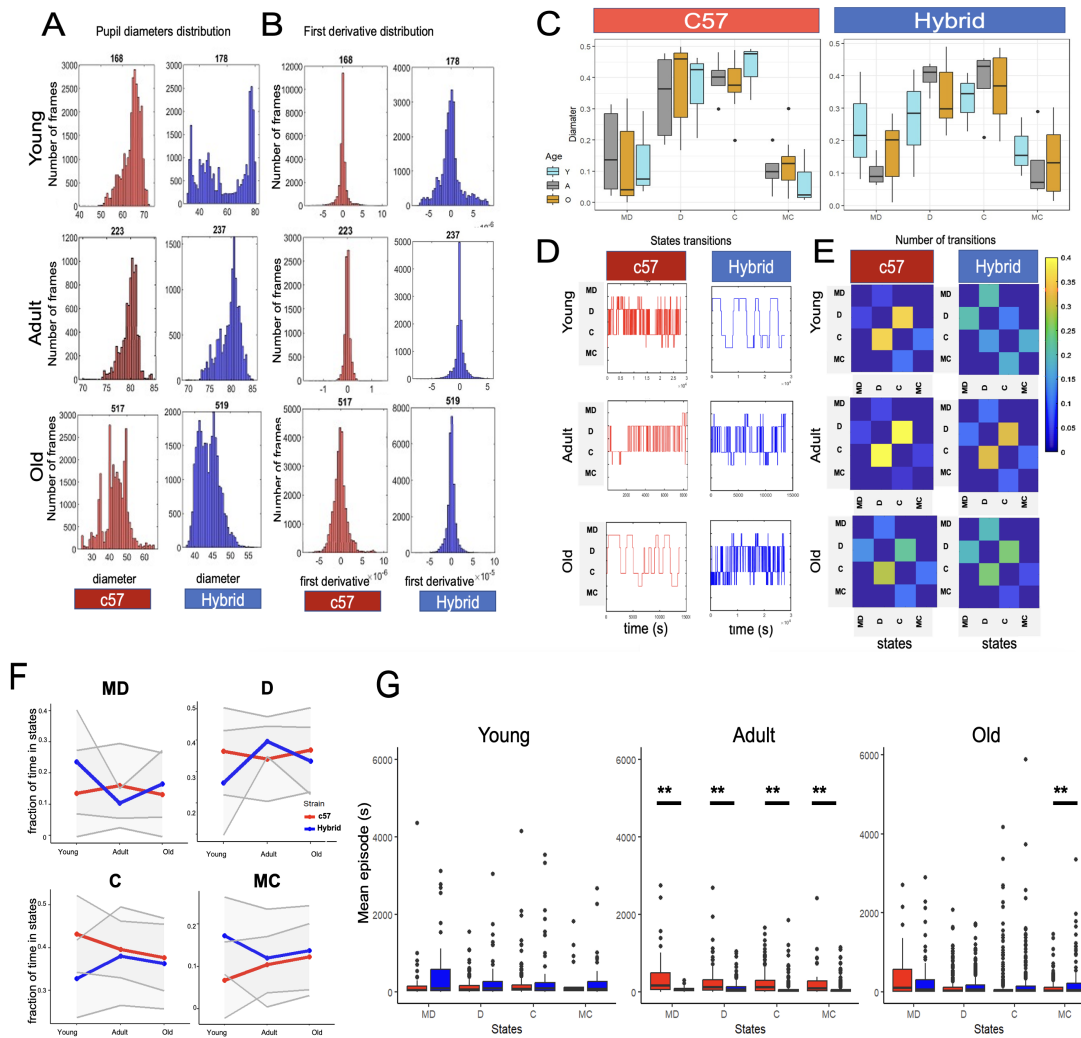
Figure 7.6: *Pupil diameter during sound presentation*

(A) Representative histograms of pupil diameter distribution in Hybrid mice (blue) and C57 (red) strains for 6 representative mice. Mice are split into 3 groups: young, middle-aged, 'adult', and old. Titles represent the ages of the mice. The number of histogram bins is 40. The distribution represents the occurrence of pupil size during the sound presentation protocol. The presented mice are the same as those used for the spontaneous figures, except for the adult Hybrid mice that did not receive natural sound auditory stimulation, we chose the closest mouse in age. (B) Same as (A) for the pupil size derivative, which is the difference between pupil size in subsequent frames. (C)Boxplots representing the fraction of time per pupil state in Hybrid mice (top panel) and C57 (bottom panel). Cyan represents young, grey represents adult, and yellow represents old age. (D) States dynamic along ageing of the same 6 mice: young (top), adult age (middle), and old (bottom), with their (E) respective colour maps representing the proportion of the number of transitions between states during the spontaneous period (colourmaps range from 0 to 0.5).(F) Interaction plot between the mean pupil diameter and age groups per mouse across ageing. Dots (blue for Hybrid mice, red for C57) represent the means, and the grey ribbon represents the standard deviation. (G) Episode duration. Mean time spent in one state when it is reached: (Total episode time (s)/number of episodes). A significant interaction between strains and meantime episodes in adults is found (Interaction effect between strain and pupil state: F(3,1)=4.1, p=.007, two-way ANOVA, with MC p=.008, C MD p<e-9, D p=.006, MD p<e-8). A significant interaction between strains and mean time episodes is also observed in old mice (Interaction effect between strain and pupil state: F(3,1)=4.1, p=.001, two-way ANOVA, with MC p=.002).

The results of our study showed that, during silence, the C57 pupil dynamic tended to be flatter than that of the Hybrid mice strain and did not change with age, whereas the pupil dynamic in Hybrid mice decreased. Although

the pupil dynamic during the sound presentation was similar in both strains, we observed strain differences in mean episode duration beginning in adulthood. These findings indicate that the C57 pupil tends to be flatter and less dynamic than Hybrid mice. These results are interesting as a correlation between pupil dynamics and spiking activity has been observed. However, this correlation needs to be tested during the sound-presentation period also. Moreover, the pupil dynamics are not consistent during silence and natural sound presentation, indicating possible differences in brain state activity during sound stimulation. However, our pipeline of pupil state categorization methods needs improvement, as they do not consider the temporal structure of the pupil dynamics or possible strain-specific effects on the pupil dynamics. Additionally, better control of the maximum pupil dilatation and constriction is needed for more accurate comparisons of pupil sizes. We also lacked in matching brain states with EEG traces as the results of the EEG are difficult to interpret due to the high artefacts observed. It would be interesting to examine the auditory cortex's local field potential oscillation to see if similar results are observed in the theta frequency band. Moreover, incorporating sleep scoring may help determine if these frequency band changes represent differences in brain integration or merely behavioural effects. Nonetheless, this analysis serves as a preliminary step towards developing a pupil states pipeline and sheds light on how pupil dynamics change over the ageing process.

> **Key findings**:
>
> ❖ The dynamics of pupil diameter correlate with the spontaneous AC spiking activity.
>
> ❖ The pupil of Hybrid mice is more dynamic during spontaneous activity compared to C57.
>
> ❖ Theta power band is higher in young C57 compared to Hybrid mice.
>
> ❖ The pupil dynamics during natural sound presentation are consistent between the two strains, however, the duration of pupil state differs starting from adult age between C57 and Hybrid mice.

Discussion
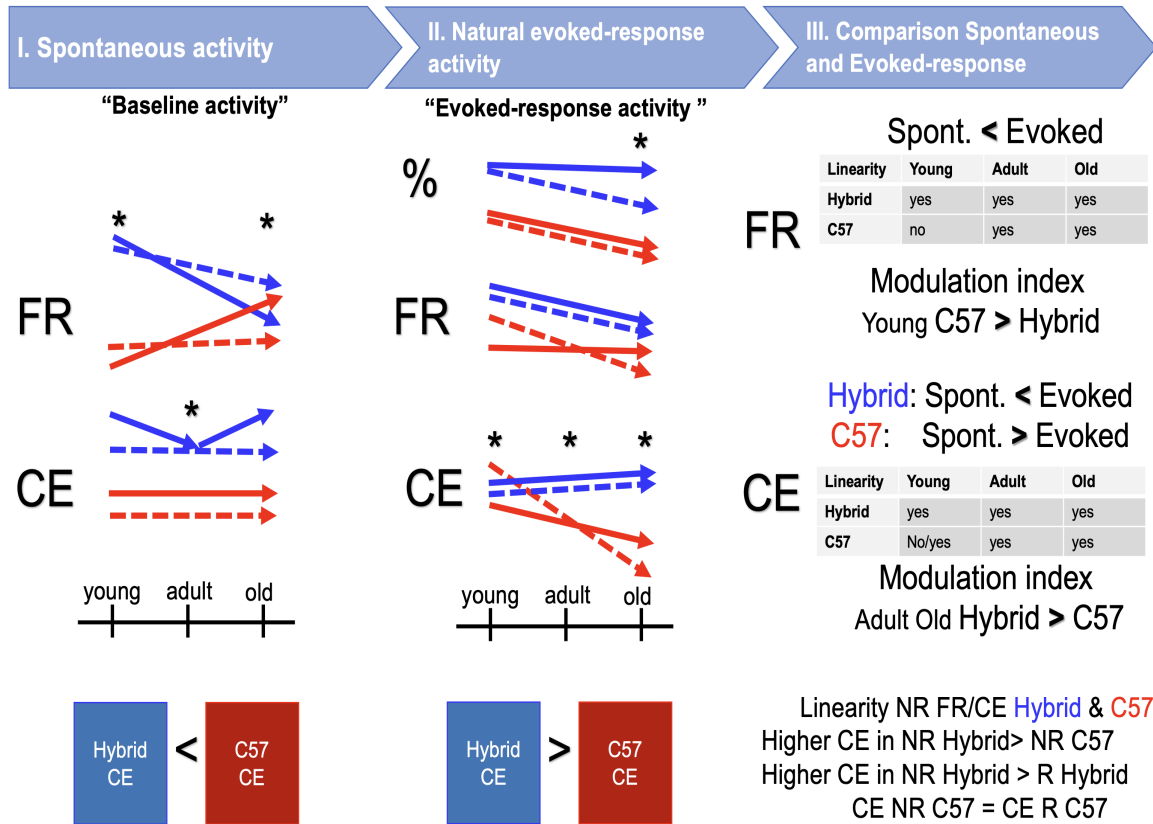
Figure 8.1: *Results summary.*
Diagram summarizing the main results in the Spontaneous, Evoked-response, and Comparison chapters. Blue lines represent the Hybrid mice results, and the red ones are the C57 results. Solid lines arrows represent the BS and the dashed line the NS FR and CE across the 3 age groups. Asterix represents the significant difference at a particular age group between C57 and Hybrid mice.

In our study, we observed age-related changes in the AC, we described these changes by the responsiveness of the AC to sounds presentations, the cells excitability and spike patterns during the spontaneous and evoked-responses (Figure 8.1). We also investigate the pupillometry metric as a marker of the brain state. We found that in the model of AC ageing, the excitability during sound and silence and the responsiveness to sounds decreases along ageing, mainly in the putative inhibitory cells, while the efficiency of the neurons transmission is maintained along ageing. This results suggests that the AC is subject to ageing deterioration of the cells, notably observed by the excitation proprieties and the MI, but that the information per spikes is maintained or increase slightly along ageing, observed by the CE and the MIs analyses. In the age related hearing-loss, we found that both excitation and efficiency of the information transmission decreases along with ageing, in comparison with the control model, this changes are even more important in inhibitory cells. This results suggest that the spike train of C57 mice AC is affected by the impairment of peripheral auditory reception.

In this Discussion Chapter, we will go over, the possible mechanisms that underline the responsiveness of the

AC to natural sound simulation, the differences in strain ageing, and the cell-type specificities. We will describe the limits of our models and the potential openings in the description of the AC code.

8.1 Analysis of the implications of the observed changes in spontaneous activity ageing of the auditory cortex during silence.

In our study, we first investigate the spontaneous activity as we hypothesise that it represents the auditory cortex structure on what the sound is received. We hypothesise that the spontaneous activity may be affected by life experience and sound reception (Wang & Bergles 2015, Tozzi et al. 2016, Longenecker & Galazyuk 2011). By then we question how the AC spontaneous activity change along age, using the FR as a marker of the cell excitability and the CE as a marker of the information carried by the spike train. We also identified the BS and NS as it represents the excitatory and inhibitory cell.

8.1.1 Discussion of the significance of the decrease in spontaneous firing rate with age in BS and NS Hybrid, as well as the increase in BS C57.

Our results show that the FR during spontaneous activity decreases in both BS and NS in Hybrid mice as a function of ageing (Murman 2015, Peters 2006, Price et al. 2017, Erb et al. 2020, Albertson et al. 2022). These findings suggest that the excitability of neurons decreases with age in both cell types. This supports several studies that indicate a decrease in brain activity and slower brain processing with ageing (Murman 2015, Peters 2006, Price et al. 2017, Erb et al. 2020, Albertson et al. 2022). However, we did not find many studies describing the changes in spontaneous FR with age in healthy models or CBA/CaJ mice. We did find a study from 1998 that compared the spontaneous FR in the IC of young (2-3.5 months old) and old (24-28 months old) CBA mice (Walton et al. 1998). In this study, they did not observe any differences in FR, despite they describing a 10% increase in low FR units in the old group compared to the young. It is worth noting that this study was conducted under anaesthesia, which could also affect the spiking rate (Plourde 2006, Filipchuk et al. 2022). Other studies investigating age-related changes in monkeys have examined how FR changes between young and old groups (Overton & Recanzone 2016, Juarez-Salinas et al. 2010). These studies have shown that older monkeys have no difference in the spontaneous activity between young and old FR compared (Juarez-Salinas et al. 2010).

In C57 mice, we observed an increase in FR during spontaneous activity as the mice aged. This increase was primarily driven by increased activity in BS. These results align with what has been reported in the literature, describing an increase in spontaneous FR in C57 mice (Bishop et al. 2022), ARHL models (Profant et al. 2015, Bishop et al. 2022, Herrmann & Butler 2021), and even in CBA mice after exposure to sound trauma (Longenecker & Galazyuk 2011). This has been usually associated with disinhibition leading to increased excitatory activity and hyperactivity (Herrmann & Butler 2021). However, in our analysis we did not observe a particular decrease in the inhibitory C57 FR, conforming to this hypothesis. However, we cannot determine whether this constant FR is due to mechanisms that maintain FR stability throughout ageing or if the number of active inhibitory cell decreases while their FR increases. Nevertheless, it is interesting to note that the kinetics of inhibitory FR in C57 mice differ from those in Hybrid mice. An increase in spontaneous activity in excitatory cell, particularly in the old

group, could lead to noise generation (Shilling-Scrivo et al. 2022), lower coding specificity, or affect neuronal synchronization (Shilling-Scrivo et al. 2022, Ramamurthy & Recanzone 2020). It may also be related to auditory hallucinations (Spooner et al. 2019, Thoma et al. 2017, Uhlhaas et al. 2009).

8.1.2 Age-related difference in spontaneous firing rate between young and old Hybrid and C57.

Comparing the two mouse strains, we found that BS FR activity is different between the C57 and Hybrid mice (Studer & Barkat 2022, Tremblay et al. 2016). Interestingly, we also found that the NS cell FR activity is not different between the two mouse strains, even though the FR decreases in the Hybrid mice. This result is interesting as it could highlight that the activity of inhibitory neurons, known to shape input signals (Studer & Barkat 2022, Tremblay et al. 2016), may play another role during spontaneous activity. We did observe a higher FR in C57 BS compared to Hybrid, suggesting that inhibitory neurons' activity might influence AC activity. However, our analysis could not determine whether the inhibitory FR similarity means that the cell are doing the same range of tasks. We hypothesise that as no sound is received, the inhibitory cell role is not in shaping the signal, and this may explain the similarity between the two strain FR.

In the BS, we found that the FR activity is higher in young Hybrid mice compared to C57 and lower in old age. The C57 mice gene mutation affects the cochlear cell starting at a young age (Ohlemiller et al. 2016, Wang & Bergles 2015, Ichimiya et al. 2000, MIKAELIAN 1979). These results suggest that the reception of the auditory input may affect the AC spontaneous activity shaping, and this effect starts from a young age, which is supported by the changes observed in the peripheral auditory pathway from a young age (Spongr et al. 1997, Ichimiya et al. 2000). In their paper of 2021, Peineau et al. showed that hair cell have a compensatory mechanism, such as an increase in the pool of vesicles ready for exocytosis in response to sound stimulation (Peineau et al. 2021). As the spontaneous activity have been though to treat the past experiences, it is possible that this higher activity in BS is representing the higher activity in processing past impaired received signal. Another possibility is that the brain is doing other than auditory treatment and that the BS are recruited by other neural networks.

Finally, as described previously, the C57 BS FR increases with age, reaching a significantly higher level compared to Hybrid mice at old age. This higher FR at old age could represent this compensatory mechanism but also represent the difference in the AC spontaneous activity between the C57 and Hybrid mice.

8.1.3 Discussion of the higher information efficiency in C57 compared to Hybrid neurons during spontaneous activity.

To investigate the information transmitted in the auditory cortex (AC), we computed the contrast entropy (CE) metric, as described by Pryluk et al. (Pryluk et al. 2019). In our study, we observed that the CE is higher in C57 mice compared to Hybrid mice during spontaneous activity. This finding suggests that the neuronal vocabulary employed by C57 cell is more flexible than that of Hybrid mice cell. By "flexible vocabulary," we mean that a neuron utilizes a broader range of words from its potential repertoire (Figure 8.3).

It is important to note that a flexible vocabulary could manifest as a neuron using, for example, all its three

possible words with their respective statistics, as opposed to a neuron utilising only one or two words out of its seven possibilities (Figure 8.3). This result indicates that peripheral impairment affects the transmission of information in the AC during spontaneous activity. However, it is crucial to emphasize that when we refer to information transmission, we are specifically addressing the transmission of information through neuronal spike trains and not the reception by post-synaptic neurons.

In the paper by Pryluk et al. (Pryluk et al. 2019), they define a high CE neuron as an efficient neuron. This definition suggests that AC C57 neurons are more efficient in transmitting information. As we did not investigate the actual reception of information and, as we do hypothesise that the efficiency of C57 AC neurons may be impaired, in particularly at old age, we will instead focus on the notion of neuron flexible vocabulary or the efficiency to use the vocabulary on the bank of possible words. Therefore, during spontaneous activity, observing neurons with a more flexible vocabulary implies that these cell transmit a broader range of information. The higher CE observed in C57 during spontaneous activity suggests that the AC is engaged in multiple tasks compared to the AC of Hybrid mice. However, a wider range of neurons vocabulary could also indicate a noisier and less specific activity during neuronal computation. This is supported by the lack of increase in the CE of the NS. An increase in the number of coded tasks per BS may coincide with an increase in NS CE, but in our study, we only observed an increase in BS.

We hypothesise that each neuron has a particular limit of possible vocabulary because of the properties of the neurons, such as the refractory period. We hypothesize that during spontaneous activity, the neurons vocabulary fluctuate depending on the ongoing activity and brain state, increasing, decreasing their CE. When a sound enters from the auditory pathway, it will be processed depending on the spontaneous state of the brain (Figure 8.2).
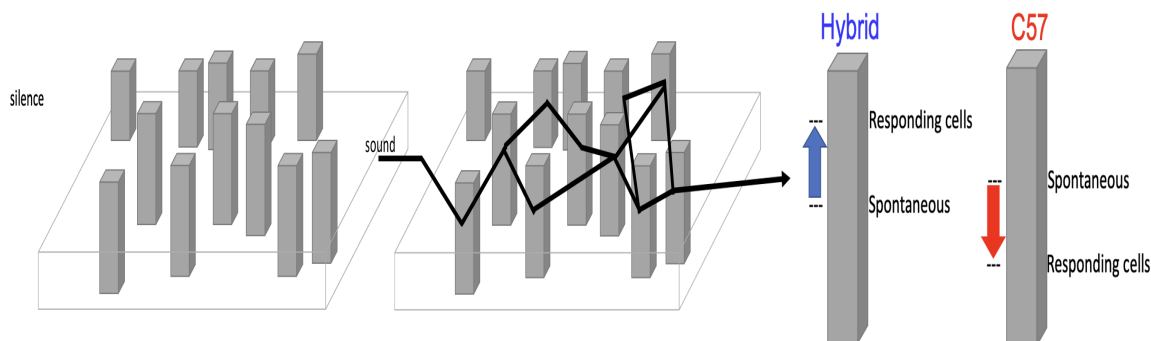
Figure 8.2: *Hypothesis on the CE and auditory reception by the AC*
Schema representing our hypothesis on the auditory cortex reception of sound in C57 and Hybrid mice. The AC neurons, represented by the grey rectangles, have a maximum set of vocabulary based on their refractory period, cellular integrity, memory etc. Theses neurons are active an a particular way during the spontaneous activity depending on the ongoing mental task and brain state. When a sound arrive, the AC shows evoked-responses and the neurons vocabulary is higher than during silence in Hybrid and lower in C57.

A review by Tozzi et al. (Tozzi et al. 2016) addressed the topic of spontaneous activity and discussed the relationship between entropy and energy in the context of brain activity. The review highlights that the brain operates at the delicate equilibrium edge, striving to minimize its thermodynamic entropy production. The concept of variational free energy, which relates to outcomes and a probability density over their causes, supports the idea

of maintaining a subtle steady-state equilibrium and limiting the number of states. The document also suggests that minimizing variational free energy leads to metabolically efficient encoding, following the principles of minimum redundancy and maximum information transfer. Furthermore, it mentions that fluctuations in power-law exponents in the brain alter the system's energy, and fractals facilitate an increase in entropy production when the system is near equilibrium.
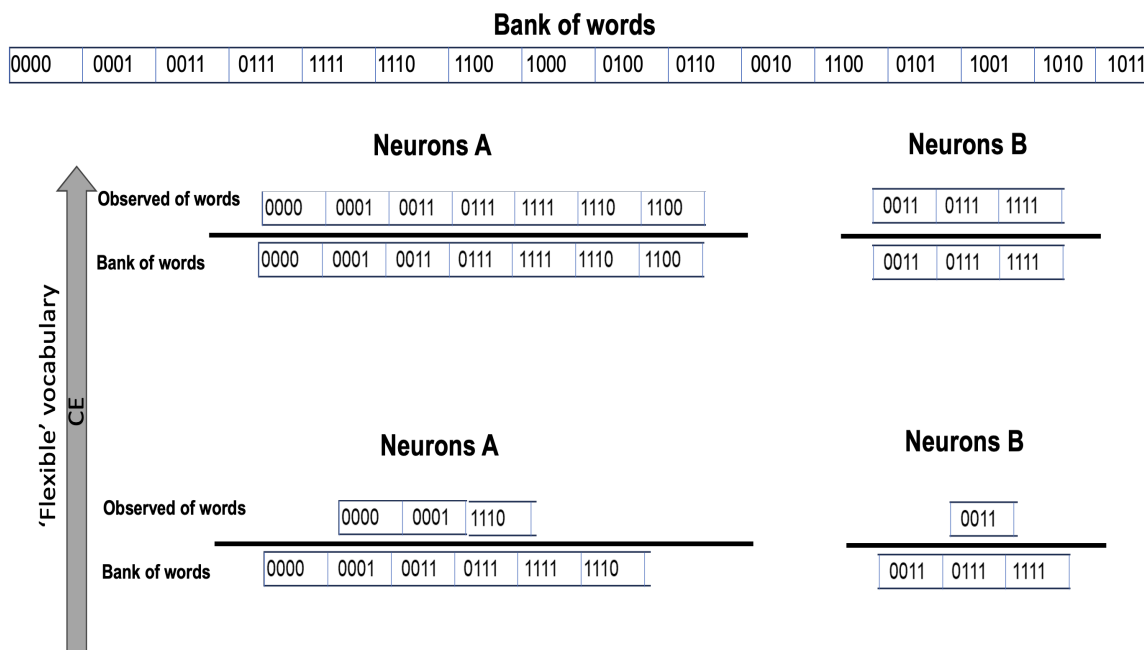
Figure 8.3: *CE and flexible vocabulary.*
This diagram represents the bank of words of a 4 letters word example. The bottom of the panel represents possible examples of neurons with higher and lower CE depending on how many words are used on the possible bank of words. Note that the related statistic of word occurrence is not explicated.

8.1.4 Interpreting the U-shaped trend with age in the CE of Hybrid and the stable CE pattern in C57 during spontaneous activity

In our investigation of age-related changes, we have observed a significant difference in the CE specifically in adult individuals. This disparity is attributed to the lower CE observed in the BS of Hybrid mice. In Hybrid mice, the CE of BS follows a U-shaped trend: it starts at a level similar to that of C57 mice in the young age group, decreases during adulthood, and then increases to the level observed in the old age group, comparable to that of C57 mice. Conversely, we did not observe this trend in the NS nor in C57.

Based on these findings, we hypothesize that the Hybrid AC BS experience a decrease in CE after the maturation of the cortex, specifically during the transition from young to adult age. When we are speaking about maturation, we are hypothesising that first the auditory cortex was shaped differently during the critical period in C57 compared to the Hybrid mice, due to the impaired received inputs (Sonntag et al. 2009, Chang & Kanold 2021), but also that the AC activity may be shaped by the experience and receiving inputs through the lifespan (Radulescu et al. 2021). Although this hypothesis was not explicitly stated or supported by p-values in the report, we tested this trend by altering the boundary between young and adult age groups from 199 days to 70 days and

still observed a decrease in CE during adulthood. These results suggest that the observed differences are not solely due to the CE of BS in the young age group but rather are associated with the adult age group.

Furthermore, we noted an increase in CE of Hybrid BS from adult to old age. We propose that this increase in entropy is a result of the ageing process in the AC. Taking into consideration the effects of ageing on the cortex (Recanzone 2018), we hypothesize that the cell increase their flexibility as a compensatory mechanism to maintain cellular integrity. For instance, we discovered a decrease in the FR of BS as they age. Therefore, the increase in CE could potentially serve as a compensatory mechanism, enhancing the power of signal transmission per BS cell. Conversely, an increase in CE could also be indicative of a detrimental effect of ageing on the AC, resulting in reduced robustness of BS cell activity and increased noise. However, it is worth noting that we did not observe a decrease in the CE of NS in the old age group, which contradicts this scenario.

8.2 Analysis of the age-related and cell type-specific changes in auditory cortex evoked responses

8.2.1 Discussion of the proportion of responding cell changes along ageing and discuss the difference between Hybrid mice and C57

In our study, we have made noteworthy findings regarding the decline in the proportion of R cell as mice age in both strains. However, a more pronounced decrease in the responding cell was observed specifically in the C57 mice. These findings are supported by considering the comparatively lower response of C57 mice to high frequencies (Lyngholm & Sakata 2019, Ison et al. 2007). Moreover, similar declines in responding cell have been documented in CBA mice as well (Shilling-Scrivo et al. 2021, Sha et al. 2008).

With specific cell types, our investigation reveals that the proportion of R BS remains stable in Hybrid mice, while it diminishes in the C57 mice. Additionally, we observed a decrease in the proportion of R NS with age in both mouse strains. Finally, our results indicate that the decrease in responsiveness is more significant in NS in C57 mice compared to Hybrid mice, thereby supporting the notion that C57 mice experience age-related hearing loss and is supported By the role of the inhibitory cell in the signal processing, (Tremblay et al. 2016). This finding is intriguing as it highlights another disparity in the auditory computation between the two mouse strains.

8.2.2 Insight on the decrease in firing rate during evoked response in Hybrid and C57 mice, as well as the difference in BS firing rate between the two strains

Regarding the FR analysis, we made interesting observations in the Hybrid mice. Specifically, we found that the FR of both BS and NS decreases with age. This suggests that the activity of the AC is affected by ageing, particularly affecting NS by significantly reducing their responsiveness and FR. However, when examining excitatory neurons, we noted a decrease in FR with ageing despite the proportion of responding cell remaining unchanged.

Considering the effect of ageing on AC activity in C57 mice, we initially anticipated a decrease in the FR in BS and NS too. However, our study only reported a decrease in NS FR, despite, both the proportion of BS and NS demonstrating responsiveness decreases to natural sound stimulation. This finding leads us to suspect that BS

may attempt to maintain a constant FR due to the reduced number of responding cell, as supported by changes in cochlear cell (Peineau et al. 2021), where they increase their burst response to compensate for the decrease in cell numbers. Moreover, this result may indicate a decrease in NS integrity in shaping BS signalling, given the substantial decrease in NS responsiveness. Additionally, it could suggest that BS may be engaged in tasks other than audition.

8.2.3 Insight on the differential processing of auditory stimuli in C57 and Hybrid mice based on contrast entropy

Comparing the CE of the AC between C57 and Hybrid mice during natural sound presentations, we observed opposite results to our spontaneous results. Interestingly, the CE is higher in Hybrid mice than in C57 mice for both cell types. This indicates that neurons in the Hybrid AC possess a more flexible range of responses during sound presentations. This may reflect the capacity of the Hybrid AC to perform a diverse set of tasks related to auditory stimulation compared to C57 (Bowen et al. 2020, Radulescu et al. 2021, Sonntag et al. 2009) and underscores the distinct responses of neurons to complex sound stimuli.

Additionally, we observed a slight increase in CE with age in Hybrid mice for both cell types, with a greater increase observed from adulthood to old age. This could potentially represent the effect of ageing on neuronal efficiency to compensate for age-related changes or could be an incorrect word choice age-related increase in noise or a decrease in specificity. Alternatively, it may signify an enhanced efficiency aimed at compensating for the effects of ageing. Intriguingly, we observed the opposite trend in C57 mice, with a significant decrease in CE for both cell types from young to adult and young to old age groups. These findings provide further insights into how AC is affected by peripheral impairments. This more robust strategy observed in C57 mice could explain the decrease in sound responses, particularly for high frequencies (Bishop et al. 2022). Moreover, it could provide insight into the difficulties experienced by individuals with presbycusis in extracting relevant sounds from a noisy background. These results are highly interesting and may serve as the focal point of our study.

Furthermore, when comparing the two mouse strains, we found that the CE differs in old age for BS. This disparity persists across all age groups for NS, suggesting difficulties in shaping signal specificity, which may manifest from a young age, as observed in young mice with presbycusis-related impairments (Ison et al. 2007). These findings further support the impact of presbycusis on inhibitory neurons. As a result, we suspect an imbalance in the excitatory/inhibitory (E/I) balance (Xue et al. 2023). Conducting a noise correlation study could shed light on the extent to which E/I functional connectivity is affected by presbycusis throughout the ageing process. Additionally, examining neuronal synchrony could provide further insights into the lower CE, as a reduced CE could potentially arise from an increase in similarly responsive neurons aimed at compensating for peripheral impairments and enhancing signal strength.

8.3 Analysis of the comparison between the Spontaneous and Evoked-response activities

In Hybrid mice, we found that the ageing AC decreased in FR during both spontaneous and evoked-response activities. These decreases are accompanied by a decrease in the responsiveness of the AC NS to sound. Inter-

estingly, we found that the CE, representing the capability to transmit information of a neuron, on the other hand, does not follow the same age-related kinetic. It is following a U-shape trend from young adult to old, while the cell are active spontaneously, and is maintained constant or increase slightly from adult to old when cell are responding to sound. Interestingly, the C57 mice present a different pattern of FR, Responsiveness, and CE AC activity than Hybrid mice. The AC FR activity increase with ageing during spontaneous activity while it decreases during sound-evoked responses. Moreover, the responsiveness of the cell is decreasing in both NS and BS along with ageing. The CE is maintained during silence and decreases importantly during sound-evoked response. These results highlight that the AC activity of the C57 is affected by peripherical impairment and seems to hardly respond to sound, moreover, the AC spontaneous activity seems to be more important than in Hybrid mice.

8.3.1 Discussion the linear relationship between spontaneous and evoked-response activity FR and age groups and cell types.

One of our interests was also to compare the spontaneous and evoked-response activity. First, we found a linear relationship between the FR and the CE between the spontaneous and evoked response periods. This linearity a linear relationship between spontaneous and evoked activity in the auditory cortex implies that the baseline or spontaneous neural activity in the cortex influences the subsequent neural responses to auditory stimuli predictably and proportionally. According to Harris' theories, the ongoing spontaneous activity in the auditory cortex can serve as a dynamic baseline against which sensory inputs are compared and processed. This relationship suggests that the level or characteristics of the spontaneous activity can modulate the responsiveness of the auditory cortex to incoming auditory stimuli (Harris & Thiele 2011, Luczak et al. 2009).

Here, we found that this relation in the FR is abolished in all cell types of young C57 and old NS C57. In the CE, we observed that the BS C57 CE linear relationship between spontaneous and evoked-response activity is also abolished in the young group. These results suggest that the predictable and proportional connection between the baseline neural activity and the subsequent neural response to auditory stimuli is no longer present. There are a few possible interpretations or implications of the abolition of this linear relationship. First, the decoupling of spontaneous and evoked activity implicates the level or characteristics of the spontaneous neural activity no longer reliably modulate the magnitude or pattern of the evoked responses. Secondly, non-linear processing could mean that the relationship between spontaneous and evoked activity may become more complex, and the responses may not change proportionally or predictably with changes in baseline activity. Non-linear processing could involve interactions between multiple factors or neural mechanisms that influence auditory perception. Finally, the abolition of the linear relationship could indicate a shift or disruption in the overall neural dynamics within the auditory cortex. Changes in the circuitry, synaptic connections, or neuromodulatory influences may contribute to the breakdown of the linear relationship between spontaneous and evoked activity (Xue et al. 2023).

It is also interesting to note the most important changes in the linearity is observed in the FR this comfort again the difference between the two metrics. This also implies that the FR could be more easily perturbed by the peripheral impairment. This makes sense knowing that the FR is a simple metric representing the excitability of the cell to a particular sound clue. If the cochlear cell's FR patterns are affected, it could affect the AC FR

too. Then, neural dynamics and mechanisms that regulate firing rates may differ from those involved in encoding contrast entropy. If there are changes in the neural dynamics or circuitry that specifically affect the modulation of firing rates, the linear relationship between spontaneous and evoked-response activity may be more susceptible to disruption. On the other hand, contrast entropy is a measure of the distribution or patterns of neural activity and may be influenced by different factors, such as population coding or temporal correlations. Therefore, disruptions or alterations in these mechanisms may impact the firing rate relationship more prominently.

In terms of cell types, the linear relationship between spontaneous and evoked-response activity is affected in both cell types and in the NS in old age. The inhibitory cell are known to play a crucial role in regulating neural activity and maintaining the balance of excitation and inhibition in neural circuits (Studer & Barkat 2022, Tremblay et al. 2016, Xue et al. 2023). Neural circuits often exhibit intricate connectivity patterns. Inhibitory cell typically provide local inhibition within a specific circuit, exerting control over the activity of nearby excitatory cell. They exert inhibitory control over excitatory cell, shaping their responses. If the inhibitory control is disrupted or compromised, it can lead to alterations in the firing rates and patterns of excitatory cell, potentially affecting the linear relationship between spontaneous and evoked responses.

8.3.2 Discussion of the higher FR during the evoked-response activity than during the spontaneous activity

Comparing the FR between the spontaneous activity and the evoked-response activity, we found that the R cell FR increase during sound presentation and this in all age groups. This indicates that sensory stimulation enhances neuronal activity in both cell types across all age groups. Interestingly, we observed that the NR cell also show a higher FR during sound presentation compared to the spontaneous activity. However, this higher activity is more important in the C57 as it is observed in BS and NS in C57 and only in the sum of BS and NS, 'All cell', in Hybrid mice. This implies that the way auditory information is processed and encoded in the auditory cortex could vary between different mouse strains. Interestingly, the higher activity observed in the NR cell during sound presentation suggests that these cell may still play a role in auditory cortex computations, despite being classified as non-responsive.

In our study, we also investigate the modulation index, a measure used to quantify the change in FR between spontaneous and evoked responses. We observed an increase in FR activity during sound presentation in both R and NR cell for both strains of mice. This suggests that sensory stimulation, specifically the presentation of sound, enhances the overall activity of neurons in the auditory cortex, regardless of their responsiveness. However, we observed a difference between strains at a young age, where the modulation index is higher in the C57 BS than Hybrid. This implies that there are strain-dependent variations in the modulation of FR during sound presentation. This support also that the difference in the AC between Hybrid mice and C57 starts at a young age and may be an increase of the neurons sensibility (Peineau et al. 2021).Interestingly, there is no difference in the modulation index for the non-responsive (NR) cell, indicating that the increased activity observed in NR cell in C57 mice is not specifically induced by the sound stimulus. Instead, it suggests that the NR cell in C57 mice exhibit a higher baseline FR activity in general, regardless of the presence of sound. This strain-specific difference in FR

modulation suggests that there may be genetic or developmental factors that influence the responsiveness and sensitivity of neurons in the auditory cortex to sound stimuli. It indicates that the processing and encoding of auditory information may vary between different strains of mice, particularly in specific cell populations such as the young C57 BS.

These findings highlight the importance of considering genetic and developmental factors when studying auditory cortex computations and the modulation of neural activity.

8.3.3   Discussion of the higher CE during the evoked-response activity than during spontaneous activity in Hybrid mice and lower in C57

When comparing the CE during evoked-response activity versus spontaneous activity in Hybrid mice, and lower contrast entropy in C57 mice within the auditory cortex. This result is really interesting in giving us how the two-strain AC responds to sound stimulation.

We hypothesise that when a specific auditory stimulus is presented, the auditory cortex engages in processing and encoding the features of that stimulus, resulting in a higher level of information processing and coding. This increased processing leads to a higher contrast entropy, indicating a more diverse and complex representation of the auditory stimulus within the neural activity. On the other hand, spontaneous activity in the auditory cortex refers to the ongoing baseline activity that occurs in the absence of any specific auditory input. During spontaneous activity, the auditory cortex is not engaged in processing specific auditory stimuli. As a result, the contrast entropy during spontaneous activity tends to be lower compared to evoked-response activity.

Observing a higher CE in Hybrid mice and C57 mice in the auditory cortex suggests that their auditory system is more responsive and capable of processing complex auditory information or able to respond to a broader range of stimulation. This increased contrast entropy indicates a greater ability to encode and represent auditory stimuli in a diverse and detailed manner. Conversely, the lower contrast entropy observed in C57 mice during evoked-response activity implies a relatively reduced capacity to process and encode auditory information. This lower contrast entropy suggests a more limited or less diverse representation of the auditory stimuli within the neural activity of C57 mice.

Investigating the modulation index between spontaneous and evoked-response CE, we found interesting observations. In Hybrid mice, we found that the modulation index remains constant across different age groups. This suggests the existence of underlying processes that work to maintain a consistent level of CE throughout the lifespan. This stability in CE modulation may be crucial for the effective processing of auditory information.

In contrast, we found a U-shaped pattern in the CE modulation index. Specifically, the modulation index decreases during adulthood and then increases again in old age. This finding implies that there are age-related changes in the modulation of CE. The decrease in CE modulation during adulthood might reflect the deficit in encoding sounds and the importance of spontaneous activity. On the other hand, the subsequent increase in CE modulation in old age suggests a potential compensatory mechanism to maintain or enhance auditory information processing as the individual ages.

These findings provide valuable insights into the dynamic nature of cortical excitability (CE) modulation and

its relationship with age in C57 and Hybrid mice. Moreover, we observed a significant decrease in CE during sound presentation compared to silence, indicating that auditory stimuli actively modulate the excitability of the auditory cortex in C57 mice.

In C57, we found that CE was initially higher in the young age group compared to Hybrid mice, specifically in NS. This suggests that the development or maturation of inhibitory neurons involved in shaping CE may be influenced in C57 mice, and this from a young age, probably trying to compensate for the first observed effect of the presbycusis mutation, increasing the neurons' sensibility (Padamsey et al. 2022) or showing a default in inhibitory neurons shaping the signal (Tremblay et al. 2016, Studer & Barkat 2022). Subsequently, we observed a notable decrease in CE in both cell types in C57 mice, while CE remained constant in Hybrid mice or exhibited a slight increase over age during the sound presentation.

These findings suggest that there may be age-related changes in the modulation of CE in the auditory cortex of C57 mice. The higher CE at the young age group and the subsequent decrease could be indicative of a maturation process or a period of stability in auditory processing during early development. However, as the mice age, CE modulation changes, with a decrease in CE during sound presentation. The U-shaped pattern observed in Hybrid mice during spontaneous activity suggests a different trajectory of CE modulation compared to C57 mice.

Overall, these findings highlight the complex interplay between CE modulation, age, and genetic factors in the auditory cortex of C57 and Hybrid mice. Further investigations into the underlying mechanisms driving these observed patterns can provide deeper insights into the developmental and functional aspects of auditory processing in different mouse strains.

8.4 Analysis of the correlations between pupil dynamics and spiking activity in the auditory cortex

In our study, we aim to examine how brain states in response to auditory stimuli change with age. To achieve this, we initially focused on measuring pupil dynamics as an indicator of brain states. Previous research has shown a relationship between pupil diameter and brain activity (Laffere et al. 2020*b*), suggesting that pupil dynamics could provide valuable insights into brain states. By analysing the variations in pupil dynamics across different auditory stimulation types and their relation to the ageing process, we compared the Hybrid and C57 strains of mice. Additionally, we will explore the correlation between pupil diameter dynamics and auditory cortex spiking activity and investigate whether specific patterns of pupil activities correspond to distinct brain states. To enhance our understanding, we will utilize frontal EEG to identify these patterns and determine if they are associated with particular EEG frequency bands. Our ultimate goal is to establish a pipeline for automatically characterizing pupil states and their potential connections to brain activity and ageing.

8.4.1 Discussion of the qualitative characterization of pupil dynamics and its relevance to brain activity.

The qualitative characterization of pupil dynamics plays a crucial role in understanding the underlying brain activity. Here, we employed a categorization approach to analysis and interpret variations in pupil size and dynamics. By examining the duration of different pupil states, transitions between states, and episode duration, we aimed to elucidate the relationship between pupil dynamics and brain activity.

In our study, we examined the correlation between pupil dynamics and spiking activity in the auditory cortex (AC). We observed that the majority of recordings showed a correlation close to zero, suggesting that the pupil predominantly reflects spiking dynamics. The spiking traces were obtained from the AC during spontaneous activity, while the mice were in a head-fixed state, minimizing the influence of locomotion or cognitive task engagement. Therefore, the observed pupil dynamics likely reflect intrinsic neural processes rather than specific external stimuli or task demands.

To use the pupil dynamic as a marker of ongoing AC activity, we then categorize the pupil dynamics into distinct states based on pupil size, we found that the fraction of time spent in an extreme state, where the pupil was maxi constricted and dilated decreases over age in Hybrid and was constantly fluctuating in middle states in C57 mice. We then correlated these results with EEG power frequency bands and found that pupil states may be represented by Alpha and Gamma powers. Furthermore, we compared the frequency band's power between the two mice strain and found that C57 mice show a higher Theta power than Hybrid mice. However, the Delta power is not different, suggesting that this difference in Theta may not be due to sleep time. Theta power is linked to memory and brain synchronization this could reflect a difference in the spontaneous ongoing activity of the C57 strain. However, this claim is too ambitious and other control needs to be done, a sleep scoring or an analysis of EMG traces could also help in shaping our understanding of the theta power difference. Another interesting aspect of our analysis is the tendency to increase higher power frequency bands with age in Hybrid mice, in particular beta, low and high-gamma frequencies. This may reflect observation done in a previous paper supporting that ageing induces an increase of desynchronised states (Waschke et al. 2017, Albertson et al. 2022), helping the cortex in the integration of signals. Moreover, we found that C57 mice do not present such trend increases, also supporting this hypothesis. It is also important to mention that our traces were highly noisy in high powers, that we cut some frequencies windows. By then, our results may be diminishing the real importance of high-frequency activities or the inverse. However, as we've been working on the spontaneous activity, and as the EEG traces were not precisely recorded at the same location for each mouse, each EEG-related claims are really hard to defend. This is why we did not go further on EEG trace analysis.

In conclusion, our qualitative characterization of pupil dynamics provides valuable insights into brain activity. The findings of our study highlight the potential of pupil measurements as a non-invasive marker of cortical activity. By examining variations in pupil size, transitions between states, and episode durations, researchers can gain a deeper understanding of cognitive processes, attentional states, and neural modulation. However, this part of our work is more of an exploration study. Further advancements in methodologies, pipelines and controls will contribute to harnessing the full potential of pupil dynamics as a valuable tool in neuroscience research and brain

state assessment.

8.5 Limitations and Future Directions

In conclusion, our study comparing two mouse strains, C57 and Hybrid, has provided valuable insights into the age-related changes in cortical excitability (CE) and firing rate (FR) in the auditory cortex. It is important to acknowledge several limitations and considerations that may impact our conclusions.

Firstly, our study focused on specific cell types, BS and NS, and did not assess sub-classes or layers within these populations. This may limit the generalisation of our findings to the entire auditory cortex. Furthermore, we did not evaluate the reception of auditory information or assess the effects of different sound structures on our results. Additionally, our measurement of CE represents the overall excitability but does not account for variations in speaking patterns or the length of words. The experimental setup also presents limitations, as the natural sound, dB, and frequency varied between the mice. While this could be problematic, it may also eliminate potential biases related to specific patterns of activity. Additionally, we did not account for the effects of sleep on our spontaneous activity analysis, nor did we specifically assess population synchronization or the impact of oscillations on spiking activity. These factors could influence the overall cortical computations and information processing. It could also be interesting to explore different way in computing the contrast entropy, maybe adding a more dynamic analysis of the neuronal vocabulary, with a non fixed number of letters per words for example. As for our language, we use different words lengths, it could be similar for the neurons, investigating the utilisation of the Lempel-ziv Markov Chain for example.

Despite these limitations, our findings suggest that age-related changes in FR and CE differ between the two strains. In Hybrid mice, FR decreases with age in both spontaneous and evoked-response activities, accompanied by a lower percentage of NS-responsive cell. However, the fraction of changes between spontaneous and evoked-response activity remains consistent, suggesting the maintenance of efficiency and even a slight increase.

In C57 mice, FR increases with age during spontaneous activity but decreases during evoked-response activity, specifically in BS and NS. This indicates that the auditory cortex adapts differently to peripheral impairment compared to "normal" ageing. Additionally, CE in C57 mice significantly decreases with age during sound presentation and is higher than in Hybrid mice during silence.

Our study reveals that the auditory cortex of C57 mice continues to respond and adapt to auditory stimuli throughout ageing despite increasing deafness with age. This suggests the presence of underlying mechanisms beyond FR, such as synaptic strength or other molecular mechanisms, that contribute to cortical computations. By elucidating the distinct patterns of FR CE modulation observed in these specific cell types, we provide initial insights into their respective functional properties and adaptations in the context of age-related changes.

8.6 Conclusion

In our study, we analysis age-related changes and cell type-specific differences in the auditory cortex (AC) of Hybrid and C57 mice. To gain insights into the auditory processing capabilities and how they are affected

by ageing and hearing loss factors, we examined various parameters describing the excitability and the spike train pattern of the AC during different auditory stimulation conditions (silence, natural sound and noise) in awake mice.

We found that the AC is subject to age-related changes, defined by a decrease in the excitability of the cells, the proportion of responsiveness and the quantity of information shared with the auditory stimuli and the spike train variability. In the AC ageing model, it is observed that excitability during sound and silence, as well as responsiveness to sounds, decrease with age, particularly in putative inhibitory cells. However, the efficiency of neuronal transmission remains constant over time. This suggests that ageing leads to deterioration of AC cells, notably affecting excitatory properties and mutual information (FR and MI), yet information per spike is either maintained or slightly increased with age, as indicated by analyses of the MIs and the CE.

In the model of age-related hearing loss, both responsiveness and excitation are impacted by aging. Additionally, there is a decrease in the quantity of transmitted information per neuron, particularly in putative inhibitory cells. These findings may explain the cocktail-party effect experienced by presbycusis patients, underscoring the significance of inhibitory cells in signal modulation. Furthermore, this conclusion is reinforced by the observation of increased interspike interval variation in putative inhibitory cells in the C57 model.

When compared to the control model of age-related changes, we noted a reduced percentage of responsive cells in both noise and natural sound stimuli presentations, indicating age-related and cell-type-specific variations in AC processing. During spontaneous activity, we observed alterations in CE and FR with age, suggesting potential cell-specific involvement in network modifications and/or the impact of peripheral inputs on AC network modulation.

Overall, our study provide an overview on the AC ageing in the C57 and the Hybrid mice. In particularly, in response to natural sound. Our thesis contributes to the understanding of age-related changes in the auditory cortex and the impact of hearing loss on the central auditory processing. The findings have implications for understanding impact of the peripheral impairment on the central process since young age, ageing processes and on the presbycusis. This study is deeply rooted in the motivation to comprehend the cortical neural code with the aim of delineating neuronal activity for potential therapeutic interventions. It underscores the importance of inserting probes to aid neuronal spiking, emphasizing the necessity of comprehending not only firing rates but also spike trains and the information conveyed per spike.

In conclusion, our thesis provides insights into the auditory cortex's functioning and its alterations during ageing, offering a foundation for future studies in the field of auditory neuroscience and age-related hearing loss.

Bibliography

Abeles, M. (1991), *Corticonics: Neural Circuits of the Cerebral Cortex*, Cambridge University Press.

Abhang, P. A., Gawali, B. W. & Mehrotra, S. C. (2016), Chapter 3 - technical aspects of brain rhythms and speech parameters, *in* P. A. Abhang, B. W. Gawali & S. C. Mehrotra, eds, 'Introduction to EEG- and Speech-Based Emotion Recognition', Academic Press, pp. 51–79.
URL: *https://www.sciencedirect.com/science/article/pii/B9780128044902000038*

Airan, R. D., Thompson, K. R., Fenno, L. E., Bernstein, H. & Deisseroth, K. (2009), 'Temporally precise in vivo control of intracellular signalling', *Nature* **458**(7241), 1025–1029.

Aizenberg, M., Mwilambwe-Tshilobo, L., Briguglio, J. J., Natan, R. G. & Geffen, M. N. (2015), 'Bidirectional regulation of innate and learned behaviors that rely on frequency discrimination by cortical inhibitory neurons', *PLoS biology* **13**(12), e1002308.

Aizenberg, M., Rolón-Martínez, S., Pham, T., Rao, W., Haas, J. S. & Geffen, M. N. (2019), 'Projection from the amygdala to the thalamic reticular nucleus amplifies cortical sound responses', *Cell reports* **28**(3), 605–615.

Akiguchi, I., Pallàs, M., Budka, H., Akiyama, H., Ueno, M., Han, J., Yagi, H., Nishikawa, T., Chiba, Y., Sugiyama, H., Takahashi, R., Unno, K., Higuchi, K. & Hosokawa, M. (2017), 'Samp8 mice as a neuropathological model of accelerated brain aging and dementia: Toshio takeda's legacy and future directions'.

Al Zoubi, O., Ki Wong, C., Kuplicki, R. T., Yeh, H.-w., Mayeli, A., Refai, H., Paulus, M. & Bodurka, J. (2018), 'Predicting age from brain eeg signals—a machine learning approach', *Frontiers in aging neuroscience* **10**, 184.

Albertson, A. J., Landsness, E. C., Tang, M. J., Yan, P., Miao, H., Rosenthal, Z. P., Kim, B., Culver, J. C., Bauer, A. Q. & Lee, J.-M. (2022), 'Normal aging in mice is associated with a global reduction in cortical spectral power and network-specific declines in functional connectivity', *NeuroImage* **257**, 119287.
URL: *https://www.sciencedirect.com/science/article/pii/S1053811922004086*

Alreja, A., Nemenman, I. & Rozell, C. J. (2022), 'Constrained brain volume in an efficient coding model explains the fraction of excitatory and inhibitory neurons in sensory cortices', *PLOS Computational Biology* **18**(1), e1009642.

Altena, E., Vrenken, H., Van Der Werf, Y. D., van den Heuvel, O. A. & Van Someren, E. J. (2010), 'Reduced orbitofrontal and parietal gray matter in chronic insomnia: a voxel-based morphometric study', *Biological psychiatry* **67**(2), 182–185.

Anderson, S., White-Schwoch, T., Parbery-Clark, A. & Kraus, N. (2013), 'A dynamic auditory-cognitive system supports speech-in-noise perception in older adults', *Hearing research* **300**, 18–32.

Bibliography

Arieli, A., Sterkin, A., Grinvald, A. & Aertsen, A. (1996), 'Dynamics of ongoing activity: Explanation of the large variability in evoked cortical responses', *Science* **273**(5283), 1868–1871.
    URL: *https://www.science.org/doi/abs/10.1126/science.273.5283.1868*

Atencio, C. A. & Schreiner, C. E. (2008), 'Spectrotemporal processing differences between auditory cortical fast-spiking and regular-spiking neurons', *The Journal of Neuroscience* **28**(15), 3897–3910.

Atencio, C. A., Sharpee, T. O. & Schreiner, C. E. (2009), 'Hierarchical computation in the canonical auditory cortical circuit'.

Attneave, F. (1954), 'Some informational aspects of visual perception.', *Psychological review* **61 3**, 183–93.

Axelrod, V., Rozier, C., Lehongre, K., Adam, C., Lambrecq, V., Navarro, V. & Naccache, L. (2022), 'Neural modulations in the auditory cortex during internal and external attention tasks: A single-patient intracranial recording study', *Cortex* **157**, 211–230.

Bahmer, A. & Gupta, D. S. (2018), 'Role of oscillations in auditory temporal processing: A general model for temporal processing of sensory information in the brain?', *Frontiers in Neuroscience* **12**, 793.

Bajo, V. M. & King, A. J. (2013), 'Cortical modulation of auditory processing in the midbrain', *Frontiers in neural circuits* **6**, 114.

Bao, J. & Ohlemiller, K. K. (2010), 'Age-related loss of spiral ganglion neurons', *Hearing Research* **264**(1-2), 93–97.
    URL: *https://dx.doi.org/10.1016/j.heares.2009.10.009*

Barlow, H. (1961), 'Possible principles underlying the transformations of sensory messages', *Sensory Communication* **1**.

Bartlett, E. L. (2013), 'The organization and physiology of the auditory thalamus and its role in processing acoustic features important for speech perception', *Brain and language* **126**(1), 29–48.

Bastos, A. M., Briggs, F., Alitto, H. J., Mangun, G. R. & Usrey, W. M. (2014), 'Simultaneous recordings from the primary visual cortex and lateral geniculate nucleus reveal rhythmic interactions and a cortical source for gamma-band oscillations', *The Journal of Neuroscience* **34**(22), 7639–7644.

Bastos, A. M., Usrey, W. M., Adams, R. A., Mangun, G. R., Fries, P. & Friston, K. J. (2012), 'Canonical microcircuits for predictive coding'.

Bean, B. (2007), 'Bean, b.p. the action potential in mammalian central neurons. nat. rev. neurosci. 8, 451-465', *Nature reviews. Neuroscience* **8**, 451–65.

Beauchamp, M. S., Oswalt, D., Sun, P., Foster, B. L., Magnotti, J. F., Niketeghad, S., Pouratian, N., Bosking, W. H. & Yoshor, D. (2020), 'Dynamic stimulation of visual cortex produces form vision in sighted and blind humans', *Cell* **181**(4), 774–783.e5.

Bibliography

Beese, C., Vassileiou, B., Friederici, A. D. & Meyer, L. (2019), 'Age differences in encoding-related alpha power reflect sentence comprehension difficulties', *Frontiers in aging neuroscience* p. 183.

Bennett, C., Arroyo, S. & Hestrin, S. (2013), 'Subthreshold mechanisms underlying state-dependent modulation of visual responses', *Neuron* **80**(2), 350–357.
URL: *https://dx.doi.org/10.1016/j.neuron.2013.08.007*

Betzel, R. F., Wood, K. C., Angeloni, C., Neimark Geffen, M. & Bassett, D. S. (2019), 'Stability of spontaneous, correlated activity in mouse auditory cortex', *PLOS Computational Biology* **15**(12), e1007360.

Beyeler, M., Rounds, E. L., Carlson, K. D., Dutt, N. & Krichmar, J. L. (2019), 'Neural correlates of sparse coding and dimensionality reduction', *PLOS Computational Biology* **15**(6), e1006908.
URL: *https://dx.doi.org/10.1371/journal.pcbi.1006908*

Bialek, W., Rieke, F., de Ruyter van Steveninck, R. R. & Warland, D. (1991), 'Reading a neural code', *Science* **252**(5014), 1854–1857.
URL: *https://www.science.org/doi/abs/10.1126/science.2063199*

Bielczyk, N. Z., Ando, A., Badhwar, A. P., Caldinelli, C., Gao, M., Haugg, A., Hernandez, L. M., Ito, K. L., Kessler, D., Lurie, D., Makary, M. M., Nikolaidis, A., Veldsman, M., Allen, C., Bankston, A., Bottenhorn, K. L., Braukmann, R., Calhoun, V., Cheplygina, V., Boffino, C. C., Ercan, E., Finc, K., Foo, H., Khatibi, A., La, C., Mehler, D. M., Narayanan, S., Poldrack, R. A., Raamana, P. R., Salo, T., Godard-Sebillotte, C., Uddin, L. Q., Valeriani, D., Valk, S. L., Walton, C. C., Ward, P. G., Yanes, J. A. & Zhou, X. (2020), 'Effective self-management for early career researchers in the natural and life sciences'.

Bishop, R., Qureshi, F. & Yan, J. (2022), 'Age-related changes in neuronal receptive fields of primary auditory cortex in frequency, amplitude, and temporal domains', *Hearing Research* **420**, 108504.
URL: *https://www.sciencedirect.com/science/article/pii/S0378595522000739*

Bitterman, Y., Mukamel, R., Malach, R., Fried, I. & Nelken, I. (2008), 'Ultra-fine frequency tuning revealed in single neurons of human auditory cortex', **451**, 197–201.

Bizley, J. K. (2017), 'Audition', *Conn's Translational Neuroscience* pp. 579–598.

Bizley, J. K. & Cohen, Y. E. (2013), 'The what, where and how of auditory-object perception', *Nature Reviews Neuroscience* **14**(10), 693–707.
URL: *https://dx.doi.org/10.1038/nrn3565*

Blackwell, J. M. & Geffen, M. N. (2017), 'Progress and challenges for understanding the function of cortical microcircuits in auditory processing', *Nature Communications* **8**(1).
URL: *https://dx.doi.org/10.1038/s41467-017-01755-2*

Blinkouskaya, Y., Caçoilo, A., Gollamudi, T., Jalalian, S. & Weickenmeier, J. (2021), 'Brain aging mechanisms with mechanical manifestations', *Mechanisms of Ageing and Development* **200**, 111575.
URL: *https://www.sciencedirect.com/science/article/pii/S0047637421001470*

Bibliography

Bories, C., Husson, Z., Guitton, M. J. & De Koninck, Y. (2013), 'Differential balance of prefrontal synaptic activity in successful versus unsuccessful cognitive aging', *Journal of Neuroscience* **33**(4), 1344–1356.

Borst, A. & Theunissen, F. E. (1999), 'Information theory and neural coding', *Nature Neuroscience* **2**, 947–957.

Bowen, Z., Winkowski, D. E. & Kanold, P. O. (2020), 'Functional organization of mouse primary auditory cortex in adult c57bl/6 and f1 (cbaxc57) mice', *Scientific Reports* **10**(1).

Bragin, A., Hetke, J., Wilson, C., Anderson, D., Engel Jr, J. & Buzsaki, G. (2000), 'Multiple site silicon-based probes for chronic recordings in freely moving rats: implantation, recording and histological verification', *Journal of neuroscience methods* **98**(1), 77–82.

Brewer, A. A. & Barton, B. (2016), 'Maps of the auditory cortex'.

Brownell, W. E. (1982), 'Cochlear transduction: an integrative model and review', *Hearing Research* **6**(3), 335–360.

Burkard, R. F. & Sims, D. (2001), 'The human auditory brainstem response to high click rates'.

Buzsáki, G. (2004), 'Large-scale recording of neuronal ensembles', *Nature neuroscience* **7**(5), 446–451.

Buzsáki, G. (2010), 'Neural syntax: cell assemblies, synapsembles, and readers', *Neuron* **68**(3), 362–385.

Buzsáki, G., Anastassiou, C. A. & Koch, C. (2012), 'The origin of extracellular fields and currents—eeg, ecog, lfp and spikes', *Nature reviews neuroscience* **13**(6), 407–420.

Buzsáki, G. (2006), *Rhythms of the Brain*, Oxford University Press.
  URL: *https://doi.org/10.1093/acprof:oso/9780195301069.001.0001*

Buzsáki, G., Anastassiou, C. A. & Koch, C. (2012), 'The origin of extracellular fields and currents — eeg, ecog, lfp and spikes', *Nature Reviews Neuroscience* **13**(6), 407–420.
  URL: *https://dx.doi.org/10.1038/nrn3241*

Buzsáki, G. & Draguhn, A. (2004), 'Neuronal oscillations in cortical networks', *Science* **304**(5679), 1926–1929.
  URL: *https://www.science.org/doi/abs/10.1126/science.1099745*

Buzsáki, G., Logothetis, N. & Singer, W. (2013), 'Scaling brain size, keeping timing: Evolutionary preservation of brain rhythms', *Neuron* **80**(3), 751–764.
  URL: *https://dx.doi.org/10.1016/j.neuron.2013.10.002*

Buzsáki, G. & Wang, X.-J. (2012), 'Mechanisms of gamma oscillations', *Annual Review of Neuroscience* **35**(1), 203–225.
  URL: *https://dx.doi.org/10.1146/annurev-neuro-062111-150444*

Byron, N., Semenova, A. & Sakata, S. (2021), 'Mutual interactions between brain states and alzheimer's disease pathology: a focus on gamma and slow oscillations', *Biology* **10**(8), 707.

Cabeza, R. (2002), 'Hemispheric asymmetry reduction in older adults: the harold model.', *Psychology and aging* **17**(1), 85.

Cantero, J. L., Atienza, M. & Salas, R. M. (2002), 'Human alpha oscillations in wakefulness, drowsiness period, and rem sleep: different electroencephalographic phenomena within the alpha band', *Neurophysiologie Clinique/Clinical Neurophysiology* **32**(1), 54–71.
  URL: *https://www.sciencedirect.com/science/article/pii/S0987705301002891*

Carcea, I., Insanally, M. N. & Froemke, R. C. (2017), 'Dynamics of auditory cortical activity during behavioural engagement and auditory perception', *Nature Communications* **8**(1), 14412.
  URL: *https://dx.doi.org/10.1038/ncomms14412*

Caron, L. (2015), 'Thomas willis, the restoration and the first works of neurology', *Medical History* **59**(4), 525–553.

Casale, J., Kandle, P. F., Murray, I. & Murr, N. (2018), 'Physiology, cochlear function'.

Caspary, D. M., Ling, L., Turner, J. G. & Hughes, L. F. (2008), 'Inhibitory neurotransmission, plasticity and aging in the mammalian central auditory system', *Journal of Experimental Biology* **211**(11), 1781–1791.

Caspary, D. M., Milbrandt, J. C. & Helfert, R. H. (1995), 'Central auditory aging: Gaba changes in the inferior colliculus', *Experimental gerontology* **30**(3-4), 349–360.

Cassidy, J. M., Wodeyar, A., Wu, J., Kaur, K., Masuda, A. K., Srinivasan, R. & Cramer, S. C. (2020), 'Low-frequency oscillations are a biomarker of injury and recovery after stroke', *Stroke* **51**(5), 1442–1450.

Catanese, J., Carmichael, J. E. & Van Der Meer, M. A. A. (2016), 'Low- and high-gamma oscillations deviate in opposite directions from zero-phase synchrony in the limbic corticostriatal loop', *Journal of Neurophysiology* **116**(1), 5–17.
  URL: *https://dx.doi.org/10.1152/jn.00914.2015*

Cessac, B., Nasser, H. & Vasquez, J.-C. (2010), 'Spike trains statistics in integrate and fire models: Exact results', *arXiv preprint arXiv:1008.5074* .

Chait, M., De Cheveigné, A., Poeppel, D. & Simon, J. Z. (2010), 'Neural dynamics of attending and ignoring in human auditory cortex', *Neuropsychologia* **48**(11), 3262–3271.
  URL: *https://dx.doi.org/10.1016/j.neuropsychologia.2010.07.007*

Chang, M. & Kanold, P. O. (2021), 'Development of auditory cortex circuits', *Journal of the Association for Research in Otolaryngology* **22**(3), 237–259.

Chase, S. M. & Young, E. D. (2007), 'First-spike latency information in single neurons increases when referenced to population onset', *Proceedings of the National Academy of Sciences* **104**(12), 5175–5180.
  URL: *https://dx.doi.org/10.1073/pnas.0610368104*

Bibliography

Chen, G., Zhang, Y., Li, X., Zhao, X., Ye, Q., Lin, Y., Tao, H. W., Rasch, M. J. & Zhang, X. (2017), 'Distinct inhibitory circuits orchestrate cortical beta and gamma band oscillations'.

Chen, Y.-C., Li, X., Liu, L., Wang, J., Lu, C.-Q., Yang, M., Jiao, Y., Zang, F.-C., Radziwon, K., Chen, G.-D. & et al. (2015), 'Tinnitus and hyperacusis involve hyperactivity and enhanced connectivity in auditory-limbic-arousal-cerebellar network', *eLife* **4**.

Chia, E.-M. (2006), 'Association between vision and hearing impairments and their combined effects on quality of life', *Archives of Ophthalmology* **124**(10), 1465.

Clinard, C. G. & Cotter, C. M. (2015), 'Neural representation of dynamic frequency is degraded in older adults', *Hearing Research* **323**, 91–98.

Clinard, C. G., Tremblay, K. L. & Krishnan, A. R. (2010), 'Aging alters the perception and physiological representation of frequency: evidence from human frequency-following response recordings', *Hearing research* **264**(1-2), 48–55.

Colin-Le Brun, I., Ferrand, N., Caillard, O., Tosetti, P., Ben-Ari, Y. & Gaïarsa, J.-L. (2004), 'Spontaneous synaptic activity is required for the formation of functional GABAergic synapses in the developing rat hippocampus.', *The Journal of Physiology* **559**(Pt 1), 129–39.
URL: *https://www.hal.inserm.fr/inserm-00484656*

Connors, B. W. & Gutnick, M. J. (1990), 'Intrinsic firing patterns of diverse neocortical neurons', *Trends in neurosciences* **13**(3), 99–104.

Cooke, J. E., Lee, J. J., Bartlett, E. L., Wang, X. & Bendor, D. (2020), 'Post-stimulatory activity in primate auditory cortex evoked by sensory stimulation during passive listening', *Scientific Reports* **10**(1).

Crowell, C. A., Davis, S. W., Beynel, L., Deng, L., Lakhlani, D., Hilbig, S. A., Palmer, H., Brito, A., Peterchev, A. V., Luber, B., Lisanby, S. H., Appelbaum, L. G. & Cabeza, R. (2020), 'Older adults benefit from more widespread brain network integration during working memory'.

Curto, C., Sakata, S., Marguet, S., Itskov, V. & Harris, K. D. (2009*a*), 'A simple model of cortical dynamics explains variability and state dependence of sensory responses in urethane-anesthetized auditory cortex', *Journal of neuroscience* **29**(34), 10600–10612.

Curto, C., Sakata, S., Marguet, S., Itskov, V. & Harris, K. D. (2009*b*), 'A simple model of cortical dynamics explains variability and state dependence of sensory responses in urethane-anesthetized auditory cortex', *The Journal of Neuroscience* **29**(34), 10600–10612.

Das, A., de los Angeles, C. & Menon, V. (2022), 'Electrophysiological foundations of the human default-mode network revealed by intracranial-eeg recordings during resting-state and cognition', *NeuroImage* **250**, 118927.
URL: *https://www.sciencedirect.com/science/article/pii/S1053811922000568*

Bibliography

Davis, A., McMahon, C. M., Pichora-Fuller, K. M., Russ, S., Lin, F., Olusanya, B. O., Chadha, S. & Tremblay, K. L. (2016), 'Aging and Hearing Health: The Life-course Approach', *The Gerontologist* **56**(Suppl$_2$), $S256 - -S267$.
URL:*https://doi.org/10.1093/geront/gnw033*

De Villers-Sidani, E., Alzghoul, L., Zhou, X., Simpson, K. L., Lin, R. C. S. & Merzenich, M. M. (2010), 'Recovery of functional and structural age-related changes in the rat primary auditory cortex with operant training', *Proceedings of the National Academy of Sciences* **107**(31), 13900–13905.
URL: *https://dx.doi.org/10.1073/pnas.1007885107*

Del Campo, H. M., Measor, K. & Razak, K. (2012), 'Parvalbumin immunoreactivity in the auditory cortex of a mouse model of presbycusis', *Hearing research* **294**(1-2), 31–39.

Destexhe, A., Contreras, D. & Steriade, M. (1999), 'Spatiotemporal analysis of local field potentials and unit discharges in cat cerebral cortex during natural wake and sleep states', *Journal of Neuroscience* **19**(11), 4595–4608.

Diaz, H., Maureira Cid, F., Otarola, J., Rojas, R., Alarcon, O. & Canete, L. (2019), 'Eeg beta band frequency domain evaluation for assessing stress and anxiety in resting, eyes closed, basal conditions', *Procedia Computer Science* **162**, 974–981.

Dimitrov, A. G., Lazar, A. A. & Victor, J. D. (2011), 'Information theory in neuroscience', *Journal of Computational Neuroscience* **30**(1), 1–5.
URL: *https://dx.doi.org/10.1007/s10827-011-0314-3*

Ding, N. & Simon, J. Z. (2012), 'Emergence of neural encoding of auditory objects while listening to competing speakers', *Proceedings of the National Academy of Sciences* **109**(29), 11854–11859.

Douglas, R. J. & Martin, K. A. (2004), 'Neuronal circuits of the neocortex', *Annu. Rev. Neurosci.* **27**, 419–451.

Dublin, W. B. (1982), 'The cochlear nuclei revisited', *Otolaryngology–Head and Neck Surgery* **90**(6), 744–760.

Eckhorn, R. & Pöpel, B. (1974), 'Rigorous and extended application of information theory to the afferent visual system of the cat. i. basic concepts', *Kybernetik* **16**(4), 191–200.

Edeline, J.-M., Dutrieux, G., Manunta, Y. & Hennevin, E. (2001), 'Diversity of receptive field changes in auditory cortex during natural sleep', *European Journal of Neuroscience* **14**(11), 1865–1880.

Eggermont, J. J. (2006), 'Properties of correlated neural activity clusters in cat auditory cortex resemble those of neural assemblies', *Journal of Neurophysiology* **96**(2), 746–764. PMID: 16835364.
URL: *https://doi.org/10.1152/jn.00059.2006*

Eggermont, J. J. (2015), 'Animal models of spontaneous activity in the healthy and impaired auditory system', *Frontiers in Neural Circuits* **9**.
URL: *https://www.frontiersin.org/articles/10.3389/fncir.2015.00019*

Bibliography

Eggermont, J. J. (2021), *The gamma, beta, and theta rhythms and nested oscillations*, Elsevier, pp. 23–42.

Ehret, G. (2009), *Tonotopic Organization (Maps)*, Springer Berlin Heidelberg, Berlin, Heidelberg, pp. 4083–4088.
   URL: *https://doi.org/10.1007/978-3-540-29678-2_{6}042*

Einevoll, G. T., Franke, F., Hagen, E., Pouzat, C. & Harris, K. D. (2012), 'Towards reliable spike-train recordings from thousands of neurons with multielectrodes', *Current Opinion in Neurobiology* **22**(1), 11–17.
   URL: *https://dx.doi.org/10.1016/j.conb.2011.10.001*

Ekdale, E. G. (2016), 'Form and function of the mammalian inner ear', *Journal of Anatomy* **228**(2), 324–337.
   URL: *https://dx.doi.org/10.1111/joa.12308*

Elliott, K. L., Fritzsch, B., Yamoah, E. N. & Zine, A. (2022), 'Age-related hearing loss: Sensory and neural etiology and their interdependence', *Frontiers in Aging Neuroscience* **14**.
   URL: *https://www.frontiersin.org/articles/10.3389/fnagi.2022.814528*

Engel, A. K., Fries, P. & Singer, W. (2001), 'Dynamic predictions: oscillations and synchrony in top–down processing', *Nature Reviews Neuroscience* **2**(10), 704–716.

Engle, J. R., Gray, D. T., Turner, H., Udell, J. B. & Recanzone, G. H. (2014), 'Age-related neurochemical changes in the rhesus macaque inferior colliculus', *Frontiers in Aging Neuroscience* **6**.
   URL: *https://www.frontiersin.org/articles/10.3389/fnagi.2014.00073*

Erb, J., Schmitt, L.-M. & Obleser, J. (2020), 'Temporal selectivity declines in the aging human auditory cortex', *eLife* **9**, e55300.
   URL: *https://doi.org/10.7554/eLife.55300*

Fairhall, A. L. (2019), 'Whither variability?', *Nature neuroscience* **22**(3), 329–330.

Faisal, A. A., Selen, L. P. & Wolpert, D. M. (2008), 'Noise in the nervous system', *Nature reviews neuroscience* **9**(4), 292–303.

Fanous, A. A. & Couldwell, W. T. (2012), 'Transnasal excerebration surgery in ancient egypt: Historical vignette', *Journal of neurosurgery* **116**(4), 743–748.

Federmeier, K. D. & Kutas, M. (2005), 'Aging in context: age-related changes in context use during language comprehension', *Psychophysiology* **42**(2), 133–141.

Federmeier, K. D., Kutas, M. & Schul, R. (2010), 'Age-related and individual differences in the use of prediction during language comprehension', *Brain and language* **115**(3), 149–161.

Feng, L. & Wang, X. (2017), 'Harmonic template neurons in primate auditory cortex underlying complex sound processing', *Proceedings of the National Academy of Sciences* **114**(5), E840–E848.
   URL: *https://dx.doi.org/10.1073/pnas.1607519114*

Bibliography

Fetoni, A. R., Troiani, D., Petrosini, L. & Paludetti, G. (2015), 'Cochlear injury and adaptive plasticity of the auditory cortex', *Frontiers in Aging Neuroscience* **7**.
URL: *https://www.frontiersin.org/articles/10.3389/fnagi.2015.00008*

Filipchuk, A., Schwenkgrub, J., Destexhe, A. & Bathellier, B. (2022), 'Awake perception is associated with dedicated neuronal assemblies in the cerebral cortex', *Nature Neuroscience* **25**(10), 1327–1338.

Finkelstein, G. (2015), 'Mechanical neuroscience: Emil du bois-reymond's innovations in theory and practice', *Frontiers in Systems Neuroscience* **9**, 133.

Fischl, B. & Dale, A. M. (2000), 'Measuring the thickness of the human cerebral cortex from magnetic resonance images', *Proceedings of the National Academy of Sciences* **97**(20), 11050–11055.

Flurkey, K., Currer, J. M. & Harrison, D. (2007), Mouse models in aging research, *in* 'The mouse in biomedical research', Elsevier, pp. 637–672.

Fox, J. & (Amsterdam), E. (2007), *The Mouse in Biomedical Research*, American College of Laboratory Animal Medicine Series, Elsevier.
URL: *https://books.google.com.gi/books?id=_VdJywAACAAJ*

Frank, L. M., Brown, E. N. & Wilson, M. A. (2001), 'A comparison of the firing properties of putative excitatory and inhibitory neurons from ca1 and the entorhinal cortex', *Journal of neurophysiology* **86**(4), 2029–2040.

Fries, P. (2009), 'Neuronal gamma-band synchronization as a fundamental process in cortical computation', *Annual Review of Neuroscience* **32**(1), 209–224.

Frisina, R. D., Singh, A., Bak, M., Bozorg, S., Seth, R. & Zhu, X. (2011), 'F1 (cba× c57) mice show superior hearing in old age relative to their parental strains: Hybrid vigor or a new animal model for "golden ears"?', *Neurobiology of aging* **32**(9), 1716–1724.

Frisina, R. D. & Walton, J. P. (2001*a*), Aging of the mouse central auditory system, *in* 'Handbook of Mouse Auditory Research', CRC press, pp. 353–394.

Frisina, R. & Walton, J. (2001*b*), 'Handbook of mouse auditory res.: From behavior to molecular biology'.

Froemke, R. C. & Jones, B. J. (2011), 'Development of auditory cortical synaptic receptive fields', *Neuroscience & Biobehavioral Reviews* **35**(10), 2105–2113.

Fuglsang, S. A., Märcher-Rørsted, J., Dau, T. & Hjortkjær, J. (2020), 'Effects of sensorineural hearing loss on cortical synchronization to competing speech during selective attention', *The Journal of Neuroscience* **40**(12), 2562–2572.

Fuksa, J., Profant, O., Tintěra, J., Svobodová, V., Tóthová, D., Škoch, A. & Syka, J. (2022), 'Functional changes in the auditory cortex and associated regions caused by different acoustic stimuli in patients with presbycusis and tinnitus', *Frontiers in Neuroscience* **16**.
URL: *https://www.frontiersin.org/articles/10.3389/fnins.2022.921873*

Bibliography

Gage, N. M. & Baars, B. J. (2018), 'Sound, speech, and music perception'.

Gates, G. A. & Mills, J. H. (2005), 'Presbycusis', *The Lancet* **366**(9491), 1111–1120.
URL: *https://www.sciencedirect.com/science/article/pii/S0140673605674235*

Gerstner, W., Kreiter, A. K., Markram, H. & Herz, A. V. M. (1997), 'Neural codes: Firing rates and beyond',
Proceedings of the National Academy of Sciences **94**(24), 12740–12741.
URL: *https://www.pnas.org/doi/abs/10.1073/pnas.94.24.12740*

Gold, C., Henze, D. A., Koch, C. & Buzsaki, G. (2006), 'On the origin of the extracellular action potential waveform:
a modeling study', *Journal of neurophysiology* **95**(5), 3113–3128.

Golumbic, E. M. Z., Ding, N., Bickel, S., Lakatos, P., Schevon, C. A., McKhann, G. M., Goodman, R. R., Emerson,
R., Mehta, A. D., Simon, J. Z. et al. (2013), 'Mechanisms underlying selective neuronal tracking of attended speech
at a "cocktail party"', *Neuron* **77**(5), 980–991.

Gong, J., Wang, J., Luo, X., Chen, G., Huang, H., Huang, R., Huang, L. & Wang, Y. (2020), 'Abnormalities of in-
trinsic regional brain activity in first-episode and chronic schizophrenia: a meta-analysis of resting-state functional
mri', *Journal of Psychiatry and Neuroscience* **45**(1), 55–68.

Grant, G. (2006), 'The 1932 and 1944 nobel prizes in physiology or medicine: rewards for ground-breaking studies
in neurophysiology', *Journal of the History of the Neurosciences* **15**(4), 341–357.

Graven, S. N. & Browne, J. V. (2008), 'Auditory development in the fetus and infant', *Newborn and infant nursing
reviews* **8**(4), 187–193.

Gray, D. T., Engle, J. R. & Recanzone, G. H. (2014), 'Age-related neurochemical changes in the rhesus macaque
cochlear nucleus', *Journal of Comparative Neurology* **522**(7), 1527–1541.
URL: *https://dx.doi.org/10.1002/cne.23479*

Greene, A. S., Horien, C., Barson, D., Scheinost, D. & Constable, R. T. (2023), 'Why is everyone talking about brain
state?', *Trends in Neurosciences* .

Gross, C. G. (1995), 'Aristotle on the brain', *The Neuroscientist* **1**(4), 245–250.

Grossman, M., Cooke, A., DeVita, C., Alsop, D., Detre, J., Chen, W. & Gee, J. (2002), 'Age-related changes in
working memory during sentence comprehension: an fmri study', *Neuroimage* **15**(2), 302–317.

Grosso, A., Cambiaghi, M., Concina, G., Sacco, T. & Sacchetti, B. (2015), 'Auditory cortex involvement in emotional
learning and memory'.

Grothe, B. & Park, T. J. (2000), 'Structure and function of the bat superior olivary complex', *Microscopy Research
and Technique* **51**(4), 382–402.

Gruters, K. G. & Groh, J. M. (2012), 'Sounds and beyond: multisensory and other non-auditory signals in the inferior
colliculus', *Frontiers in neural circuits* **6**, 96.

Bibliography

Grégoire, A., Deggouj, N., Dricot, L., Decat, M. & Kupers, R. (2022), 'Brain morphological modifications in congenital and acquired auditory deprivation: A systematic review and coordinate-based meta-analysis', *Frontiers in Neuroscience* **16**.
URL: *https://www.frontiersin.org/articles/10.3389/fnins.2022.850245*

Gu, Y., Gagnon, J.-F. & Kaminska, M. (2023), 'Sleep electroencephalography biomarkers of cognition in obstructive sleep apnea', *Journal of Sleep Research* **n/a**(n/a), e13831.

Guo, W., Chambers, A. R., Darrow, K. N., Hancock, K. E., Shinn-Cunningham, B. G. & Polley, D. B. (2012), 'Robustness of cortical topography across fields, laminae, anesthetic states, and neurophysiological signal types', *The Journal of Neuroscience* **32**(27), 9159–9172.

Hackett, T. A., Barkat, T. R., O'Brien, B. M., Hensch, T. K. & Polley, D. B. (2011), 'Linking topography to tonotopy in the mouse auditory thalamocortical circuit', *Journal of Neuroscience* **31**(8), 2983–2995.

Hackett, T. A., Rinaldi Barkat, T., O'Brien, B. M. J., Hensch, T. K. & Polley, D. B. (2011), 'Linking topography to tonotopy in the mouse auditory thalamocortical circuit', *The Journal of Neuroscience* **31**(8), 2983–2995.

Haines, D. & Mihailoff, G. (2017), *Fundamental Neuroscience for Basic and Clinical Applications*, Elsevier Health Sciences.
URL: *https://books.google.fr/books?id=ONoyDwAAQBAJ*

Hamilton, L. S., Sohl-Dickstein, J., Huth, A. G., Carels, V. M., Deisseroth, K. & Bao, S. (2013*a*), 'Optogenetic activation of an inhibitory network enhances feedforward functional connectivity in auditory cortex', *Neuron* **80**(4), 1066–1076.

Hamilton, L. S., Sohl-Dickstein, J., Huth, A. G., Carels, V. M., Deisseroth, K. & Bao, S. (2013*b*), 'Optogenetic activation of an inhibitory network enhances feedforward functional connectivity in auditory cortex', **80**, 1066–1076.

Harmony, T. (2013), 'The functional significance of delta oscillations in cognitive processing', *Frontiers in Integrative Neuroscience* **7**.
URL: *https://www.frontiersin.org/articles/10.3389/fnint.2013.00083*

Harris, K. C. & Dubno, J. R. (2017), 'Age-related deficits in auditory temporal processing: unique contributions of neural dyssynchrony and slowed neuronal processing', *Neurobiology of aging* **53**, 150–158.

Harris, K. D. & Shepherd, G. M. (2015), 'The neocortical circuit: Themes and variations'.

Harris, K. D. & Thiele, A. (2011), 'Cortical state and attention', *Nature Reviews Neuroscience* **12**(9), 509–523.
URL: *https://dx.doi.org/10.1038/nrn3084*

Haykin, S. & Chen, Z. (2005), 'The cocktail party problem'.

Bibliography

He, D. Z. (1997), 'Relationship between the development of outer hair cell electromotility and efferent innervation: a study in cultured organ of corti of neonatal gerbils', *Journal of Neuroscience* **17**(10), 3634–3643.

He, H., Hong, L. & Sajda, P. (2023), 'Pupillary response is associated with the reset and switching of functional brain networks during salience processing', *PLOS Computational Biology* **19**(5), e1011081.

He, N.-j., Mills, J. H. & Dubno, J. R. (2007), 'Frequency modulation detection: effects of age, psychophysical method, and modulation waveform', *The Journal of the Acoustical Society of America* **122**(1), 467–477.

Heilbron, M. & Chait, M. (2018), 'Great expectations: is there evidence for predictive coding in auditory cortex?', *Neuroscience* **389**, 54–73.

Henao, D., Navarrete, M., Valderrama, M. & Le Van Quyen, M. (2020), 'Entrainment and synchronization of brain oscillations to auditory stimulations', *Neuroscience Research* **156**, 271–278.

Henry, K. R. (1982), 'Influence of genotype and age on noise-induced auditory losses', *Behavior Genetics* **12**(6), 563–573.

Henry, M. J., Herrmann, B., Kunke, D. & Obleser, J. (2017), 'Aging affects the balance of neural entrainment and top-down neural modulation in the listening brain', *Nature communications* **8**(1), 1–11.

Herculano-Houzel, S. (2009), 'The human brain in numbers: a linearly scaled-up primate brain', *Frontiers in human neuroscience* p. 31.

Herrmann, B., Buckland, C. & Johnsrude, I. S. (2019), 'Neural signatures of temporal regularity processing in sounds differ between younger and older adults', *Neurobiology of Aging* **83**, 73–85.

Herrmann, B. & Butler, B. E. (2021), Chapter 17 - aging auditory cortex: the impact of reduced inhibition on function, *in* C. R. Martin, V. R. Preedy & R. Rajendram, eds, 'Assessments, Treatments and Modeling in Aging and Neurological Disease', Academic Press, pp. 183–192.
URL: *https://www.sciencedirect.com/science/article/pii/B9780128180006000172*

Hess, E. H. & Polt, J. M. (1964), 'Pupil size in relation to mental activity during simple problem-solving', *Science* **143**(3611), 1190–1192.

Hirrlinger, J. & Nave, K.-A. (2014), 'Adapting brain metabolism to myelination and long-range signal transduction', *Glia* **62**(11), 1749–1761.

Hodgkin, A. L. & Huxley, A. F. (1952), A quantitative description of membrane current and its application to conduction and excitation in nerve, *in* 'J. Physiol', pp. 500–544.

Holley, M. C. (2005), 'Keynote review: The auditory system, hearing loss and potential targets for drug development', *Drug discovery today* **10**(19), 1269–1282.

Hong, G. & Lieber, C. M. (2019), 'Novel electrode technologies for neural recordings', *Nature Reviews Neuroscience* **20**(6), 330–345.

Bibliography

Horton, C., D'Zmura, M. & Srinivasan, R. (2013), 'Suppression of competing speech through entrainment of cortical oscillations', *Journal of neurophysiology* **109**(12), 3082–3093.

Howarth, A. & Shone, G. R. (2006), 'Ageing and the auditory system', *Postgraduate Medical Journal* **82**(965), 166–171.
URL: *https://dx.doi.org/10.1136/pgmj.2005.039388*

Hubel, D. H. & Wiesel, T. N. (1962), 'Receptive fields, binocular interaction and functional architecture in the cat's visual cortex', *The Journal of physiology* **160**(1), 106.

Hudspeth, A. (2013), 'Snapshot: auditory transduction', *Neuron* **80**(2), 536–e1.

Humphries, C., Liebenthal, E. & Binder, J. R. (2010), 'Tonotopic organization of human auditory cortex', **50**, 1202–1211.

Ichimiya, I., Suzuki, M. & Mogi, G. (2000), 'Age-related changes in the murine cochlear lateral wall'.

Ingham, N. J., Bleeck, S. & Winter, I. M. (2006), 'Contralateral inhibitory and excitatory frequency response maps in the mammalian cochlear nucleus', *European Journal of Neuroscience* **24**(9), 2515–2529.

Ingham, N. J., Pearson, S. A., Vancollie, V. E., Rook, V., Lewis, M. A., Chen, J., Buniello, A., Martelletti, E., Preite, L., Lam, C. C. & et al. (2019), 'Mouse screen reveals multiple new genes underlying mouse and human hearing loss', *PLOS Biology* **17**(4), e3000194.
URL: *https://dx.doi.org/10.1371/journal.pbio.3000194*

Ison, J. R., Allen, P. D. & O'Neill, W. E. (2007), 'Age-related hearing loss in c57bl/6j mice has both frequency-specific and non-frequency-specific components that produce a hyperacusis-like exaggeration of the acoustic startle reflex', *Journal of the Association for Research in Otolaryngology* **8**(4), 539–550.
URL: *https://dx.doi.org/10.1007/s10162-007-0098-3*

Jackson library, C. H. (2017), 'When are mice considered old? jackson laboratory', `https://www.jax.org/news-and-insights/jax-blog/2017/november/when-are-mice-considered-old#`, note = Accessed: 2022-03-10.

Jaramillo, S. & Zador, A. M. (2011), 'The auditory cortex mediates the perceptual effects of acoustic temporal expectation', *Nature Neuroscience* **14**(2), 246–251.
URL: *https://dx.doi.org/10.1038/nn.2688*

Jayakody, D. M., Friedland, P. L., Martins, R. N. & Sohrabi, H. R. (2018), 'Impact of aging on the auditory system and related cognitive functions: a narrative review', *Frontiers in neuroscience* p. 125.

Jeng, J., Johnson, S. L., Carlton, A. J., De Tomasi, L., Goodyear, R. J., De Faveri, F., Furness, D. N., Wells, S., Brown, S. D. M., Holley, M. C. & et al. (2020), 'Age-related changes in the biophysical and morphological characteristics of mouse cochlear outer hair cells', *The Journal of Physiology* **598**(18), 3891–3910.

Bibliography

Jensen, O. & Mazaheri, A. (2010), 'Shaping functional architecture by oscillatory alpha activity: Gating by inhibition', *Frontiers in Human Neuroscience* **4**.
URL: *https://www.frontiersin.org/articles/10.3389/fnhum.2010.00186*

Jia, X. & Kohn, A. (2011), 'Gamma rhythms in the brain', *PLOS Biology* **9**(4), e1001045.
URL: *https://dx.doi.org/10.1371/journal.pbio.1001045*

Jiang, C., Luo, B., Manohar, S., Chen, G.-D. & Salvi, R. (2017), 'Plastic changes along auditory pathway during salicylate-induced ototoxicity: Hyperactivity and cf shifts', *Hearing Research* **347**, 28–40.
URL: *https://dx.doi.org/10.1016/j.heares.2016.10.021*

Joshi, S., Li, Y., Rishi & Joshua (2016), 'Relationships between pupil diameter and neuronal activity in the locus coeruleus, colliculi, and cingulate cortex', *Neuron* **89**(1), 221–234.
URL: *https://dx.doi.org/10.1016/j.neuron.2015.11.028*

Juarez-Salinas, D. L., Engle, J. R., Navarro, X. O. & Recanzone, G. H. (2010), 'Hierarchical and serial processing in the spatial auditory cortical pathway is degraded by natural aging', *The Journal of Neuroscience* **30**(44), 14795–14804.

Jung, R. & Berger, W. (1979), 'Hans bergers entdeckung des elektrenkephalogramms und seine ersten befunde 1924–1931', *Archiv für Psychiatrie und Nervenkrankheiten* **227**(4), 279–300.

Kandler, K., Clause, A. & Noh, J. (2009), 'Tonotopic reorganization of developing auditory brainstem circuits', *Nature neuroscience* **12**(6), 711–717.

Karakaş, S. (2020), 'A review of theta oscillation and its functional correlates', *International Journal of Psychophysiology* **157**, 82–99.
URL: *https://www.sciencedirect.com/science/article/pii/S0167876020300763*

Kavalali, E. T. (2014), 'The mechanisms and functions of spontaneous neurotransmitter release', *Nature Reviews Neuroscience* **16**, 5–16.

Keller, G. B. & Mrsic-Flogel, T. D. (2018), 'Predictive processing: a canonical cortical computation', *Neuron* **100**(2), 424–435.

Kerlin, J. R., Shahin, A. J. & Miller, L. M. (2010), 'Attentional gain control of ongoing cortical speech representations in a "cocktail party"', *Journal of Neuroscience* **30**(2), 620–628.

Keshmiri, S. (2020), 'Entropy and the brain: An overview', *Entropy* **22**(9), 917.

Khullar, S. & Babbar, R. (2011), 'Presbycusis and auditory brainstem responses: a review', *Asian Pacific Journal of Tropical Disease* **1**(2), 150–157.

Kielan, P., Kciuk, M. & Piecyk, J. (2020), 'Biofeedback therapy application with eeg signal visualization and the optimization of success factor algorithm', *International Journal of Electronics and Telecommunications* **66**, 607–612.

Bibliography

King, A. J., Hammond-Kenny, A. & Nodal, F. R. (2019), *Multisensory Processing in the Auditory Cortex*, Springer Handbook of Auditory Research, p. 105–133.

King, A. J., Teki, S. & Willmore, B. D. (2018*a*), 'Recent advances in understanding the auditory cortex', *F1000Research* **7**, 1555.
   URL: *https://dx.doi.org/10.12688/f1000research.15580.1*

King, A. J., Teki, S. & Willmore, B. D. (2018*b*), 'Recent advances in understanding the auditory cortex', *F1000Research* **7**.

Kipke, D. R., Shain, W., Buzsáki, G., Fetz, E., Henderson, J. M., Hetke, J. F. & Schalk, G. (2008), 'Advanced neurotechnologies for chronic neural interfaces: new horizons and clinical opportunities', *Journal of Neuroscience* **28**(46), 11830–11838.

Klimesch, W. (2012), 'Alpha-band oscillations, attention, and controlled access to stored information', *Trends in Cognitive Sciences* **16**(12), 606–617.
   URL: *https://dx.doi.org/10.1016/j.tics.2012.10.007*

Koops, E. A., Renken, R. J., Lanting, C. P. & Van Dijk, P. (2020), 'Cortical tonotopic map changes in humans are larger in hearing loss than in additional tinnitus', *The Journal of Neuroscience* **40**(16), 3178–3185.

Kopp-Scheinpflug, C., Sinclair, J. L. & Linden, J. F. (2018), 'When sound stops: offset responses in the auditory system', *Trends in neurosciences* **41**(10), 712–728.

Kotak, V. C., Fujisawa, S., Lee, F. A., Karthikeyan, O., Aoki, C. & Sanes, D. H. (2005), 'Hearing loss raises excitability in the auditory cortex', *The Journal of Neuroscience* **25**(15), 3908–3918.

Kral, A. & Sharma, A. (2023), 'Crossmodal plasticity in hearing loss', *Trends in Neurosciences* **46**(5), 377–393.
   URL: *https://www.sciencedirect.com/science/article/pii/S0166223623000450*

Kropotov, J. D. (2009), Chapter 3 - beta rhythms, *in* J. D. Kropotov, ed., 'Quantitative EEG, Event-Related Potentials and Neurotherapy', Academic Press, San Diego, pp. 59–76.
   URL: *https://www.sciencedirect.com/science/article/pii/B9780123745125000037*

Krueger, C. & Garvan, C. (2014), 'Emergence and retention of learning in early fetal development', *Infant Behavior and Development* **37**(2), 162–173.
   URL: *https://www.sciencedirect.com/science/article/pii/S0163638313001185*

Kujawa, S. G. & Liberman, M. C. (2015), 'Synaptopathy in the noise-exposed and aging cochlea: Primary neural degeneration in acquired sensorineural hearing loss', *Hearing Research* **330**, 191–199.
   URL: *https://dx.doi.org/10.1016/j.heares.2015.02.009*

Kwan, T., White, P. M. & Segil, N. (2009), 'Development and regeneration of the inner ear', *Annals of the New York Academy of Sciences* **1170**(1), 28–33.

Bibliography

Laffere, A., Dick, F. & Tierney, A. (2020*a*), 'Effects of auditory selective attention on neural phase: individual differences and short-term training', *NeuroImage* **213**, 116717.
URL: *https://www.sciencedirect.com/science/article/pii/S1053811920302044*

Laffere, A., Dick, F. & Tierney, A. (2020*b*), 'Effects of auditory selective attention on neural phase: individual differences and short-term training', *NeuroImage.* **213**, 116717.

Langers, D. R. & van Dijk, P. (2012), 'Mapping the tonotopic organization in human auditory cortex with minimally salient acoustic stimulation', *Cerebral cortex* **22**(9), 2024–2038.

Larsen, R. S. & Waters, J. (2018), 'Neuromodulatory correlates of pupil dilation', *Frontiers in neural circuits* **12**, 21.

Leaver, A. M. & Rauschecker, J. P. (2010), 'Cortical representation of natural complex sounds: Effects of acoustic features and auditory object category', *The Journal of Neuroscience* **30**(22), 7604–7612.

Lee, C. C. (2013), 'Thalamic and cortical pathways supporting auditory processing', *Brain and Language* **126**(1), 22–28.
URL: *https://dx.doi.org/10.1016/j.bandl.2012.05.004*

Lee, C. C. & Sherman, S. M. (2012), 'Intrinsic modulators of auditory thalamocortical transmission', *Hearing Research* **287**(1-2), 43–50.
URL: *https://dx.doi.org/10.1016/j.heares.2012.04.001*

Lee, C. C., Yanagawa, Y. & Imaizumi, K. (2015), 'Commissural functional topography of the inferior colliculus assessed in vitro', *Hearing research* **328**, 94–101.

Lee, E. K., Balasubramanian, H., Tsolias, A., Anakwe, S. U., Medalla, M., Shenoy, K. V. & Chandrasekaran, C. (2021), 'Non-linear dimensionality reduction on extracellular waveforms reveals cell type diversity in premotor cortex', *eLife* **10**.

Lee, R. S., Hermens, D. F., Porter, M. A. & Redoblado-Hodge, M. A. (2012), 'A meta-analysis of cognitive deficits in first-episode major depressive disorder', *Journal of Affective Disorders* **140**(2), 113–124.
URL: *https://www.sciencedirect.com/science/article/pii/S0165032711006720*

Lejko, N., Larabi, D. I., Herrmann, C. S., Aleman, A. & Ćurčić Blake, B. (2020), 'Alpha power and functional connectivity in cognitive decline: A systematic review and meta-analysis', *Journal of Alzheimer's Disease* **78**(3), 1047–1088.

Lesica, N. A. (2018), 'Why do hearing aids fail to restore normal auditory perception?', *Trends in Neurosciences* **41**(4), 174–185.
URL: *https://www.sciencedirect.com/science/article/pii/S0166223618300328*

Lesicko, A. M. & Llano, D. A. (2017), 'Impact of peripheral hearing loss on top-down auditory processing', *Hearing Research* **343**, 4–13.
URL: *https://dx.doi.org/10.1016/j.heares.2016.05.018*

Bibliography

Li, C.-L. & Jasper, H. (1953), 'Microelectrode studies of the electrical activity of the cerebral cortex in the cat', *The Journal of physiology* **121**(1), 117.

Li, H.-S. (1992), 'Influence of genotype and age on acute acoustic trauma and recovery in cba/ca and c57bl/6j mice', *Acta Oto-Laryngologica* **112**(6), 956–967. PMID: 1481666.
URL: *https://doi.org/10.3109/00016489209137496*

Li, H.-S. & Hultcrantz, M. (1994), 'Age-related degeneration of the organ of corti in two genotypes of mice', *ORL* **56**(2), 61–67.

Li, K., Su, W., Chen, M., Li, C.-M., Ma, X.-X., Wang, R., Lou, B.-H., Zhao, H., Chen, H.-B. & Yan, C.-Z. (2020), 'Abnormal spontaneous brain activity in left-onset parkinson disease: A resting-state functional mri study', *Frontiers in Neurology* **11**.
URL: *https://www.frontiersin.org/articles/10.3389/fneur.2020.00727*

Li, L.-y., Xiong, X. R., Ibrahim, L. A., Yuan, W., Tao, H. W. & Zhang, L. I. (2015), 'Differential receptive field properties of parvalbumin and somatostatin inhibitory neurons in mouse auditory cortex', *Cerebral cortex* **25**(7), 1782–1791.

Liberman, M. C. (2017), 'Noise-induced and age-related hearing loss: new perspectives and potential therapies', *F1000Research* **6**, 927.
URL: *https://dx.doi.org/10.12688/f1000research.11310.1*

Lim, S., Mckee, J. L., Woloszyn, L., Amit, Y., Freedman, D. J., Sheinberg, D. L. & Brunel, N. (2015), 'Inferring learning rules from distributions of firing rates in cortical neurons', *Nature Neuroscience* **18**(12), 1804–1810.
URL: *https://dx.doi.org/10.1038/nn.4158*

Lin, F. R., Thorpe, R., Gordon-Salant, S. & Ferrucci, L. (2011), 'Hearing Loss Prevalence and Risk Factors Among Older Adults in the United States', *The Journals of Gerontology: Series A* **66A**(5), 582–590.
URL: *https://doi.org/10.1093/gerona/glr002*

Linden, J. F. & Schreiner, C. E. (2003), 'Columnar transformations in auditory cortex? a comparison to visual and somatosensory cortices', *Cerebral cortex* **13**(1), 83–89.

Lindenberger, U. & Baltes, P. B. (1997), 'Intellectual functioning in old and very old age: cross-sectional results from the berlin aging study.', *Psychology and aging* **12**(3), 410.

Livingston, G., Sommerlad, A., Orgeta, V., Costafreda, S. G., Huntley, J., Ames, D., Ballard, C., Banerjee, S., Burns, A., Cohen-Mansfield, J. & et al. (2017), 'Dementia prevention, intervention, and care', *The Lancet* **390**(10113), 2673–2734.

Llinás, R. R. (2014), 'Intrinsic electrical properties of mammalian neurons and cns function: a historical perspective', *Frontiers in Cellular Neuroscience* **8**.
URL: *https://www.frontiersin.org/articles/10.3389/fncel.2014.00320*

Bibliography

Lomber, S. G. (2017), 'What is the function of auditory cortex when it develops in the absence of acoustic input?'.

Longenecker, R. J. & Galazyuk, A. V. (2011), 'Development of tinnitus in cba/caj mice following sound exposure', *Journal of the Association for Research in Otolaryngology* **12**(5), 647–658.
URL: *https://dx.doi.org/10.1007/s10162-011-0276-1*

Lopez-Poveda, E. A. (2018), 'Olivocochlear efferents in animals and humans: From anatomy to clinical relevance', *Frontiers in Neurology* **9**.
URL: *https://www.frontiersin.org/articles/10.3389/fneur.2018.00197*

Lozano, A. M., Lipsman, N., Bergman, H., Brown, P., Chabardes, S., Chang, J. W., Matthews, K., McIntyre, C. C., Schlaepfer, T. E., Schulder, M. et al. (2019), 'Deep brain stimulation: current challenges and future directions', *Nature Reviews Neurology* **15**(3), 148–160.

Luczak, A., Barthó, P. & Harris, K. D. (2009), 'Spontaneous events outline the realm of possible sensory responses in neocortical populations', *Neuron* **62**(3), 413–425.
URL: *https://dx.doi.org/10.1016/j.neuron.2009.03.014*

Luebke, J., Chang, Y.-M., Moore, T. & Rosene, D. (2004), 'Normal aging results in decreased synaptic excitation and increased synaptic inhibition of layer 2/3 pyramidal cells in the monkey prefrontal cortex', *Neuroscience* **125**(1), 277–288.

Lyngholm, D. & Sakata, S. (2019), 'Cre-dependent optogenetic transgenic mice without early age-related hearing loss', *Frontiers in Aging Neuroscience* **11**, 29.

Mackay, D. M. & McCulloch, W. S. (1952), 'The limiting information capacity of a neuronal link', *Bulletin of Mathematical Biology* **14**, 107–107.

Madisen, L., Mao, T., Koch, H., Zhuo, J.-m., Berenyi, A., Fujisawa, S., Hsu, Y.-W. A., Garcia, A. J., Gu, X., Zanella, S. et al. (2012), 'A toolbox of cre-dependent optogenetic transgenic mice for light-induced activation and silencing', *Nature neuroscience* **15**(5), 793–802.

Magri, C., Whittingstall, K., Singh, V., Logothetis, N. K. & Panzeri, S. (2009), 'A toolbox for the fast information analysis of multiple-site lfp, eeg and spike train recordings', *BMC Neuroscience* **10**(1), 81.
URL: *https://dx.doi.org/10.1186/1471-2202-10-81*

Malsburg, C. v. d. (1994), The correlation theory of brain function, *in* 'Models of neural networks', Springer, pp. 95–119.

Markocsan, N., Nylén, P., Wigren, J., Li, X.-H. & Tricoire, A. (2009), 'Effect of thermal aging on microstructure and functional properties of zirconia-base thermal barrier coatings', *Journal of Thermal Spray Technology* **18**(2), 201–208.

Mathis, A., Mamidanna, P., Cury, K. M., Abe, T., Murthy, V. N., Mathis, M. W. & Bethge, M. (2018), 'Deeplabcut: markerless pose estimation of user-defined body parts with deep learning', *Nature neuroscience* **21**(9), 1281–1289.

Bibliography

Matthew, Stephen & David (2015), 'Cortical membrane potential signature of optimal states for sensory signal detection', *Neuron* **87**(1), 179–192.
   URL: *https://dx.doi.org/10.1016/j.neuron.2015.05.038*

Matthews, P. B. C. (1999), 'The effect of firing on the excitability of a model motoneurone and its implications for cortical stimulation', *The journal of physiology.* **518**(3), 867–882.

Mattson, M. P. & Arumugam, T. V. (2018), 'Hallmarks of brain aging: adaptive and pathological modification by metabolic states', *Cell metabolism* **27**(6), 1176–1199.

Mattson, M. P. & Magnus, T. (2006), 'Ageing and neuronal vulnerability', *Nature Reviews Neuroscience* **7**(4), 278–294.
   URL: *https://dx.doi.org/10.1038/nrn1886*

Mazelová, J., Popelar, J. & Syka, J. (2003), 'Auditory function in presbycusis: peripheral vs. central changes', *Experimental gerontology* **38**(1-2), 87–94.

Mazelová, J., Popelar, J. & Syka, J. (2003), 'Auditory function in presbycusis: peripheral vs. central changes', *Experimental Gerontology* **38**(1), 87–94. Proceedings of the 6th International Symposium on the Neurobiology and Neuroendocrinology of Aging.
   URL: *https://www.sciencedirect.com/science/article/pii/S0531556502001559*

McAlinden, N., Gu, E., Dawson, M. D., Sakata, S. & Mathieson, K. (2015), 'Optogenetic activation of neocortical neurons in vivo with a sapphire-based micro-scale led probe', *Frontiers in Neural Circuits* **9**.
   URL: *https://www.frontiersin.org/articles/10.3389/fncir.2015.00025*

McCormick, D. A., Connors, B. W., Lighthall, J. W. & Prince, D. A. (1985), 'Comparative electrophysiology of pyramidal and sparsely spiny stellate neurons of the neocortex', *Journal of neurophysiology* **54**(4), 782–806.

McFadden, S. L. & Willott, J. F. (1994), 'Responses of inferior colliculus neurons in c57bl/6j mice with and without sensorineural hearing loss: Effects of changing the azimuthal location of a continuous noise masker on responses to contralateral tones'.

McGinley, M. J., David, S. V. & McCormick, D. A. (2015), 'Cortical membrane potential signature of optimal states for sensory signal detection', *Neuron* **87**(1), 179–192.

McKay, C. M., Lim, H. H. & Lenarz, T. (2013), 'Temporal processing in the auditory system', *Journal of the Association for Research in Otolaryngology* **14**(1), 103–124.

McNair, S. W., Kayser, S. J. & Kayser, C. (2019), 'Consistent pre-stimulus influences on auditory perception across the lifespan', *Neuroimage* **186**, 22–32.

Menardo, J., Tang, Y., Ladrech, S., Lenoir, M., Casas, F., Michel, C., Bourien, J., Ruel, J., Rebillard, G., Maurice, T., Puel, J. L. & Wang, J. (2012), 'Oxidative stress, inflammation, and autophagic stress as the key mechanisms of premature age-related hearing loss in samp8 mouse cochlea'.

Bibliography

Mendelson, J. & Ricketts, C. (2001), 'Age-related temporal processing speed deterioration in auditory cortex', *Hearing research* **158**(1-2), 84–94.

Menon, V. (2023), '20 years of the default mode network: A review and synthesis', *Neuron* .
    URL: *https://www.sciencedirect.com/science/article/pii/S0896627323003082*

Meredith, M. A. & Lomber, S. G. (2011), 'Somatosensory and visual crossmodal plasticity in the anterior auditory field of early-deaf cats', *Hearing Research* **280**(1-2), 38–47.
    URL: *https://dx.doi.org/10.1016/j.heares.2011.02.004*

Meyer-Baese, L., Watters, H. N. & Keilholz, S. (2022), 'Spatiotemporal patterns of spontaneous brain activity: a mini-review', *Neurophotonics* **9**(3), 032209.
    URL: *https://doi.org/10.1117/1.NPh.9.3.032209*

Michalski, N. & Petit, C. (2022), 'Central auditory deficits associated with genetic forms of peripheral deafness', *Human Genetics* **141**(3-4), 335–345.

Miettinen, R., Sirviö, J., Riekkinen Sr, P., Laakso, M., Riekkinen, M. & Riekkinen Jr, P. (1993), 'Neocortical, hippocampal and septal parvalbumin-and somatostatin-containing neurons in young and aged rats: correlation with passive avoidance and water maze performance', *Neuroscience* **53**(2), 367–378.

MIKAELIAN, D. O. (1979), 'Development and degeneration of hearing in the c57/b16 mouse'.

Mitra, A., Kraft, A., Wright, P., Acland, B., Snyder, A. Z., Rosenthal, Z., Czerniewski, L., Bauer, A., Snyder, L., Culver, J. et al. (2018), 'Spontaneous infra-slow brain activity has unique spatiotemporal dynamics and laminar structure', *Neuron* **98**(2), 297–305.

Montes-Lourido, P., Kar, M., David, S. V. & Sadagopan, S. (2021), 'Neuronal selectivity to complex vocalization features emerges in the superficial layers of primary auditory cortex', *PLOS Biology* **19**(6), e3001299.

Moore, A. K. & Wehr, M. (2013), 'Parvalbumin-expressing inhibitory interneurons in auditory cortex are well-tuned for frequency', *Journal of neuroscience* **33**(34), 13713–13723.

Moore, B. C. J. (2016), 'A review of the perceptual effects of hearing loss for frequencies above 3khz', *International Journal of Audiology* **55**(12), 707–714.
    URL: *https://dx.doi.org/10.1080/14992027.2016.1204565*

Morrison, J. H. & Baxter, M. G. (2012), 'The ageing cortical synapse: hallmarks and implications for cognitive decline', *Nature Reviews Neuroscience* **13**(4), 240–250.

Murman, D. L. (2015), The impact of age on cognition, *in* 'Seminars in hearing', Vol. 36, Thieme Medical Publishers, pp. 111–121.

Musk, E. (2019), 'An integrated brain-machine interface platform with thousands of channels', *Journal of Medical Internet Research* **21**(10), e16194.

Bibliography

Neher, E. & Sakmann, B. (1976), 'Single-channel currents recorded from membrane of denervated frog muscle fibres', *Nature* **260**(5554), 799–802.

Nelken, I., Rotman, Y. & Yosef, O. B. (1999*a*), 'Responses of auditory-cortex neurons to structural features of natural sounds', *Nature* **397**(6715), 154–157.

Nelken, I., Rotman, Y. & Yosef, O. B. (1999*b*), 'Responses of auditory-cortex neurons to structural features of natural sounds', *Nature* **397**(6715), 154–157.

Nishi, S. & North, R. (1973), 'Intracellular recording from the myenteric plexus of the guinea-pig ileum', *The Journal of physiology* **231**(3), 471.

Nishimura, H., Hashikawa, K., Iwaki, T., Watanabe, Y., Kusuoka, H., Nishimura, T., Kubo, T. et al. (1999), 'Sign language 'heard' in the auditory cortex', *Nature* **397**(6715), 116–116.

Noben-Trauth, K., Zheng, Q. Y. & Johnson, K. R. (2003), 'Association of cadherin 23 with polygenic inheritance and genetic modification of sensorineural hearing loss', *Nature Genetics* **35**(1), 21–23.
URL: *https://dx.doi.org/10.1038/ng1226*

Noudoost, B. & Moore, T. (2011), 'The role of neuromodulators in selective attention', *Trends in Cognitive Sciences* **15**(12), 585–591.
URL: *https://dx.doi.org/10.1016/j.tics.2011.10.006*

Nuñez, A. & Buño, W. (2021), 'The theta rhythm of the hippocampus: From neuronal and circuit mechanisms to behavior', *Frontiers in Cellular Neuroscience* **15**.
URL: *https://www.frontiersin.org/articles/10.3389/fncel.2021.649262*

Oertel, D., Wright, S., Cao, X.-J., Ferragamo, M. & Bal, R. (2011), 'The multiple functions of t stellate/multipolar/chopper cells in the ventral cochlear nucleus', *Hearing research* **276**(1-2), 61–69.

Oghalai, J. S. (2004), 'The cochlear amplifier: augmentation of the traveling wave within the inner ear', *Current Opinion in Otolaryngology Head Neck Surgery* **12**(5), 431–438.

Ohlemiller, K., Frisina, R., Schacht, J., Popper, A. & Fay, R. (2008), 'Auditory trauma, protection, and repair', *US: Springer* pp. 145–194.

Ohlemiller, K. K. (2002), 'Reduction in sharpness of frequency tuning but not endocochlear potential in aging and noise-exposed balb/cj mice', *Journal of the Association for Research in Otolaryngology* **3**(4), 444–456.
URL: *https://dx.doi.org/10.1007/s10162-002-2041-y*

Ohlemiller, K. K. (2004), 'Age-related hearing loss: The status of schuknecht's typology'.

Ohlemiller, K. K. (2009), 'Mechanisms and genes in human strial presbycusis from animal models', *Brain Research* **1277**, 70–83.
URL: *https://dx.doi.org/10.1016/j.brainres.2009.02.079*

Bibliography

Ohlemiller, K. K., Jones, S. M. & Johnson, K. R. (2016), 'Application of mouse models to research in hearing and balance', *Journal of the Association for Research in Otolaryngology* **17**(6), 493–523.
URL: *https://dx.doi.org/10.1007/s10162-016-0589-1*

Ohyama, K., Kanda, T., Miyazaki, T., Tsujino, N., Ishii, R., Ishikawa, Y., Muramoto, H., Grenier, F., Makino, Y., Mchugh, T. J., Yanagisawa, M., Greene, R. W. & Vogt, K. E. (2020), 'Structure of cortical network activity across natural wake and sleep states in mice', *PLOS ONE* **15**(5), e0233561.

Oliver, D. L., Beckius, G. E., Bishop, D. C., Loftus, W. C. & Batra, R. (2003), 'Topography of interaural temporal disparity coding in projections of medial superior olive to inferior colliculus', *Journal of Neuroscience* **23**(19), 7438–7449.

Opoku-Baah, C., Schoenhaut, A. M., Vassall, S. G., Tovar, D. A., Ramachandran, R. & Wallace, M. T. (2021), 'Visual influences on auditory behavioral, neural, and perceptual processes: A review', *Journal of the Association for Research in Otolaryngology* **22**(4), 365–386.

Ouda, L. & Syka, J. (2012), 'Immunocytochemical profiles of inferior colliculus neurons in the rat and their changes with aging', *Frontiers in Neural Circuits* **6**, 68.

Overton, J. A. & Recanzone, G. H. (2016), 'Effects of aging on the response of single neurons to amplitude-modulated noise in primary auditory cortex of rhesus macaque', *Journal of Neurophysiology* **115**(6), 2911–2923. PMID: 26936987.
URL: *https://doi.org/10.1152/jn.01098.2015*

Pachitariu, M., Lyamzin, D. R., Sahani, M. & Lesica, N. A. (2015), 'State-dependent population coding in primary auditory cortex', *The Journal of Neuroscience* **35**(5), 2058–2073.

Pachitariu, M., Steinmetz, N. A., Kadir, S. N., Carandini, M. & Harris, K. D. (2016), 'Fast and accurate spike sorting of high-channel count probes with kilosort', *Advances in neural information processing systems* **29**.

Padamsey, Z., Katsanevaki, D., Dupuy, N. & Rochefort, N. L. (2022), 'Neocortex saves energy by reducing coding precision during food scarcity', *Neuron* **110**(2), 280–296.e10.

Palomero-Gallagher, N. & Zilles, K. (2019), 'Cortical layers: Cyto-, myelo-, receptor-and synaptic architecture in human cortical areas', *Neuroimage* **197**, 716–741.

Park, S. N., Back, S. A., Park, K. H., Kim, D. K., Park, S. Y., Oh, J. H., Park, Y. S. & Yeo, S. W. (2010), 'Comparison of cochlear morphology and apoptosis in mouse models of presbycusis'.

Paul, M. S. et al. (2019), 'Neuroanatomy, superior and inferior olivary nucleus (superior and inferior olivary complex)'.

Peelle, J. E., Troiani, V., Grossman, M. & Wingfield, A. (2011), 'Hearing loss in older adults affects neural systems supporting speech comprehension', *The Journal of Neuroscience* **31**(35), 12638–12643.

157

Bibliography

Peelle, J. E. & Wingfield, A. (2016), 'The neural consequences of age-related hearing loss', *Trends in Neurosciences* **39**(7), 486–497.
URL: *https://dx.doi.org/10.1016/j.tins.2016.05.001*

Peineau, T., Belleudy, S., Pietropaolo, S., Bouleau, Y. & Dulon, D. (2021), 'Synaptic release potentiation at aging auditory ribbon synapses', *Frontiers in Aging Neuroscience* **13**.
URL: *https://www.frontiersin.org/articles/10.3389/fnagi.2021.756449*

Pelvig, D. P., Pakkenberg, H., Stark, A. K. & Pakkenberg, B. (2008), 'Neocortical glial cell numbers in human brains', *Neurobiology of aging* **29**(11), 1754–1762.

Peng, A. W. & Ricci, A. J. (2011), 'Somatic motility and hair bundle mechanics, are both necessary for cochlear amplification?', *Hearing research* **273**(1-2), 109–122.

Pernia, M., Díaz, I., Colmenárez-Raga, A., Rivadulla, C., Cudeiro, J., Plaza, I. & Merchán, M. (2020), 'Cross-modal reaction of auditory and visual cortices after long-term bilateral hearing deprivation in the rat', *Brain Structure and Function* **225**(1), 129–148.

Peters, R. (2006), 'Ageing and the brain', *Postgraduate Medical Journal* **82**(964), 84–88.
URL: *https://dx.doi.org/10.1136/pgmj.2005.036665*

Phillips, D. P., Hall, S. & Boehnke, S. (2002), 'Central auditory onset responses, and temporal asymmetries in auditory perception', *Hearing research* **167**(1-2), 192–205.

Piasini, E. & Panzeri, S. (2019), 'Information theory in neuroscience', *Entropy* **21**(1), 62.
URL: *https://dx.doi.org/10.3390/e21010062*

Pichora-Fuller, M. K. & Singh, G. (2006), 'Effects of age on auditory and cognitive processing: Implications for hearing aid fitting and audiologic rehabilitation', *Trends in Amplification* **10**(1), 29–59.

Pickles, J. O. (2015), Chapter 1 - auditory pathways: anatomy and physiology, *in* M. J. Aminoff, F. Boller & D. F. Swaab, eds, 'The Human Auditory System', Vol. 129 of *Handbook of Clinical Neurology*, Elsevier, pp. 3–25.
URL: *https://www.sciencedirect.com/science/article/pii/B9780444626301000019*

Pivovarov, A. S., Calahorro, F. & Walker, R. J. (2019), 'Na+/k+-pump and neurotransmitter membrane receptors', *Invertebrate Neuroscience* **19**(1).
URL: *https://dx.doi.org/10.1007/s10158-018-0221-7*

Plack, C. J., Barker, D. & Prendergast, G. (2014), 'Perceptual consequences of "hidden" hearing loss', *Trends in Hearing* **18**(0), 233121651455062.
URL: *https://dx.doi.org/10.1177/2331216514550621*

Plourde, G. (2006), 'Auditory evoked potentials'.

Bibliography

Podvalny, E., Flounders, M. W., King, L. E., Holroyd, T. & He, B. J. (2019), 'A dual role of prestimulus spontaneous neural activity in visual object recognition', *Nature communications* **10**(1), 1–13.

Poulet, J. F. & Crochet, S. (2019), 'The cortical states of wakefulness', *Frontiers in systems neuroscience* **12**, 64.

Poulisse, C., Wheeldon, L., Limachya, R., Mazaheri, A. & Segaert, K. (2020), 'The oscillatory mechanisms associated with syntactic binding in healthy ageing', *Neuropsychologia* **146**, 107523.

Pouzat, C., Mazor, O. & Laurent, G. (2002), 'Using noise signature to optimize spike-sorting and to assess neuronal classification quality', *Journal of neuroscience methods* **122**(1), 43–57.

Powell, D. S., Oh, E. S., Reed, N. S., Lin, F. R. & Deal, J. A. (2022), 'Hearing loss and cognition: What we know and where we need to go', *Frontiers in Aging Neuroscience* **13**.
    URL: *https://www.frontiersin.org/articles/10.3389/fnagi.2021.769405*

Price, D., Tyler, L. K., Neto Henriques, R., Campbell, K. L., Williams, N., Treder, M., Taylor, J. R. & Henson, R. N. A. (2017), 'Age-related delay in visual and auditory evoked responses is mediated by white- and grey-matter differences', *Nature Communications* **8**(1).

Profant, O., Tintěra, J., Balogová, Z., Ibrahim, I., Jilek, M. & Syka, J. (2015), 'Functional changes in the human auditory cortex in ageing', *PLOS ONE* **10**(3), e0116692.
    URL: *https://dx.doi.org/10.1371/journal.pone.0116692*

Pryluk, R., Kfir, Y., Gelbard-Sagiv, H., Fried, I. & Paz, R. (2019), 'A tradeoff in the neural code across regions and species', *Cell* **176**(3), 597–609.

R Core Team (2022), *R: A Language and Environment for Statistical Computing*, R Foundation for Statistical Computing, Vienna, Austria.
    URL: *https://www.R-project.org/*

Radulescu, C. I., Cerar, V., Haslehurst, P., Kopanitsa, M. & Barnes, S. J. (2021), 'The aging mouse brain: cognition, connectivity and calcium', *Cell Calcium* **94**, 102358.
    URL: *https://www.sciencedirect.com/science/article/pii/S0143416021000129*

Raichle, M. E. (1998), 'Behind the scenes of functional brain imaging: A historical and physiological perspective', *Proceedings of the National Academy of Sciences* **95**(3), 765–772.

Ramamurthy, D. L. & Recanzone, G. H. (2020), 'Age-related changes in sound onset and offset intensity coding in auditory cortical fields a1 and cl of rhesus macaques', *Journal of Neurophysiology* **123**(3), 1015–1025.

Rauschecker, J. P. (1999), 'Auditory cortical plasticity: a comparison with other sensory systems', *Trends in Neurosciences* **22**(2), 74–80.
    URL: *https://www.sciencedirect.com/science/article/pii/S0166223698013034*

Bibliography

Rauschecker, J. P. & Scott, S. K. (2009), 'Maps and streams in the auditory cortex: nonhuman primates illuminate human speech processing', *Nature neuroscience* **12**(6), 718–724.

Ray, S., Crone, N. E., Niebur, E., Franaszczuk, P. J. & Hsiao, S. S. (2008), 'Neural correlates of high-gamma oscillations (60–200 hz) in macaque local field potentials and their potential implications in electrocorticography', *The Journal of Neuroscience* **28**(45), 11526–11536.

Read, H. L., Winer, J. A. & Schreiner, C. E. (2002), 'Functional architecture of auditory cortex'.

Recanzone, G. (2018), 'The effects of aging on auditory cortical function', *Hearing Research* **366**, 99–105. International Conference on Auditory Cortex 2017.
   URL: *https://www.sciencedirect.com/science/article/pii/S0378595517306275*

Rees, A. (2009), *Medial Geniculate Body*, pp. 2275–2279.

Reich, D. S., Mechler, F., Purpura, K. P. & Victor, J. D. (2000), 'Interspike intervals, receptive fields, and information encoding in primary visual cortex', *The Journal of Neuroscience* **20**(5), 1964–1974.

Reichenbach, T. & Hudspeth, A. (2010), 'A ratchet mechanism for amplification in low-frequency mammalian hearing', *Proceedings of the National Academy of Sciences* **107**(11), 4973–4978.

Reimer, J., Froudarakis, E., Cathryn, Yatsenko, D., George & Andreas (2014), 'Pupil fluctuations track fast switching of cortical states during quiet wakefulness', *Neuron* **84**(2), 355–362.
   URL: *https://dx.doi.org/10.1016/j.neuron.2014.09.033*

Reinagel, P. (2000), 'Information theory in the brain', *Current Biology* **10**(15), R542–R544.

Renshaw, B., Forbes, A. & Morison, B. (1940), 'Activity of isocortex and hippocampus: electrical studies with micro-electrodes', *Journal of neurophysiology* **3**(1), 74–105.

Revill, A. L. & Fuglevand, A. J. (2017), 'Inhibition linearizes firing rate responses in human motor units: implications for the role of persistent inward currents', *The journal of physiology.* **595**(1), 179–191.

Rey, H. G., Pedreira, C. & Quiroga, R. Q. (2015), 'Past, present and future of spike sorting techniques', *Brain research bulletin* **119**, 106–117.

Rhode, W. S., Roth, G. L. & Recio-Spinoso, A. (2010), 'Response properties of cochlear nucleus neurons in monkeys', *Hearing research* **259**(1-2), 1–15.

Ribeiro, M. & Castelo-Branco, M. (2022), 'Slow fluctuations in ongoing brain activity decrease in amplitude with ageing yet their impact on task-related evoked responses is dissociable from behavior', *eLife* **11**, e75722.
   URL: *https://doi.org/10.7554/eLife.75722*

Rieke, F., Bodnar, D. A. & Bialek, W. (1995), 'Naturalistic stimuli increase the rate and efficiency of information transmission by primary auditory afferents', *Proceedings of the Royal Society B: Biological Sciences* **262**(1365), 259–265.

Bibliography

Rieke, F., Warland, D., Van Steveninck, R. d. R. & Bialek, W. (1999), *Spikes: exploring the neural code*, MIT press.

Riva, C., Donadieu, E., Magnan, J. & Lavieille, J.-P. (2007), 'Age-related hearing loss in cd/1 mice is associated to ros formation and hif target proteins up-regulation in the cochlea', *Experimental Gerontology* **42**(4), 327–336.
URL: *https://www.sciencedirect.com/science/article/pii/S0531556506003317*

Rogalla, M. M. & Hildebrandt, K. J. (2020), 'Aging but not age-related hearing loss dominates the decrease of parvalbumin immunoreactivity in the primary auditory cortex of mice', *eneuro* **7**(3), ENEURO.0511–19.

Rossant, C., Kadir, S. N., Goodman, D. F., Schulman, J., Hunter, M. L., Saleem, A. B., Grosmark, A., Belluscio, M., Denfield, G. H., Ecker, A. S. et al. (2016), 'Spike sorting for large, dense electrode arrays', *Nature neuroscience* **19**(4), 634–641.

Rossignol, E. (2011), 'Genetics and function of neocortical gabaergic interneurons in neurodevelopmental disorders', *Neural Plasticity* **2011**.

Rossignol, E., Kruglikov, I., Van Den Maagdenberg, A. M., Rudy, B. & Fishell, G. (2013), 'Cav2. 1 ablation in cortical interneurons selectively impairs fast-spiking basket cells and causes generalized seizures', *Annals of neurology* **74**(2), 209–222.

Rothschild, G., Cohen, L., Mizrahi, A. & Nelken, I. (2013), 'Elevated correlations in neuronal ensembles of mouse auditory cortex following parturition', *Journal of Neuroscience* **33**(31), 12851–12861.

Rothschild, G., Nelken, I. & Mizrahi, A. (2010), 'Functional organization and population dynamics in the mouse primary auditory cortex'.

Rozycka, A. & Liguz-Lecznar, M. (2017), 'The space where aging acts: Focus on the gaba ergic synapse', *Aging cell* **16**(4), 634–643.

Rubio, J. E. & Holden, A. V. (1975), 'The response of a model neurone to a white noise input', *Biological Cybernetics* **19**(4), 191–195.

Sadaghiani, S., Hesselmann, G., Friston, K. & Kleinschmidt, A. (2010), 'The relation of ongoing brain activity, evoked neural responses, and cognition', *Frontiers in Systems Neuroscience* **4**.
URL: *https://www.frontiersin.org/articles/10.3389/fnsys.2010.00020*

Sadagopan, S., Kar, M. & Parida, S. (2023), 'Quantitative models of auditory cortical processing', *Hearing Research* **429**, 108697.
URL: *https://www.sciencedirect.com/science/article/pii/S0378595523000096*

Sakata, S. (2016), 'State-dependent and cell type-specific temporal processing in auditory thalamocortical circuit', *Scientific reports* **6**(1), 1–13.

Sakata, S. & Harris, K. D. (2009), 'Laminar structure of spontaneous and sensory-evoked population activity in auditory cortex'.

Bibliography

Sanju, H. K. & Kumar, P. (2016), 'Enhanced auditory evoked potentials in musicians: A review of recent findings'.

Saxe, G. N., Calderone, D. & Morales, L. J. (2018), 'Brain entropy and human intelligence: A resting-state fmri study', *PLOS ONE* **13**(2), e0191582.
URL: *https://dx.doi.org/10.1371/journal.pone.0191582*

Scharf, R., Tsunematsu, T., Mcalinden, N., Dawson, M. D., Sakata, S. & Mathieson, K. (2016), 'Depth-specific optogenetic control in vivo with a scalable, high-density microled neural probe', *Scientific Reports* **6**(1), 28381.
URL: *https://dx.doi.org/10.1038/srep28381*

Scheeringa, R., Bastiaansen, M. C., Petersson, K. M., Oostenveld, R., Norris, D. G. & Hagoort, P. (2008), 'Frontal theta eeg activity correlates negatively with the default mode network in resting state', *International Journal of Psychophysiology* **67**(3), 242–251.
URL: *https://dx.doi.org/10.1016/j.ijpsycho.2007.05.017*

Schjetnan, A. G. P. & Luczak, A. (2011), 'Recording large-scale neuronal ensembles with silicon probes in the anesthetized rat', *Journal of Visualized Experiments* (56).
URL: *https://dx.doi.org/10.3791/3282*

Schmitzer-Torbert, N. ., Jackson, J., Henze, D., Harris, K. & Redish, A. (2005), 'Quantitative measures of cluster quality for use in extracellular recordings', *Neuroscience* **131**(1), 1–11.

Schroeder, C. E., Wilson, D. A., Radman, T., Scharfman, H. & Lakatos, P. (2010), 'Dynamics of active sensing and perceptual selection', *Current opinion in neurobiology* **20**(2), 172–176.

Schröger, E., Marzecová, A. & SanMiguel, I. (2015), 'Attention and prediction in human audition: a lesson from cognitive psychophysiology', *European Journal of Neuroscience* **41**(5), 641–664.

Schwiening, C. J. (2012), 'A brief historical perspective: Hodgkin and huxley', *The Journal of physiology* **590**(Pt 11), 2571.

Seymour, R. A., Rippon, G. & Kessler, K. (2017), 'The detection of phase amplitude coupling during sensory processing', *Frontiers in Neuroscience* **11**.
URL: *https://www.frontiersin.org/articles/10.3389/fnins.2017.00487*

Sha, S. H., Kanicki, A., Dootz, G., Talaska, A. E., Halsey, K., Dolan, D., Altschuler, R. & Schacht, J. (2008), 'Age-related auditory pathology in the cba/j mouse'.

Shafto, M. A. & Tyler, L. K. (2014), 'Language in the aging brain: the network dynamics of cognitive decline and preservation', *Science* **346**(6209), 583–587.

Shannon, C. E. (1948), 'A mathematical theory of communication', *Bell System Technical Journal* **27**(3), 379–423.
URL: *https://dx.doi.org/10.1002/j.1538-7305.1948.tb01338.x*

Bibliography

Shilling-Scrivo, K., Mittelstadt, J. & Kanold, P. O. (2021), 'Altered response dynamics and increased population correlation to tonal stimuli embedded in noise in aging auditory cortex', *The Journal of Neuroscience* **41**(46), 9650–9668.

Shilling-Scrivo, K., Mittelstadt, J. & Kanold, P. O. (2022), 'Decreased modulation of population correlations in auditory cortex is associated with decreased auditory detection performance in old mice', *The Journal of Neuroscience* **42**(49), 9278–9292.

Siveke, I., Leibold, C., Schiller, E. & Grothe, B. (2012), 'Adaptation of binaural processing in the adult brainstem induced by ambient noise', *The Journal of Neuroscience* **32**(2), 462–473.

Smith, P. H. & Populin, L. C. (2001), 'Fundamental differences between the thalamocortical recipient layers of the cat auditory and visual cortices', *Journal of Comparative Neurology* **436**(4), 508–519.

Sohal, V. S., Zhang, F., Yizhar, O. & Deisseroth, K. (2009), 'Parvalbumin neurons and gamma rhythms enhance cortical circuit performance'.

Solyga, M. & Barkat, T. R. (2021), 'Emergence and function of cortical offset responses in sound termination detection', *eLife* **10**.

Sonntag, M., Englitz, B., Kopp-Scheinpflug, C. & Rübsamen, R. (2009), 'Early postnatal development of spontaneous and acoustically evoked discharge activity of principal cells of the medial nucleus of the trapezoid body: Anin vivostudy in mice', *The Journal of Neuroscience* **29**(30), 9510–9520.

Spongr, V. P., Flood, D. G., Frisina, R. D. & Salvi, R. J. (1997), 'Quantitative measures of hair cell loss in CBA and C57BL/6 mice throughout their life spans', *The Journal of the Acoustical Society of America* **101**(6), 3546–3553.
URL: *https://doi.org/10.1121/1.418315*

Spooner, R. K., Wiesman, A. I., Proskovec, A. L., Heinrichs-Graham, E. & Wilson, T. W. (2019), 'Rhythmic spontaneous activity mediates the age-related decline in somatosensory function', *Cerebral Cortex* **29**(2), 680–688.
URL: *https://dx.doi.org/10.1093/cercor/bhx349*

Stahnisch, F. W. (2017), 'How the nerves reached the muscle: Bernard katz, stephen w. kuffler, and john c. eccles—certain implications of exile for the development of twentieth-century neurophysiology'.

Steinmetz, P. N., Roy, A., Fitzgerald, P., Hsiao, S., Johnson, K. & Niebur, E. (2000), 'Attention modulates synchronized neuronal firing in primate somatosensory cortex', *Nature* **404**(6774), 187–190.

Steriade, M. & Timofeev, I. (2003), 'Neuronal plasticity in thalamocortical networks during sleep and waking oscillations', *Neuron* **37**(4), 563–576.

Steriade, M., Timofeev, I. & Grenier, F. (2001), 'Natural waking and sleep states: a view from inside neocortical neurons', *Journal of neurophysiology* **85**(5), 1969–1985.

Bibliography

Stiebler, I., Neulist, R., Fichtel, I. & Ehret, G. (1997), 'The auditory cortex of the house mouse: left-right differences, tonotopic organization and quantitative analysis of frequency representation', *Journal of Comparative Physiology A* **181**(6), 559–571.

Strauß, A., Henry, M. J., Scharinger, M. & Obleser, J. (2015), 'Alpha phase determines successful lexical decision in noise', *Journal of Neuroscience* **35**(7), 3256–3262.

Stringer, C., Pachitariu, M., Steinmetz, N., Reddy, C. B., Carandini, M. & Harris, K. D. (2019), 'Spontaneous behaviors drive multidimensional, brainwide activity', *Science* **364**(6437), eaav7893.

Strouse, A., Ashmead, D. H., Ohde, R. N. & Grantham, D. W. (1998), 'Temporal processing in the aging auditory system', *The Journal of the Acoustical Society of America* **104**(4), 2385–2399.
URL: *https://doi.org/10.1121/1.423748*

Studer, F. & Barkat, T. R. (2022), 'Inhibition in the auditory cortex', *Neuroscience and Biobehavioral Reviews* **132**, 61–75.
URL: *https://www.sciencedirect.com/science/article/pii/S0149763421005145*

Südhof, T. C. & Malenka, R. C. (2008), 'Understanding synapses: Past, present, and future', *Neuron* **60**(3), 469–476.
URL: *https://dx.doi.org/10.1016/j.neuron.2008.10.011*

Tabak, J., Rinzel, J. & O'Donovan, M. J. (2001), 'The role of activity-dependent network depression in the expression and self-regulation of spontaneous activity in the developing spinal cord', *The Journal of Neuroscience* **21**(22), 8966–8978.

Tacik, P., Alfieri, A., Kornhuber, M. & Dressler, D. (2012), 'Gasperini's syndrome: its neuroanatomical basis now and then', *Journal of the History of the Neurosciences* **21**(1), 17–30.

Theunissen, F. E. & Elie, J. E. (2014), 'Neural processing of natural sounds', *Nature Reviews Neuroscience* **15**(6), 355–366.
URL: *https://dx.doi.org/10.1038/nrn3731*

Theunissen, F. E., Sen, K. & Doupe, A. J. (2000), 'Spectral-temporal receptive fields of nonlinear auditory neurons obtained using natural sounds', *The Journal of Neuroscience* **20**(6), 2315–2331.

Thoma, R. J., Meier, A., Houck, J., Clark, V. P., Lewine, J. D., Turner, J., Calhoun, V. & Stephen, J. (2017), 'Diminished auditory sensory gating during active auditory verbal hallucinations', *Schizophrenia Research* **188**, 125–131.
URL: *https://dx.doi.org/10.1016/j.schres.2017.01.023*

Thwaites, A., Glasberg, B. R., Nimmo-Smith, I., Marslen-Wilson, W. D. & Moore, B. C. J. (2016), 'Representation of instantaneous and short-term loudness in the human cortex', *Frontiers in Neuroscience* **10**.
URL: *https://www.frontiersin.org/articles/10.3389/fnins.2016.00183*

Timme, N. M. & Lapish, C. (2018), 'A tutorial for information theory in neuroscience', *eneuro* **5**(3), ENEURO.0052–18.

Bibliography

Tomar, R. (2019), 'Review: Methods of firing rate estimation', *Biosystems* **183**, 103980.

Tozzi, A., Zare, M. & Benasich, A. A. (2016), 'New perspectives on spontaneous brain activity: dynamic networks and energy matter', *Frontiers in human neuroscience* **10**, 247.

Tremblay, K. L. & Miller, C. W. (2014), 'How neuroscience relates to hearing aid amplification', *International Journal of Otolaryngology* **2014**, 1–7.
URL: *https://dx.doi.org/10.1155/2014/641652*

Tremblay, R., Lee, S. & Rudy, B. (2016), 'Gabaergic interneurons in the neocortex: From cellular properties to circuits', *Neuron* **91**(2), 260–292.
URL: *https://dx.doi.org/10.1016/j.neuron.2016.06.033*

Tsunematsu, T., Patel, A. A., Onken, A. & Sakata, S. (2020), 'State-dependent brainstem ensemble dynamics and their interactions with hippocampus across sleep states', *eLife* **9**.

Uhlhaas, P., Pipa, G., Lima, B., Melloni, L., Neuenschwander, S., Nikolić, D. & Singer, W. (2009), 'Neural synchrony in cortical networks: history, concept and current status', *Frontiers in Integrative Neuroscience* **3**.
URL: *https://www.frontiersin.org/articles/10.3389/neuro.07.017.2009*

Upadhyay, J., Silver, A., Knaus, T. A., Lindgren, K. A., Ducros, M., Kim, D.-S. & Tager-Flusberg, H. (2008), 'Effective and structural connectivity in the human auditory cortex', *The Journal of Neuroscience* **28**(13), 3341–3349.

Vago, D. R. & Zeidan, F. (2016), 'The brain on silent: mind wandering, mindful awareness, and states of mental tranquility', *Annals of the New York Academy of Sciences* **1373**(1), 96–113.
URL: *https://dx.doi.org/10.1111/nyas.13171*

Valderrama, J. T., de la Torre, A. & McAlpine, D. (2022), 'The hunt for hidden hearing loss in humans: From preclinical studies to effective interventions', *Frontiers in Neuroscience* **16**.
URL: *https://www.frontiersin.org/articles/10.3389/fnins.2022.1000304*

Van Lier, B., Hierlemann, A. & Knoflach, F. (2018), 'Parvalbumin expression and gamma oscillation occurrence increase over time in a neurodevelopmental model of nmda receptor dysfunction', *PeerJ* **6**, e5543.

Van Putten, M. J. A. M. (2020), *Basics of the EEG*, p. 129–152.

VanRullen, R. (2016), 'How to evaluate phase differences between trial groups in ongoing electrophysiological signals', *Frontiers in neuroscience* **10**, 426.

Verkhratsky, A., Krishtal, O. A. & Petersen, O. H. (2006), 'From galvani to patch clamp: the development of electrophysiology', *Pflügers Archiv* **453**(3), 233–247.

Vicencio-Jimenez, S., Weinberg, M. M., Bucci-Mansilla, G. & Lauer, A. M. (2021), 'Olivocochlear changes associated with aging predominantly affect the medial olivocochlear system', *Frontiers in Neuroscience* **15**.
URL: *https://www.frontiersin.org/articles/10.3389/fnins.2021.704805*

Bibliography

Vonderschen, K. & Chacron, M. J. (2011), 'Sparse and dense coding of natural stimuli by distinct midbrain neuron subpopulations in weakly electric fish', *Journal of Neurophysiology* **106**(6), 3102–3118.
URL: *https://dx.doi.org/10.1152/jn.00588.2011*

Walton, J., Orlando, M. & Burkard, R. (1999), 'Auditory brainstem response forward-masking recovery functions in older humans with normal hearing', *Hearing research* **127**(1-2), 86–94.

Walton, J. P. (2010), 'Timing is everything: Temporal processing deficits in the aged auditory brainstem', *Hearing Research* **264**(1-2), 63–69.

Walton, J. P., Frisina, R. D. & O'Neill, W. E. (1998), 'Age-related alteration in processing of temporal sound features in the auditory midbrain of the cba mouse', *The Journal of Neuroscience* **18**(7), 2764–2776.

Walton, J. P., Simon, H. & Frisina, R. D. (2002), 'Age-related alterations in the neural coding of envelope periodicities', *Journal of Neurophysiology* **88**(2), 565–578. PMID: 12163510.
URL: *https://doi.org/10.1152/jn.2002.88.2.565*

Wang, H. C. & Bergles, D. E. (2015), 'Spontaneous activity in the developing auditory system', *Cell and Tissue Research* **361**(1), 65–75.

Wang, H.-F., Zhang, W., Rolls, E. T., Li, Y., Wang, L., Ma, Y.-H., Kang, J., Feng, J., Yu, J.-T. & Cheng, W. (2022), 'Hearing impairment is associated with cognitive decline, brain atrophy and tau pathology', *eBioMedicine* **86**, 104336.

Wang, J. & Puel, J.-L. (2020), 'Presbycusis: An update on cochlear mechanisms and therapies', *Journal of Clinical Medicine* **9**(1), 218.

Wang, M., Gamo, N. J., Yang, Y., Jin, L. E., Wang, X.-J., Laubach, M., Mazer, J. A., Lee, D. & Arnsten, A. F. (2011), 'Neuronal basis of age-related working memory decline', *Nature* **476**(7359), 210–213.

Wang, S., Zhao, Y., Zhang, L., Wang, X., Wang, X., Cheng, B., Luo, K. & Gong, Q. (2019), 'Stress and the brain: Perceived stress mediates the impact of the superior frontal gyrus spontaneous activity on depressive symptoms in late adolescence', *Human Brain Mapping* **40**(17), 4982–4993.
URL: *https://onlinelibrary.wiley.com/doi/abs/10.1002/hbm.24752*

Wang, X.-J., Tegner, J., Constantinidis, C. & Goldman-Rakic, P. S. (2004), 'Division of labor among distinct subtypes of inhibitory neurons in a cortical microcircuit of working memory', *Proceedings of the National Academy of Sciences* **101**(5), 1368–1373.

Waschke, L., Wöstmann, M. & Obleser, J. (2017), 'States and traits of neural irregularity in the age-varying human brain', *Scientific reports* **7**(1), 1–12.

Wen, X., Wu, X., Liu, J., Li, K. & Yao, L. (2013), 'Abnormal baseline brain activity in non-depressed parkinson's disease and depressed parkinson's disease: A resting-state functional magnetic resonance imaging study', *PLOS*

ONE **8**(5), e63691.

URL: *https://dx.doi.org/10.1371/journal.pone.0063691*

Willmore, B. D. B., Cooke, J. E. & King, A. J. (2014), 'Hearing in noisy environments: noise invariance and contrast gain control', *The Journal of Physiology* **592**(16), 3371–3381.

URL: *https://dx.doi.org/10.1113/jphysiol.2014.274886*

Willmore, B. D. B. & King, A. J. (2023), 'Adaptation in auditory processing', *Physiological Reviews* **103**(2), 1025–1058. PMID: 36049112.

URL: *https://doi.org/10.1152/physrev.00011.2022*

Willott, J. F. (1991), 'Aging and the auditory system', *Anatomy, Physiology, and Psychophysics* pp. 168–201.

Wilson, C. A., Fouda, S. & Sakata, S. (2020), 'Effects of optogenetic stimulation of basal forebrain parvalbumin neurons on alzheimer's disease pathology', *Scientific reports* **10**(1), 1–9.

Wingfield, A. & Grossman, M. (2006), 'Language and the aging brain: patterns of neural compensation revealed by functional brain imaging', *Journal of neurophysiology* **96**(6), 2830–2839.

Wlotko, E. W., Lee, C. L. & Federmeier, K. D. (2010), 'Language of the aging brain: Event-related potential studies of comprehension in older adults', *Linguistics and Language Compass* **4**, 623–638.

Wong, L. L. N., Yu, J. K. Y., Chan, S. S. & Tong, M. C. F. (2014), 'Screening of cognitive function and hearing impairment in older adults: A preliminary study', *BioMed Research International* **2014**, 1–7.

URL: *https://dx.doi.org/10.1155/2014/867852*

Woods, D. L., Wyma, J. M., Yund, E. W., Herron, T. J. & Reed, B. (2015), 'Age-related slowing of response selection and production in a visual choice reaction time task', *Frontiers in human neuroscience* **9**, 193.

Wöstmann, M., Lim, S.-J. & Obleser, J. (2017), 'The human neural alpha response to speech is a proxy of attentional control', *Cerebral cortex* **27**(6), 3307–3317.

Wu, P.-Z., O'Malley, J. T., De Gruttola, V. & Liberman, M. C. (2020), 'Age-related hearing loss is dominated by damage to inner ear sensory cells, not the cellular battery that powers them', *The Journal of Neuroscience* **40**(33), 6357–6366.

Xue, B., Meng, X., Kao, J. P. & Kanold, P. O. (2023), 'Age-related changes in excitatory and inhibitory intra-cortical circuits in auditory cortex of c57bl/6 mice', *Hearing Research* **429**, 108685.

URL: *https://www.sciencedirect.com/science/article/pii/S0378595522002532*

Yague, J. G., Tsunematsu, T. & Sakata, S. (2017), 'Distinct temporal coordination of spontaneous population activity between basal forebrain and auditory cortex', *Frontiers in Neural Circuits* **11**.

URL: *https://www.frontiersin.org/articles/10.3389/fncir.2017.00064*

Bibliography

Yang, T., Liu, Q., Fan, X., Hou, B., Wang, J. & Chen, X. (2021), 'Altered regional activity and connectivity of functional brain networks in congenital unilateral conductive hearing loss', *NeuroImage: Clinical* **32**, 102819.
URL: *https://www.sciencedirect.com/science/article/pii/S2213158221002631*

Yerkes, R. M. & Dodson, J. D. (1908), 'The relation of strength of stimulus to rapidity of habit-formation', *Journal of Comparative Neurology and Psychology* **18**(5), 459–482.

Yizhar, O., Fenno, L. E., Davidson, T. J., Mogri, M. & Deisseroth, K. (2011), 'Optogenetics in neural systems', *Neuron* **71**(1), 9–34.

Young, E. D. (2008), 'Neural representation of spectral and temporal information in speech', *Philosophical Transactions of the Royal Society B: Biological Sciences* **363**(1493), 923–945.
URL: *https://dx.doi.org/10.1098/rstb.2007.2151*

Yuzgeç, O., Prsa, M., Zimmermann, R. & Huber, D. (2018), 'Pupil size coupling to cortical states protects the stability of deep sleep via parasympathetic modulation'.

Zanto, T. P. & Gazzaley, A. (2009), 'Neural suppression of irrelevant information underlies optimal working memory performance', *The Journal of Neuroscience* **29**(10), 3059–3066.

Zanto, T. P. & Gazzaley, A. (2014), 'Attention and ageing.'.

Zdebik, A. A., Wangemann, P. & Jentsch, T. J. (2009), 'Potassium ion movement in the inner ear: insights from genetic disease and mouse models', *Physiology* **24**(5), 307–316.

Zerlaut, Y. & Destexhe, A. (2017), 'Enhanced responsiveness and low-level awareness in stochastic network states', *Neuron* **94**(5), 1002–1009.

Zhang, X., Li, X., Chen, J. & Gong, Q. (2018), 'Background suppression and its relation to foreground processing of speech versus non-speech streams', *Neuroscience* **373**, 60–71.
URL: *https://www.sciencedirect.com/science/article/pii/S0306452218300253*

Zimmerman, B., Rypma, B., Gratton, G. & Fabiani, M. (2021), 'Age-related changes in cerebrovascular health and their effects on neural function and cognition: A comprehensive review', *Psychophysiology* **58**(7).